PCIC EUROPE
PETROLEUM & CHEMICAL INDUSTRY COMMITTEE

becomes

PCiC energy

18th PCIC Europe Annual Electrical and Automation Knowledge Sharing Event

Electrical and Instrumentation Applications & Automation

June 7nd-9th, 2022

London, United Kingdom

Partners

pcic.energy

ISBN Information: 978-3-9524799-7-1

PCIC Europe Mission

To provide an international forum for the exchange of electrical applications technology and automation relating to the petroleum and chemical industry, to sponsor appropriate standards activity for that industry, and to provide opportunity for professional development.

PCIC Europe Strategies

1. The PCIC Europe Annual Technical Conference will be held in locations of industry strength, and its location will be rotated annually in an effort to attract national and international participation.
2. PCIC Europe will proactively promote participation by a broad base of PCIC Europe representatives, with an emphasis on both younger and retired engineers.
3. Attendees will be encouraged to participate in technical activities including authorship of papers and standards development.
4. The quality of PCIC Europe paper offerings is essential for the PCIC Europe mission to succeed and will be given highest priority. Preference will be given to application oriented papers.
5. The technical content of the PCIC Europe Annual Conference will be continuously evaluated and updated to reflect the evolving needs of the industry.
6. Participation of users, manufacturers, consultants and contractors will be encouraged in the activities of PCIC Europe to strengthen the conference technical base.
7. PCIC Europe will offer tutorials directed towards enhancing the technical, communication, and interpersonal skills of petroleum and chemical industry engineers.

PCIC Europe Topics

The main topics of the PCIC Europe conference are:

The UN COP26 conference will set the forward agenda for decades to come, consequently the hottest topics for our next iDEAS 2022 events will be the energy transition and support to positioning our industry on climate risk, opportunity, and strategy specifically in relation to technology application and implementation. In respect of the conference themes for iDEAS this means:

1. **Electrification, energy storage and integration of renewables**
2. **Life cycle management and integration of digitization**

NB. You will find the table of contents at the end of this document.

PAST PCIC EUROPE CONFERENCES

PCIC Europe 2004
May 27-28 Basel, Switzerland
Chair: Uwe Klausmeyer

PCIC Europe 2005
October 26-28 Basel, Switzerland
Chair: René Ouëndag

PCIC Europe 2006
June 7-9 Amsterdam, The Netherlands
Chair: René Ouëndag

PCIC Europe 2007
June 13-15 Paris, France
Chair: Patrick Leroux

PCIC Europe 2008
June 10-12 Weimar, Germany
Chair: Patrick Leroux

PCIC Europe 2009
May 26-28 Barcelone, Spain
Chair: Patrick Leroux

PCIC Europe 2010
June 15-17 Oslo, Norway
Chair: Patrick Leroux

PCIC Europe 2011
June 7-9 Rome, Italy
Chair: Patrick Leroux

PCIC Europe 2012
June 19-21 Prague, Czech Republic
Chair: Patrick Leroux

PCIC Europe 2013
May 28-30 Istanbul, Turkey
Chair: Jean-Charles Guilhem

PCIC Europe 2014
June 3-5 Amsterdam, The Netherlands
Chair: Jean-Charles Guilhem

PCIC Europe 2015
June 9-11 London, United Kingdom
Chair: Jean-Charles Guilhem

PCIC Europe 2016
June 14-16, Berlin, Germany
Chair: Jean-Charles Guilhem

PCIC Europe 2017
May 16-18, Vienna, Austria
Chair: Peter Pieters

PCIC Europe 2018
June 5th-7th, Antwerp, Belgium
Chair: Peter Pieters

PCIC Europe 2019
May 7th-9th, Paris, France
Chair: Peter Pieters

PCIC Europe 2021 VIRTUA1 Event
June 22nd-24th, Digital Event
Chair: Justin Mason

PCIC EUROPE COMMITTEE MEMBERS

Executive & Technical Program Committee
Justin Mason Trydanol Energy Solutions (UK), Executive Committee Chair
Jeremy Andrews, Siemens (UK), Secretary & Executive Committee Vice-Chair
Jan Verstraten, Dow (NL), Treasurer
Paul Donnellan, Shell (NL), Technical Committee Chair
Diedrich Thaden (D), Technical Committee Vice-Chair Automation
Cécile Gaudeaux, Air Liquide (F), Tutorials
Luigi Bellofatto, IMESA Spa (I), Technical Secretary
Kim Fumagalli, Technor Italsmea (I), Assistant Technical Secretary
Bert Engbers, ABB (NL), Sponsors Chair
Chris Thomason (UK), PCIC Europe Local Committee Chair
Florent Baldeck, WEG (F), PCIC Middle East Local Committee Chair
Caroline Bishop, Exertherm (UK)
Caroline Vollet, Schneider Electric (F)
Allen Gibson, CAPE Industries (USA)
Bruno Leforgeais, TotalEnergies (F)
Ben Johnson, Thermon (USA)
Philippe Angays, Technip Energies (F)
Edouard Thibaut, TotalEnergies (F)

Third-parties
Melynda McCabe, Martin Marketing (USA)
Bob Martin, Martin Marketing (USA)
Thibaut Jouvet, Thera (F)

Supervisory Board
Jean-Charles Guilhem, 2B1st Consulting (F), Supervisory Board Chair
Patrick Leroux, Retired from Total (F), Supervisory Board Vice-Chair
Peter Pieters, Sabic (NL), Member

FLASHOVER CAUSED BY ELECTROSTATIC DISCHARGE DURING TRANSFORMER ROUTINE SWITCHING

Paper No. PCIC Europe EUR22_02

Georgios Fotiou
Aramco Oil Company
Dhahran
Saudi Arabia

Omar K Arfaj
Aramco Oil Company
Dhahran
Saudi Arabia

Hussain M Suwaidan
Aramco Oil Company
Dhahran
Saudi Arabia

Abstract - When switching on a power transformer, the coupling of the applied step voltage function to the stray capacitance and inductance of the secondary winding is generating an oscillatory transient voltage. The existence of a resonant point close to that oscillation frequency can amplify the surge severity above the insulation withstand and lead to insulation breakdown or flashovers. In addition, factors affecting the transformer capacitance, like the oil degradation, might shift the resonance point and impact the surge severity.

Index Terms — Capacitive Coupling, Electrostatic Discharge, Flashover.

I. INTRODUCTION

During a routine energization of an unloaded 100MVA 230000 Grd Y / 132790 - 13200Y / 7621 - 13200Y / 7621 transformer (T701), through a 230kV SF6 breaker, the differential protection picked up and issued a trip. The site survey after the incident revealed signs of flashover at both 13.2kV breakers heat radiators in all three phases. In addition, a comparative evaluation of the breaker condition identified that the insulation barriers between the breaker poles were not covering the heat radiators entirely, and the clearance on air for the exposed parts was 86mm. The disturbance recordings of the 230kV transformer feeder protection relay confirmed the survey findings, indicating a phase B to phase C fault, which rapidly developed to a bolted short circuit. During the energization, the personnel close to the transformer didn't report any out-of-the-ordinary humming or hammering sound effects. The transformer was in service for more than 20 years and was repeatedly energized, without any concerns. The power supply was recently shifted from an old AIS substation to new GIS switchgear via 160m of 230kV cable.

Fig. 1 Carbonization at the 13.2kV Breaker Radiators

II. ANALYSIS

A. Modeling for EMTP simulation

The electrostatic discharge analysis requires an accurate representation of the transformer capacitances and inductances, the interconnecting cable geometry, and the energizing breaker capacitances, pre-strike behavior, pole asymmetry, and point on wave switching. The transformer saturation, voltage ratio, and magnetic properties do not affect the analysis.

B. Transformer Model

The three winding transformer classical approach modeling was used, enhanced with the stray and interwinding capacitances. Due to the prolonged age of the transformer, those values were not available either in the company database or the vendor archives. They were calculated from the insulation power factor SAT and FAT test reports. The connection topology for those tests requires short-circuiting the three windings to avoid unwanted inductances affecting the accuracy of the results; thus, the measured capacitance values involve all the windings. Multiplying the overall values by 0.33 provides an estimate of the individual per phase winding capacitances. Reference [3] presents a straightforward method to determine the transformer capacitance. Fig 13.8 in [3] provides the total capacitance value to the ground of the highest voltage windings on a per-phase basis as per the IEEE working group. Considering that the T701 transformer size is 33.3MVA per phase, the below plot yields the highest voltage winding capacitance to ground (CH) of 5000pF. Since the transformer winding is grounded [3], this capacitance is 5000 x 0.33 or 1650pF. Consecutively from [6] and [4], CL = 3 x 1650 or 4950pf and CLH = 4 x 1650 or 6600pf.

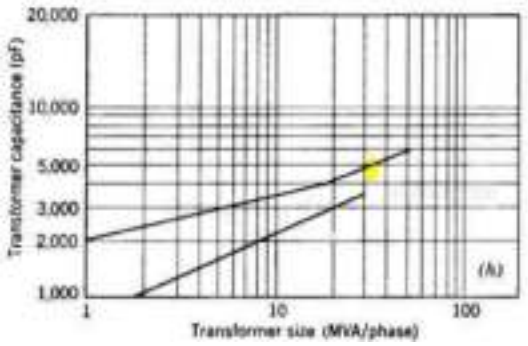

Fig. 2 Transformer capacitance graph as per [3]

Fig. 3 SAT (Top) and FAT (Bottom) capacitance measurement test reports

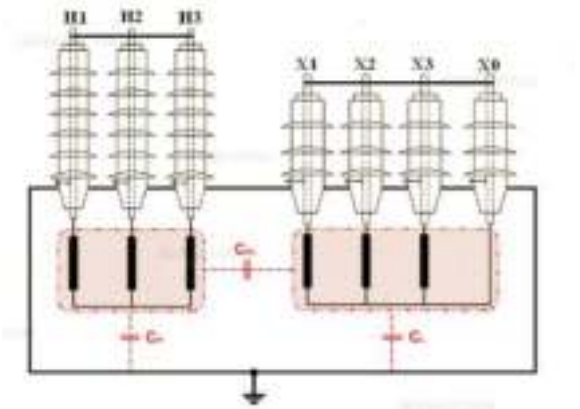

Fig. 4 FAT and SAT test connection topology

The following table summarizes the calculated capacitance values from the FAT, SAT, and the theoretical approach.

TABLE I
TRANSFORMER CAPACITANCES

Per Phase	Fault Currents and Resulted Voltage in LV side of ESP		
	FAT Test (pF)	SAT Test (pF)	Theoretical (pF)
CH	1850	1901	1650
CL	4576	4321	4950
CHL	3340[a]	1511	6600
CT	4270	4609	4950
CHT	3340	1488	n.a.
CLT	4433	158	n.a.

[a] the missing CHL measurement was replaced with CHT as the windings are identical and symmetrical placed in reference to the primary.

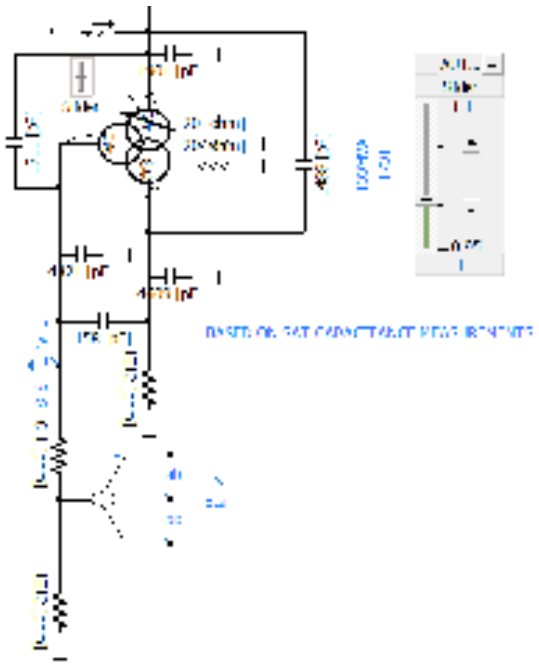

Fig. 5 Transformer Model for EMTP simulation

C. Cable Model

The cable was modeled as frequency-dependent to capture the surge propagation and reflections and investigate any possible resonance frequency matching the transformer, leading to very high voltages at the secondary [7].

As per the provided datasheet, the existing 230kV cable between the new GIS and the transformer T601 is an "*LS-cable and system*," XLPE 630mm^2 single-pole cable with copper conductor and corrugated aluminum metallic sheath.

Fig. 6 Cable data from the vendor catalog

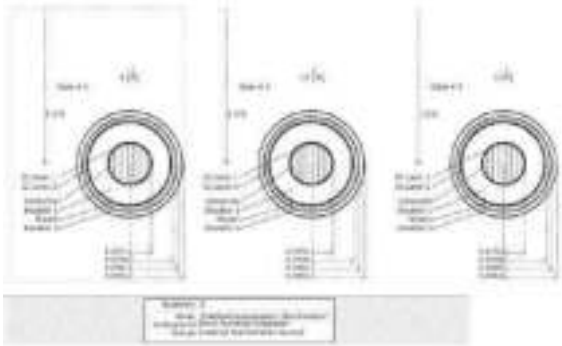

Fig. 7 Cable parametrization for EMTP simulation

D. Breaker Model

The breaker parameterized as a frequency-dependent model with the stray and the open pole capacitances based on vendor data. A statistical breaker simulated the pre-strike behavior, following a normal distribution with a standard deviation of 4, a minimum time delay of zero, and a maximum delay of 4msec. Although the worst case is switching at the voltage peak, we performed a subsequential closing with 2 msec intervals across a complete 60Hz power cycle.

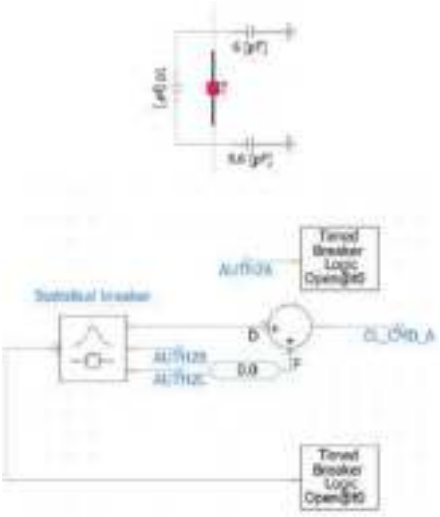

Fig. 8 Statistical breaker model for EMTP simulation

E. Validation of the Model

The model was verified against the steady-state load flow and short circuit results from a phasor domain analysis software and the latest available energization recordings from the available DFR. Figure 9 and 10 visualizes the simulated voltage waveforms as well as the recorded voltage waveforms. The obtained pattern indicates that the model is already tuned to produce the actual system response to the transient. However, the curves do not match perfectly as other factors like remnant flux, voltage transformer characteristics, and measurement instrument characteristics affect the recorded waveform.

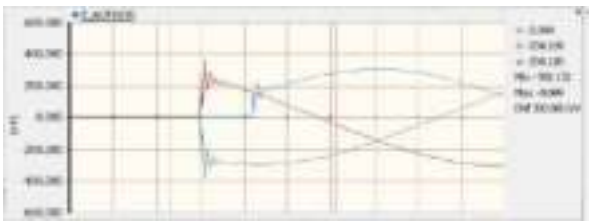

Fig. 9 Simulated Waveform

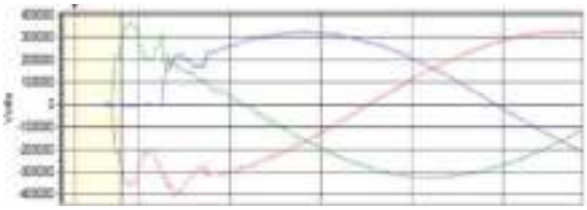

Fig. 10 Recorded Waveform

III. RESULTS

The simulation was performed for the two transformer capacitance data sets as calculated from the FAT and the SAT reports.

A. Frequency Scan

The frequency scan of the power network, comprising the 230kV cable and the 230/13.8/13.8kV transformer, is illustrated in Figure 11.

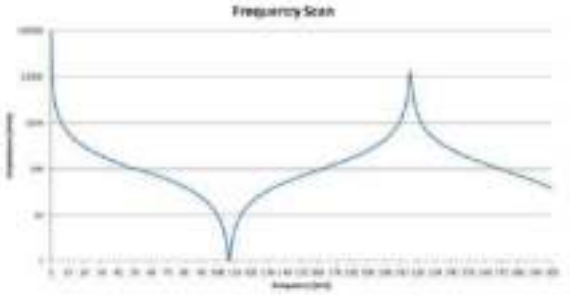

Fig. 11 Recorded Waveform

The scan identifies a series resonance point at 106.86 kHz and a parallel resonance point at 215.22kHz. The series resonance point is associated with very low impedance, so if excited by a voltage source at the resonant frequency would result in a high current flow. While a parallel resonance point is associated with high impedance, so if excited by a current source at the resonant frequency would result in a high voltage escalation

B. Analysis Based on FAT Tests

Utilizing the FAT distributed capacitance measurements and switching over a cycle in 2msec steps, while accounting for the pre-strike behavior and a single-pole closing delay of 1.2msec as recorded at the site, the simulation yields the below results.

Fig. 12 Secondary side ph-ph and ph-grd voltage surge (kV peak – FAT)

The front time of the voltage surge is 3μsec, and the time to half is 6msec. The oscillation frequency is approximately 125kHz, close to the resonance point of 106.86 kHz.

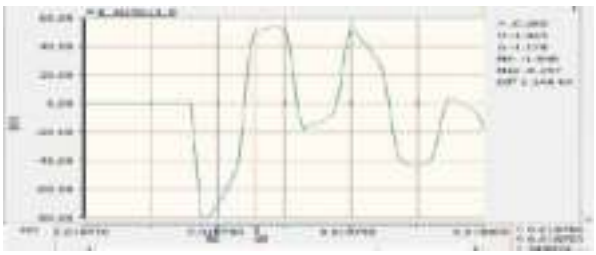

Fig. 13 Electrostatic discharge waveform (3/6μsec)

The calculated maximum phase to ground voltage surge amplitude is 130.6kV, which violates the transformer LV winding BIL level of 110kV and the MV Breaker BIL level of 95kV. The maximum phase to phase surge amplitude is 136.8kV, indicating a minimum clearance on air of 228mm as per IEEE Std. 1410.

C. Analysis Based on SAT Tests

Repeating the previous analysis, utilizing the capacitance values as measured in SAT tests, the study yields the below results.

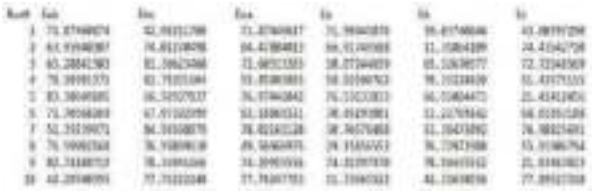

Fig. 14 Secondary side ph-ph and ph-grd voltage surge (kV peak – SAT)

In this case, the transformer LV winding and 13.2kV breaker BIL levels are not violated. The worst-case phase to phase overvoltage is 84.4kV between phase B and C, indicating a minimum required phase to phase clearance on air of 140mm.

The front time of the voltage surge waveform is 3 μsec while the time half 5μsec. The oscillation frequency is approximately 125kHz, close to the resonance point of 106.86 kHz.

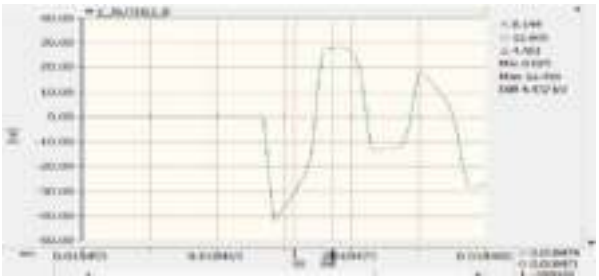

Fig. 15 Electrostatic discharge waveform (3/5μsec)

D. Transferred Surge to the Secondary Side

The 230kV/13.8kV transformers are equipped with 230kV Surge Arresters at the primary side, protecting the primary windings from receiving surges. Those chopped receiving voltage waves propagate to the transformer secondary side through the electrostatic coupling between the windings.

Based on [5] the initial voltage spike can be calculated from the following expressions:

$$V_{ls} = S*p*V_{pl} \quad (1)$$

$$S = C_{hl} / (C_{hl} + C_{lg} + C_{ext}) \quad (2)$$

Where:

V_{ls} Surge transferred to the secondary of the transformer

S Factor depending upon the transformer winding capacitance of low voltage side connections

p Factor, which allows superimposition of incoming surge voltage over power frequency voltage. P=1.05 for wye-wye and delta-delta connected transformers and p=1.15 for delta-wye connected transformers.

V_{pl} Primary surge protective level of the surge arresters

C_{hl} The distributed capacitance between the high and the low voltage winding

C_{lg} The distributed capacitance of the low-voltage winding

C_{ext} Secondary side external capacitance, i.e., cables connected to the transformer

The installed surge arrester at the 230kV side has a lightning impulse residual voltage crest of 457kV peak for a discharge current of 20kA. Compared to the transformer HV winding BIL level of 900kV, it is safe to conclude that the primary side has adequate protection against incoming surges. As the transformer's connection to the upstream GIS is through underground cables, the basis of our assessment is the switching residual voltage for 2kA of 383kV peak.

Utilizing the SAT transformer capacitance measurements from table 1, we can calculate the S factor from (2) to 0.25. Using a p factor equal to 1.05, the transferred surge to the secondary side can be estimated to 102kV, which is well within the LV BIL level of 110kV.

Similarly, utilizing the FAT measurements from table 1, the resulted transferred surge is calculated to 167.5kV, whereas for the theoretical values, the result is 227kV.

TABLE II
OUTDOOR SURGE ARRESTER RATINGS

Arrester Rating	192kV rms
MCOV	152kV rms
Ten second TOV capability	210kV rms
One second TOV capability	223kV rms
FOW Residual Voltage at 20kA (0.5sec)	486kV peak
Lightning Impulse Residual Voltage	457kV peak
Switching residual Voltage at 2kA	283kV peak

The table below summarizes the available measurements and highlights the requirement for installing a surge arrester on the MV side.

TABLE III
TRANSFERRED SURGE

Basis of Capacitance	Transferred Surge (kV)	Surge Arrester	LV BIL (kV)
FAT	167.5	YES	110
SAT	102	NO	110
Theoretical	227	YES	110

E. Oil Degradation Effects on Capacitance

It is well proven from the literature [8] that the polarization index of the degraded transformer oil is higher than the pure one. The dielectric constant and the transformer capacitance are governed from the following expressions:

$$\varepsilon_r = (P / \varepsilon_0 * E) + 1 \quad (3)$$

$$C = \varepsilon_0 * \varepsilon_r * ((\int E * ds) / V) \quad (4)$$

From (3) and (4), we can conclude that a transformer with degraded oil manifests higher capacitances, resulting in higher discharge surges to the secondary side during energization.

IV. CONCLUSION

Based on EMTP analysis results and the device data provided during the related fault investigation, our analysis identified a high probability of flashover due to reduced air to air clearance between the 13.2kV breaker live parts at the heat sink area of approximately 86mm.

The study indicated that during the transformer energization and under specific switching conditions, the feeder demonstrates an operation very close to its series resonance point of 106.86kHz. The resulting surge can lead to a BIL violation for both transformer LV winding and MV breaker based on FAT capacitance measurements. The addition of the 230kV interconnecting cable to revert the power supply from the old AIS switchgear to the newly constructed GIS substation altered the frequency footprint of the network. The installation of surge arresters at the LV side can mitigate the disastrous effects of the discharged surge.

The transformer oil degradation is causing an increase in capacitance. This behavior can potentially shift the resonant point close to the electrostatic discharge oscillation frequency and increase the severity of the surge.

V. NOMENCLATURE

SAT	Site acceptance Tests
FAT	Factory Acceptance tests
GIS	Gas Insulated Switchgear
AIS	Air Insulated Switchgear
EMTP	Electromagnetic Transient Analysis Program
DFR	Disturbance Fault Recorder

VI. REFERENCES

[1] IEEE Std. 1410, IEEE Guide for Improving the Lightning Performance of Electric Power

[2] IEEE Std. 1313, IEEE Guide for the Application of Insulation Coordination

[3] Allan Greenwood, Electrical Transients in Power Systems, Second Edition, John Wiley & Sons, 1991.

[4] Modeling and Analysis of System Transient Using Digital Programs IEEE PES Special Publication, Working Group 15.08.09, A.J.F Keri, et al. 99TP133-0, 1998.

[5] IEEE Database, Surges Transferred Through Transformers, J.C. Das, Sr MIEE, PE.

[6] Applications of PSCAD EMTDC.

[7] IEEE Transactions on Power Delivery, Vol. 10, No. 1, January 1995, Overvoltages in Power Transformers caused by no-load switching, Gerardus Chr. Paap, Abraham A. Alkema, Lou van der Sluis.

[8] Effect of Insulating Oil Degradation on power Transformer Capacitance, 2012 7th International Conference on Electrical and Computer Engineering, 20-22 December 2012, Dhaka, Bangladesh, Salman Habib, Q. Ahsan.

[9] IEEE Transactions on Power Delivery, Vol. 10, No.1, January 1995, Overvoltages in Power Transformers Caused by No-Load Switching.

VII. VITA

Georgios Fotiou, the corresponding author, graduated from the Democritus University of Thrace in 1999 with an MSc degree. He has more than 20 years of experience in substation automation and control, advanced system studies, conceptual and detail design. He worked as a senior engineer in ABB SA for eight years and a lead engineer in JP AVAX for six years. He has been a protection and systems studies engineer for Aramco Oil Company since 2012.
George.fotiou@aramco.com

Omar K Arfaj, Omar Alarfaj, P.E. (IEEE S '15, M' 18) is an Electrical Engineer with Saudi Aramco in the Consulting Services Department. He received the B.Sc degree in electrical engineering from the King Fahd University of Petroleum and Minerals, Dhahran, Saudi Arabia, in 2008, and the M.A.Sc. and the Ph.D. degrees in electrical and computer engineering from the University of Waterloo, Waterloo, ON, Canada, in 2014 and 2018, respectively. After graduation with a B.Sc degree in 2008, he joined Saudi Aramco as an electrical maintenance engineer serving the company's facilities in Ras Tanura area under Power Operations Department and Ras Tanura Refinery Engineering Department. After completing his graduate studies, he joined Saudi Aramco's Consulting Services Department as an Electrical Engineer providing technical support and consultancy to various Aramco oil and gas plant operations. He is a licensed Professional Engineer in Saudi Arabia.
Omar.arfaj@aramco.com

Hussain M Suwaidan, Hussain Suwaidan graduated from King Fahd University of Petroleum and minerals (KFUPM) in 2008, and MSs from Colorado schools of mines, USA, in 2015. He has 13 years of experience with Saudi Aramco as a specialist for switchgears and transformers. He has experience in the design, manufacturing, testing, and operation of HV, MV, LV switchgears, and power transformers.
Hussain.suwaidan@aramco.com

RISK MANAGEMENT OF ELECTRIC VEHICLE CHARGING ON FUEL FORECOURTS AND ENCLOSED CAR PARKS

Paper No. PCIC Europe EUR22_04

Jeff McQueen
bp
London. United Kingdom

Abstract – As the rapid adoption of electric vehicles (EV) across the globe increases, so does the need to charge these vehicles. Charging locations now include fuel forecourts and enclosed car parks, e.g., basements and multistorey car parks. Risks associated with a battery fire during charging have been poorly understood by the industry.
This paper will use the familiar industry bow tie analysis model for risk management as a framework to represent the preventative and mitigation barriers to manage the risk events. Relevant detail will be shared on each barrier.
The result will be a globally applicable process and tool to identify, manage and communicate risks related to electric vehicle charging in challenging locations.

Index Terms — Electric vehicle charging, risks, EV fires, lithium-ion, bow tie model, forecourts, enclosed car parks, safety, barriers.

I. INTRODUCTION

Factors to consider when charging an EV include location (open air, forecourts and enclosed areas) and charging speed. Open-air locations pose a lower risk in the event of an EV fire and will not be specifically referenced in this paper.

Fuel forecourts are increasingly being used as high power/ultra-fast charging locations as charging speeds aim to replicate the current hydrocarbon re-fuelling duration. (Charging power ranges from home charging: 7-20kW; destination: 50-70kW; fast: 100-200kW; ultra-fast >200kW. Hydrocarbon refuelling rates: ca. 300kWh/min)

With land being a key factor in identifying suitable charging locations, building basements and multistorey car parks appear attractive opportunities.

Both enclosed areas and forecourt locations present safety risks should a lithium-ion EV battery ignite. EV batteries are notoriously difficult to extinguish and can continue burning for days[1]. This differentiates risks between fires of internal combustion engine (ICE) vehicles and EVs.

Lithium-ion batteries fail due to mechanical, electrical and thermal abuse which may lead to cell thermal runaway and once ignited, may burn uncontrolled, producing intense local heat, noxious gasses and toxic contaminants.

For home charging cases, the density of charging EVs is less (1 or 2 EVs at any one location), and the charging rate is usually lower. The consequences are less (although dire for the homeowner), so whilst still carrying a safety risk, this scenario will not be considered specifically. Parallels do exist, and the risk mitigation proposed within this paper could be used.

The reader will be introduced to the bow tie analysis for risk management. This will serve as the framework to represent the preventative and mitigation barriers to manage the risk event(s). Pragmatic recommendations will be discussed for industry to develop, implement and verify the health of each barrier.

II. RISK AND THE BOW TIE MODEL

A. Risk

Risk is the product of consequence and impact. While a **hazard**, is something that can cause harm or result in a negative situation, a **risk** is the chance (likelihood, or probability - high or low), that any **hazard** will cause a negative outcome (risk event) and the consequences of that negative event. Identifying and mitigating the hazards in EV charging installations can be represented on a bow tie diagram.[2] See figure 1.

B. Barrier bow tie Model

Following the catastrophic Piper Alpha platform event in 1988, the Cullen report [16] concluded that there was insufficient understanding of hazards and their accompanying risks. Originally developed by Imperial Chemistry Industry (ICI) and further standardised and adopted by the Petrochemical industry, the bow tie model has gained support in industry as a visual tool, useful to assure that appropriate risk controls are implemented consistently.

The bow tie (figure 1) examines chains of events, or accident scenarios and then identifies control measures to prevent these events. The left-hand side of the bow tie uses a typical fault tree methodology (Boolean AND/OR gate) to model causal relationships between events, while the right-hand side utilises an event tree thinking. Using the Swiss Cheese model (James Reason ca. 1990's), the bow tie identifies control measures, known as barriers.

C. Barriers

Barriers are independent, mutually exclusive and able to prevent an event from occurring or escalating. Preventative barriers sit on the left-hand side and represent those control measures in place to prevent the cause from producing the risk event. Mitigation barriers are right hand side controls that prevent the risk event from escalating to the anticipated consequences. [2]

The Swiss Cheese metaphor considers that barriers are never 100% effective. At some stage, the deficiencies (holes in the cheese) in all the barriers along a causal path may fail (line up), resulting in the risk event from occurring (LHS Preventative barriers), or the risk event escalating to the Consequences (RHS, Mitigation barriers)

Unlike risk management techniques such as Fault Tree, layers of protection analysis (LOPA) or Risk graph, the bow tie method does not consider likelihood or frequency but rather if the controls are available, healthy and effective.

Figure 1 Bow tie risk assessment model

D. Determining if barriers are healthy.

Determining barrier effectiveness is a key factor when considering risk management. An ineffective barrier will not prevent the risk event from happening. Key questions to consider regarding barriers and risk are:

- What is the risk?
- What are the barriers?
- Who owns them?
- Do they work?
- How do you know?

Representing barrier health on a bow tie is a very useful visual tool for communicating a complex message to a wide audience.

III. EV CHARGING HAZARDS

Hazards involved in charging EV's include the use of electrical energy. When not controlled, this energy can become an ignition source or result in electrocution.

Hydrocarbon re-fuelling activities on forecourts create hazardous areas within which the use of non-rated electrical equipment is restricted.

The stored electrical energy within lithium-ion batteries is a hazard if the battery or control/safety system fails.

IV. EV CHARGING RISKS

The frequency of EV charging incidents is relatively low although the number of incidents may be increasing as rapid EV adoption occurs. Low likelihood, high consequence events do occur and as a responsible charge point operator (CPO), these need to be addressed.

The main two risk events related to EV charging are electrocution of personnel and fire from a failed lithium-ion battery.

A. Electrocution

Working on or near electrical equipment can pose a risk of electrocution. EV charger outputs range from 7kW home chargers to megawatt charging (trucks, busses). At these power levels, sites may require high voltage installations, transformers, low voltage switchgear and concomitant supporting infrastructure.

Installation, maintenance and operation activities can expose personnel to electrocution risks if these are not addressed appropriately.

Being mostly industrial standard equipment, the preventative and mitigation barriers around this equipment are well understood. Nevertheless, as the EV charging business escalates, so parties less well versed with applying the applicable safety standards are active and hence, electrocution risks remain a key contributor to overall site risks.

B. Fire

EVs are currently powered by Lithium-ion batteries. They are also used as energy storage systems in battery buffered high power charge points. Failures within cells can quickly lead to fire and explosion of adjacent cells. Uncontrolled thermal runaway follows.

Increasing reports of EV battery and Energy Storage System fires have led to vehicle and property destruction, injuries, and major EV recalls in the US, Europe, and Asia, e.g. Hyundai's recall of its Kona EV's earlier this year. In the Battery Energy Storage System (BESS) segment there have been 38 large BESS fires since 2018 and in July 2021 Tesla's 450 MWh Megapack project in Victoria, Australia caught fire, requiring 7 days and 150 firefighters to extinguish. 23 BESS fires in South Korea (2017 to 2019), resulting in losses valued at $32 million. A 2019 grid-scale battery storage system fire in Arizona caused extensive injuries and damage. High profile BESS fire incidents have affected insurers' risk tolerance. [3,4,5]

When discussing battery fires, it is useful to appreciate how EV batteries are constructed and their failure mechanisms.

1) Li-ion battery construction

An EV battery consists of multiple smaller cells that are constructed with an anode and cathode separated by a porous electronically insulating separator. (See Figure 2)

During discharge, lithium leaves the anode as lithium-ion (Li+) and an electron (e-). The Li+ flows through the ion conducting electrolyte and separator to the cathode. [1]

As the separator is electronically insulated, the electron must flow via an external circuit where useful work is done.

During re-charge, the Li+ ions and electrons on the anode recombine on the cathode to form lithium on the cathode electrode.

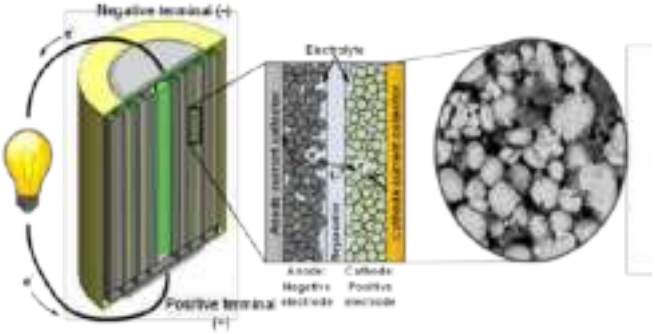

Figure 2. Li-ion battery construction and operation

The heavy EV batteries are usually located in the lower, central section of an EV within an enclosed casing of robust construction. Access is restricted and any firefighting opportunities are particularly challenging (figure 3).

Figure 3. Typical location and construction of EV battery pack. Batteries contained in the chassis base. *(Credit Autocar.co.uk)*

2) Li-ion battery failure modes – manufacturing defect

Contaminants in raw materials, damages during construction and the high number of cell components within a battery result in challenges in the defect detection during manufacturing. These defects are seldom identified during quality control, testing or operation. [17]

3) Li-ion battery failure modes – degradation [1,6]

Li-ion batteries can degrade over time or fail rapidly.

Degradation can be caused by high or low temperature, high current/loading, high or low voltage/state of charge per cell, number of cycles, chemical or mechanical stress.

The degradation mechanism includes growth or decomposition of the solid electrolyte interphase layer, lithium plating or dendrite formation piercing through the separator, and general failure of the battery component parts.

This leads to the loss of lithium inventory, active anode material or active cathode material and results in a capacity loss or power fade.

While degradation is usually a time related occurrence, accidents to EV or BESS batteries can result in a rapid deterioration, due to failure of the battery monitoring management system (control system).

4) Li-ion battery failure modes – rapid failure/accidents

Accidents related to lithium-ion battery failures can be caused by:

Mechanical abuse – deformation or separator tearing (e.g. crash, shock, crush or penetration).

Electrical abuse – internal short circuit, lithium dendrite growth leading to the piercing of the separator (e.g. internal short circuit, over discharge, over charge).

Thermal abuse – high temperature leading to a collapse of the separator (e.g. overheating).

All the above can result in an internal battery short circuit leading to thermal runaway.

This failure may occur in a single cell, but as these are closely packed within the EV or BESS, thermal runaway can quickly lead to flames, explosion, oxygen release, high temperature and a myriad of noxious gasses (hydrogen fluoride (HF), phosphorus pentafluoride (PF_5), hydrogen cyanide (HCN) and carbon monoxide (CO)) being released. Studies into the failure mechanisms of many battery types included the gaseous emissions and toxicity [1, 7, 8]

5) Identifying failures in Li-ion batteries

Li-ion battery failures are time dependent, however failure can occur rapidly after damage or abuse.

Consider the following failure detection options:

- Electrolyte vapour detection: The event in which the cell case vents due to a rise in internal pressure of the cell is termed off gas. (NFPA 855/UL 9540A). [6, 7] This unique event is useful to determine incipient faults within the battery construction. At the early stages of failure, lower explosion limit sensors or voltage, temperature and current measurement variations are not easily detected, as the characterises have not changed much. However, the electrochemical reaction inside the battery creates a noticeable amount of gas at this early stage. Some commercially available detectors use gas sensors to monitor and detect off gassing events a few seconds after failure occurs and long before battery measurements are effective. Early detection coupled with a correctly designed shutdown system is an effective safety barrier. Note, this method cannot predict the state of the battery.
- Measure terminal voltage variations using battery management system. This is a widely used monitoring method with redundancy and comparative measurements assumed to be providing integrity, but due to the complexity of programmable systems and a lack of segregation between control and protective safety systems this assumption may not result in the required integrity and is difficult to validate. This method is not very fast at identifying early stages of thermal runaway.
- Monitor the battery temperature using embedded fibre Bragg grating optical temperature sensors or electrochemical impedance spectroscopy measurements. This method provides an accurate temperature measurement but adds cost and complexity to battery packaging.
- Measure current variations (short circuits). The BMS can be configured to measure current flow. Any abnormal rate of current flow or load-requested level can trigger an alarm indicating a potential short circuit. Usually irreversible failure has occurred at this stage.
- Measure mechanical deformation or delamination of electrode coatings. Other than visual or x-rays, no commercially viable passive method is employed.

6) Li-ion battery fire management.

Internal short circuits consequences can be discussed in 3 levels as summarised in Table 1.

TABLE 1
BATTERY FAILURE CHARACTERISTICS.

Level	Cell voltage	Cell temperature	Identification and consequences
Level 1	At cell voltage, but slow decrease	Slow increase, self-discharge, no/low obvious heat	Off gas detection Electrical approach, BMS identification. Self-extinguish behaviour.
Level 2	Fast decrease	Rapid increase, Joule heating	Electrical-thermal coupled approach. Consequences depends on heat dissipation.
Level 3	No voltage	Thermal runaway. Joule + chemical reactions	Too late. Unstoppable consequence.

The temperature increases rapidly over time up to about 100°C, increases slowly further up to about 200°C after which the separator and electrolyte separating the anode and cathode fails leading to a significant rapid increase in temperature to well above 500°C. Figure 4 represents an example of different cathode materials.

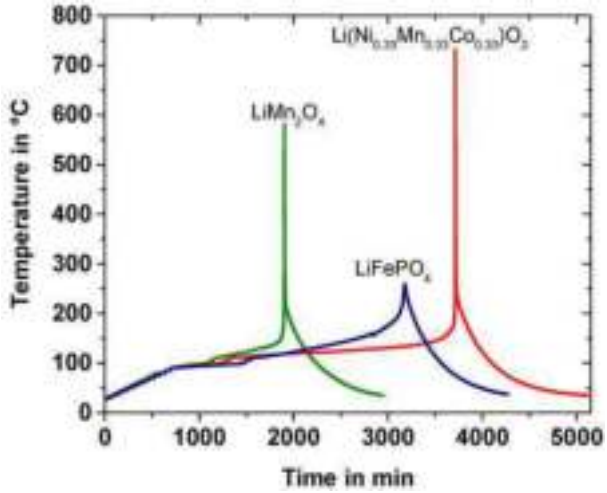

Figure 4 Typical temperature versus time of different cathode material failures [18]

As the heat from an internal cell fire and the resulting thermal runaway causes lithium to generate oxygen and react with water to form hydrogen, fire water only serves as a cooling mechanism rather than oxygen depletion. Cooling water can also act as a conduction medium between voltage containing parts of the failing battery or vehicle. As such, a Li-ion battery can burn and continue to burn for many days. This poses new and significant challenges to the fire services and affected parties and may have environmental consequences for the CPO.

Currently, the industry is generally inadequately prepared for Li-ion battery fire prevention and the resulting consequences.

7) Battery or BESS bow tie

While the bow tie concept will be discussed in the following sections, for completeness, Appendix A [13] offers a typical risk bowtie of a Lithium-ion cell failure in a typical battery of BESS system.

V. CAUSES OF EV CHARGING RISKS

While many activities can lead to an EV charging risk event happening, the causes can be combined into the following categories:

A. Working or operating on or near live electrical equipment

This includes human interaction with live electrical equipment, including batteries during installation, operating, maintenance as well as the public exposure to EVSE.

B. Operating above the safe design limits

This cause includes equipment being required to operate above design value or environment. This may be due to operator or user requirement or external factors affecting the equipment capability.

C. Failure of equipment

Whilst an obvious cause of a risk event, failure of the equipment can include all EVSE, the EV charger (EVC), cable, any component parts or the battery. It includes component parts of the equipment (e.g. insulation exposing live parts)

D. Ignition of battery or flammable fuels

The failure and subsequent ignition of a Li-ion battery will cause a risk event. Flammable fuels, e.g. a forecourt fuels spillage, will contribute to this risk event.

VI. CONSEQUENCES OF EV CHARGING RISKS

A. Injury, Electrocution or fatality

A credible consequence of a failure of the electrical equipment – be it equipment integrity, operation or any related activities, can vary from a mild electrical shock to electrocution and even a fatality. High power levels are in use by a wide range of personnel competencies.

B. Property or reputational damage and/or loss of business.

Any safety incident, or fire could result in damage to the operator's reputation or even in a closure of the site, or, if significant, the business itself. Whilst legally the Landlord or EV driver may be the responsible party, the CPO may face an unintended reputational risk.

Other minor consequences e.g. environmental impact, consequential escalation damage were considered and merged into the two mentioned above.

VII. APPLICATION OF THE BOW TIE MODEL TO EV CHARGING SITES

A. Basic bow tie model [2]

Representing the causes, risk event and consequences on a bow tie presents the model shown in Figure 5.

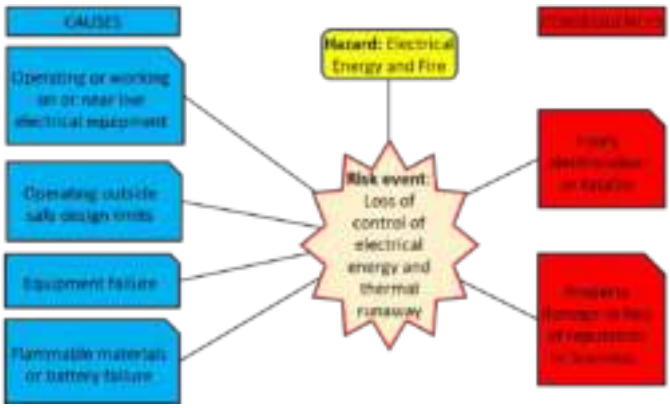

Figure 5. Bow tie model showing causes, risk events and consequences of EV charging hazards.

B. Barrier bow tie model

To prevent the risk event from happening, or to reduce the consequences of the risk event should it occur, we use barriers. Representing these on the bow tie offers the model shown in figure 6 (see Appendix B for a larger format.)

Figure 6. Barriers added to the bow tie model

C. Interpreting the bow tie model

To understand and apply the bow tie, it is useful to learn how to read the model.

A situation may have a hazard. In this case, we have combined two hazards for simplicity. These are electrical energy and fire.

Hazards result in a risk event. Loss of control of electrical energy and Fire are the highest risk events from the hazards identified.

A risk event is caused by a condition, action or threat. Combining causes results in the four listed in section V (Working on or near electrical equipment; operating above the safe design limits; failure of equipment and ignition of fuel or battery) Note, many other causes are possible. These are combined into credible causes without losing any content.

A risk event may result in a consequence. The possible consequences are electrocution or fatality, and damage to property or reputation. Essentially these are personnel and non-personnel consequences. Other minor consequences are possible but merged for clarity.

Barriers prevent or mitigate the risk event. They stop or reduce the "risk event from happening or getting worse".

Preventative barriers prevent the cause or threat causing the risk event from happening, i.e., they reduce the likelihood of the undesirable situation from happening.

Mitigation barriers minimise or limit the consequence of the risk event, after it has occurred, i.e., they stop things getting worse. They may also be labelled Recovery barriers.

Every barrier has control measures to determine the barrier health. Examples include maintenance, competence, standards, processes, tools, etc. These should not be seen as barriers in themselves, as maintenance, for example, will not prevent a faulty piece of equipment from electrocuting someone. It will however strengthen that barrier (e.g., equipment integrity) or a lack of a control measure (maintenance) will weaken a barrier. Often this is down to interpretation, but ultimately it is better to represent barriers as per their definition – independent and mutually exclusive.

Having interpreted the bow tie model, the real benefit lies in its application.

Barriers should be designed, tested, reviewed, assured or verified to determine their health or effectiveness. Barrier health can be represented as:

- In place, available and effective.
- In place, available with opportunities to improve.
- Not in place, not available, or not fully effective.
- Not tested or insufficient data available.

Representing these with various colours of choice, helps to create a graphical representation of the current risk profile of the site. If all barriers on a causal line are not in place, not available or not fully effective, then, per the Swiss Cheese model, one should expect the risk event to occur/escalate.

This simple model has been used across the globe to represent a myriad of risk events, ranging from health status, oil and gas operations, financial models, and many other scenarios. Exploiting proven tools across the wider industry benefits nascent businesses.

VIII. EV CHARGING RISKS BARRIERS

The core of this paper discusses each barrier and a list of recommendations to consider are offered to the reader.

These are based on experience and are not exhaustive. Some recommendations are based on international standards, or regulations and should be read as requirements, whilst others are recognised and generally accepted as good engineering practices.

A. Preventative barriers [9,10,11, 15]

1) Equipment Integrity.

a) Site feasibility and design:

Equipment integrity considerations should start at the initial site feasibility and appraisal stage.

Consider the location of equipment with respect to existing hazardous areas, fire risk (e.g., enclosed parking areas) and fire mitigation/extinguishment. [5]

A site check list which includes access, traffic flow, hazardous area considerations, electrical supply options and requirements, fire risk and mitigations, customer requirements, etc is useful.

Consider equipment size, weight (enclosed car parks may have a point load restriction (N/m^2)), access to maintain or operate.

Early-stage considerations can affect the type of equipment which in turn may affect its integrity.

b) Design of EVSE:

Apply international and local equipment standards which cover both AC and DC EVSE, battery energy storage, the plugs, sockets, cable connectors, vehicle inlets, and all associated supply equipment. (e.g., high voltage grid connection, HV/LV switchgear, transformer and associated equipment) and functional safety of control, protection and mitigation systems implemented using electrical/ electronic/ programmable electronic systems.

For forecourt designs, ensure designers are experienced in hazardous areas management and incorporate these into the design of the equipment and site.

For EVC cable management, consider cable abrasion, vehicle drive-over, DC insulation protection, electromagnetic compatibility risks, screened/shielded cables, cable management systems and return-to-holder management via human machine interface (HMI) or mobile application. Consider cable length with respect to vehicle parking practices, personal injuries (slips and trips) and access for disabled persons.

Inspection and maintenance activities include safety functions testing, diagnostics, electrical protection, cyber security and the management of ventilation of the EVC and EVSE. Consider dust, pollution, the local environment and the Original Equipment Manufacturer's recommendations and frequencies when creating an inspection and maintenance plan.

Consider the use of interconnected devices that perform functions with a high level of autonomy (smart devices) that can provide remote monitoring and control functionality. This can monitor equipment health status, condition monitoring and to receive and manage any alarms, trips and other

communications. This is particularly useful when the CPO has many EV charging sites across a wide geography, Consider the increasing cyber security risks ranging from every payment to the whole CPO back-office operation.

Use physically separate, diverse and possibly redundant systems for control, protection and mitigation systems to reduce the likelihood of common failure.

EVC display screens can be configured to view and manage the equipment integrity. These include EVC diagnostics, charging statistics and battery integrity. Most algorithms include a cable and connection self-test prior to energisation, thereby managing the cable and connector integrity, charge stop or alerts to the operator can be configured within the HMI.

Consider EVC algorithms or handshake protocol logic that inhibit known EVs with poor batteries from being charged. ISO 15118 [12] supports vehicle to grid charging and in particular plug and charge – which addresses secure communication between EVs and EVCs, EVSE and the Utility grid.

Consider the source of manufacturing integrity of BESS batteries.

c) Off gas detection [6, 7, 8]

Consider gas detectors aimed to identify any incipient off-gas emissions from a failing battery. These may prove very useful as some manufactured products identify gaseous emissions many seconds before any significant voltage or thermal activity can be measured.

2) Earthing/ grounding and bonding

As pressurised systems in industrial plant use relief valves to mitigate overpressure situations, the electrical equivalent is a robust earthing system that sinks fault current into the mass of the earth. Ensuring that this barrier is effective is vital to prevent a causal path developing into a risk event.

Consider the type of earthing system to implement. Most countries require EV chargers to be TT earthed. (Terra- terra - direct earth connection). In the UK, the neutral and protective conductor may be combined after the HV/LV transformer secondary winding, resulting in a TN-C (Terra Neutral Combined system). A separated system (TN-S) is required for EV charging.

When high voltage equipment is required, consider the earth/ground potential rise (EPR) or (GPR). This occurs when a large current (e.g., fault current) flows to earth through an earth grid impedance. The potential is the highest at the point where current enters the ground and declines with distance from the source. The EPR around a substation may cause the voltage over distance (potential gradient) to be dangerously high between a person's two feet or between the ground on which the person is standing and a metal object. Any conducting object connected to the substation earth ground, such as re-fuelling equipment, rails, fences, or metallic piping, may also be energized at the ground potential of the substation. This transferred potential is a hazard to people and equipment outside the substation area.

Soil resistivity, underground metal objects and the distance between high and low voltage substations affect EPR. This may result in the HV and LV substations being up to 20 m apart. Many forecourts do not have this available space, resulting in the site being unsuitable for EV charging. Specialist software exists to calculate EPR and provides a complete earthing study (e.g., Current Distribution, Electromagnetic fields, Grounding and Soil Structure Analysis – CDEGS)

Lightning protection of the site should be considered for high-risk areas and included into the electrical design.

Extraneous bonding should comply with the earthing philosophy adopted.

3) Personnel and equipment electrical protection systems

A robust barrier of personnel and equipment protection is necessary to prevent uncontrolled electrical energy from harming people or equipment. Basic electrical protection against shock and faults provides automatic disconnection or separation of the supply.

Grading and protection studies are recommended to provide the correct discrimination. These should include thermal, over current and earth leakage protection. Some LV systems require restricted earth fault protection. Consider filters to mitigate harmonics generated by the connected thyristor-based load.

Consider the type of personnel protection provided in the EVC circuit. Some countries require a residual current device (RCD) to be part of the supply circuit. Any DC leakage current over 6mAdc is not identified by a normal AC type A RCD. A type B (or F) RCD is required. These are orders of magnitude more expensive, and some designers or equipment providers may not install them. Much debate has ensured over this barrier.

Consider the requirements of galvanic isolation between the AC and DC circuits in EVC designs.

Consider DC protection to include DC insulation monitoring of the charging cable. This is the main electrical interface experienced by the public. Any DC contactors should be suitably rated as interrupting DC is physically more difficult that AC as the voltage does not pass through a zero point.

Some fuel forecourts require that the site emergency shutdown isolates all EVSEs. Consider how this may affect payment transactions, storing of the last measured values and any similar connectivity when hardwired into site ESD system.

Consider the use of fibre optic cable to connect circuits from different supplies together (e.g. a signal from the site LV supply to isolate the separately supplied EVSE).

Whilst not electrical protection as such, physical barriers like posts or bollards prevent vehicles colliding with EVSE, reducing any electrocution risk potential.

Administrative controls are viewed as lower down in the hierarchy of control table. However, these remain independent and mutually exclusive barriers. The following barriers support these control measures.

4) Isolation, intervention and reinstatement.

Consider a suitable control of work process to manage the safe interaction of personnel with electrical equipment or other such work on an EV charging site. This may include a permit to work system, lock out tag out process or safe authorisation of personnel procedure.

Consider if the type of equipment to be designed and procured will meet these systems. Suitable locking arrangements are recommended.

5) Electrical Safety rules

Consider employing suitable electrical safety rules which are clear, communicated, used and verified.

It is recommended that these rules clearly define requirements, competence and authorisation for working on or near live equipment, isolation and provide a duty of care.

6) Restricted access

Physical separation is one of the best means to prevent electrocution risks.

Consider adequate separation of the public from any live EVSE.

Consider locks or special tools to secure doors and panels. Consider separate locks for LV and HV equipment access. This assists in managing access for different authorisation levels of competent personnel.

Consider adequate signage to address live equipment dangers, no unauthorised access, or warnings of separate sources of supply.

To ensure adequate supervision at forecourts, consider charging only when the forecourt is supervised.

7) Location

EVSE should be located outside of any hydrocarbon gaseous hazardous area zones. These include the sealed forecourt apron, dispensers, tanker offloading, fill, drain and vent points or emergency exit routes.

Consider all ventilation systems to prevent possible hydrocarbon vapour entry. This includes sealing of any ducts or conduits that may interconnect a hazardous zone to a safe zone.

Storing BESS away from the public provides separation in the event of a fire.

Consider the proximity of the EVC site to other combustibles or hazards given that an EV battery may be left to burn until it self-extinguishes.

B. Mitigation barriers

Mitigation barriers are required after the risk event has occurred. Their primary purpose is to reduce the severity of the risk event to escalate to the determined consequences.

1) Secondary protection systems after an incident.

For an electrical incident to occur, the local circuit has not operated effectively, and the fault has escalated. Upstream circuitry is now required to clear the fault. Adequate protection and earthing/grounding systems are necessary to absorb the increased fault current post an incident.

Consider a high integrity earthing and grounding system of upstream circuits and protection systems.

It is recommended to grade the electrical protection system with the upstream circuit included. The integrity of this discrimination will determine the effectiveness of this barrier.

2) Ignition prevention

As both risk events can include sources of ignition, if these occur on a fuel forecourt during a fuel spillage, the risk event could escalate.

Consider means to remove ignition sources. These can include isolation of EVSE. Usually, the main emergency stop within the forecourt shop/office is linked to the relevant isolation points of the EVSE. Any battery buffered EVCs or BESS isolation will require special considerations.

Consider other flammables within the vicinity that can support escalation from the risk event.

Gas detection, as with the preventative barrier, can identify emissions leading to the escalation of heat leading to thermal runaway.

3) Emergency response.

Two types of emergency response fall within this barrier – personnel and fire related.

Consider how emergency response for an electrocution would be performed. Consider adequate signage, training, equipment, means of notification, and space around the equipment.

It is recommended that every site has a bespoke emergency response plan. This should include access and egress of people, emergency services (particularly challenging for enclosed car parks), fire mitigation measures, (sprinklers, fire doors, suppression systems) and alarm and response systems to reduce possible escalation.

Consider the extended duration of a Li-ion battery fire. In some cases, these can last for days. The heat and explosive nature of failing cells can rapidly escalate to adjacent vehicles.

Consider the consequences of excessive fire water which could be contaminated with hydrofluoric acid and other pollutants. This may affect water courses; the weight bearing loading in basements or present a flooding risk.

IX. EV CHARGING RISKS BARRIERS IN ENCLOSED AREAS

Special considerations are required when charging EV's in basements or enclosed car parks.

In the event of a fire or incident, the level of mental alertness affects one's ability and speed of evacuation from a building.

Building regulations consider residential accommodation (in particular hotels) and shops/commercial properties. higher risk category than commercial premises due to high occupancy densities, more potential for disorientating layouts, unfamiliar occupants and increased potential for rapid fire development. Commercial properties historically have a lower life risk, with buildings often involving large volumes and effective smoke control with occupants generally more alert. [14]

Assembly/recreational, may sit between these two. Life risk in offices is understood to be low where occupants are generally familiar with the premises and fire loads are consistent and appropriately managed.

A. Risks

A different probability of disorderly evacuation applies when calculating the risk for different building types.

The CPO has no control over the EV or EV battery condition. The CPO does have control over any owned BESS.

A car fire in a parking bay is already a known risk. An ICE fire has the same heat release rate as an EV (although EV battery may burn longer and create more focused heat, similar to a jet or plastic fire)

Charging an EV presents a slightly higher risk of EV battery failure than simply parking. However the frequency of fire in a BESS as part of, or in support of EVSE is not well understood and with a much larger energy capacity, could potentially result in hazards with greater consequences.

In most cases, CPO reputational impact is perceived to be the key risk differential from introducing chargers. There could be legal repercussions if failure of the EVSE leads to injury or fatality.

B. Bow tie

Further to the general bow tie shown above for EV charging sites, a specific risk bow tie helps frame the enclosed parking barriers.

Figure 7 (see Appendix B for a larger format) shows the specific bow tie applicable to enclosed areas.

Figure 7 Enclosed area EV charging bow tie

The following apply:

1) Hazard:

Lithium-ion batteries within EV or BESS

2) Risk:

Fire. While electrocution is still a risk, in this case the focus is solely on fire.

3) Causes:

a) Failure of equipment

Include the battery, EVC, or any EVSE.

b) Operating outside equipment's safe operating limits.

Include battery failure initiators discussed above (electrical, mechanical or chemical abuse)

c) Flammable materials.

Consider the risk of other vehicles or any other combustible material that may propagate a fire.

4) Preventative Barriers

a) Equipment integrity – charging and charged.

EVCs without BESS are relatively low risk failure items as they consist mainly of electrical components. A range of detection features should be considered including temperature, electrical overload, over current and earth fault protection, DC insulation and internal faults.

EVCs incorporating BESS can be supplied with preventative systems such as BMS achieving a known level of functional safety integrity e.g. SIL2, and mitigation systems such as smoke detection, gas and temperature monitoring. The CPO has a duty to understand these risks and specify the correct type and number of barriers to control these risks. The CPO has better control over the risks of BESS.

b) Mechanical protection

Physical protection to prevent mechanical damage from an impact to equipment can include bollards, kerbs or wheel stops.

Consider encasing batteries in a robust construction. EVs usually design crash-proof casings to house the battery systems.

c) Battery management system (within vehicle)

Over charging, charging at too high a rate or charging failing/failed batteries can lead to battery integrity concerns. The BMS should be configured to detect these occurrences. As the BMS is part of the vehicle, as CPO, this is a challenging barrier to manage.

5) Mitigation barriers

Due to the uniqueness of each installation, local regulations etc. for every site should develop a specific emergency response plan that includes the barriers below.

a) Passive fire protection

A key mitigation barrier includes the thermal rating of the surrounding concrete construction. (e.g., a fire rating of 4 hours is recommended by the London Fire Brigade [10]). A suitable concrete basement ceiling can offer significant fire-withstand properties to the building above.

Consider smoke management – natural or forced ventilation – and how the latter is energised. Note the reflected heat off the ceiling and walls in an enclosed area is significantly more than in an open area.

b) Detection, alarms and isolation

Consider how fires may be detected within a battery (see Preventative barrier – Equipment integrity) and within a building.

Smoke alarms may be required within EVC's or other electrical equipment.

Consider how these alarms communicate to a place where an effective response can be made.

Consider how fire alarms are communicated to the wider affected or at-risk population.

c) Active fire protection

Consider sprinkle or suppression systems. Although unlikely to quench an EV or Li-ion battery fire, these may mitigate escalation.

Consider internal fire water mains in terms of sizing, back up, integrity and the ability to operate in the event of a battery fire.

d) Evacuation systems

All fire evacuation plans should be well signposted. These should be visible even when there is a power outage.

e) Emergency response procedures

Consider firefighting access, length of hoses from most suitable hydrant, routes and any alternative routes.

Alert the local fire brigade of the additional risk of EV charging and update any fire risk procedures.

f) Event response

Consider the effects of copious quantities of water on the building design – weight of water, flooding of lower floors, and contaminated water management.

Consider the effects of smoke damage to the building and or its neighbours and occupants.

6) Consequences

As per above, the same main consequences result when considering enclosed car parking areas.

a) Injury, Electrocution or fatality

As this scenario does not deal with electrical energy, the personnel-related consequence focusses on injury or fatality from a fire or as a result of a fire within an enclosed car park.

b) Property or reputational damage and/or loss of business.

As per the example above, any safety incident, or fire could result in damage to the operator's reputation or even in a closure of the site, or, if significant, the business itself. Escalation risks affecting any building above or adjacent to the enclosed car park can be significant.

Regardless of the legal responsibility, the CPO may face an unintended reputational risk.

These consequences should drive CPO's to seriously consider the risks of enclosed areas for EV charging or BESS storage locations.

X. GENERAL EV CHARGING RISK MITIGATIONS

A. STANDARDS

ISO 15118 – "Road Vehicles – Vehicle to grid communication interface" provides a well-designed and documented, future-proof standard addressing vehicle to EVC communications. Globally applicable, covering AC, DC, wireless and vehicle to grid (V2G) charging within a constrained utility grid capacity, this standard makes it possible to match the grid's capacity to the energy demands of a growing number of EVs

B. *Application of process safety to EVSE.*

Applying functional safety. Hazard identification (HAZID), Hazard and Operability (HAZOP) studies and risk assessment are some of the tools industries are applying to identify risks. These tools now include equipment manufacturers and thus the whole industry benefits.

C. *Off gas emission detection*

Recent developments in incipient cell failure identification equipment connected to a suitable shutdown system can greatly reduce the escalation risks of battery failures. Traditional gas detection methods have been less effective. This is seen as a significant fire management strategy that currently meets many insurance company requirements.

XI. CONCLUSION

This paper discusses the use of a bow tie model for risk assessment and applies this to EV charging sites with special focus on high-risk sites, namely fuel forecourts and enclosed locations. Preventive and mitigation barriers are discussed with key points for the reader to consider.

While many barriers are common to industry today and can be implemented effectively, the issue of lithium-ion battery integrity remains a challenge for industry. EV batteries are encased deep within the vehicle and not within the CPO's control. Detecting battery failure is difficult. Li -ion batteries fail catastrophically and currently there few effective fire management methods of early extinguishment known to CPOs.

As the number of EVs in use increase, charging locations become increasingly difficult to site. BESS is promoted where electrical infrastructure cannot support fast charging EVSE. These risks may escalate with the concomitant negative consequences.

Industry would do well to heed the advice offered and remain abreast of other risk management mitigations within this growing industry.

NOMENCLATURE

BESS	Battery energy storage systems
CPO	Charge point operator
EPR	Earth potential rise
EV	Electric vehicle
EVC	Electric vehicle charger
EVSE	Electric vehicle supply equipment
GPR	Ground potential rise
HMI	Human machine interface
ICE	Internal combustion engine vehicle
RCD	Residual current device

II. ACKNOWLEDGEMENTS

The author would like to thank Nick Davies, Gholam-Hasan Molayem, Alex Waslin and the PCIC Technical committee for their review.

XII. REFERENCES

[1] B Wu and L Bravo Diaz, "Electric Vehicle lithium-ion batteries" Imperial College London
[2] "Bow ties in Risk Management", bp standard
[3] https://liiontamer.com/south-korea-identifies-top-4-causes-that-led-to-ess-fires/
[4] Arizona battery fire's lessons can be learned by industry to prevent further incidents, DNV GL says - Energy Storage News (energy-storage. news)
[5] https://www.thefpa.co.uk/news/lithium-ion-battery-fires-cost-uk-100m-yearly
[6] https://www.dnv.com/Publications/technical-reference-for-li-ion-battery-explosion-risk-and-fire-suppression-165062
[7] J. McNamara "How to prevent thermal runaway in li-ion batteries" Xtralis Li-ionTamer
[8] Considerations for ESS Fire Safety Consolidated Edison New York, NY Report No.: OAPUS301WIKO(PP151894), Rev. 3 January 18th, 2017
[9] APEA/EI "Guidance for Design, Construction, Modification, Maintenance and Decommissioning of Filling Stations" 4th Edition
[10] "Electric vehicle supply equipment", bp standard
[11] IEC 62619, Secondary cells and batteries containing alkaline or other non-acid electrolytes – Safety requirements for secondary lithium cells and batteries, for use in industrial applications
[12] ISO 15118 "Road Vehicles – Vehicle to grid communication interface."
[13] Lithium-ion battery thermal runaway bowtie. Shell projects and Technology
[14] APEA/LFB, Jan 2017. Requirements and rationale for the acceptance of petrol filling stations located under residential, hotels or commercial property,
[15] Code of Practice for Electric Vehicle Charging Equipment Installation, 4th Edition
[16] The Public Enquiry into the Piper Alpha Disaster. Hon Lord Cullen 1990 https://www.hse.gov.uk/offshore/piper-alpha-public-inquiry-volume1.pdf
[17] Roberto Sebastiano Faranda, Kim Fumagalli, Massimiliano Bielli, Lithium-ion Batteries for Explosive Atmosphere, EUR19_32, PCIC PARIS
[18] Experimental Analysis of Thermal Runaway in 18650 Cylindrical Li-Ion Cells Using an Accelerating Rate Calorimeter

XIII. VITA

Jeff McQueen graduated from the University of Natal, Durban South Africa in 1990 with a BSc EE degree, University of South Africa with a B. Commerce in 1995 and PMI PMP in 2005. He has been working in the electrical discipline in the petrochemical industry since. He is currently an Advisor to all electrical mobility activities in bp and global development engineering manager to the EV charging business. He has authored three previous papers for PCIC and is a Fellow of the IET.

Jeffmcqueen1@gmail.com

XIV. APPENDIX

A. *APPENDIX A*

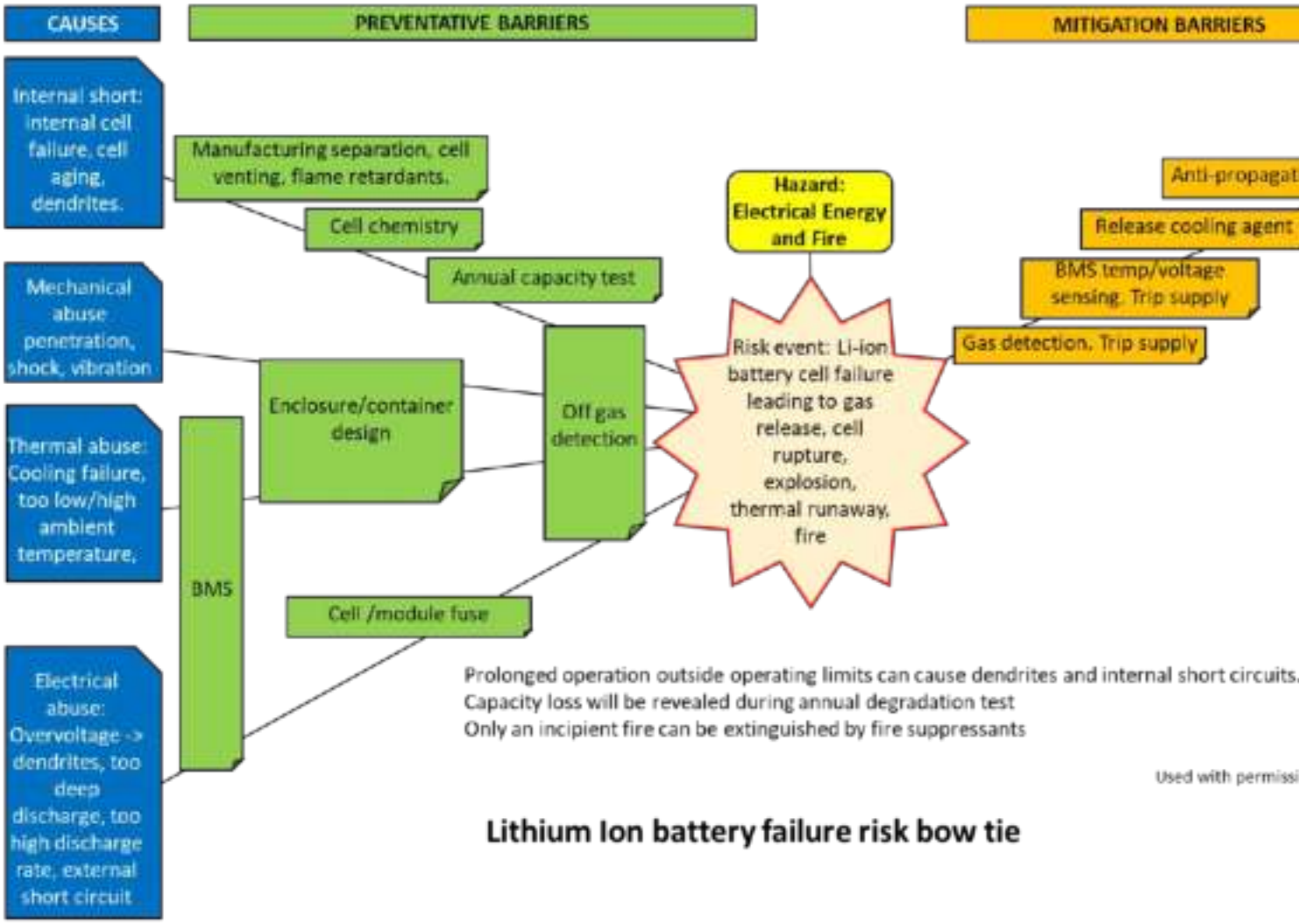

Lithium Ion battery failure risk bow tie

B. APPENDIX B

FIGURES IN DETAIL

The following figures are shown in a larger format for clarity.

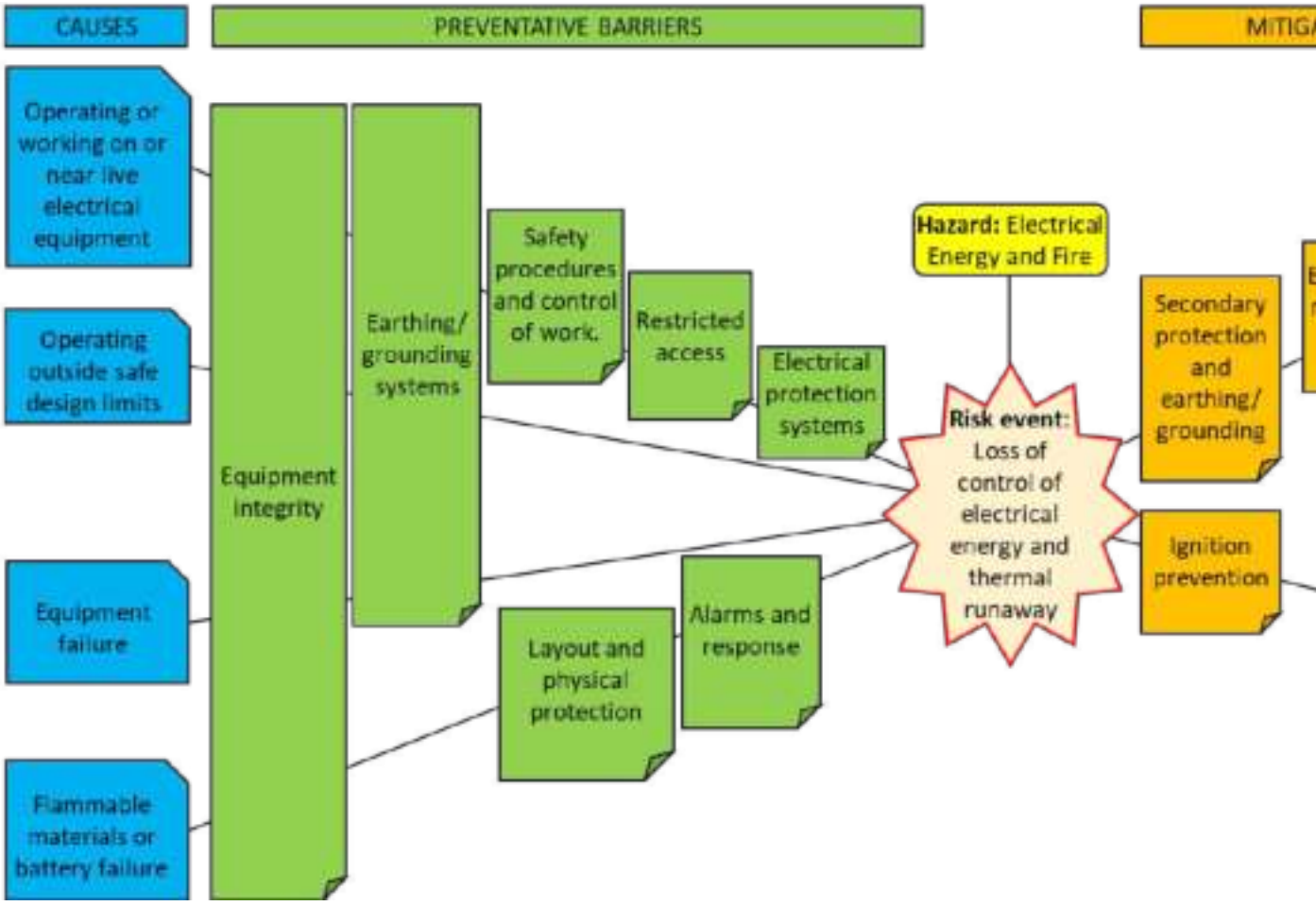

Figure 6. Barriers added to the bow tie model

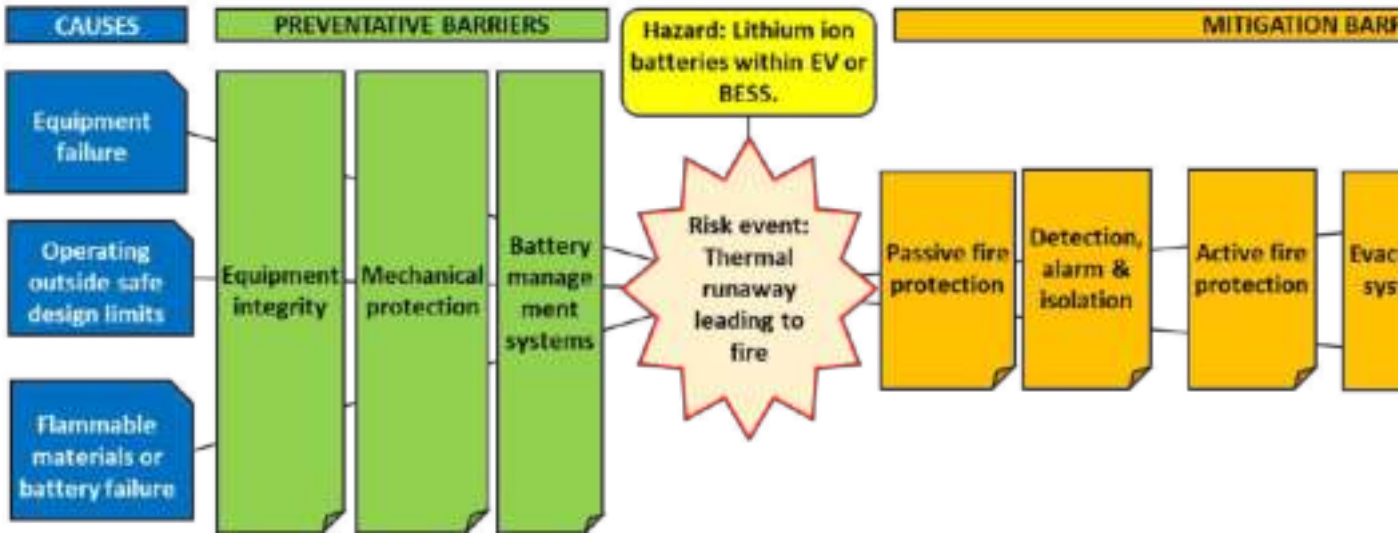

Figure 7 Enclosed area EV charging bow tie

SYMPATHETIC INRUSH STUDY CASE

Paper No. PCIC Europe EUR22_05

Georgios Fotiou
Aramco Oil Company
Dhahran
Saudi Arabia

Hussain Al-Awami. Sr IEEE
Aramco Oil Company
Dhahran
Saudi Arabia

Abstract – Sympathetic inrush is the transient current which is drawn by an already energized transformer while another transformer is being energized and connected in parallel. Depending on the severity of this phenomenon, these currents may have many adverse effects, like false triggering of protection system, electrical and mechanical stressing to equipment, and generally demotion to the network quality. The magnitude and the duration of this currents are mainly related to the involved transformers electromagnetic and mechanical characteristics, network source impedance, load conditions, breaker point of wave switching, etc. This paper shows some analysis using fast electromagnetic transient modelling on existing network to show the sympathetic inrush current effects on the voltage profile at the LV side of the paralleled transformer. It also studies some solutions to improve the voltage drop.

Index Terms — Sympathetic inrush, paralleled transformers, fast electromagnetic transient modelling, residual flux, ESP.

I. INTRODUCTION

There has been some reported severe voltage drop for an existing offshore 13.8kV distribution network during energization one of two 50MVA step down transformers (115/13.8kV) while the other one is in service. Depending on the severity of these disturbances, a number of Electrical Submersible Pumps (ESP's) were dropping out. The investigation reports for these disturbances concluded that the cause of these tripping ESP's is the under-voltage condition due to sympathetic inrush on the running transformer. The electrical system network of the system in concern is shown in Fig 1.

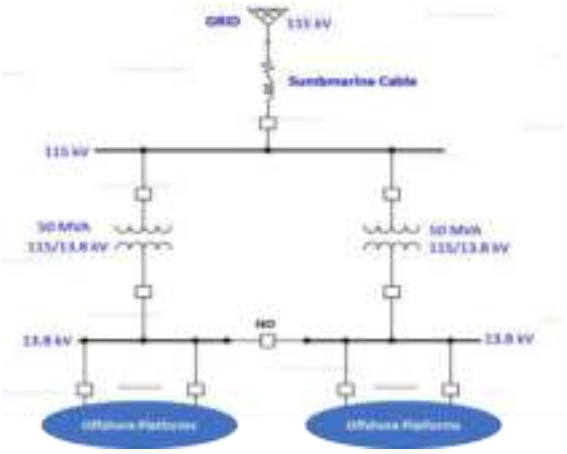

Fig 1. System network

The aim of this paper is to verify the above conclusion and asses the severity of the phenomena. It would also investigate the possibility of applying short term mitigation solutions targeting on identifying specific operating scenarios.

II. METHODOLOGY

The analysis of the electrical network model is based on fast electromagnetic transient modelling software. The network configuration, the source impedance parameters, the cable characteristics, as well as the transformer data were collected from actual power system modelling model of the system. The fast electromagnetic transient modelling model was verified by comparing the power system modelling short circuit and the load flow results. The model was tuned based on the actual loading data taken from the online measurement of the system. By doing so, a trustable model capable to reflect the actual operating conditions and the responses to the transient events was accomplished.

The sympathetic inrush study was carried considering two stages. The first stage is to identify the exact point on-wave switching that results in highest sympathetic inrush current for specific operating scenarios which are load condition, residual flux, and the source impedance. The pole discrepancy for the switching has severe impact on the transformer current inrush but it would not be considered because it was not justified with the available recording.

In the second stage, the effect of the tap changer position, transformer residual flux, and the source impedance which were kept fixed in the first stage was studied using the identified the point on-wave switching and breaker pole asymmetry identified in the first stage. This is to simulate the worst-case scenario in terms of sympathetic inrush current amplitude for any possible short time mitigation options.

With regards to the submarine cables modeling, the 115kV submarine cable was modeled using frequency dependent model. The other cables were modeled as coupled PI sections as they are short and the interest here is focused on the fundamental frequency and steady state conditions. For the loading, the total active power measured at the 13.8kV system is 15.08MW and the reactive power at the 115kV side is 14.91MVAR. Since the loads are identical, the active and reactive power consumption for each load was modeled to be 780kW and 690kVar. Furthermore, the historical HV side voltage was reported as 116.4kV while the MV side voltage was reported to be 14.0 kV.

III. ANALYSIS

A. Transformer T602 Tap at 1.0pu

For this case, the subject transformer T602 to be energized was considered to be at nominal tap or 1pu. The worst-case scenario identified is run#274 where the

voltage drop at the LV side of the transformer T601 (running transformer) dropped from 13.99kV to 13.166kV as shown in Fig 2. The inrush currents in the energized transformer as well the sympathetic inrush in the running transformer are shown in Fig 3 & Fig 4 respectively. The exact breaker switching moment and poles closing asymmetry were:

Phase A	Phase B	Phase C
1.50855 sec	1.50840 sec	1.50910 sec

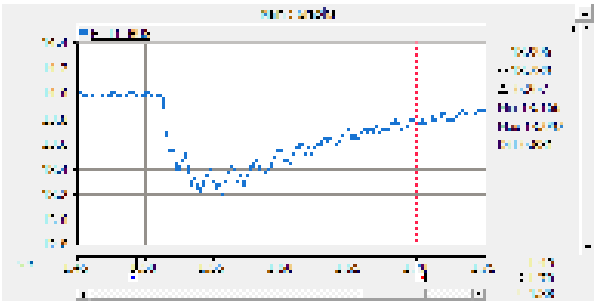

Fig 2. T601 LV side voltage for case A

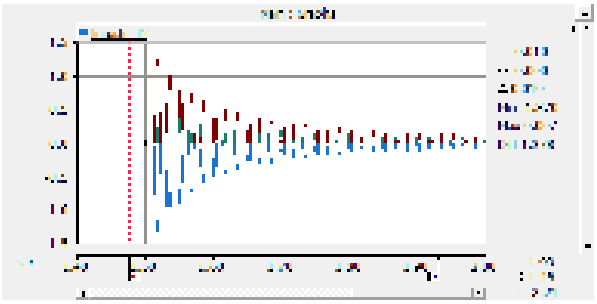

Fig 3. T602 inrush current for case A

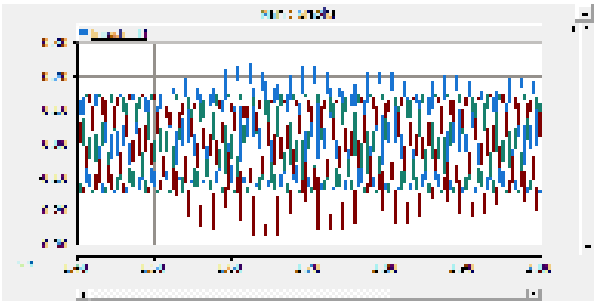

Fig 4. T602 Sympathetic Inrush current for case A

The highest voltage drop is found to be in load# 162/170 with amount of 6.96%. The voltage profile of subject load is shown in Fig 5. The maximum voltage drop in the connected loads is summarized in Table I.

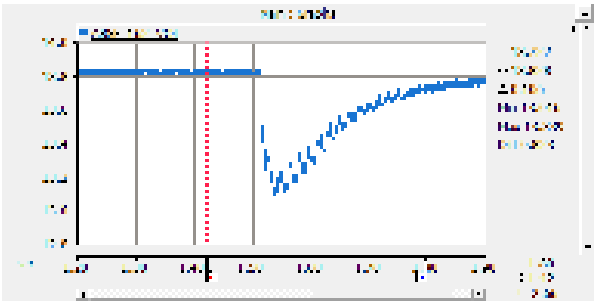

Fig 5. Load#162/170 voltage profile for case A

TABLE I
LOADS VOLTAGE DROP FOR CASE A

Load#	Dist (km)	Cable Size	Min V (kV)	ΔV%
119, 121/128	15.994	3/C 1000 AWG	13.055	6.683
100/106	3.512	3/C 4/0 AWG	13.107	6.312
36/41	6.407	3/C 350 AWG	13.088	6.447
17/22	1.908	3/C 4/0 AWG	13.124	6.190
172/180	7.765	3/C 185 mm2	13.040	6.791
23/28	10.106	3/C 350 AWG	13.046	6.748
62, 129/127	6.221	3/C 4/0 AWG	13.062	6.633
51, 57/61	2.602	3/C 4/0 AWG	13.121	6.212
48, 52/56	13.681	3/C 750 AWG	13.056	6.676
XFRT-3001	0.033	3/C 2 AWG	13.161	5.926
90/99	2.561	3/C 4/0 AWG	13.122	6.204
TP1	3.488	3/C 4/0 AWG	13.108	6.305
64/69	16.797	3/C 1000 AWG	13.050	6.719
162-170	5.427	3/C 120 mm2	13.016	6.962
70/75	8.029	3/C 350 AWG	13.070	6.576
30/35, 138/139	5.673	3/C 4/0 AWG	13.073	6.555
10/15	8.839	3/C 350 AWG	13.061	6.640
42/47, 140/141	4.948	3/C 4/0 AWG	13.084	6.476

B. Transformer T602 Tap at 1.1pu

For this case, the T602 tap changer position was set at maximum upper position which is 1.1pu. The peak of the transformer inrush current was significantly reduced when a bigger portion of the winding is energized. The effect in the sympathetic inrush is investigated. A full analysis was performed and the worst case was found in run#79 with the closing time of:

Phase A	Phase B	Phase C
1.51045 sec	1.51125 sec	1.51015 sec

The voltage at the transformer secondary dropped to 13.34kV which indicates 1.33% improvement from the previous case. The highest voltage drop is 5.733% at load# 162/170. Table II shows the voltage drop for all loads.

TABLE II
LOADS VOLTAGE DROP FOR CASE B

LOAD#	Min Vol (kV)	ΔV%
119, 121/128	13.231	5.425
100/106	13.283	5.054
36/41	13.264	5.189
17/22	13.300	4.932
172-180	13.216	5.533
23/28	13.222	5.490
62, 129/127	13.238	5.375
51, 57/61	13.297	4.954
48, 52/56	13.231	5.425
XFRT-3001	13.338	4.660
90/99	13.298	4.946
TP1	13.284	5.046
64/69	13.225	5.468
162-170	13.188	5.733
70/75	13.246	5.318
30/35, 138, 139	13.249	5.297
10/15	13.237	5.382
42/47, 140. 141	13.260	5.218

C. T602 Tap at 0.9pu

The full analysis was repeated where T602 tap position was set to the minimum regulation of 0.9pu. The loads voltage drop is shown in Table III.

TABLE III
LOADS VOLTAGE DROP FOR CASE C

LOAD#	Min Vol (kV)	ΔV%
119, 121/128	12.833	8.270
100/106	12.884	7.906
36/41	12.866	8.034
17/22	12.901	7.784
172-180	12.818	8.377
23/28	12.824	8.335
62, 129/127	12.840	8.220
51, 57/61	12.898	7.806
48, 52/56	12.834	8.263
XFRT-3001	12.939	7.513
90/99	12.899	7.798
TP1	12.885	7.898
64/69	12.828	8.306
162-170	12.790	8.578
70/75	12.847	8.170
30/35, 138, 139	12.850	8.149
10/15	12.838	8.234
42/47, 140. 141	12.862	8.063

The aim is to acquire the complete footprint of the OLTC on the sympathetic inrush currents. The worst case was found on run#34 and the highest voltage drop at load#162-170 side was found to be 8.578%. The exact breaker closing times were:

Phase A	Phase B	Phase C
1.51175 sec	1.51245 sec	1.51185 sec

D. T601 Tap at 1.0pu

The effected of involving more winding from the running transformer T601 is investigated under this scenario. This was achieved by raising the grid voltage to 1.05pu and set the tap position of T601 to 1.0pu instead of 0.96875pu used in previous analysis. `The voltage for the ESPs needs to be maintained for safe operation of these loads.

The simulation results are shown in Table IV and the transformer T601 voltage curves are shown in Fig 6 & Fig 7. The simulation outcomes show that the situation is not improving the voltage drop at the load side.

TABLE IV
LOADS VOLTAGE DROP FOR CASE D

	T601 TAP =1pu T602 TAP=1.1pu V=120kV		T601 TAP=1pu T602 TAP=1pu V=120kV	
Load#	Min Vol (kV)	ΔV%	Min Vol (kV)	ΔV%
119, 121/128	13.198	5.755	13.038	6.898
100/106	13.251	5.377	13.096	6.484
36/41	13.232	5.513	13.072	6.655
17/22	13.268	5.256	13.108	6.398
172-180	13.184	5.855	13.024	6.998
23/28	13.190	5.813	13.030	6.955
62, 129/127	13.206	5.698	13.046	6.841
51, 57/61	13.265	5.277	13.105	6.420
48, 52/56	13.199	5.748	13.039	6.891
XFRT-3001	13.306	4.984	13.145	6.134
90/99	13.266	5.270	13.105	6.420
TP1	13.252	5.370	13.091	6.520
64/69	13.193	5.791	13.033	6.934
162-170	13.155	6.063	12.996	7.198
70/75	13.213	5.648	13.053	6.791
30/35, 138, 139	13.216	5.627	13.056	6.769
10/15	13.204	5.713	13.044	6.855
42/47, 140. 141	13.228	5.541	13.068	6.684

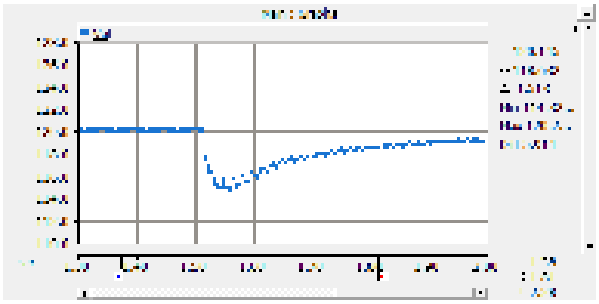

Fig 6. T601 Primary voltage curve for case D

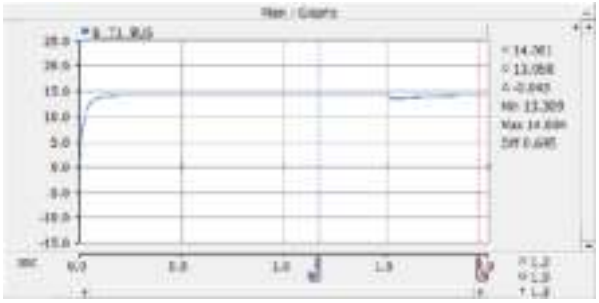

Fig 7. T601 Secondary voltage curve for case D

E. T601 Tap at 0.9125 and T602 at Tap 1.1pu

Under this scenario, the system voltage is reduced to the lowest possible level that still guarantees safe operation for the ESPs. The tap position for T601 is set at 0.9125pu.

Lowering the system voltage in order to utilize a lower position at the running transformer T601 did not improve the situation significantly as it can be seen in Table V. Furthermore, this scenario is not practical to be used as a short term mitigation since the upstream network is not regulated by the company and it is under the control of the Grid. The T601 primary and secondary voltages are shown in Fig 8 & Fig 9 in addition to its sympathetic inrush in Fig 10. The T602 inrush current is shown in Fig 11.

TABLE V
LOADS VOLTAGE DROP FOR CASE E

	T601 TAP = 0.9125pu T602 TAP=1.1 Vprimary=111.29kV	
Load#	Min Vol (kV)	ΔV%
119, 121/128	13.431	5.362
100/106	13.484	4.989
36/41	13.465	5.123
17/22	13.502	4.862
172-180	13.416	5.468
23/28	13.422	5.426
62, 129/127	13.438	5.313
51, 57/61	13.499	4.883
48, 52/56	13.432	5.355
XFRT-3001	13.541	4.587
90/99	13.5	4.876
TP1	13.485	4.982
64/69	13.426	5.397
162-170	13.387	5.672
70/75	13.446	5.256
30/35, 138, 139	13.449	5.235
10/15	13.437	5.320
42/47, 140. 141	13.461	5.151

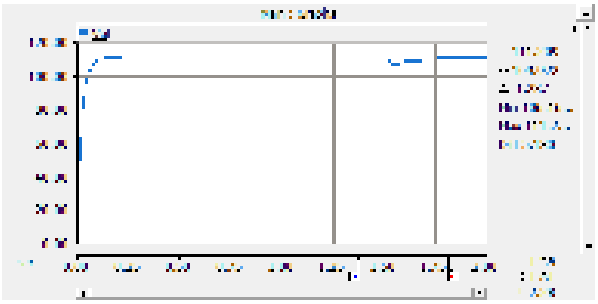

Fig 8. T601 primary voltage for case E

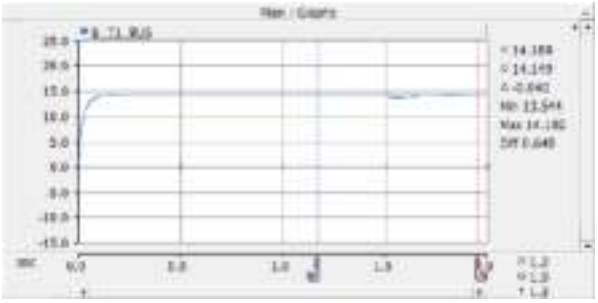

Fig 9. T601 secondary voltage for case E

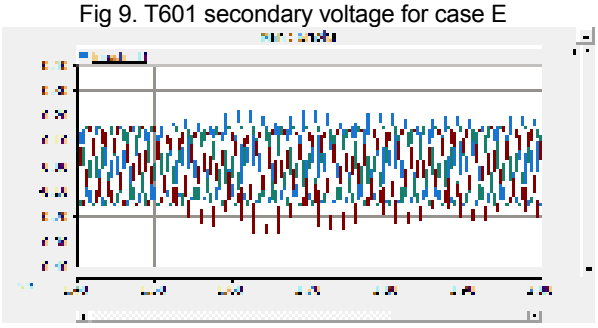

Fig 10. T601 sympathetic inrush current for case E

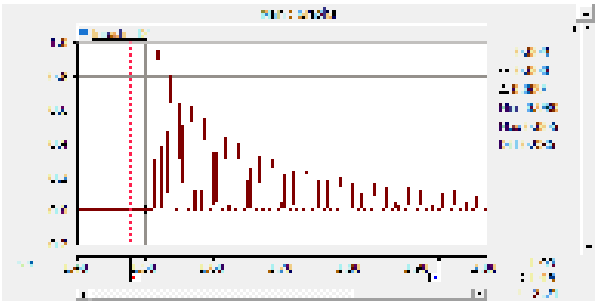

Fig 11. T602 inrush current for case E

F. T601 Tap at 0.9pu and T602 at 1.1pu

Under this scenario, the T601 was set at its lowest tap position. The results shown in Table VI did not show voltage drop more then 5%. The drawback for this case that the voltage level in the ESP's are exceeding the 15kV due to the cable Ferranti which is stressing the insulation above it is nominal limits.

TABLE VI
LOADS VOLTAGE DROP FOR CASE F

	T601 TAP = 0.93125pu T602 TAP=1.1 Vprimary=116.4kV	
LOAD#	**MIN VOLTAGE (kV)**	**ΔV%**
119, 121/128	14.26	4.93
100/106	14.32	4.53
36/41	14.30	4.67
17/22	14.34	4.40
172-180	14.25	5.00
23/28	14.25	5.00
62, 129/127	14.27	4.87
51, 57/61	14.33	4.47
48, 52/56	14.26	4.93
XFRT-3001	14.38	4.13
90/99	14.33	4.47
TP1	14.32	4.53
64/69	14.26	4.93
162-170	14.22	5.20
70/75	14.28	4.80
30/35, 138, 139	14.28	4.80
10/15	14.27	4.87
42/47, 140. 141	14.29	4.73

G. T601 Tap at 0.93125pu and T602 at 1.1pu

Under this case, the optimum operation scenario to address the severe voltage dip and not to exceed the voltage nominal level of 15kV. This is achieved by keeping T601 tap at 0.93125pu (14.6kV) and T602 at 1.1 tap. This is to avoid the excessive overvoltages and maintaining the ESP's minimum voltage not below its rating of 13.8kV. the simulation results are shown in table VII.

TABLE VII
LOADS VOLTAGE DROP FOR CASE G

	T601 TAP = 0.93125pu T602 TAP=1.1 Vprimary=116.4kV	
LOAD#	**MIN VOLTAGE (kV)**	**ΔV%**
119, 121/128	13.81	4.93
100/106	13.86	4.53
36/41	13.84	4.67
17/22	13.88	4.40
172-180	13.79	5.00
23/28	13.80	5.00
62, 129/127	13.82	4.87
51, 57/61	13.88	4.47
48, 52/56	13.81	4.93
XFRT-3001	13.92	4.13
90/99	13.88	4.47
TP1	13.86	4.53
64/69	13.80	4.93
162-170	13.76	5.20
70/75	13.82	4.80
30/35, 138, 139	13.83	4.80
10/15	13.81	4.87
42/47, 140. 141	13.84	4.73

H. Design Load of 1.2MW & 690kVar per ESP

The purpose of this case is to study the influence in the total voltage drop was the load size is increased to match the available ESP's nameplates. The load size is distributed equally between the locations. The simulation was carried at different tap positions for T601 & T602. Fig 12 shows an example for the secondary voltage for T601 and Table VI shows the voltage drops at the ESP's for different cases.

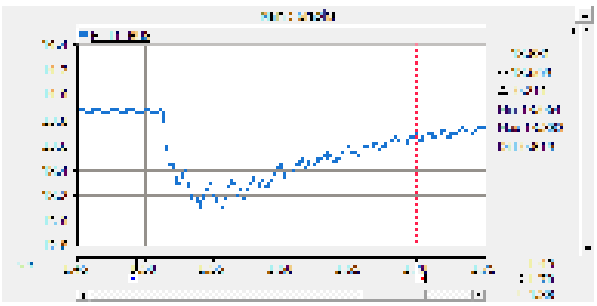

Fig 12. T601 Secondary voltage for case H

The worst voltage drop was noticed at ESP#162. The voltage drop reached 7.37% as shown in Fig 13.

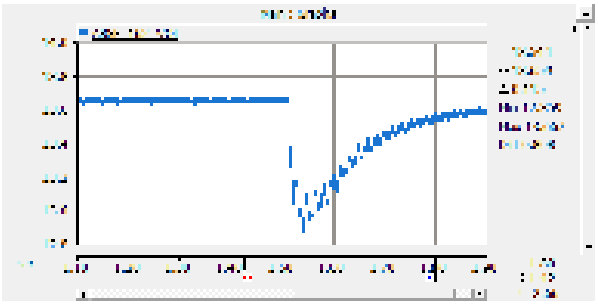

Fig 13. ESP# 162 voltage curve for case H

TABLE VIII
LOADS VOLTAGE DROP FOR CASE H

	T601 TAP=0.96875pu T602 TAP=1pu Vprimary=116.4kV		T601 TAP=0.95625 T602 TAP=1 Vprimary=116.4kV		T601 TAP=0.96875pu T602 TAP=1.1pu Vprimary=116.4kV	
Load#	Min Vol (kV)	ΔV%	Min Vol (kV)	ΔV%	Min Vol (kV)	ΔV%
119, 121/128	12.932	6.837	13.092	6.845	13.081	5.763
100/106	12.985	6.455	13.146	6.461	13.140	5.338
36/41	12.964	6.606	13.124	6.617	13.119	5.490
17/22	13.012	6.260	13.173	6.269	13.167	5.144
172-180	12.897	7.089	13.056	7.101	13.051	5.979
23/28	12.909	7.002	13.069	7.009	13.063	5.893
62, 129/127	12.924	6.894	13.084	6.902	13.079	5.778
51, 57/61	13.005	6.311	13.165	6.326	13.16	5.194
48, 52/56	12.928	6.865	13.088	6.873	13.083	5.749
XFRT-3001	13.060	5.915	13.221	5.927	13.216	4.791
90/99	13.006	6.304	13.166	6.318	13.161	5.187
TP1	12.987	6.440	13.147	6.454	13.142	5.324
64/69	12.926	6.880	13.085	6.895	13.080	5.770
162-170	12.857	7.377	13.016	7.386	13.011	6.268
70/75	12.940	6.779	13.1	6.788	13.095	5.662
30/35, 138, 139	12.939	6.786	13.099	6.795	13.093	5.677
10/15	12.928	6.865	13.088	6.873	13.082	5.756
42/47, 140. 141	12.954	6.678	13.114	6.688	13.109	5.562

I. Design Load of 1.6MW & 690kVar per ESP

By increasing the 1.2MW load size of the previous case for each ESP 1.6MW and keeping the same voltage regulation at the transformer tap changers, the secondary voltage dropped to 12.96kV. This is expected to have worse voltage drop during transformer sympathetic inrush current when the load size is increased. The voltage curve for T601 secondary voltage is shown in Fig 14 and the highest voltage drop was at ESP#162 as its voltage curve is shown in Fig 15. The summary of the ESP's voltage drop is shown in Table IX.

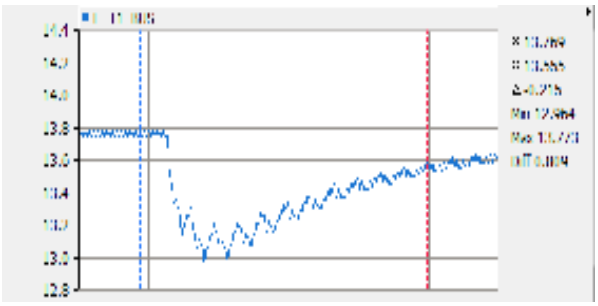

Fig 14. T601 secondary voltage curve for case I

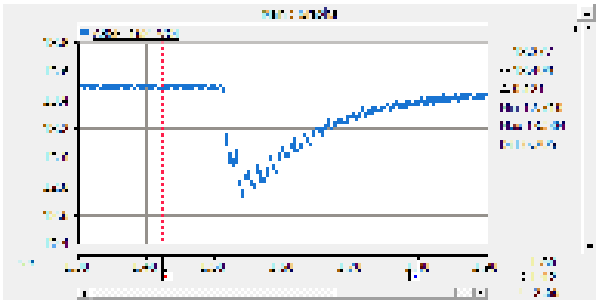

Fig 15. ESP#162 Voltage Curve

TABLE IX
LOADS VOLTAGE DROP FOR CASE I

	T601 TAP=0.96875pu T602 TAP=1pu Vprimary=116.4kV		T601 TAP=0.96875pu T602 TAP=1.1pu Vprimary=116.4kV		T601 TAP=0.9125pu T602 TAP=1.1pu Vprimary=110.55kV	
Load#	Min Vol (kV)	ΔV%	Min Vol (kV)	ΔV%	Min Vol (kV)	ΔV%
119, 121/128	12.813	6.97	12.964	5.87	13.159	5.636
100/106	12.867	6.57	13.019	5.47	13.215	5.235
36/41	12.844	6.74	12.996	5.64	13.191	5.407
17/22	12.903	631	13.055	5.21	13.252	4.970
172-180	12.759	7.36	12.909	6.27	13.104	6.031
23/28	12.777	7.23	12.928	6.13	13.123	5.895
62, 129/127	12.791	7.13	12.942	6.03	13.137	5.794
51, 57/61	12.892	6.39	13.044	5.29	13.241	5.048
48, 52/56	12.805	7.02	12.957	5.92	13.151	5.694
XFRT-3001	12.960	5.90	13.114	4.78	13.311	4.546
90/99	12.893	6.38	13.045	5.28	13.242	5.041
TP1	12.869	6.56	13.021	5.46	13.217	5.221
64/69	12.805	7.028	12.957	5.925	13.152	5.687
162-170	12.709	7.725	12.859	6.636	13.053	6.397
70/75	12.814	6.963	12.966	5.859	13.161	5.622
30/35, 138, 139	12.810	6.992	12.961	5.896	13.156	5.658
10/15	12.800	7.065	12.951	5.968	13.146	5.730
42/47, 140. 141	12.829	6.854	12.981	5.750	13.176	5.515

J. Submitted Nameplate Loads

In order to acquire a more realistic footprint of the network transient behavior, some individual platforms nameplate loading were adopted. The effect of the new load in the transformer secondary side voltage is almost identical to the previous case as shown in Fig 16. The summary of the ESPs voltage is shown in Table VIII. The most severe voltage drop is in load# 162-170 platform which is 7.36%.

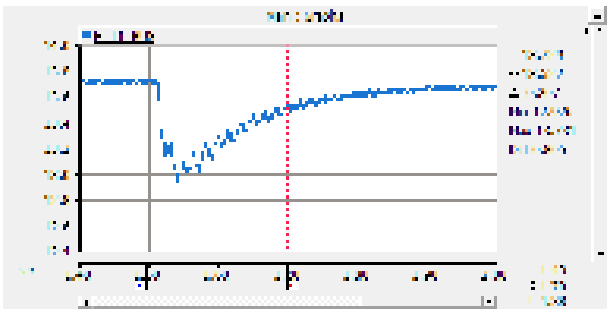

Fig 16. T601 LV Bus for case J

TABLE VIII
LOADS VOLTAGE DROP FOR CASE J

	T602 TAP 1pu		T602 TAP 1.1pu	
LOCATION	**MIN VOLTAGE (kV)**	**ΔV%**	**MIN VOLTAGE (kV)**	**ΔV%**
119, 121/128	12.766	7.028	12.917	5.928
100/106	12.820	6.635	12.972	5.528
36/41	12.823	6.613	12.975	5.506
17/22	13.878	6.212	13.031	5.098
172-180	12.774	6.970	12.926	5.863
23/28	12.792	6.839	12.943	5.739
62, 129/127	12.734	7.261	12.885	6.161
51, 57/61	12.865	6.307	13.017	5.200
48, 52/56	12.806	6.737	12.958	5.630
XFRT-3001	12.922	5.892	13.075	4.778
90/99	12.859	6.351	13.012	5.236
TP1	12.830	6.562	12.983	5.448
64/69	12.795	6.817	12.947	5.710
162-170	12.720	7.363	12.871	6.263
70/75	12.788	6.868	12.940	5.761
30/35, 138, 139	12.769	7.006	12.920	5.906
10/15	12.801	6.773	12.953	5.666
42/47, 140. 141	12.803	6.758	12.954	5.659

IV. CONCLUSION

In this paper, the effect of the transformer tap changer position on the sympathetic inrush was studied. It showed that the tap changer position has direct effect on the voltage profile during transformer energization. Also, the running loads size in addition to the Grid voltage have some impact on the system.

V. REFERENCES

[1] CIGRE Working Group C4.307, 'Transformer Energization in Power Systems : A Study Guide', vol. 568, ed. France : CIGRE Publication February 2014, pp.8-73.

[2] Manitoba HVDC, 'Applications of PSCAD/EMTDC', 2018.

[3] Manitoba HVDC, 'PSCAD User Guide'.

[4] J. Peng, 'Assessment of Transformer Energization Transients and their Impacts on Power Systems', PhD Thesis, School of Electrical and Electronics Engineering, The Univercity of Manchester, 2013.

[5] U. Rudez, R. Mihalic, 'Sympathetic Inrush Current Phenomenon with Loaded Transformers.', Elec. Power Systems Research, vol. 138, Sep2010.

[6] P.C.Y. Ling and A. Basak, 'Investigation of Magnetizing Inrush Current in a Single Phase Transformer', IEEE Trans. on Magnetics, vol.24, no.6, pp. 3217-3222, November 1988.

VI. VITA

Georgios Fotiou, the corresponding author, graduated from the Democritus University of Thrace in 1999 with an MSc degree. He has more than 20 years of experience in substation automation and control, advanced system studies, conceptual and detail design. He worked as a senior engineer in ABB SA for eight years and a lead engineer in JP AVAX for six years. He has been a protection and systems studies engineer for Aramco Oil Company since 2012.
George.fotiou@aramco.com

Hussain Al-Awami, graduated from King Fahad University of Petroleum & Minerals(KFUPM) with a BScEE degree in 2004 and received his MSc in EE in year 2010. He has been working as protection and power system engineer in Saudi Aramco since 2004. He received his IEEE senior membership in year 2018 and he is licensed Professional Engineer in Saudi Arabia. He has been involved in many mega projects and major electrical interruptions.
Hussain.awami.3@aramco.com

ELECTRIC HEATING SYSTEMS FOR ELECTRIC THERMAL ENERGY STORAGE (ETES)

Paper No. PCIC Europe EUR22_06

Dennis Long
Watlow
St Louis, MO
USA
dlong@watlow.com

Eric Ludwig
Watlow
St Louis, MO
USA
eludwig@watlow.com

Abstract – Many thermal energy storage technologies are competing for shares in the energy storage market. The thermal energy input into the systems will frequently come from electric heating systems. These systems typically have process temperature needs of 560 to 900+ ° C. [1]

The systems normally use megawatts of power from renewable energy sources. The electrical heating systems are often designed at or near the peak available power to maximize the amount of energy stored. As such, the electrical heating systems require control system solutions not normally needed in electrical process heaters operating well below the available power.

This paper will show the design of very large megawatt heating system for electric thermal energy storage, including both the heaters and the control system. Special emphasis will be placed on the needs of control systems to assure reliable operation in situations that are consuming all or nearly all of the available power, with consideration of the needed durability and reliability.

Index Terms — Thermal Energy Storage, Control Systems for Electric Process Heating, Process Heating

I. INTRODUCTION

The use of renewable electricity for the electrification of process heating and many other applications to reduce or eliminate carbon dioxide emissions is well underway. The intermittency of renewable electricity generation sources such as wind, photovoltaic and concentrated solar power results in a desire to store any excess produced energy. Energy storage technology results in the possibility of renewable based electricity around the clock. Energy storage is essential to cope with the intermittency of renewables. [2] Energy storage is also used to reduce the imbalances that occur due to differences in energy demand and energy production.

There are several energy storage sciences to choose from. Energy storage sciences include thermal, chemical, liquid, mechanical, gas, magnetic field and electric field technologies. Thermal energy storage is a proven technology that is in widespread use today primarily in large electrical power generation plants. The storage media used in thermal storage systems include different types of salts, igneous rock, metals, silica and others.

Sometimes it is desirable for the energy producer to divert all or nearly all the available power to the energy storage system to provide rapid recharging or to facilitate load dumping. In electric thermal energy storage (ETES) systems, the heat source is frequently an electrical resistance type process heater that creates heat energy, which is then transferred to the target storage media via conduction, convection, radiation or combinations of these heat transfer modes. In these cases, the process heater control system must be capable of assuring the heater surfaces do not exceed specified maximum skin temperature. In addition, the control system must have the capability to assure that connection of the electrical supply to the process heater loads is managed appropriately to prevent damage or unbalanced situations from occurring to the generation source.

II. OVERVIEW OF ETES HEATING SYSTEM

A. ETES Technologies

There are a variety of technologies for ETES. The technologies typically fall under one of the following types: sensible heat, latent heat or thermo-chemical storage. Sensible heat examples include molten salt or similar types of mass that can be increased in temperature and subsequently lowered in temperature to provide heat energy for the electricity generation loop. The electricity generation loop is frequently driven by a steam powered turbine. The heat source for sensible systems could be solar in addition to electric resistance type heaters.

The second type are latent heat storage systems in which the target heat source undergoes a phase change. An example is aluminum, which can be heated to transform from a solid state to a liquid state. The primary idea behind latent heat storage is to provide for higher energy density as compared to other technologies.

The third type is thermo-chemical thermal energy storage. This type of thermal energy storage occurs due to a chemical reaction that has high energy. This type of storage consists of two main processes, thermochemical reactions and sorption processes. In this paper, we will focus on sensible heat systems.

ETES systems that use electric resistance type heaters as the charging source can be rated at many megawatts. System sizes from 10 to 150+ megawatts are well within the capabilities of the heater technology. The recommended physical size of the electric process heater is a function of thermodynamic analysis and manufacturing capabilities. The thermodynamic analysis is the most frequent determining factor of the physical size because the sensible heat systems are frequently forced convection systems. It is desirable to achieve the best possible mass flow rate through the electric heat

exchanger and still meet targets for pressure drop, flow induced vibration and metal erosion. This design analysis approach results in the smallest practical physical size for the electric heat exchanger. The physical size is a consideration of both the heat exchanger shell diameter and length. Smaller exchanger shell diameters not only help with fluid velocities but also help to keep the shell wall thickness as thin as possible while meeting construction standards (such as the ASME B&PVC or PED).

B. Example of Large Megawatt ETES Heat Exchanger

The flow of the heated medium can be through a series of electric heat exchangers, or through a series parallel arrangement as shown in Figure 1.

Fig. 1 Series-Parallel Heating Train

The actual arrangement could be a wide combination of heaters completely in series or series-parallel arrangement. In addition to the thermodynamic considerations, the end user may have redundancy or reliability targets that affect the final solution. The heat exchangers don't necessarily need to be the same physical size. It is common to use different SKU numbers in the series arrangement that consist of heat exchangers with the highest heat flux density nearest the inlet of the system. Since these are sensible systems that add heat energy the inlet temperature is always lower than the outlet temperature. This results in the opportunity to use the highest flux densities near the inlet while assuring the target heater maximum skin temperature is not exceeded.

These series-parallel trains require control of the temperature within each individual heat exchanger. The skin temperature of the heater sheaths within each heat exchanger is also an important control consideration. Skin temperatures that exceed the maximum specified could result in decomposition of the heated fluid or corrosion rates that exceed the specifications. Either of these situations will result in unplanned downtime and replacement costs.

In addition to the individual heat exchangers, the process temperature of the entire system must also be tightly controlled within the requirements of the end user. Failure to meet the outlet temperature requirements means the target fluid will not possess the intended amount of heat energy. Ultimately this means the system cannot be recharged in the intended time range, or the temperature of the target fluid is not reached. Either situation will result in less energy available to produce electricity on demand.

The control systems for these large megawatt systems are typically switching low voltage. Low voltage in this case normally means 380 to 690 volts. A 10-megawatt system operating on a 3-phase supply, connected to 690 volts, will draw approximately 8368 amps. This amperage results in necessary design considerations for heat dissipation. Control systems located adjacent to the heat exchangers might result in the lowest cost for connection cables. However, adjacent location might also result in the most expensive solution for removal of heat from the control system panel.

III. OPERATION AND CONTROL OF AN ETES HEATING SYSTEM

A. Operational Considerations and Scenarios

ETES applications can present numerous operational scenarios that result in the need to engineer the system in consideration of process temperature needs and the electrical power supply. Some examples of operational scenarios include:

- Preheat – the systems are typically made of metal that are preheated prior to introducing the target heated fluid
- Startup – raising the system temperature from preheat to normal with the target heated fluid
- Phase change protection – mode to assure the minimum fluid temperature is maintained
- Normal operation
- Idle mode – not shutdown, startup or normal
- Routine planned maintenance
- Hybrid scenarios – somewhere in-between any of the scenarios previously listed

These operational scenarios create many system operational variables that the control system must handle without causing thermal or electrical problems that result in unplanned downtime or unsafe conditions. The various operational scenarios result in varying temperatures, flow rates, and pressure. In addition, the available power for the electric heat exchangers could vary for different operational scenarios.

The intended maximum process temperature and skin temperature vary in each operational scenario. One control system must be capable of handling varying inlet and outlet process temperature needs. In addition, the maximum allowable skin temperature of the heating elements varies between scenarios. For systems that are partially or fully controlled via signals from temperature sensors, even the selection of which sensors to use for input to the control system can change with each scenario.

The fluid flow rate also varies among the operational scenarios. A range of planned fluid velocities will occur between the normal, idle and hybrid scenarios. The control system must have turndown ratio capabilities that effectively change the average heat flux to prevent skin temperature excursions beyond what is allowed for the operational scenario. The maximum skin temperature allowed in the various operational scenarios ultimately determines the amount of power (heat energy) that can be input into the system. The power input determines the rate of temperature rise in any of the operational scenarios.

The system pressure is also an operational scenario variable that can be used to control the system. Pressure measurements can be used as confirmation of the operational scenario and as an indicator of system changes over time that are anticipated. Abnormal

changes in pressures are good indicators of situations that require immediate system maintenance intervention.

Finally, the available power may also vary with the operational scenarios. The available power will determine the time needed to raise the temperature of the target fluid to the intended outlet process temperature at a given flow rate and inlet temperature. Conversely, the available power will also determine the maximum possible process outlet temperature that can be achieved at the actual flow rate and inlet temperature.

B. System Design Considerations – Heat Exchanger

Electric resistance type process heaters are exactly what the name implies; i.e. resistive devices. The resistance type process heaters are Joule heating devices. In Joule heating, the energy of the electric current is converted into heat as is flows through a resistance. The devices are primarily resistive with a very small (negligent) amount of capacitance. Keeping in mind Ohm's Law (see Figure 2), the tolerance of the resistance and applied voltage determine the available power.

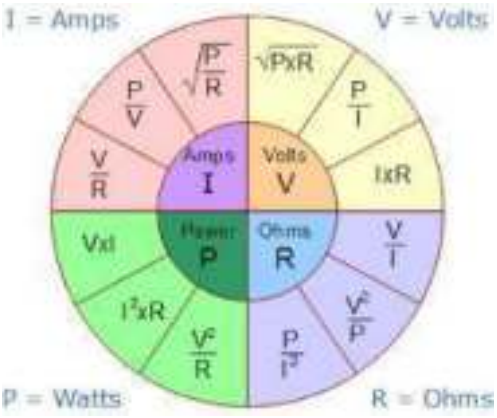

Fig. 2 Ohm's Law

When users want to maximize the energy input into their thermal energy storage system, the voltage and resistance tolerances are of great importance. A 5% drop in the connection voltage will drop the available power by about 10%. In addition, any percentage increase in the resistance beyond the nominal specifications (because of the manufacturing process) will result in a proportional decrease in the power. For megawatt systems, this loss of available power can become a major consideration in the system design.

It is worth noting that once the electric heater is manufactured, the resistance while operating is essentially a fixed value. Based on the principles of Ohm's Law, as the voltage supply increases or decreases, the current draw will also increase or decrease by the same ratio. As the voltage varies, so does the current, so the overall power consumed (P(real)) or converted would also vary. This is governed by the following equation:

P (real) = V*I*sqrt3

Voltage (V) and current (I) can swing by the overall tolerance of the supply voltage. As an example, a heater that is nominally designed with a resistance value to produce 6MW at 690V would have the following …

Nominal Values:
Effective Resistance (each leg) = R = 0.24 ohms
Effective Power (each leg, line to line) = 2.0 MW
Effective Power (3PH, 3 leg total) = 6.0 MW
Voltage = 690VAC Line to Line, 3PH
Resulting Current = I = P/(V*sqrt3) = 5021 A
P = V*I*sqrt3 = 690*5020*1.732 = 6.0 MW

At +10% voltage (#'s rounded):
Voltage = 759V
Effective Resistance stays constant, as it is a factor of the heater design = 0.24 ohms (each leg)
Effective Power (each leg, line to line) = 2.42 MW
Effective Power (3PH, 3 leg total) = 7.26 MW
Resultant Current = 5523 A
P = V*I*sqrt3 = 690*5523*1.732 = 7.26 MW

Likewise, at -10% Voltage, the system, by similar analysis, would equate to 4.86MW. Based on this, the effective thermal output of this heater could vary between 4.86MW and 7.26MW depending on the voltage input (if the voltage were to vary by +/-10%). These ranges must be taken into consideration when designing the overall system to ensure the proper heat is available as needed. In addition to the overall size of the heater, these voltage fluctuations will impact the overall feeder power necessary to run the system

In addition to as-manufactured resistance tolerances and voltage supply tolerances, parasitic losses also need to be determined. In addition to the heat energy needed to raise the temperature of the target fluid, both electrical and thermal parasitic losses need to be calculated and considered to understand the overall power needs. On the electrical side, all terminations result in some amount of voltage drop. The connection cables from the control system to the process heater terminal enclosure also have some electrical resistance and thus some voltage drop. The power loss can be calculated using the classical equation associated with Joule's First Law, I^2R.

On the thermal side, the heat exchanger cannot be perfectly insulated, and will have some thermal losses to the atmosphere. A convection cooling section between the pressure vessel tube sheet and the process heater terminal enclosure is purposefully left uninsulated in the field, as shown in Figure 3. This design method assures terminal enclosure temperatures remain at or below the design intention. [3] This is another source of thermal heat losses. Even touch safe surfaces have some thermal loss to the atmosphere.

Fig. 3 Process Heater Convective Cooling Section

In addition to the thermal losses associated with the heater, there are also thermal losses associated with the control system and power panel. These manifest through current carrying parts within those systems, and result in additional I^2R losses. Therefore, even a highly efficient technology like Joule heating is not capable of putting all the heat energy input into the target fluid. Careful analysis can do an adequate estimate of the losses to the atmosphere. This is an important point and consideration as it pertains to the thermal design of large megawatt size thermal energy systems.

C. System Design Considerations – Power Switching

Power switching devices cycle the power to maintain certain temperatures within the system. There are two main types of switching hardware used to turn the circuits of a large system heater on and off: contactors and thyristors (also known as SCRs). Contactors switch the power on or off to each circuit based on a digital control signal from the main process controller. These devices are immediate, meaning the power is switched as soon as the device receives the signal. As such, the power switch may occur anywhere within the waveform of the sinusoidal cycle. Typically, this will create some harmonics in the system, due to the connection/disconnection of the load at random points within the voltage waveform. Due to their mechanical nature, contactors also have a limited lifespan, which is dependent on the number of on/off cycles. It is important to understand how often the system circuits will need to cycle, as well as the anticipated life of the system, to determine if contactor control is adequate. For circuits that will need to be cycled often, this may not be the best method of power switching, as the life expectancy of the contactor may not be sufficient.

The thyristor (i.e. SCR) power switching method is based on solid state technology. This allows much more flexibility in how and when the power is switched on/off to the circuit. There are two basic modes of control within a thyristor … phase angle firing and zero cross duty cycle.

In phase angle firing, each voltage half sine wave is "chopped" to only allow a certain portion of the sine wave through, as shown in Figure 4.

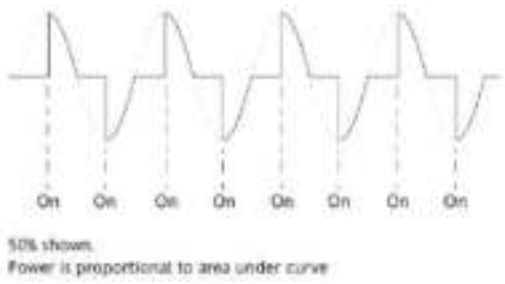

Fig. 4 50% Chopped Sine Wave

The power can be switched anywhere along the half wave. During the "on" portion of the waveform, only the voltage waveform through a specified angular value (0-180 degrees) is delivered to the load circuit. During the "off" portion of the waveform, no voltage or current is available to the load circuit. The resulting power to the load circuit is equal to the area under the curve, or, in simpler terms, equal to the proportional amount of the waveform during the "on" cycle. Examples of the power profile over time using various phase angle fired values on a 500kW load circuit (i.e. Pmax = 500kW) are shown below. At 100% (full time on) the result in depicted in Figure 5. Note the power profile is a constant value, at 100% (500kW), and does not fluctuate with time.

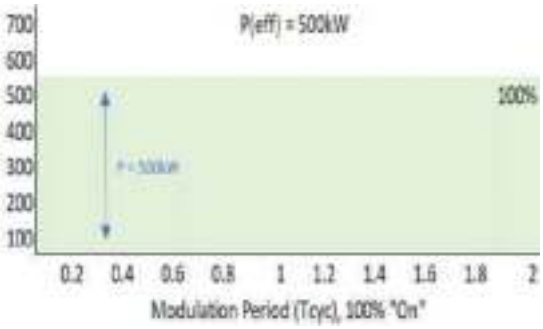

Fig. 5 100% "On" Switched Load

At 60% (partially on) the result is depicted in Figure 6. Note, again, the power profile is a constant value, at 300kW, and does not fluctuate with time.

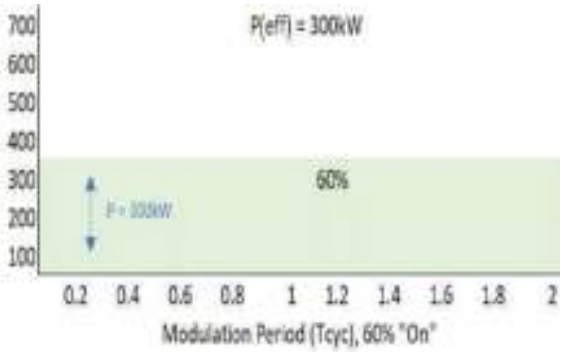

Fig.6 60% "On" Switched Load

Zero Cross Duty Cycle control only switches the power when the voltage waveform is at its zero value within the sinusoidal waveform. This eliminates much of the harmonic and electrical noise issues associated with switching while power is applied. The drawback, however, is that power can only be switched a couple of times within a single mains cycle (at each zero cross). To accomplish this, and produce adequate control, the thyristor depends on a modulation period for control. This modulation period (Tcyc) can be user defined, and is typically set to ensure the system is fast enough to respond to any changes (based on thermal time constants or other factors). Typical modulation periods can be anywhere from fractions of a second (for fast response systems) to 10-20 seconds (on slower response systems). Within the modulation period, the power is "on" (Ton) for a specified time period and "off" (Toff) for the remaining time. During the "on" period, full voltage and current is delivered to the load circuit, while no voltage and current are delivered during the "off" portion. The specified time duration the power is "on" is called the duty cycle. Overall, the voltage and current are turned on at the zero-cross point within the modulation period, and stays on for a percentage portion of that period, turning off at the next zero cross point. See the Figure 7 diagram for a depiction of the resulting waveform:

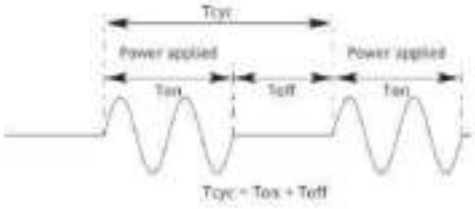

Fig. 7 Zero Off with Modulation

Using the same 500kW load circuit as before, with a modulation period of 1 second, and a 100% duty cycle (full on), the resulting power profile would be as shown in Figure 8. Note that the power profile is a constant value due to the nature of 100% of the voltage waveform being "on" with this duty cycle setting.

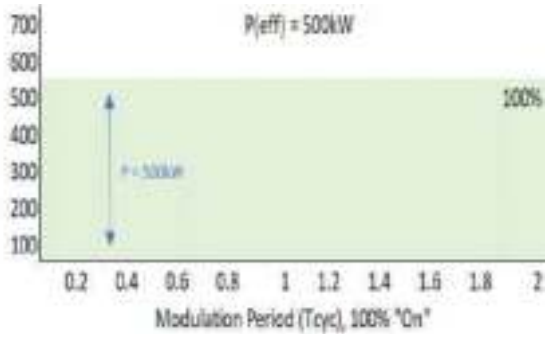

Fig. 8 100% Duty Cycle with 1 Second Modulation

At 60% Duty Cycle the output graph is depicted in Figure 9. Note the power profile in this case is not constant, rather is 100% (500kW) during "on" portion of the modulation period, and 0% (0kW) during the "off" portion of the modulation period.

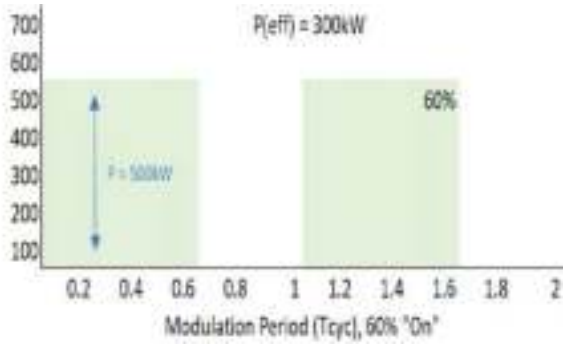

Fig. 9 60% Duty Cycle with 1 Second Modulation

Readers will notice a distinct difference in the power profiles between the phase angle fired and duty cycle controlled modes. Since the zero-cross duty cycle control is effectively turning the load on and off, the instantaneous power consumed during the "on" cycle is the full load power of the load circuit (i.e. 500kW). Over the complete modulation period, this averages to a value proportional to the duty cycle to produce and average power to the load at the desired value (i.e. 300kW over 1 second in the above example).

There are advantages and disadvantages to each type of power switching technique. Many users cannot withstand the harmonics and electrical noise associated with high power phase angle fired thyristors. As such, it is typically desired to use the zero-cross technology when switching high power loads. Managed correctly, this can help prevent additional parasitic losses, instability and nuisance electrical noise issues within the power system.

Overall, the best technology for power switching the entire electric heater system is typically a "hybrid" approach, where some circuits would be controlled using contactors, and some with thyristors. This is also referred to as "base load plus trim" system. The base load, which cycles infrequently, would be suited for contactor control. The more variable load, with needs to switch more often, would be managed using the thyristor technology. As will become apparent in latter parts of this paper, coordination between all these circuits becomes critical to maintain a stable electrical system.

D. System Design Considerations – Control System

Within the system, a main process controller will be used to collect the performance parameters from the process, and convert those into the appropriate signals for the power switching devices to maintain the desired temperatures. As with the power switching technology, there are several modes of control that can be utilized; however, given the amount of power being switched in most of these applications, it is desirable to have a closed loop feedback control system. This would typically deploy a standard PID loop that ensures the temperature at the outlet of the system is properly maintained. Where there are many electric heaters in series to perform this task, or where several different items need to be temperature controlled using the power from the electric heaters, a control technique called cascade control is often used. This control technique is functionally as shown in Figure 10.

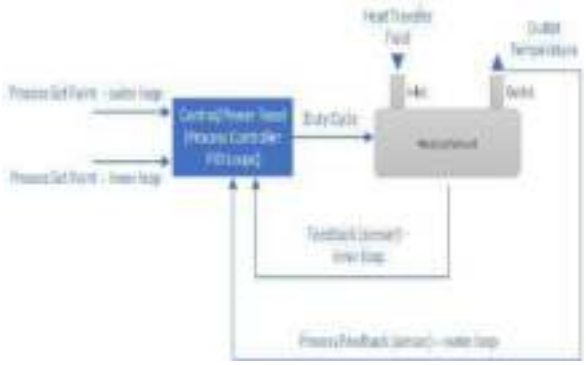

Fig. 10 PID Cascade Control Loop

In this example, the outlet process temperature is controlled to a certain set point. In addition, a specific parameter inside the vessel (example – the element sheath temperature) is also controlled to a certain set point, different than the previous outlet process temperature setpoint. The controller then appropriately controls the power to the heating elements to maintain both within their control limits. This type of control methodology works well for various modes of operation. During pre-heating of the system, it may be desirable to heat up the heater/vessel, but still ensure the heater elements are protected from overtemperature. During this mode of operation, the vessel temperature may be used as the outer loop, and the heating element temperature for the inner loop. When switching to normal operation, the outer loop sensor may switch over to the outlet temperature sensor.

Yet a further refinement of this cascade control system should be considered if there will be fast transients within the process flow. By adding a feedforward input to the process controller as shown in Figure 11, this can be used to predict and scale the response of the system. [4] The prediction algorithm can start to throttle or accelerate the power through the duty cycle output, which in turn, will throttle or accelerate the heat applied. Depending on the thermal inertia and latency associated with the measurement devices, this method can help speed up the response to protect both the fluid media and/or the heating elements themselves.

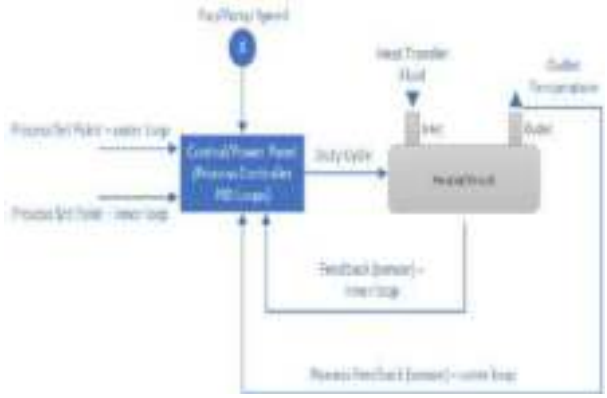

Fig. 11 Control with Feed Forward

E. System Design Considerations – Load Management

Another important aspect of the control system will be its ability to manage the sequencing of the power switching to ensure a stable power profile. Electricity disruptions are estimated to cost the economy roughly $80 billion or more annually and seriously endanger public health and safety. [5] The size of these ETES systems equates to hundreds of amperes being switched within a circuit. Many of these systems have multiple circuits, adding up to thousands of amperes. The simultaneous switching of these circuits on/off could cause power factor issues and/or instability within the power system if not adequately balanced and controlled.

As discussed in the power switching section of this paper, a contactor and/or zero cross duty cycle controlled thyristor circuit will produce 100% instantaneous power when the circuit is “on”. Each of these circuits will need to be switched on/off to maintain temperatures at the outlet of the electric heater. To illustrate the issue, the following example, as shown in Figures 12 and 13, is used:

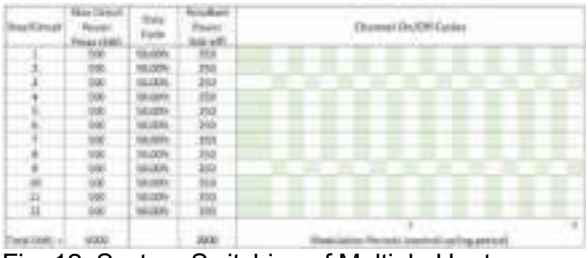

Fig. 12 System Switching of Multiple Heaters

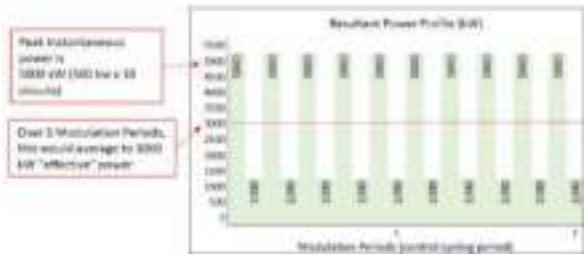

Fig. 13 Power Profile of Figure 12

The twelve circuits that make up the heater are all switching independently. With the random nature of this independent control, there could be situations where the power switching for the circuits occurs at the same moment in time. For this case, with a 50% duty cycle, the instantaneous power while any single circuit is on equates to 500kW. Overall, for the twelve circuits, this equates to an instantaneous power draw of 5000kW if ten of the twelve circuits are on simultaneously. Since the duty cycle is 50%, the ten circuits turn off in the second half of the modulation period, while the other two circuits are on. Overall, this creates an instantaneous power swing of 4000kW in the power system. Over the entire modulation period, the power is averaged to the effective duty cycle (in this case 3000kW), and the system is adequately heated. In doing so, however, it puts a great strain on the power feeder network.

To alleviate this, it is important for the power control system to incorporate a load sharing and management algorithm. This coordinates the switching times of all the circuits together to ensure a stable demand on the power feeder. In the above example, if a system needs 3000kW of power to adequately heat, and has the same twelve circuits, a more stable profile of switching is needed to

balance the input power. By manipulating the times these circuits can switch, one can eliminate the large swings in instantaneous power. By managing the circuits together, rather than independently, the switching sequence can be manipulated to provide the same thermal response without the large swings. The results of managing the circuits as described is shown visually in Figures 14 and 15.

Fig. 13 Managed Power Switching

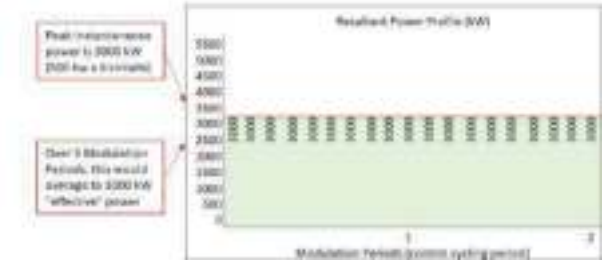

Fig. 14 Stable Power Demand

IV. Conclusion

Energy storage is a vital component of the energy future, particularly from intermittent renewable energy sources. Thermal energy storage is a viable technology for assuring renewable energy sources can be available 24 hours per day. Thermal energy storage systems can be effectively charged using electric resistance type process heaters or electric heat exchangers, even when the system requires hundreds of megawatts of power.

Electric Thermal Energy Storage (ETES) systems can be designed and operated successfully within the many operational scenarios that are required. Sufficient planning and analysis, and thoughtful application of technologies available today will result in systems that work well with the available electricity source while delivering the intended amount of power.

V. Nomenclature

P	Power (watts).
V	Voltage(emf).
A	Amperage (amps).
I	Amperage (amps).
R	Resistance (ohms).
MW	Megawatts (watts).
kW	Kilowatts (watts).
PID	Proportional, Integral and Derivative.

VI. Acknowledgment

The authors would like to acknowledge the contributions of Trevor Smith, Mike Bange and Scott Boehmer of Watlow Electric Manufacturing Company. Their thermal system engineering skills helped postulate portions of the context presented in this paper.

VII. References

[1] Toru Okazaki, “Electric Thermal Energy Storage and Advantage of Rotating Heater Having Synchronous Inertia”, 12 November 2019

[2] U.S. Department of Energy, Grid energy storage. https://www.energy.gov/sites/prod/files/2014/09/f18/Grid%20Energy%20Storage%20December%202013.pdf , December 2013

[3] Scott Boehmer and Mike Bange, “Better Predicting Terminal Enclosure Temperature to Improve Heater Reliability, Digital Refining, Feb-2020

[4] “Understanding Feedforward Control”, Control Engineering, April 1, 2019

[5] LaCommare, K.; Eto, J. “Cost of Power Interruptions to Electricity Consumers in the United States.” Ernest Orlando Lawrence Berkeley National Laboratory for the U.S. Department of Energy, 2006

VIII. VITA

Dennis Long graduated from Truman State University in 1982 with a BS Industrial Technology degree. He has been in numerous engineering and technical positions with Watlow since 1982. He sits on several Underwriters Laboratories Standards Technical Panels (STP). He is a member of API SCHTE Unfired Consensus Group. He is an inventor on 7 patents. He has authored numerous published articles.
dlong@watlow.com

Eric Ludwig graduated from Missouri S&T (formally known as the University of Missouri – Rolla) with a Bachelor’s of Science Degree in Electrical Engineering in 1995, and a Master’s of Science in Electrical Engineering, emphasizing in Power and Controls, in 1996. After working for a capital equipment manufacturer for the first 8 years of his career, he joined Watlow in 2004, where he is still employed today. Throughout his career, he has designed, developed, and analyzed many high-power heater and control system applications for the nuclear, power, oil and gas industries. He is a member of the National Fire Protection Agency (NFPA), a member of IEEE, versed in many of the international regulatory standards governing heaters and power panels, and authored numerous published articles.
eludwig@watlow.com

LESSONS LEARNED THROUGH COMMISSIONING, LIVENING, AND OPERATING SWITCHGEAR

Paper No. PCIC Europe EUR22_07

Matthew Watkins
Schweitzer Engineering Laboratories, Inc.
101 East Park Blvd Ste 1180
Plano, Texas 75074
United States

Kamran Heshami
Schweitzer Engineering Laboratories, Inc.
3760 14th Ave, Ste 200
Markham, Ontario L3R 6H3
Canada

Michael T. Mendiola
Tengizchevroil
2007 Rice Mill Dr
Katy, Texas 77493
United States

Nilushan K. Mudugamuwa
Tengizchevroil
9 Stockbridge Rd
Fleet Hampshire
GU51 1AR
United Kingdom

Abstract — During commissioning, verifying the functionality of protective relays and wiring prior to livening is standard practice in the oil and gas industry. For protective relays, verification is complex due to their increased capabilities and the sophisticated control schemes that use them. This paper presents lessons learned from an industrial project of approximately 12 000 protective relays in a 110, 35, 10, 6, and 0.38 kV power generation, transmission, and distribution system.

The paper discusses power-system-related events from commissioning to after handover. Some events involve a single relay; others include complex schemes involving multiple electronic devices, communication protocols, and their impact on overall power system performance. Each event includes detailed analysis using relay waveform captures, sequential event reports, logic diagrams, instruction manuals, and functional design specifications to determine the root cause and corrective action.

Index Terms — Event Reports, Relay Protection, Generator Control, Root Cause.

I. INTRODUCTION

This paper highlights six different events that occurred during commissioning or just after system handover to the client. These events include a generator slow-response control event where a zero MW reading resulted in offloading of generation and how a failed surge arrester led to the field engineers finding an 87L line current differential relay disabled. A transformer compensation matrix setting error that resulted in a transformer differential trip for an external fault is also described, along with how mysterious feeder trips revised line construction practices. The remaining events include how a loss of 52A status resulted in two different trips for similar reasons, and how a load bank commissioning test uncovered an incorrect directional relay setting error. In sharing these events, the authors shall teach about the issues found during commissioning, describe how to use event reports to determine root cause, and illustrate how to avoid similar issues in the future.

II. SLOW-RESPONSE CONTROL SYSTEM EVENT

The commissioning team was tasked with updating relay communications settings for an in-service primary line protective relay. The protection scheme consisted of redundant line relays protecting a 110 kV line running from the utility. To follow the best-practice method for modifying relay settings for an in-service relay, the approved procedure included the team isolating the relay trip outputs by inserting a test plug and relying on the redundant relay to protect the line. Upon isolating the in-service relay, the facility's slow-response generator control system detected an unexpected dip in utility power import from 6 MW to 0 MW due to a loss of voltage in the relay and the relay being used as the control system's source of line megawatts. This resulted in the gradual offloading of the facility generation in an attempt to increase the utility import back to the desired tie-flow set point. The slow-response generator control system drove up the utility import from 6 MW to 73 MW until the system operators could get the situation under control. Fig. 1 depicts the power import from the utility during this incident, which was measured by another relay sensing the utility currents and voltages.

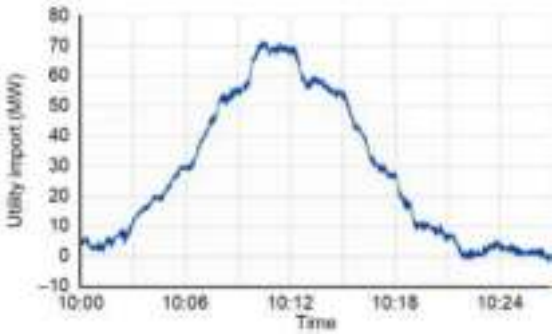

Fig. 1 Utility power import during the incident

The trip output contacts and voltage transformer inputs to the primary line Relay A were wired to the relay sharing the same 14-pole test block. All 14 poles of the test block were isolated by inserting the test plug in the test block socket, resulting in a loss-of-voltage measurement by the primary relay. The desired system response to a loss-of-voltage measurement is to switch the power-flow measurement source to the redundant backup Relay B, as described in the data-flow diagram in Fig. 2.

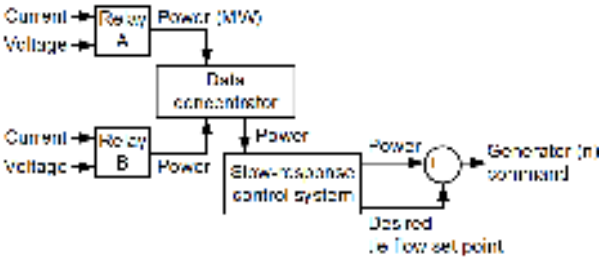

Fig. 2 Data-flow diagram

As shown in the data-flow diagram in Fig. 2, relay power measurements are communicated to the slow-response generator control system through a data concentrator. This is also shown in the process diagram in Fig. 3. The logic flow depicted in the process diagram is performed by the data concentrator.

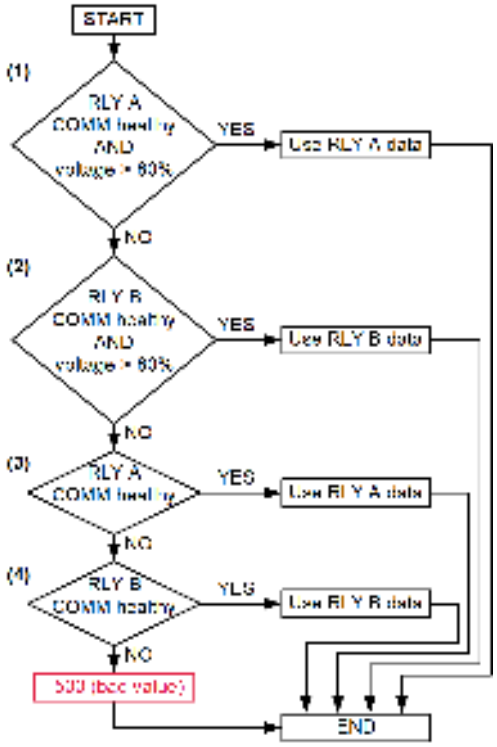

Fig. 3 Process diagram

As mentioned, the desired system response to a loss-of-voltage measurement is to switch the power-flow measurement source to the redundant relay. Decision Gate 1 in the process diagram evaluated to NO because of the loss of voltage in Relay A. Decision Gate 2 evaluated YES because Relay B communications were healthy and its voltage inputs were unaffected. Therefore, the power-flow measurement should have switched to Relay B as the source, and the slow-response generator control system should have taken no action.

In investigating the issue, the field engineers found that although communication between the data concentrator and Relay B appeared to be healthy to the electrical control system, the data received by the slow-response control system's data concentrator were flagged with having bad data quality. The active IEC 61850 configuration file was retrieved from Relay B; it confirmed that the data set being polled by the slow-response control system's data concentrator was set as a spare data set with blank data. Therefore, the Decision Gate 2 result in the process diagram was NO, and Relay A remained as the primary power-flow measurement source, which provided a reading of 0 MW to the slow-response control system. The corrective action to address the bad data quality was to update the IEC 61850 configuration, perform laboratory testing to verify correct functionality, and load the configuration file into Relay B.

If the sudden rise in the utility power import and facility generation offloading had gone unnoticed by the system operators, this condition could have caused power system instability, leading to potential islanding of the facility and frequency load-shedding to restore system stability. The process diagram also shows that even with healthy communications with both devices, the same outcome would have been expected for a simultaneous loss-of-potential condition on both relays caused by a blown voltage transformer (VT) fuse, because both relays are connected to the same VT.

To solve this problem, the team recommended sending a value of –500, which is identified by the slow-response control system as a bad value, if Decision Gates 3 and 4 evaluate to YES. The expected action of the slow-response control system when receiving that bad value is to take no action, which addresses the concern about the loss-of-potential condition. This recommendation is currently under review.

III. FAILED 110 KV SURGE ARRESTER REVEALS DISABLED LINE RELAY

In this event, a line current differential (87L) relay detected a line fault and tripped both line terminals. Power system operators quickly identified the root cause as a failed surge arrester. Fig. 4 is a photo of the failed surge arrester counter. Although this was a correct trip event, further analysis found that both the primary and backup 87L relay detected the fault, but only the backup 87L relay tripped. Fig. 5 and Fig. 6 show the backup and primary relay performances, respectively. Fig. 5 shows a trip issued by the backup relay and Fig. 6 shows that the primary relay did not trip.

Fig. 4 Failed surge arrester counter

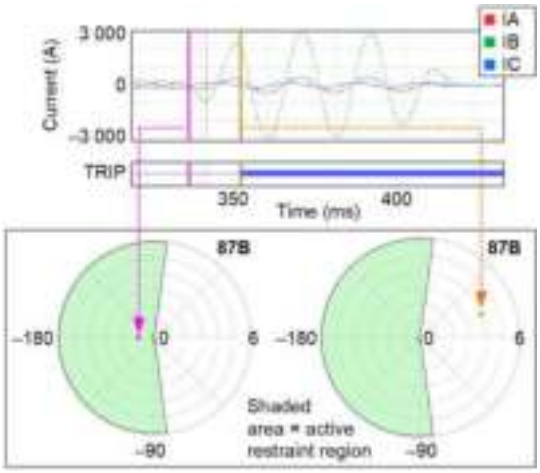

Fig. 5 Backup relay performance

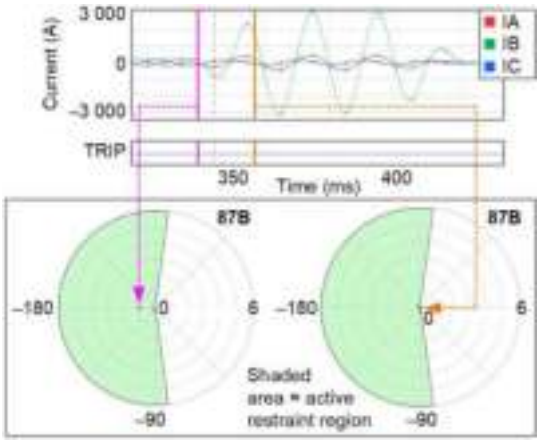

Fig. 6 Primary relay performance

Reference [1] describes the current-based alpha plane characteristic. In both Fig. 5 and Fig. 6, the pre-fault condition accurately plots at –1, indicating that the relay is secure (no trip condition). However, during the fault condition, both relays plot in the tripping region of the alpha plane, yet only the backup relay issued a trip.

After further investigation, the relay technician found that a communications channel watchdog alarm disabled the primary relay 87L protection. The communications channel watchdog alarm warns the user when an 87L protection element operation is repeatedly avoided by the disturbance detector or if the relay repeatedly receives an 87L direct transfer trip without an accompanying pickup of the disturbance detector. This alarm can occur during local or remote relay testing and, if not reset, can result in a disabled 87L relay element. The addition of the communications watchdog alarm is a security improvement in the relay design to help prevent undesired operations that can occur from communications-channel-based single event upsets (SEUs), as detailed in [1].

As a result of this event, the engineering team implemented several report changes to monitor the alarm counters and watchdog alarm status. Relay test engineers now include this report in the relay test documentation and verify proper operation prior to putting a relay into service.

Several months later, commissioning engineers used these updated reports and correctly identified a need to reset the 87L watchdog alarms prior to putting a line into service. Power system operators removed a 110 kV line from service and powered down the relays for a change in current transformer (CT) wiring. Local relay testing for the change in CT ratio occurred 11 days later. When this occurred, the watchdog alarm status (87ERR2) correctly asserted and disabled the 87L relay element. Fig. 7 shows an example report.

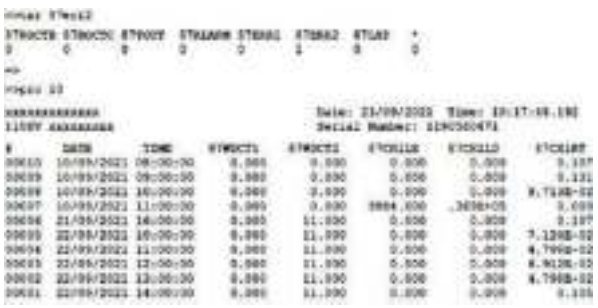
Fig. 7 Example report

Commissioning engineers reviewed the relay's sequential event report, verifying the test activity that occurred and resulted in an assertion of the 87L watchdog alarm. Then, they cleared the watchdog alarm before putting the relay back into service, and made sure that 87L protection was enabled.

IV. TRANSFORMER TRIP

The transformers in this system are protected using microprocessor-based protective relays. These relays have advanced calculation methods that can accommodate any transformer arrangement. The user-configurable set points of the protective relays were programmed according to the protection study report, and the user-configurable logic was programmed according to the logic diagrams issued by the engineering team. In addition, the protective relay has embedded logic with predefined algorithms for certain functions to ensure the correct operation of the relays. Verifying the correct implementation of the engineering design is part of the precommissioning and commissioning processes.

The main protection scheme used to protect transformers at this installation is transformer differential protection. It was important to set the current transformer phase-angle compensation setting [2] correctly to match the physical construction of the transformer, the phase-to-bushing connections, and the CT connections. Incorrect settings could lead to undesired operations. It was also important to verify the settings and wiring during commissioning and to properly record and manage changes until the system went into service.

The event described in this section includes an undesired operation of the transformer differential relay for an out-of-zone fault and an incomer relay trip for a feeder fault during the livening process. As shown in Fig. 8, the system is comprised of a step-up delta-wye transformer from a 10.5 kV brownfield feeder to a 35 kV greenfield substation. The transformer is protected with a transformer protective relay that provides differential and restricted earth fault protection. The incomer protective relay provides inverse-time overcurrent protection.

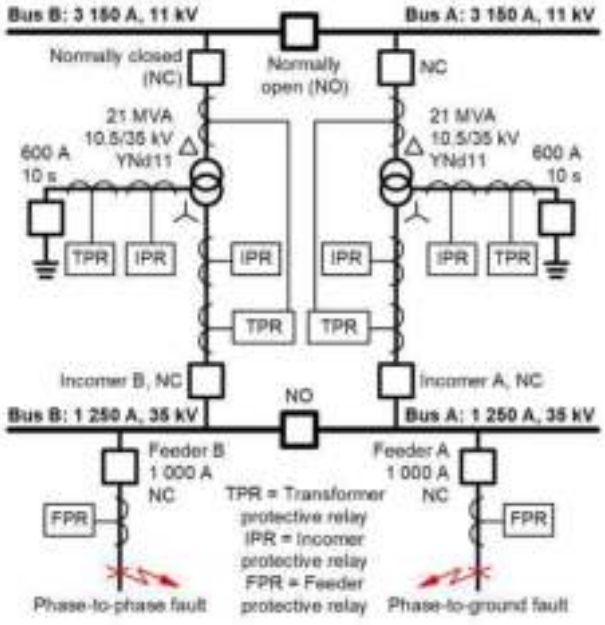

Fig. 8 System where transformer protection trip occurred

The 35 kV switchboard was energized using standard livening procedures after the precommissioning and commissioning procedures were completed. As the next step, the feeders were precommissioned and commissioned. The first feeder energized was reconductored because it used part of an existing line. During the livening process of that feeder in Bus B, multiple events were recorded and the protection tripped the Incomer B breaker.

Preliminary investigation found a BC phase-to-phase fault at the 35 kV Feeder B. Although the expectation was that the feeder would be tripped, the Incomer B breaker was tripped by both the transformer protective relay, for differential protection, and the incomer protective relay, for instantaneous overcurrent protection.

Event reports for each relay were extracted by the commissioning team to further understand the event. Fig. 9 shows the fault current waveform recorded at the feeder. It clearly shows the magnitude of the fault current around 1 500 A in Phase B and Phase C, lasting for five cycles. However, the trip (TR) Relay Word bit was not asserted either from 51P (600 A pickup) or 50P (2 700 A pickup). Instead, the incomer cleared the fault, suggesting a discrimination issue between Incomer B and Feeder B.

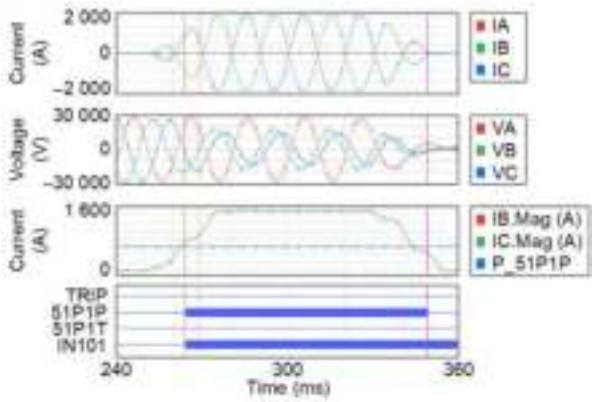

Fig. 9 Feeder event report

Fig. 10 shows the waveform recorded at the 35 kV Incomer B relay, where fault current with a magnitude of 1 500 A was seen on Phase B and Phase C, lasting close to five cycles. The 50P1P element picked up as soon as it hit the set point (1 000 A) and triggered a trip on 50P1T after 15 ms. The breaker opened (52A deasserted) 50 ms later.

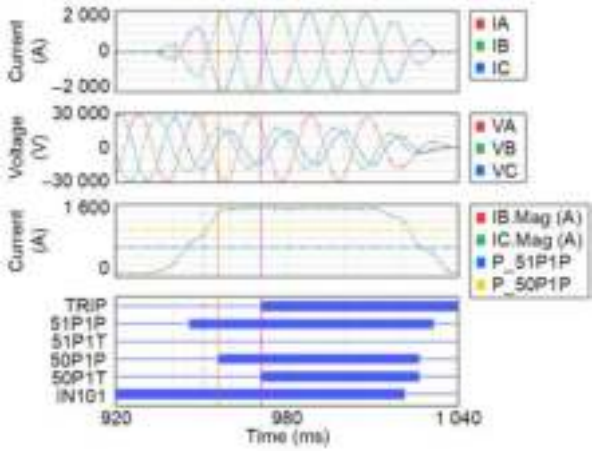

Fig. 10 Incomer B event report

A similar pattern can be seen when reviewing the event record on the transformer protective relay. The fault current was experienced in both the primary and secondary windings, and it was cleared within 60 ms after the Phase A restrained differential element (87RA) Relay Word bit was asserted, as shown in Fig. 11.

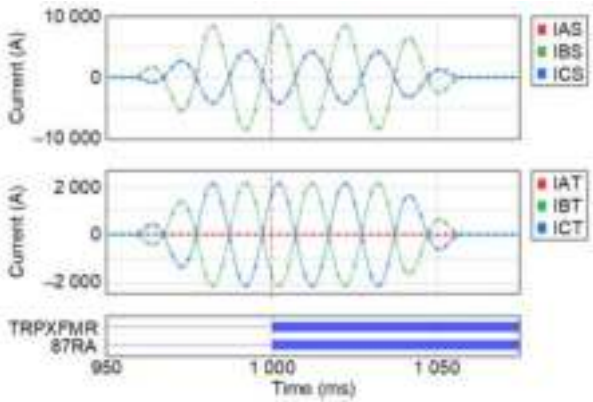

Fig. 11 Transformer relay event report

Fig. 12 explores further the operating current (IOP) and restraint current (IRT) measured during the event with the 87RA element assertion. Equation (1) shows the method of calculating operating (differential into the zone) and restraint (through the zone) current. Based on relay design, the “k” coefficient in (1) can vary. In the case of the relay in question, k = 1, and for an external fault, IOP should be zero. For an internal fault, IOP should ideally be equal to the IRT. As per (1) and Fig. 12, the fault impacts all three phases in the delta winding, and Phase B and Phase C experience fault current for the wye-connected secondary.

$$IRT = \frac{|\mathbf{I_1}| + |\mathbf{I_2}|}{k} \qquad IOP = |\mathbf{I_1} + \mathbf{I_2}| \qquad (1)$$

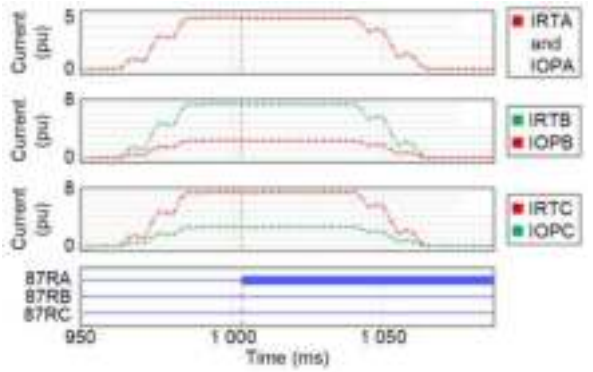

Fig. 12 Further exploration of 87RA assertion

Detailed analysis of this fault showed that the transformer protective relay determined an in-zone fault where Phase A operated, as the operating and restraint current pair plotted in the trip region of the percentage differential element. After performing basic tests, the team confirmed that the transformer was fault-free. Simultaneously, a detailed review of the set points was performed on the transformer protective relay.

It is important to set the compensation settings to match the transformer nameplate (an example nameplate is shown in Fig. 13), taking into account the phase-to-

bushing connections and the CT connections. These settings define the amount of compensation that the relay applies to each set of winding currents. For example, this correction is needed if both wye and delta power transformer windings are present but both sets of CTs are connected in wye. The effect of the compensation is to create phase shift and to remove zero-sequence current components [3].

Fig. 13 Internal connection and vector arrangement taken from the transformer nameplate (21 MVA)

After the review, it was found that the compensation settings were set to TSCTC = 0 (Winding 1 S input, 10.5 kV) and TTCTC = 11 (Winding 2 T input, 35 kV) to compensate for a YNd11 arrangement. According to Fig. 14 and Fig. 15, the set points were incorrect [2]. The commissioning engineers concluded that the settings should have been TSCTC = 0 (S input, 10.5 kV) and TTCTC = 1 (T input, 35 kV) to correctly compensate the differential currents for the step-up transformer.

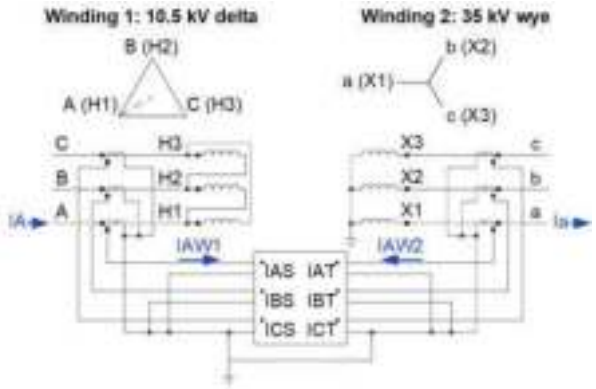

Fig. 14 Delta-wye transformer

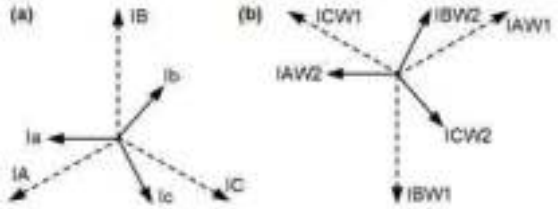

Fig. 15 Phase currents a) on system and b) at relay

A recalculation of IOP and IRT with correct settings was performed to verify the correct operation of the relay. If TTCTC = 1 for this fault, a replay of the event using the modified compensation settings, shown in Fig. 16, proves that the relay would have been secure (all operate current would be approximately 0 and restraint current would be 5 to 10 pu on all phases) for this operation [4].

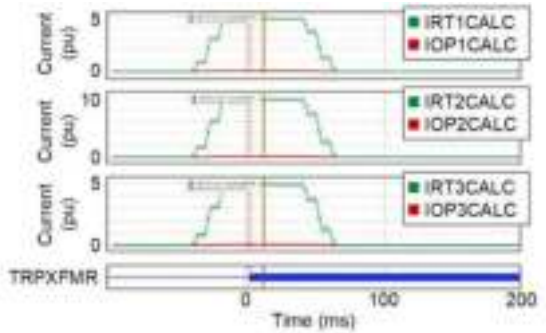

Fig. 16 IOP and IRT based on custom calculations using modified compensation setting TTCTC =1

Further analysis concluded that this error was detected on the protection study report during transformer primary injection testing and that the relay settings were then corrected; however, during the precheck phase of the livening process, the settings were reverted to match the latest protection study report, which failed to capture the red-line markup of the protection study made earlier.

Fig. 10, the Incomer B relay event report, shows a trip triggered from the instantaneous overcurrent (50P1T) set point. The incomer relay should not clear a downstream feeder fault; instead, the downstream feeder protection should clear the fault to maintain trip discrimination and allow the remaining feeders to continue to supply their load.

Fig. 17 shows the trip curve for both the incomer and feeder relays on this switchboard (not to scale). The instantaneous pickup (1 000 A) was mapped incorrectly to the trip equation of the incomer relay. The Feeder B instantaneous protection pickup (50P) was set at 2 700 A with a 400 ms time delay; however, the fault current seen in this scenario would not trigger a trip for 50P. Instead, a 51P element set at a standard inverse curve (IEC Class A) would have triggered in approximately one second to maintain discrimination between the upstream and downstream feeders with no changes to the set points.

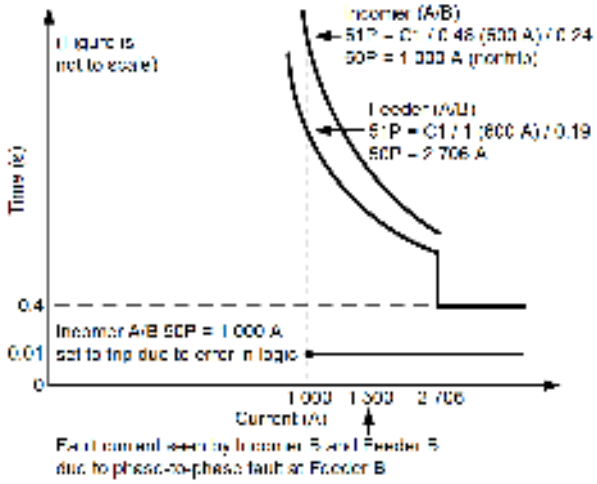

Fig. 17 Trip curve for incomer and feeder relays

After a design review, the team confirmed that the instantaneous element was supposed to block the automatic transfer scheme operation. However, the element was mapped to the trip equation incorrectly in the logic diagram. It was subsequently removed from the trip equation and the logic diagrams were updated.

Thorough review of the final set points and the logic diagram as part of the overall design can identify errors like this in commissioning activities while safe energizing practices are still maintained. In addition, it is important to carefully control changes made after commissioning to avoid overriding the corrections made during commissioning activities.

V. MYSTERIOUS TRIPS ON 35 KV FEEDER A

During the investigation of the 35 kV Incomer B (trip-logic error) and Incomer B transformer protective relay (compensation error), the team observed that the same errors were made for Incomer A and the Incomer A transformer relay. At this time, Incomer B was isolated and all feeders were energized only through Incomer A. This increased the overall load on Incomer A and elevated the operate and restraint current in the Incomer A transformer protective relay. A trip would isolate all power flow for all critical downstream feeders.

Prior to the implementation of changes to the transformer protective Relay A and the Incomer A relay, the Incomer A breaker tripped while it was single-ended, and power to all downstream feeders was lost. However, unlike the previous event on Incomer B, ground current was observed in this scenario. Analysis of the transformer relay event record shown in Fig. 18 revealed a through fault on the ground. The 35 kV wye-winding zero-sequence current and the transformer neutral current were 180 degrees apart with identical magnitudes, confirming that the fault was out-of-zone.

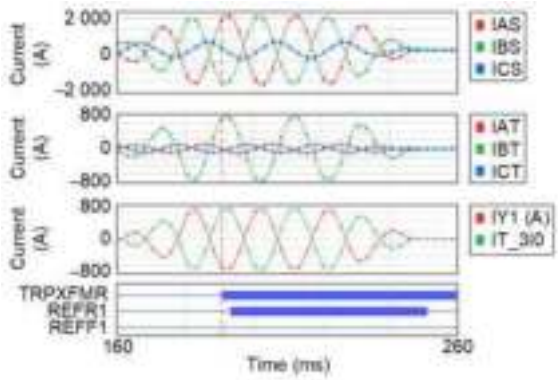

Fig. 18 Transformer relay event report

Analysis of the event report shown in Fig. 19 further confirmed that a downstream Phase-B-to-ground fault was experienced by the incomer relay. The incomer relay 50N1 protection picked up without issuing a trip. No trip was recorded in the feeder relay for the first trip event. This was due to the 600 ms time delay set on the ground protection; the fault was cleared by the transformer protective relay before 600 ms elapsed. Further investigation showed that the sequential event recorder feature in the protective relay used in this project to record the event was not set correctly to record ground fault pickups.

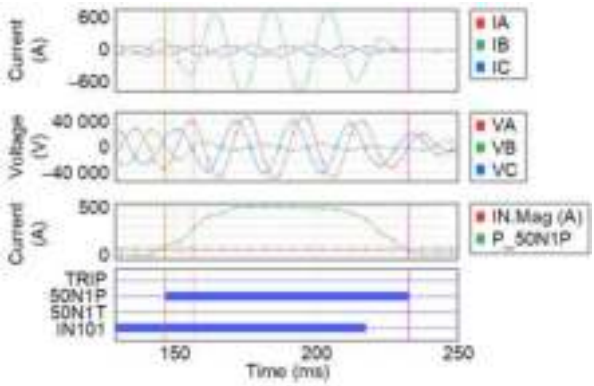

Fig. 19 Incomer A trip event report

Because of the criticality of the downstream loads, and the cause of the trip was established in the previous event, the 35 kV switchgear was livened using Incomer A and Incomer B. The bus tie was opened under normal operating conditions after correcting the transformer protection settings on both transformer relays and correcting the trip logic on both incomer relays. However, following the Phase-B-to-ground fault where the operations team did not find conclusive evidence for the cause of the trip events, power was restored to Feeder A, and the protection subsequently tripped two more times.

Fig. 8 shows the switchgear arrangement and the possible fault location on Feeder A. Fig. 20 shows the fault current recorded at the feeder relay for the first of the two Feeder A trips. The fault current gradually declined, then increased and remained stable until the fault was cleared. The fault was cleared soon after the 600 ms time delay included for discrimination purposes.

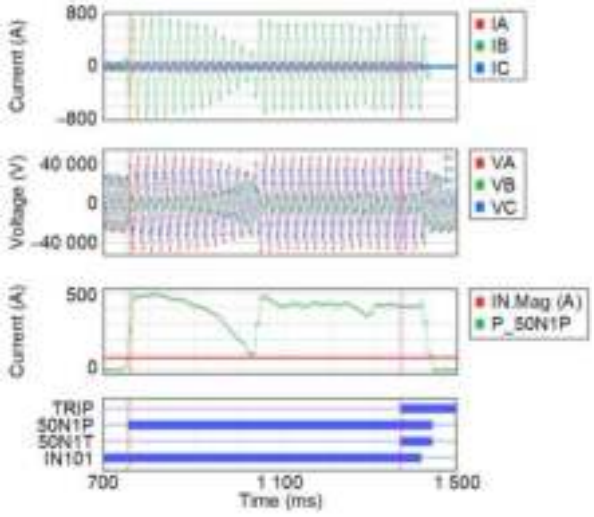

Fig. 20 Fault current recorded for first Feeder A trip

Fig. 21 shows the fault current recorded at the feeder relay for the second Feeder A trip.

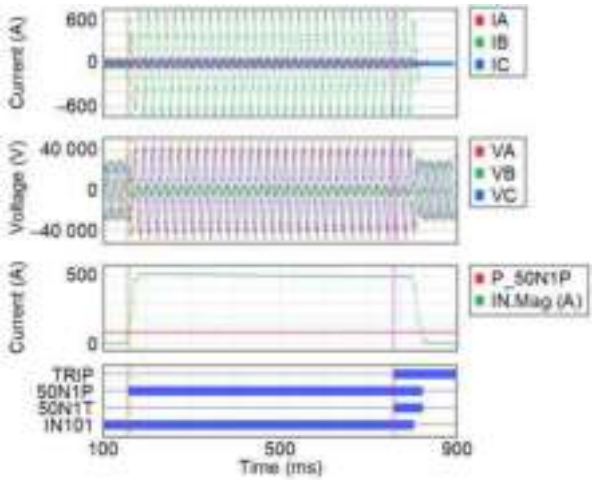

Fig. 21 Fault current recorded for second Feeder A trip

Unfolding the cause of the trips was not an easy task with the protective relays set incorrectly and with a fault that was not present all the time. An elimination method was used to pinpoint the fault location. After the initial trip on Incomer B, the major equipment was tested for insulation resistance and the engineers ran procedural tests prior to reenergization. (The details of these tests are not included here because they are tangential to the event analysis of the protective relay records.)

After the first trip on Feeder A, the team concluded that the fault was still present. However, without conclusive evidence, and because the load feeding the line was critical, the line was re-energized.

Similarly, the second trip on Feeder A was cleared soon after the 600 ms time delay. Because there was no conclusive evidence of equipment failure, the team walked the overhead line span to observe any physical damage. Initial investigation found nothing. After another walk of the line on a windy day (with westerly winds moving from west to east), the team observed that the separation between the overhead line for Phase B and the concrete poles was minimal, as shown in Fig. 22.

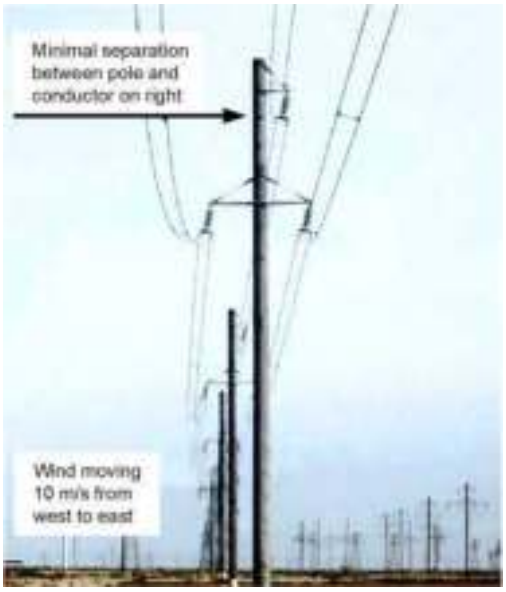

Fig. 22 Concrete pole with minimal conductor separation

The minimal separation meant that it was possible for the Phase B line to flashover to the pole. Analysis of wind data also confirmed that this geographical location is prone to receiving high-speed winds. With this information in hand, the operations team walked the line again and visually inspected poles using binoculars. They found signs of flashover damage on a couple of the concrete poles. Fig. 23 shows one example.

Fig. 23 Flashover damage on concrete pole

Because the operations team observed the overhead line during a westerly wind, their observations of the minimal line separation prompted them to investigate this issue in detail. They concluded that the repeated trips on Feeder A (after the initial trip due to incorrect settings) occurred with the transformer protective relay set correctly for transformer differential protection. They further concluded that the incomer relay was set correctly (as per the lessons learned from the previous event), with the instantaneous protection trip removed from the trip equation and instead used to block the automatic transfer scheme.

The feeder relay's sequential event recorder feature was updated to identify pickup fault current prior to trips, to help investigate any future trips. The team concluded that a combination of short crossarm length on the concrete poles and high westerly winds was the cause of the trip, although the existing installation did meet the project specifications. The construction team replaced the crossarms of the concrete poles with longer lengths to resolve the issue.

VI. PEER-TO-PEER COMMUNICATION TRIP EVENTS

This section discusses the lessons learned from two separate events that occurred on in-service feeder protective relays installed on a 35 kV switchgear. The system, which consists of a 35 kV switchgear with a main-tie-main bus configuration, a 380 V station service switchgear with a main-tie-main bus configuration (located in the same substation), and multiple 6 kV switchgears located downstream of the substation that also have main-tie-main bus configurations. All three main-tie-main

switchgears are equipped with transfer controllers for automatic and manual source transfer. These controllers are labeled 35kV_ATS, 6kV_ATS, and 380V_ATS in the single-line diagram. At the time of the event, only a single 6 kV switchgear was in service; therefore, only one 6 kV switchgear is depicted in the simplified diagram in Fig. 24.

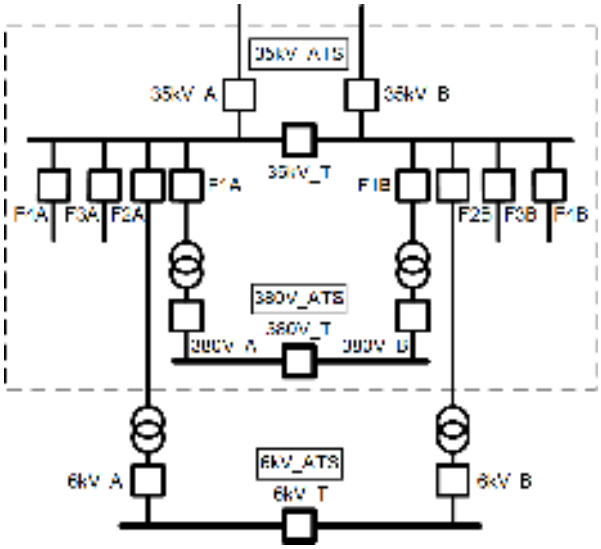

Fig. 24 Simplified single-line system diagram

The interlocking and an intertripping scheme between the relays used a peer-to-peer communication protocol. There is a peer-to-peer communication link between each pair of upstream and downstream relays; for example, the relays at Breakers F1A and 380V_A transmit data over a dedicated communications channel. One bit transmitted from upstream to downstream that is significant in the two events discussed in this section is the upstream breaker's status. Opening of the upstream breaker (e.g., F1A) results in the opening of the downstream incomer breaker (e.g., 380V_A) and the initiating of fast automatic transfer to the opposite source through the closing of the bus-tie breaker (e.g., 380V_T).

Event 1 occurred when new approved settings changes were being uploaded to the F1A relay. During the process of uploading new settings to the relay, the engineer loading the settings noticed switching operation in the 380 V switchgear located in the same substation. Once the settings upload to the F1A relay was successful, the engineer retrieved the sequence of events from the F1A, 380V_A, 380V_B, and 380V_T relays, as well as the 35kV_ATS and 380V_ATS controllers, for analysis. Examination of the sequence of events reports showed that a fast source transfer was initiated by 380V_A as the relay detected a momentary opening of the upstream F1A breaker.

Event 2 occurred during the replacement of the relays at F3B and F4B. The construction contractor accidentally created a short circuit on the control circuit, which caused the miniature circuit breaker (MCB) supplying control voltage to all Bus B relays to trip. There were reports of switching operation at both the local downstream 380 V switchgear and the remote downstream 6 kV switchgear shortly after the MCB tripped. Interrogation of the relays and controller at both the 380 V and 6 kV switchgears showed fast transfer initiation by the 380_B Incomer B relay due to the detection of the upstream Breaker 35kV_F1B opening.

In both Event 1 and Event 2, the root cause was determined to be an incorrect declaration of breaker-open logic in the upstream relay that was then transmitted downstream. Fig. 25 shows an excerpt from the F1A relay sequence of events from Event 1.

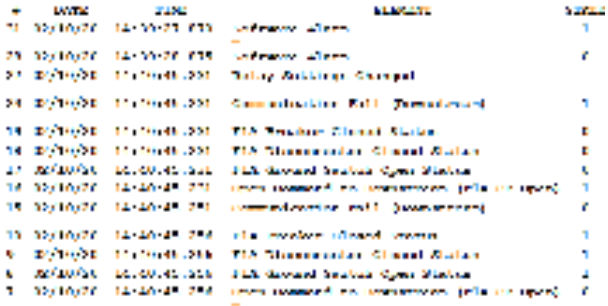

Fig. 25 F1A relay report excerpt for Event 1

Line 31 corresponds to the relay engineer logging into the relay write-access level, which triggered a software alarm and then self-reset after one second. New relay settings were uploaded to the relay in Line 27, which caused the relay to disable temporarily while accepting the new settings. Peer-to-peer communication with the downstream relay was also temporarily lost during this period for a total duration of 20 ms (Lines 23 to 15).

In this application, a second peer-to-peer channel was also enabled to communicate with an input/output (I/O) module to transmit and receive additional I/O, including breaker open (52b) status, breaker closed (52a) status, disconnect switch open/close status, and ground switch open/close contacts. As with the peer-to-peer communications channel with the downstream relay, the channel with the remote I/O module was also lost temporarily. During a period of time when the relay has poor peer-to-peer communication, it does not process any received bits on this channel, and instead maps these bits to user-defined default values, which in this case were all zeros. The 52a status deasserted for the duration of the communications channel failure (Line 19) and then reasserted (Line 10). During this time, both the 52a and 52b statuses were logically zero as seen by the relay. There is a period between Lines 15 and 7 when the communication with the downstream relay returned as healthy while the upstream relay was also sending an unexpected active-open command to the downstream relay.

Fig. 26 shows an excerpt from the 380V_A relay sequence of events. The command to trip the 380 V incomer breaker was issued in Line 51, which corresponds to the same time that the peer-to-peer communications became healthy again between the two relays.

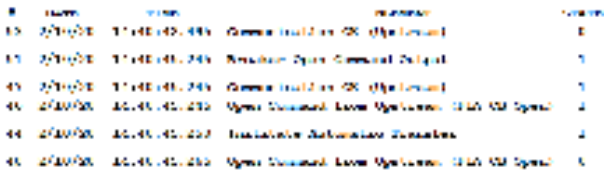

Fig. 26 380V_A relay report excerpt for Event 1

The open-command-to-downstream (F1A circuit breaker [CB] open) logic programmed in the F1A relay is

shown in Fig. 27. This is not a fail-safe logic, because the scenario described above would result in a false open command being issued to the downstream relay. Additionally, a failure of an I/O module, or a failure of the communications media between the relay and the I/O module, would also result in a false open command being issued to the downstream relay. The logic needs to be improved to remain secure for such conditions.

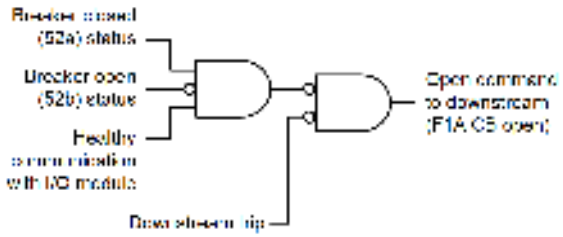

Fig. 27 F1A relay open-command-to-downstream logic

The loss of control voltage supply that occurred in Event 2 caused all relay and I/O module inputs to evaluate to logical zero (similar to what was experienced in Event 1). As a result, the upstream relays issued a false open command to the downstream relay, and in Event 2 this affected all relays on Bus B. All feeder relays on the 35 kV switchgear are programmed with open-command-to-downstream logic similar to that programmed in the F1A relay. Fig. 28 and Fig. 29 are sequence of events excerpts from the F1B and F2B relays, respectively. These reports show that both relays sent false open commands to the downstream relay after the 52a status deasserted.

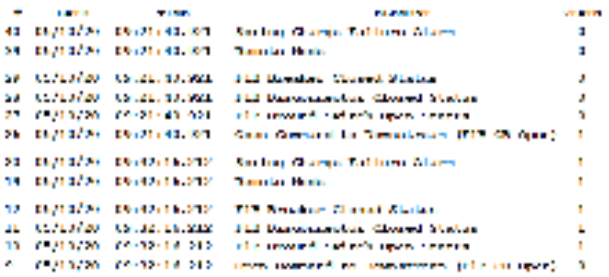

Fig. 28 F1B relay report excerpt for Event 2

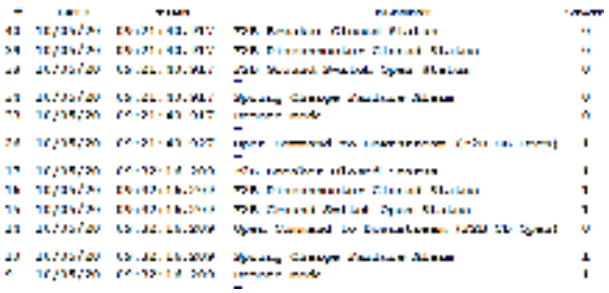

Fig. 29 F2B relay report excerpt for Event 2

The desired relay operation for both Event 1 and Event 2 was for the relays to remain secure and not issue an open command on either end of the feeder. The corrective action was to make this logic fail-safe for the scenarios described: sending settings to the relay, the failure of an I/O module, the failure of communications between a relay and I/O module, and the loss of control voltage supply. The logic depicted in Fig. 30 was implemented to address this. The logic does not use the inverted 52a status, and the total number of logical operators is significantly reduced to simplify the logic. The inverted downstream trip-received signal is used to supervise the logic to avoid sending the trip command back to the downstream relay where it originated.

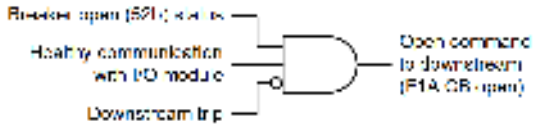

Fig. 30 Updated logic that addresses listed scenarios

VII. 380 V LOAD BANK TESTING

A 1 MW load bank test was performed by commissioning engineers on a new 380 V switchgear with a connected standby diesel generator (SDG). Fig. 31 shows a simple one-line diagram.

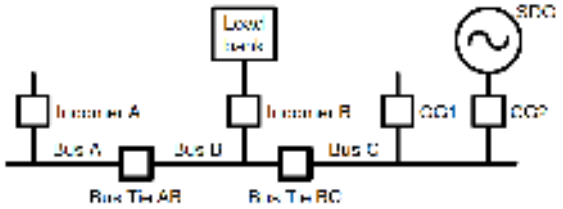

Fig. 31 One-line diagram for 380 V switchgear setup

The test required the SDG to energize Bus C and feed through a connected load bank on Incomer B. At the start of the test, both Bus Tie AB and Bus Tie BC were open. Bus A was isolated and energized by temporary generation to power auxiliary loads. When the test began, test engineers closed Bus Tie BC to connect the SDG to the load bank.

After the engineers closed the Bus Tie BC breaker, Breaker CG2 immediately tripped on a relay's directional phase overcurrent element. Fig. 32 shows the event report retrieved from one of the relays protecting Breaker CG2.

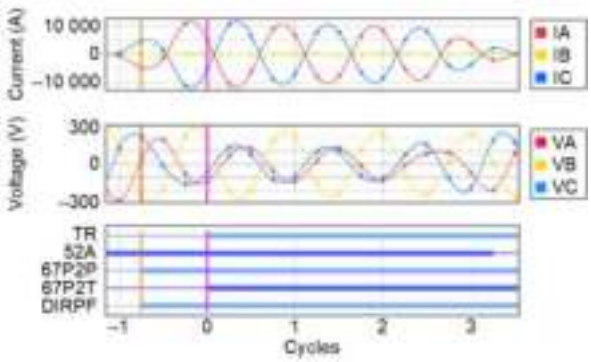

Fig. 32 Breaker CG2 relay event report

After analyzing the event report, commissioning engineers reviewed the cable connections from the load bank to Incomer B. Due to the temporary 1 MW load bank test connections to the motor control center (MCC), the commissioning contractor used two cables per phase to connect the load bank to the incomer. Two cables were correctly connected from the load bank Phase B to the incomer Phase B. However, when the four remaining

cables for Phase A and Phase C were connected, two of the cables were swapped, creating a 10 000 A phase-to-phase fault upon energization. Although this was the root cause of the trip, further analysis of the tripping times revealed another problem.

The protection for Breaker CG2 consists of two relays: a generator protective relay and a directional relay designed to trip for faults on the SDG side of the breaker. According to the event report, the directional relay asserted a trip in 15 ms. The directional element was set to the forward direction and based on the phase-to-phase fault on the Incomer B load bank; the directional relay should not have tripped. For this specific fault, Bus Tie BC should have tripped. Although the Bus Tie BC relay did pick up, the definite time (50) element of the CG2 backup directional relay was faster than the 51 element in the Bus Tie BC relay.

Upon review of the drawings, the engineering team found a discrepancy: the side (bus or generator) to which the CT star point was connected changed between design revisions (typical drawings, versus as-built). The relay settings engineer developed the settings based on the relay typical drawings and not the as-built drawings. Following this event and a review of the CT wiring, the commissioning team updated the settings to match the relay's intended zone of operation.

VIII. CONCLUSIONS

This paper detailed multiple events covering a wide range of applications in a 110, 35, 10, 6, and 0.38 kV power generation, transmission, and distribution system. The lessons learned from each event were described, as well as the solutions that the engineers applied.

In summary, proper settings management of as-left settings is critical. Engineering teams should clear any 87L communication watchdog alarms after local relay testing that might result in a blocking of the protection when a relay is placed in service. Microprocessor-based relay reporting functionalities should be used to their full advantage to continuously monitor for communication watchdog alarms.

For system design, it is important to document the basis for each relay set point change made during commissioning and to manage changes for all affected design documentation (such as protection settings studies). An example fail-safe intertripping logic design for peer-to-peer communications was shown in this paper. Engineers should also review CT-polarity-sensitive protection elements against as-built drawings to confirm the intended design.

The lessons learned by the teams working on this particular system can be applied to future projects by other engineers working on switchgear commissioning, livening, and operation.

IX. REFERENCES

[1] K. Zimmerman and D. Costello, "A Practical Approach to Line Current Differential Testing," proceedings of the 66th Annual Conference for Protective Relay Engineers, 2013.

[2] B. Edwards, D. G. Williams, A. Hargrave, M. Watkins, and V. K. Yedidi, "Beyond the Nameplate – Selecting Transformer Compensation Settings for Secure Differential Protection," proceedings of the 70th Annual Georgia Tech Protective Relaying Conference, 2016.

[3] *SEL-487E-3, -4 Transformer Protection Relay Instruction Manual*. Available: selinc.com.

[4] A. Hargrave, M. Watkins, and S. N. Ananthan, "Using Custom Calculations in SYNCHROWAVE Event to Apply Transformer Compensation Matrices," SEL Application Guide (AG2015-26), 2015. Available: selinc.com.

X. VITA

Matthew Watkins, PE, received his BS, summa cum laude, from Michigan Technological University in 1996 and an MBA from Cardinal Stritch University, Wisconsin, in 2003. He worked for five years as a distribution protection engineer responsible for the application of reclosers throughout the distribution system. In 2005, Matthew joined Schweitzer Engineering Laboratories, Inc. (SEL) as a product manager and later served as a field application engineer. He presently holds the title of senior engineer in SEL's engineering services division in Plano, Texas. He is a senior member of IEEE and a registered professional engineer in the state of Texas.
matt_watkins@selinc.com

Kamran Heshami, PEng, received his BASc in electrical engineering from the University of Waterloo in 2015. In 2015, he joined Schweitzer Engineering Laboratories, Inc. (SEL) as a project engineer in SEL's engineering services division in Toronto, Canada. He is a registered professional engineer in the Canadian provinces of Ontario, Manitoba, Newfoundland and Labrador, Nova Scotia, New Brunswick, and Prince Edward Island.
kamran_heshami@selinc.com

Michael T. Mendiola received both his bachelor's and master's degrees in electrical engineering from California Polytechnic State University, San Luis Obispo, in 2008. He joined Chevron in 2007, working in Chevron's Engineering Technology Company as an electrical engineering power systems specialist based in Houston, Texas. Since 2011, he has worked as a project electrical discipline engineer on a major capital project for Tengizchevroil (TCO). He is a member of IEEE.
mendiolam@chevron.com

Nilushan K. Mudugamuwa received his PhD in renewable energy from the University of Surrey, United Kingdom, in 2009, and BEng (honors) in electrical and electronic engineering at City University London, in 2004. He joined KBR London in 2010 as an electrical engineer and worked on a variety of projects. In 2015, he went on secondment to Azerbaijan and became responsible for onsite electrical engineering design for two offshore platforms. Since 2018, he has worked for Tengizchevroil (TCO) in Kazakhstan as an electrical protection relay discipline engineer. He is a Member of the Institution of Engineering and Technology (MIET) and has been registered as a Chartered Engineer from the Institution of Engineering and Technology, United Kingdom (IET UK) since 2014.
nmgn@chevron.com

SMART SENSOR FOR ADVANCED ELECTRIC MOTORS CONDITION MONITORING

Paper No. PCIC Europe EUR22_08

Jose Antonino-Daviu
Universitat Politècnica de València
Instituto Tecnologico de la Energia
Camino de Vera s/n
46022, Valencia
SPAIN

Israel Zamudio-Ramirez
Univ. Politècnica de València
Dep. Ingeniería Eléctrica
Camino de Vera s/n
46022, Valencia
SPAIN

Roque A Osornio-Rios
Univ. Autonoma de Queretaro
Engineering Faculty
San Juan del Rio 76806

MEXICO

Larisa Dunai
Universitat Politècnica de València
CITG
Camino de Vera s/n
46022, Valencia
SPAIN

Abstract - This paper exposes the recent advances of the authors' research group related to the development of proprietary intelligent sensors that combine the analysis of different electrical and thermal quantities. More specifically, the smart sensor relies on the analysis of currents, stray fluxes, and thermograms which can be measured in a non-invasive way and with simple primary sensors. The smart sensor combines the application of traditional tools based on stationary analysis (e.g., MCSA) with modern powerful methods relying on the analysis of transient currents and fluxes (ATCSA), which have proven to yield a high reliability for the diagnosis. Moreover, the sensor enables not only to analyze such quantities but also to provide a direct conclusion of the motor health thanks to the artificial intelligence tools that enable an automatic diagnosis. The paper explains the results obtained when diagnosing different faults in real machines, proving the powerfulness of the developed methodologies.

Index Terms — Electric motors, fault diagnosis, smart sensors, reliability, predictive maintenance, rotor faults, misalignments.

I. INTRODUCTION

Electric motors are core elements in many processes taking place in petrochemical plants. In a single plant there may be thousands of motors driving a diversity of loads such as pumps, fans, compressors, blowers, etc. According to some surveys, these machines can demand more than 40% of the energy generated in an industrialized country [1], which gives an idea of their importance in the industrial sector of nowadays societies.

Most of the electric motors operating in petrochemical plants are cage induction motors (IM). This is due to the higher reliability and lower cost of these machines in comparison with other alternative solutions that require a more complex maintenance or that have higher costs (e.g., synchronous motors). In spite of these facts, IM are not immune to the occurrence of different types of faults that are, indeed, rather common in these machines. Among them, rotor faults (broken rotor bars, cracked end rings), bearing failures (damages in bearing elements, lubrication problems, circulation of bearing currents, etc.), insulation faults (turn or ground wall insulation problems), stator asymmetries, core damages, coupling system problems (pulleys/belts systems problems or gear damages) have been reported as relatively frequent faults in these machines having, each of them, different fault occurrence rates [2]. These faults can have a negative impact both on the *motor reliability* and on the *motor efficiency*. Regarding the reliability, the occurrence of these failures can lead to motor outages with catastrophic effects in some parts of the motor that sometimes imply complex repairs and long production downtimes, as well as potential hazards to the process and to the own users. On the other hand, regarding the efficiency, the presence of these faults, even if they are at an incipient stage, implies a reduction on the motor efficiency, as it has been reported in previous works [3]. This means that, even if high efficiency motors are employed in the considered process, their actual efficiency will be much lower than the rated one if they operate with one of the aforementioned anomalies.

As a consequence of the previous facts, it becomes crucial to develop condition -based maintenance (CBM) methods that are able to reliably determine the motor condition, avoiding false indications (positive and negative) that can have very costly repercussions for the corresponding company. In this context, an intensive research effort has been carried out over recent decades to develop CBM methods based on monitoring and subsequently analyzing different motor quantities (vibrations, currents, fluxes, temperatures, torque, powers, acoustic emissions, partial discharges, etc.) with the aim of reaching a reliable conclusion about the health of the diagnosed motor parts. However, despite a huge number of different methods have been proposed, it has been proven that each of these approaches works well for the detection of specific failures and, even for these failures for which a technique may work well, there may be some situations in which it can fail, due to specific operating conditions or constructive characteristics of the diagnosed machine. In practice, each specific technique has been applied separately for the diagnosis of a certain range of faults for which it is considered to provide good results. For instance, current analysis has been typically employed to detect faults as rotor problems or eccentricities, while vibration analysis is the preferred option to detect mechanical failures (bearing damages, coupling system problems), while partial discharge analysis is mainly employed for monitoring the insulation condition.

Given the previous facts, a recent trend in the electric motors condition monitoring area relies on developing systems that combine the information obtained from the analysis of different quantities; since each quantity enables the diagnosis of a certain part of the machine, the combined information from all these quantities would allow obtaining a complete 'picture' of the motor condition. Despite some of these systems have been developed and are even commercially available, they mainly rely on the analysis of raw machine data or RMS values of the aforementioned quantities; they do not take advantage of the powerful information provided by most modern

techniques that have proven to give a more robust and reliable diagnoses of the motors (such as the recent technologies based on the transient analysis of currents and fluxes). This fact limits the reliability and accuracy of the few currently available solutions in this area.

This paper presents a novel smart sensor solution for induction motors condition monitoring. It is based on the joint analysis of current, stray-flux and infrared thermography data. For the analysis of current and stray flux signals, both classical methods based on the Fourier analysis of stationary signals and modern approaches based on the time-frequency analysis of transient signals are employed. These latter have shown very powerful results for the diagnosis of different faults, avoiding the occurrence of false indications that can be derived when using some techniques [4]. The smart sensor performs the measurement of the aforementioned quantities and their automatic processing, by applying the commented advanced approaches. Moreover, the smart sensor enables to reach an automatic diagnosis of the machine condition, since it is equipped with artificial intelligence methods that enable to interpret the results of the analyses and reach an automatic diagnosis conclusion.

II. UNDERLYING FAULT DIAGNOSIS METHODS

A. Analysis of motor currents

The analysis of current signals is one of the techniques that have been widely accepted in industry for the diagnosis of certain faults in electrical machines. The possibility of performing a remote condition monitoring (i.e., the current can be measured at the motor control center), the broad availability of different current sensors, and the relatively wide fault coverage of this technique, makes it a relevant diagnosis method for the detection of different faults, namely: rotor-related faults, eccentricities, bearing faults, and misalignments [5].

The most popular current-based approach that has been extensively used is the Motor Current Signature Analysis (MCSA). This technique relies on the application of the Fourier transform to the steady state current signals for monitoring specific fault-related frequency components, which are amplified when the motor is working under a fault condition. So then, it is known that different faults yield the amplification of different harmonics according to the severity of the fault (see Table I) [5], [6]. For example, it has been shown that broken rotor failures in cage motors will lead to the amplification of frequency components f_{BRB}, given by (1) and (2).

$$f_{BRB} = \left[1 \pm \frac{k}{p} \cdot (1 - s)\right] \cdot f_s \quad (1)$$

$$f_{BRB} = [1 \pm 2 \cdot k \cdot s] \cdot f_s \quad (2)$$

where f_s = fundamental frequency, *s*= slip, *k/p=1,3,5…*in (1) and *k*= 1, 2, 3, … in (2).

Nevertheless, despite the great advantages provided by the MCSA method, there are some drawbacks that need to be considered when performing a final diagnosis. In this regard, it is known that the relatively low sensitivity due to the attenuation of the fault signature at higher frequencies makes it difficult to detect eccentricity or bearing failures, especially in noisy field environments [5]. Therefore, the analysis of current signals for detecting mechanical defects related to the bearing, eccentricity, or load may require special signal processing techniques and methods able to extract relevant information. On the other hand, since this technique relies on the amplitude comparison of a limited number of frequency components. Consequently, non-fault-related phenomena such as constructive characteristics or operating conditions of the machine can sometimes mask/amplify similar frequency components [7] yielding potential false indications.

To avoid the previous problems, novel techniques based on the analysis of the current demanded by the motor under starting have been recently proposed (ATCSA) [7]-[8]. This approach has showed that the identification of the patterns created by the fault components under that transient by using appropriate time-frequency (t-f) tools is a suitable method to diagnose the presence of different faults in electric motors under a more robust basis. In this regard, recent investigations have reported problems of MCSA related to false indications caused by certain operating conditions of the motor (fluctuating loads, unloaded motors…) or constructive characteristics of the machine (presence of rotor cooling axial ducts, magnetic anisotropy issues) which can be easily avoided with the use of ATCSA [7]-[8].

Consequently, recent methods relying on current analysis are based on combining different methods such as MCSA and ATCSA to obtain a more robust diagnosis [9]. Even though, the combination with alternative techniques is desired to expand the range of motor faults that can be diagnosed since current analysis covers a specific range of motor failures. In this context, stray flux analysis and infrared thermography are excellent technologies to this end.

B. Analysis of stray fluxes

The analysis of stray flux signals has proven to be a useful tool, both for the diagnosis of faults in electric machines by yielding comparable results to those of well-established techniques, and as a complement to other fault detection methods (such as MCSA) due to its diverse advantages and capabilities such as very low cost of the required sensors (Hall-effect sensors, coil-based sensors, flexible probe sensors, etc.), non-invasive nature (no sensors are required inside the machine), efficient and reliable in cases where conventional techniques produce false indications (i.e., rotor axial air ducts, rotor magnetic anisotropy, low frequency load oscillations, etc.), and flexibility / simplicity for the installation of the available sensors [10]-[11].

The techniques based on the analysis of stray flux rely on the fact that the different components of the magnetic field that is present around the electric motor (i.e., radial stray flux, axial stray flux, axial + radial stray flux) are caused by the stator and rotor currents, which are modified when the electric motor operates under a fault condition [10]. Conventional methods perform a Fourier analysis to the steady state stray flux signals for monitoring specific frequency components, which are amplified when the analyzed motor is working under a

fault condition. Table I shows the most common frequency contents amplified in the stray flux signals when the motor operates under a specific fault. These fault-related components have been validated in several research papers [12]. In this way, stray-flux-based techniques turn to be very efficient and reliable for the detection of several faults, namely: broken rotor bars, eccentricities, misalignments, bearing-related faults, and inter-turn short circuits. Thus, plenty of information can be obtained by analyzing the different stray flux components by using suitable time-frequency decomposition tools and specific methods adapted for these purposes. However, these conventional methods are restricted due to intrinsic contraints inherent to the Fourier transform (i.e., non-suitable for non-stationary signals, potential false indications caused by constructive characteristics or operating conditions of the machine, etc.).

In this regard, the proposed smart sensor takes advantage of the high amount of harmonic information, and it discerns the diverse fault-related patterns according to the fault and its evolution during the startup by applying suitable time frequency decomposition tools and artificial intelligence methods. In this way, the false diagnosis encountered in traditional methods may be overcome since the patterns observed during the startup turn to be a very reliable indicator of a fault.

TABLE I. MAIN FREQUENCY COMPONENTS AMPLIFIED BY DIFFERENT FAULTS IN THE CURRENT AND STRAY FLUX SIGNALS

CURRENT	
Rotor faults	$f_{BRB} = \left[1 \pm \frac{k}{p} \cdot (1-s)\right] \cdot f_s$ $f_{BRB} = [1 \pm 2 \cdot k \cdot s] \cdot f_s$
Eccentricities/ misalignments	$f_{ecc}=f_s \cdot \pm f_r$
Bearing outer race	$f_{BO} = f_s \pm k \frac{N}{2} f_r \left(1 - \frac{D_b}{D_c}\cos(\beta)\right)$
Bearing inner race	$f_{BO} = f_s \pm k \frac{N}{2} f_r \left(1 + \frac{D_b}{D_c}\cos(\beta)\right)$
STRAY FLUX	
Rotor faults	$s \cdot f$, $3 \cdot s \cdot f$ (axial) $f \cdot (1 \pm 2 \cdot s)$ (radial)
Eccentricities	$f_{ecc}= f \cdot \pm f_r$
Stator interturn short circuits	$f_{stator} = k_{odd} \cdot f_s \pm n \cdot f_r$
where f_r=Rotor rotational speed, k: integer (= 1, 2, 3, …), N: number of balls, k_{odd} is an odd integer and n is an integer different than $6 \cdot j \pm 1$ (j is an integer)	

C. Analysis of infrared data

Infrared thermography (IRT) is a noninvasive technique that has taken a great relevance in the last years due to the significant advances in the features of infrared cameras and their progressive availability. Additionally, the remarkable advance in image processing techniques and their feasibility to be implemented in electronic devices has allowed to acquire thermograms and process them in situ, which opens a wide variety of possibilities and applications that demand online diagnosis schemes.

Currently, the techniques and methodologies implemented in the field of electric motor fault detection are essentially based on the application of various image processing techniques and parameter extraction at various stages. In this regard, most of the methodologies found in the literature perform an image pre-processing stage in which the background noise is extracted from the image. Subsequently, a feature extraction stage obtains some parameters related to a fault, and finally a feature selection is performed to gather the most significant characteristics. Besides these common stages, some papers have proposed the integration of artificial intelligence techniques to automate the final diagnosis task, as these methods are able to classify data among different classes. These techniques have shown good results for the diagnosis of different faults such as bearing-related faults, fan failures, broken rotor bars, stator unbalances, misalignments, and transmission system problems [13]. However, most of the proposed methodologies require to manually enter some parameters to the IRT camera, such as relative humidity, condition temperature, emissivity, absolute temperature, and distance to the inspected object, which under practical terms limits its application [13]. Additionally, thermographers in the industry have created their own thresholds, adapted for each specific machine, which have been derived from their own experience in the field, thus increasing the dependence on the thermographer expertise and making the application of the technique more subjective.

Therefore, novel techniques must be able to adapt to different operating and installation conditions, in such a way that the results must be invariable to the abovementioned parameters. Moreover, it is highly relevant to generate methodologies able to incorporate thermographic sensors that do not require external calibration, since in practical terms it is not feasible to regulate the camera with external devices each time the application requires it. In this sense, the proposed smart sensor implements image processing techniques capable of generating automatic diagnoses regardless of the position in which the thermographic sensor is installed, which do not require a calibration through external modules. In this way, an invariable methodology to installation-related problems is achieved. On the other hand, by extracting parameters obtained from thermographic images and processing them through artificial intelligence techniques, the proposal is able to combine the information from various variables to generate a more robust final diagnosis.

III. SMART SENSOR STRUCTURE

The proposed smart sensor is essentially based on a processing unit / user interface, a primary thermographic sensor, a primary current sensor and a primary triaxial stray flux sensor. All these components can be observed in Fig 1. This Figure also shows a schematic diagram detailing the general overview of the proposal. As it can be seen there, the smart sensor has the ability to remotely intercommunicate with the different sensors through wireless protocols. Logically, in this way, the information coming from the different sensors (which is related to the various failures that usually occur in electrical machines)

can be processed remotely, providing flexibility and practicality of operation to the proposal. In addition, by means of integrated wired connectors it is possible to acquire the signals in a wired approach for the cases in which the application demands this feature. This attribute may be very helpful in noisy environments where the wireless signals may be lost or mixed due to interferences.

The processing unit, which is the main element where all the signal processing and classification tasks are performed, is enabled to perform different operations, namely: acquisition and processing of the signals collected by the different sensors, development of an automatic assessment of the general condition of the electric machine under analysis, and display of the final results to the end user. These final results are displayed by means of a graphical user interface that indicates the overall health status of the machine. Thus, with the proposed approach it is possible to continuously and wirelessly monitor the health of the electric motor, being able to alert the end users of the occurrence of any anomaly related to a fault in a component of the machine under analysis in an effective and timely manner, this is, before any catastrophic and irreversible failure may occur.

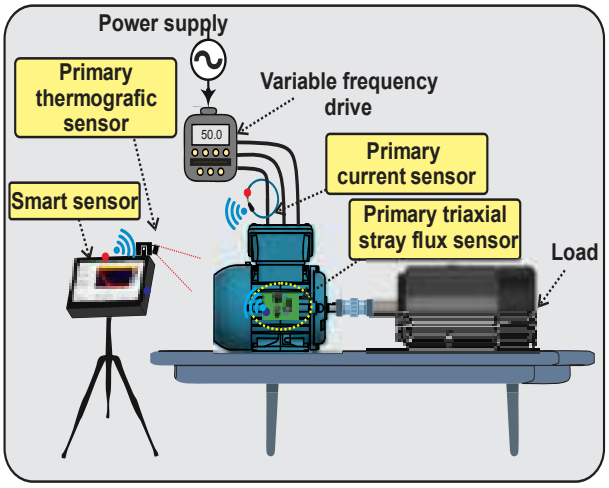

Fig. 1. Smart sensor general overview.

On the other hand, the architecture and configurability of the smart sensor enable the implementation of a wide variety of functions, algorithms and specialized data processing and classification techniques, specific to each of the stages of the proposed methodology. Fig. 2 shows the general architecture of the processing unit and its essential elements. As observed, in the first stage, the different primary sensors (i.e., triaxial stray flux sensor, current sensor, and thermographic sensor) that provide fundamental information for the final diagnosis of the health of the machine are connected to the main processing unit. Subsequently, a signal acquisition module (DAS) is prepared for conditioning the signals coming from the different sensors in such a way that their output can be handled by the analog-to-digital converter. Once the signals are digitized (output of the DAS module), the single board computer (SBC) enables to process the signals simultaneously through the implementation and application of specialized signal processing and classification techniques. Finally, a user interface allows to generate an interaction between the smart sensor and the end user (by means of a touch screen), and provides an automated final diagnosis.

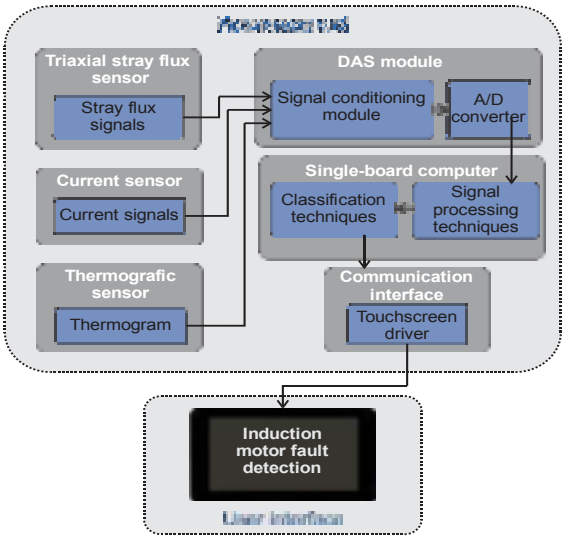

Fig. 2. Block diagram of the proposed smart–sensor general architecture.

IV. RESULTS

This section shows and describes the results obtained with the developed smart sensor when it is installed in a kinematic chain based on an induction motor rated 2P, 1 hp, 220 V (WEG 00236ET3E145T-W22), a belt and pulleys transmission system, and an alternator acting as a load (set at 25% of the rated load). The results shown below correspond to screenshots obtained from the smart sensor display.

Fig. 3 shows the main screen that displays the results obtained from the automatic diagnosis performed by the sensor. As it can be observed, the condition of different motor parts is evaluated, informing on different possible faults taking place in the machine, namely: broken rotor bars, misalignments, eccentricity faults, bearing faults, unbalance-related faults and transmission system problems. Moreover, the severity of each fault is assessed and displayed according to a color scale using a traffic light system: green (indicating that the corresponding part of the motor is operating under health conditions), yellow (informing on an alert, i.e., the motor is operating under incipient fault conditions) and red (the most critical alarm status, indicating a severe level of failure that requires imminent attention). Thus, the different failure levels evaluated by the smart sensor allow the end user to schedule adequate maintenance actions. Additionally, if any indicator reaches a critical state, an alarm signal is sent to the end user, indicating the origin of the failure, hence avoiding irreversible failures that may cause high repair costs. For example, Fig. 3 (c) shows the results obtained for a motor operating under a broken rotor bar alert state (in this case, the motor was operating under one broken rotor bar). As the results show, a yellow flag is set, indicating an alert related to the rotor condition. On the other hand, the misalignment, eccentricity, and bearings state are indicated by a green traffic light, denoting a healthy condition (the induction motor under study was operating in good condition apart from the one broken rotor bar). Finally, the smart sensor provides an estimation of the power supply frequency and slip, as shown in Fig. 3 (a). Moreover, an indication of the captured signals is displayed, as shown by Fig. 3 (b).

Fig. 3. Main screen of the smart-sensor graphical user interface showing an automatic final diagnosis: (a) estimated power supply frequency, (b) available captured signals, (c) automated final diagnosis.

On the other hand, the smart sensor can provide in-situ relevant information in addition to the automatic health assessment of the motor (which is generated by analyzing the combination of current, stray flux, and thermographic signals). In this regard, it is possible to observe the acquired infrared images, which allow a deeper study of expert users, in case that it is of interest. Fig. 4 shows an example of the results provided by the smart sensor when analyzing an induction motor under misalignment fault conditions. In this Figure, the hottest points can be observed in the belts and pulleys transmission system (shown by a color palette), where the blue color indicates the coldest point, and the red color indicates the hottest point.

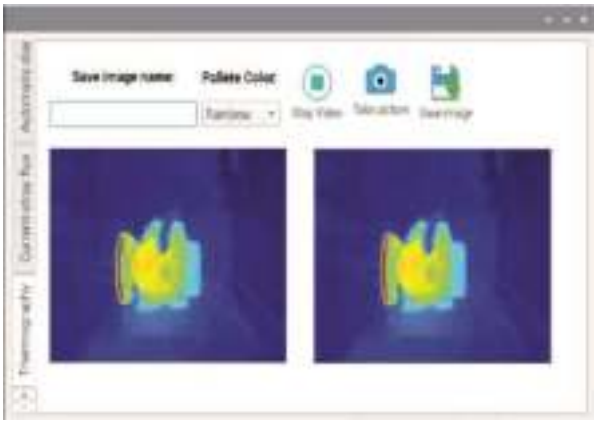

Fig. 4. In-situ infrared thermal images provided by the smart-sensor.

Additionally, if even more specific data is required, the smart sensor can provide the Fourier spectra of the different acquired signals (i.e., stray flux signals, and current signals), once it automatically detects that the machine is not operating under transient states. In this way, the end user can obtain immediate information (without needing to transfer the signals to a PC) in order to obtain more detailed conclusions, which can help to get a general idea of the motor health, and to determine the amplitudes of specific failure-related components.

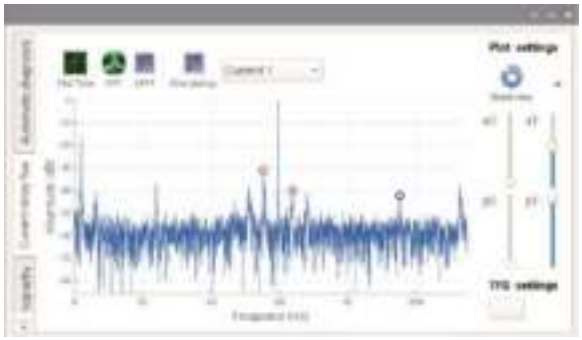

Fig. 4. In-situ FFT spectrum provided by the smart-sensor when analyzing an induction motor having one broken rotor bar.

Last but not least, the smart-sensor is able to automatically determine and isolate the transient startup state of the motor to subsequently compute the short-time Fourier transform (STFT) (ATCSA approach) and display a time-frequency map of the startup transient to the end user. In this regard, Fig. 4 shows a time-frequency map (provided by the smart sensor) obtained by analyzing an induction motor operating under two broken rotor bars. In this way, it is possible to determine and observe the existence of fault patterns evolving during the starting, thus providing a wide number of diagnostic options for an end-user requiring more specific and detailed analysis.

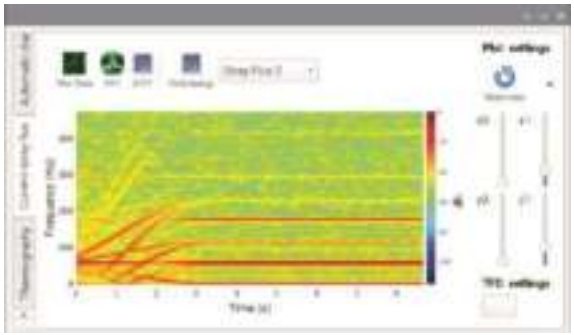

Fig. 4. In-situ time-frequency map provided by the smart-sensor when analyzing the startup of an induction motor having two broken rotor bars.

V. CONCLUSIONS

This paper presents a novel smart sensor based on the advanced analysis of stray flux, current signals, and thermographic data for the diagnosis of failures in induction motors. The proposal relies on the analysis of these quantities by means of advanced signal processing techniques at stationary and transient conditions. In this way, the excellent advantages that each of the techniques provide are obtained, providing a much higher reliability for the detection of faults. To achieve this, the research group has developed novel methodologies and implemented advanced time-frequency signal processing techniques that can capture the fault-related evolution patterns during transient states, especially during the start-up transient, which allow obtaining a robust and reliable final diagnosis. Moreover, the incorporation of artificial intelligence techniques allows the extraction and retention of the most relevant characteristics that each of

the analyzed magnitudes contains, in such a way that it allows for the fusion of information, which is used simultaneously in order to obtain a final diagnosis. Finally, the results obtained show the excellent performance achieved by the smart sensor, in such a way that a wide variety of faults can be diagnosed automatically in an online way, enabling to achieve optimum maintenance actions, preventing unscheduled downtimes and reducing maintenance costs. In its current version, the proposed smart sensor, can automatically diagnose: broken rotor bars, misalignment failures, eccentricity failures, bearing-related failures, and transmission system problems.

VI. ACKNOWLEDGEMENTS

This work was supported by the Spanish 'Ministerio de Ciencia Innovación y Universidades' and FEDER program in the framework of the 'Proyectos de I+D de Generación de Conocimiento del Programa Estatal de Generación de Conocimiento y Fortalecimiento Científico y Tecnológico del Sistema de I+D+i, Subprograma Estatal de Generación de Conocimiento' (ref: PGC2018-095747-B-I00).

VII. REFERENCES

[1] F. S. Al Badawi and M. Al Muhaini, "Reliability modelling and assessment of electric motor driven systems in hydrocarbon industries," IET Electr. Power Appl., vol. 9, no. 9, pp. 605–611, 2015, doi: 10.1049/iet-epa.2015.0089.

[2] W. T. Thomson and M. Fenger, "William T. Thomson and Mark Fenger," IEEE Ind. Appl. Mag., no. August, 2001.

[3] M. Garcia, P. A. Panagiotou, J. A. Antonino-Daviu, and K. N. Gyftakis, "Efficiency assessment of induction motors operating under different faulty conditions," IEEE Trans. Ind. Electron., vol. 66, no. 10, pp. 8072–8081, 2019, doi: 10.1109/TIE.2018.2885719.

[4] J. A. Ramirez-Nunez et al., "Evaluation of the Detectability of Electromechanical Faults in Induction Motors Via Transient Analysis of the Stray Flux," IEEE Trans. Ind. Appl., vol. 54, no. 5, pp. 4324–4332, 2018, doi: 10.1109/TIA.2018.2843371.

[5] S. Bin Lee et al., "Condition Monitoring of Industrial Electric Machines: State of the Art and Future Challenges," IEEE Ind. Electron. Mag., vol. 14, no. 4, pp. 158–167, 2020, doi: 10.1109/MIE.2020.3016138.

[6] M. Riera-Guasp, J. A. Antonino-Daviu, and G. A. Capolino, "Advances in electrical machine, power electronic, and drive condition monitoring and fault detection: State of the art," IEEE Trans. Ind. Electron., vol. 62, no. 3, pp. 1746–1759, 2015, doi: 10.1109/TIE.2014.2375853.

[7] J. Antonino-Daviu, S.B. Lee and E. Wiedenbrug, "Reliable Detection of Rotor Bar Failures in Induction Motors Operating in Petrochemical Plants", *PCIC Europe Conference Record",* 2014.

[8] J. Antonino-Daviu, J. Pons_llinares and S.B. Lee, "Advanced Rotor Fault Diagnosis for High Voltage Induction Motors via Continuous Transforms", *PCIC Europe Conference Record",* 2015.

[9] J. Antonino-Daviu, A. Quijano-Lopez, V. Climente-Alarcon, and C. Garin-Abellan, "Reliable Detection of Rotor Winding Asymmetries in Wound Rotor Induction Motors via Integral Current Analysis," IEEE Trans. Ind. Appl., vol. 53, no. 3, pp. 2040–2048, 2017, doi: 10.1109/TIA.2017.2672524.

[10] Y. Park et al., "Stray flux monitoring for reliable detection of rotor faults under the influence of rotor axial air ducts," IEEE Trans. Ind. Electron., vol. 66, no. 10, pp. 7561–7570, 2019, doi: 10.1109/TIE.2018.2880670.

[11] J. A. Ramirez-Nunez et al., "Evaluation of the Detectability of Electromechanical Faults in Induction Motors Via Transient Analysis of the Stray Flux," IEEE Trans. Ind. Appl., vol. 54, no. 5, pp. 4324–4332, 2018, doi: 10.1109/TIA.2018.2843371.

[12] I. Zamudio-Ramirez, R. A. A. Osornio-Rios, J. A. Antonino-Daviu, H. Razik, and R. de J. Romero-Troncoso, "Magnetic Flux Analysis for the Condition Monitoring of Electric Machines: A Review," IEEE Trans. Ind. Informatics, vol. 3203, no. c, pp. 1–14, 2021, doi: 10.1109/TII.2021.3070581.

[13] R. Alfredo Osornio-Rios, J. A. Antonino-Daviu, and R. De Jesus Romero-Troncoso, "Recent industrial applications of infrared thermography: A review," IEEE Trans. Ind. Informatics, vol. 15, no. 2, pp. 615–625, 2019, doi: 10.1109/TII.2018.2884738.

VIII. VITA

Jose A. Antonino-Daviu received the M.Sc. and Ph.D. degrees in electrical engineering, both from the Universitat Politècnica de València, Valencia, Spain, in 2000 and 2006, respectively. He has worked for IBM, involved in several international projects. He is currently an Full Professor in the Department of Electrical Engineering, Universitat Politècnica de València. He was an Invited Professor at Helsinki University of Technology, Finland, in 2005 and 2007, Michigan State University, USA, in 2010, Korea University, South Korea, in 2014, Université Claude Bernard Lyon 1, France, and Coventry University, U.K., in 2016. He is a coauthor of more than 260 papers published in technical journals and conference proceedings. He is also the coauthor of one international patent.

Dr. Antonino-Daviu is an Associate Editor of the IEEE TRANSACTIONS ON INDUSTRIAL INFORMATICS and a member of the Editorial Board. He received the IEEE Second Prize Paper Award of the Electric Machines Committee of the IEEE Industry Applications Society (2013). He also received the Best Paper Award in the conferences IEEE ICEM 2012, IEEE SDEMPED 2011and IEEE SDEMPED 2019 and the "Highly Commended Recognition" of the IET Innovation Awards in 2014 and in 2016. He was the General Co-Chair of SDEMPED 2013 and is a member of the Steering Committee of IEEE SDEMPED. In 2016, he received the Medal of the Spanish Royal Academy of Engineering (Madrid, Spain) for his contributions in new techniques for predictive maintenance of electric motors. In 2018, he has been awarded with the prestigious 'Nagamori Award' from the Nagamori Foundation (Kyoto, Japan). In 2019, he received the SDEMPED diagnostic achievement Award (Toulouse, France) for his contributions to electric motors advanced diagnosis.

joanda@die.upv.es

Israel Zamudio-Ramírez received his M.S. degree in mechatronic from the Autonomous University of

Queretaro, Mexico, in 2019. He is currently working towards the Ph.D. degree at the Autonomous University of Queretaro with the Department of Mechatronics, Mexico and at the Universitat Politècnica de València with the Department of Electrical Engineering, Spain. His research interests include monitoring and diagnosis of electrical machines, embedded systems and hardware signal processing for engineering applications on FPGA.

Roque A. Osornio-Rios received the Ph.D. degree in mechatronics from the Autonomous University of Queretaro, Queretaro, Mexico, in 2007. Dr. Osornio-Rios is a National Researcher level 2 with the Mexican Council of Science and Technology, CONACYT. He is currently a Head Professor with the University of Queretaro, Mexico. He is advisor for more than 80 theses, and a coauthor of more than 100 technical papers published in international journals and conferences. His fields of interest include hardware signal processing and mechatronics. Dr. Osornio-Rios is fellow of the Mexican Academy of Engineering. Prof Osornio-Rios received the National Award in Investigation 2016 for Mexican Academy of Science. He is part of the editorial board of Journal and Scientific and Industrial Research.

Larisa Dunai, Associate Professor at Universitat Politecnica de Valencia (UPV), obtained her MSc degree in Electronic Engineering in 2003 from Technical University of Moldova. Afterwards, she joined that University as an Assistant professor at the Radio electronics and Telecommunications Department. In 2007 she started working as a researcher in the Research Center in Graphic Technology (CITG) of the UPV. In November 2008 she became Assistant professor of the Graphic Design Department. In 2010 obtained her PhD at UPV. In 2013 she received the MIT Innovators Award for Spain and in 2014 the Michael Richey Medal from Royal Institute of Navigation (UK).

SUPPORTING DECARBONISATION – AN INTRODUCTION TO ELECTRO-MECHANICAL ASD

Paper No. PCIC Europe EUR22_09

Simon Turnbull
Voith Turbo Ltd
United Kingdom

Justin Mason CEng FIET
Trydanol Energy Solutions Cyf.
United Kingdom

Michael Rimmer
Costain Ltd
United Kingdom

Wissam Moubarak
J.M. Voith SE & Co. KG
Germany

Abstract - Electrification of energy plants is an evolving trend as operators look to decarbonise facilities. This paper focuses on electro-mechanical ASD which can be an effective solution to turbine driver replacement or new plant versus large power electronic ASD, for speed regulation of driven equipment up to 20MW.

Electro-mechanical ASD utilize the power split principle which can result in efficiency gains of up to 2.5% versus a full-scale power electronic ASD. The drive consists of a fixed speed motor, two smaller servomotors connected to a regenerative ASD providing control power and the main planetary gearbox which connects to the driven equipment.

The paper evaluates the underlying theory behind the technology, benefits in comparison to full-scale ASD, starting performance, reliability and availability. Assessment of TOTEX including lifecycle energy consumption and carbon dioxide emissions savings of the hybrid electro-mechanical ASD in comparison to the alternative traditional full-scale ASD are included. Finally, a case study is presented detailing a 5MW pump drive train upgrade.

Index Terms — Adjustable Speed Drive (ASD) also known as Variable Frequency Drive (VFD), this paper uses ASD according to IEC 61800 series [1] and NEMA ICS7 terminology [2]

I. INTRODUCTION

The energy sector has historically been a significant contributor to individual country green house gas emissions. Annual reporting as part of the United Nations Framework Convention on Climate Change (UNFCCC) Nationally Determined Contributions (NDCs) [3] as part of the Paris Agreement detail work at country level to reduce national CO_2 emissions and adjust to the effect of climate change. Ultimately this effort demonstrates individual nation`s policies to progressively reduce their CO_2 emissions over time. Regional incentives such as EU Emissions Trading System (ETS) [4] provide a cap and trade system to encourage polluters in energy intensive industries to reduce their emissions over time through provision of a fiscal mechanism to offset individual installation CO_2 by trading of carbon credits.

Within the energy sector, high-power compressor and pump drive trains are typically deployed on critical process applications. As the energy sector works to reduce its CO_2 emissions impact in the context of more aggressive forward reducing NDCs and more widespread adoption of ETS, more energy efficient drive train solutions are needed to reduce OPEX exposure to both emissions and prime energy usage costs.

Traditionally steam or gas turbine variable speed drive train solutions have been adopted due to the availability of gas or steam for driver power, perceived flexibility, technical simplicity and footprint considerations but are challenged in terms of their overall energy efficiency, reliability and hence CO_2 emissions.

As process plant operators in the energy sector look to replace these installations using more energy efficient solutions for drive trains in order to and reduce their emissions intensity through electrification of existing installations or base case electrification of new plants, motor driven variable speed solutions become more attractive.

A. Requirements for electric motor driven variable speed drive trains

When selecting technology for the variable speed trains in replacement applications or new projects the following requirements are often considered as supplemented by IEEE 958 [5]:

1) The torque speed characteristic of the motor and driven equipment.

2) Operating speed range: Expected duration of operation at upper and lower speed limits, critical speed bands and mode of operation at these points for the variable speed drive train.

3) Electric supply grid: Expected short circuit level and power quality at the point of common coupling for the variable speed solution during expected process plant operating scenarios including start-up and controlled shutdown.

4) Reliability and Availability: Mean time between failure (MTBF) and mean time to repair (MTTR) of the drive train and associated sub-components is in line with the user ranking of the criticality of the associated process equipment and the expected process plant planned maintenance frequency.

5) Safety: The process safety aspect of the drive train implementation leads to an overall reduction in the risks associated with operation of the process equipment. This can include redundancy in drive train topology design and identification single points of failure. Subsequent failure of drive train sub-components allows for a controlled ramp-down or controlled process shutdown.

6) Efficiency of the variable speed drive train: Higher efficiency means that losses are reduced, typically this is a reduction in thermal losses from energy conversion from electricity to motive power. This implies minimization of operating losses effectively reducing CO_2e emissions. This has a direct impact on OPEX in terms of direct energy costs and as ancillary equipment count and complexity is reduced, then maintenance costs also fall.

7) Total expenditure (TOTEX): Consideration of initial CAPEX investment and OPEX lifecycle expenditure in determining the total cost ownership of the variable speed solution and associated ancillary equipment needed. OPEX in this instance is both energy and component maintenance/replacement.

8) Footprint / weight: Both on-plant for the drive train and electrical rooms are important either on new facilities where for example plot allocation may be limited or on brownfield developments

9) Maintenance: Improvements in process plant internal inspections through adoption of technology solutions have progressively increased the running periods between turnarounds and reduced the duration of the turnarounds themselves. This places an increased emphasis on the reliability of the variable speed solution and the need for enhanced digitized condition monitoring techniques for the variable speed solution to ensure that its maintenance is not the critical path item determining turnaround frequency or duration.

B. Electric motor driven variable speed solutions

There are various electric motor driven variable speed solutions available, a selection are summarized below. Often a variable speed drive is selected based on the specific project scenario and the requirements listed previously may be ordered by priority, which can differ project to project, as per Fig. 1a and Fig. 1b.

1) Constant speed electric motor driven hydrodynamic fluid couplings: optionally including gear stages(s)
2) Constant speed electric motor driven hydrodynamically controlled superimposing planetary gear
3) Full-scale ASD with gear box
4) Full-scale ASD without gear box (high speed motor)

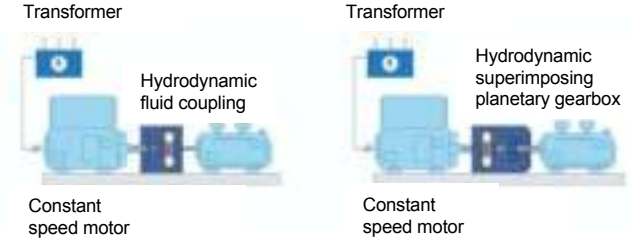

Fig. 1a Constant speed electric motor driven variable speed solutions

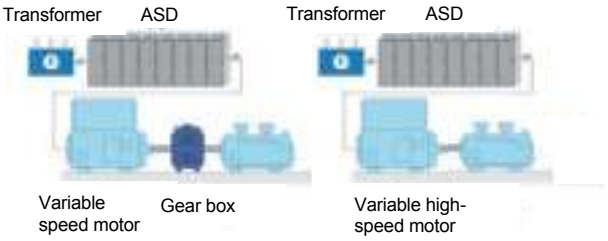

Fig. 1b Full-scale ASD solutions

Therefore, electro-mechanical ASDs offer a further solution, with the aim of supporting the requirements for variable speed drives previously described with a focus of improving efficiencies across operating speed ranges of the driven equipment. Full-scale ASDs with gearboxes to step up the motor speed are often used where the motor is controlled by the ASD, placed in line, and designed to full power. This paper will focus and draw comparison to such full-scale ASD solutions.

C. Technology evolutions for electrical driven equipment

Electrical ASDs are based on semi-conductors that have evolved through the years. In the 1950's diodes have been the first type of semi-conductors used for ASDs to convert AC to DC. Then the evolution of semi-conductors to the thyristors family allowed to have the first Current Source Inverter (CSI) AC to AC ASDs as the Load Commutated Inverter (LCI) or Cycloconverters in the 1970's. These ASDs can drive only synchronous motors and are capable to reach high power levels. In the late 1980's Insulated Gate Bipolar Transistor (IGBT) have been developed allowing to have Voltage Source Inverters (VSI) AC to AC ASDs driving synchronous or induction motors. Over the years the VSIs were capable to reach higher voltages and currents and drive high power motors thanks to the development of the MV IGBTs. Motors as well have been evolving from DC motors to Synchronous motors or Induction Motors. The evolution of ASDs towards VSIs have pushed the evolution of the induction motors to higher power and speed allowing to reach on some cases load operating points without gear box (high speed motors).

The different evolution of components in the system have led to different system improvements either on power, quality, efficiency, etc. At the same time, system re-arrangement of existing components can lead to a system improvement as for the electro-mechanical ASDs

II. INTRODUCTION TO ELECTRO-MECHANICAL ASD

Electro-mechanical ASD can provide variable speed regulation for pumps and compressors up to a 20MW rating and 15,000 rpm rated output speed, operating typical pump operating ranges of 50-100% and compressor operating ranges of 70-105%. The solution (Fig. 2) consists of a constant speed main motor (typically a four-pole induction motor connected to a medium voltage grid) which drives a superimposing planetary gearbox, which is connected to the driven machine.

Two control servomotors controlled by a regenerative ASD are connected either side of the superimposing planetary gearbox which creates an (electro-mechanical) superimposing planetary gearbox (ESPG). The servomotors are specified to a low percentage of rated

power, which means only a small percentage of power is used as control power by the servomotors and ASD. The driven machine`s speed can then be achieved and regulated by a combination of constant input speed from the main motor and regulation speed provided by the ESPG.

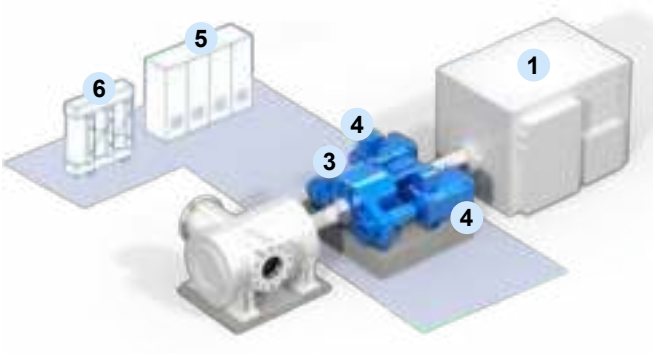

(1) Constant speed main motor (2) Driven machine (3) (Electro-mechanical) superimposing planetary gearbox (4) Servomotors (5) ASD (6) Transformer

Fig. 2 Electro-mechanical ASD layout

A. Evolution towards electro-mechanical ASD

Electro-mechanical ASD, as previously noted, is based on the rearrangement of improved single components within the system to improve the full system. It consists of using proven and widely used main components, already referenced in the energy industries. Table I highlights a breakdown and compliance with Industry standards. The one partial deviation in electro-mechanical ASD is the gearbox, parallel shaft gearboxes are considered as standard with superimposing planetary gearboxes being widely used in the energy industry.

TABLE I
Using proven & widely used main components

Main component	Industry Standards i.e., IOGP JIP 33	Industry References Proven
ASD Transformer	✓	✓
ASD	✓	✓
Main Motor	✓	✓
Gearbox	✗	✓
Servomotors	✓	✓

The innovation with the electro-mechanical ASD allows to have significant power and size reduction of the electrical components when comparing to full-scale ASD (Fig.3). As per the power-split principle (described in section IIC), all powers are added together. The result is reducing the electrical ASD and its transformer to ~15% of the total power, and the main motor to ~85% of the total power while adding two servomotors of a total power of ~15% to reach a total of 100% on the load side. The reduction of power allows footprint and weight savings to be made and auxiliaries can also be reduced such as cooling needed for the ASD.

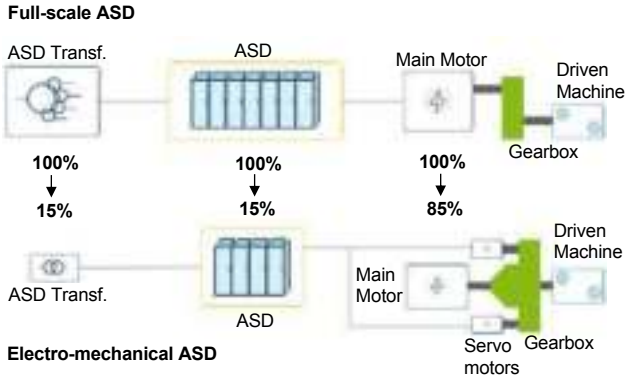

Fig.3 Electrical power reduction of electro-mechanical ASD

B. Theory behind the technology – bringing electrical and mechanical together

Reference to Fig.4 the ring gear (3) of the superimposing planetary gearbox is connected to the main motor (1) by the input shaft (2) and is driven at the motors constant speed. The sun gear (4) is connected to the output shaft (6) which provides the variable speed to the driven machine. The sun gear is then orbited by the planet gears (5) which are housed in a planet carrier (8) and then enclosed by the ring gear. The two control servomotors (7) are indirectly connected to the planet gear via the planet carrier. The servomotors are operating in a bi-directional way which changes the direction and speed of the planet carrier, therefore providing variable speed regulation to the driven machine.

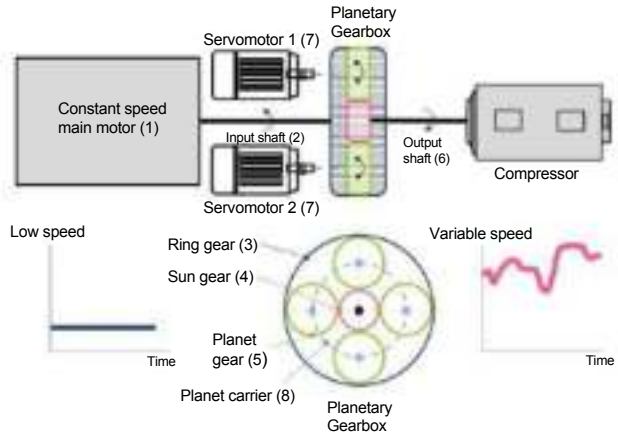

Fig.4 Theory behind electro-mechanical ASD

To increase the output speed the planet carrier is driven by the servomotors in the same direction as the sun gear, and to reduce the output speed the planet carrier must rotate in the opposite direction to the sun gear (Fig.5)

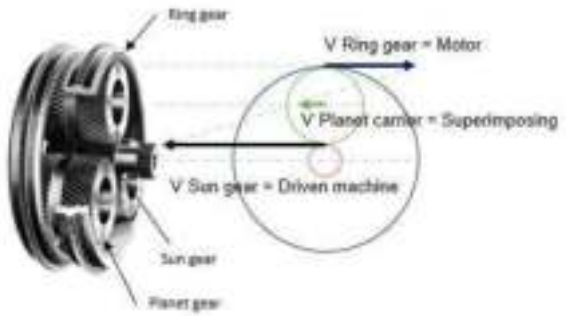

$V = \omega * r$

$V = \pi * n * r / 30$

where

V	Circumferencial speed (m/s)
ω	Angular frequency (1/s)
r	Radius (m)
n	Speed (rpm)

Fig.5 Speed diagram of the ESPG [6]

C. The power splitting principle (at rated point)

Electro-mechanical ASD utilizes two power flows to provide the desired output power for the driven machine. When the driven machine operates at rated point, as an example, the main motor will typically provide 85% of power to the driven machine and the remaining 15% power would be provided by the ASD and servomotors, this is called the power splitting principle. When comparing to full-scale ASD, 100% full power is provided by the main variable speed motor and ASD, which are installed inline. (Fig.6)

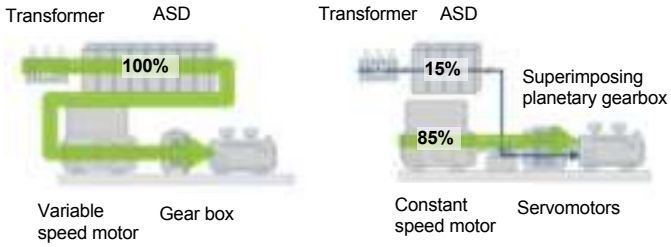

Fig.6 Full-scale ASD vs Power splitting principal

III. EFFICIENCY COMPARISON WITH FULL SCALE ASD

A. Main drive train equipment

An efficiency comparison can be made between electro-mechanical ASD and full-scale ASD with gearbox (Fig. 1b)

As previously discussed at rated point, an electro-mechanical ASD uses 15% as control power for providing variable speed, this means the ASD losses are proportional to 15% of power. In full-scale ASD due to the inline arrangement the losses are subjected and proportional to the full (100%) power flow (Fig.6)

Here the power splitting principle supports increased efficiencies due to only a small portion of power flowing through the ASD line and the majority of power transmitted purely mechanically. Therefore, the following equation (1) can be used to describe the underlying theory at rated point:

$$\eta_{Train} = (0.15 \times \eta_{Tr} \times \eta_{ASD} \times \eta_{SM} + 0.85 \times \eta_{MM}) \times \eta_{PG} \times 100\% \quad (1)$$

At rated point the following equation (2) can be used to define the full scale ASD efficiency:

$$\eta_{Train} = \eta_{Tr} \times \eta_{ASD} \times \eta_{MM} \times \eta_{PSG} \times 100\% \quad (2)$$

where

η_{Train}	Drive train efficiency
η_{Tr}	Transformer efficiency
η_{ASD}	ASD efficiency
η_{SM}	Servomotor efficiency
η_{MM}	Main motor efficiency
η_{PG}	Superimposing planetary gear efficiency
η_{PSG}	Parallel shaft gear efficiency

Table II shows an efficiency comparison between the two technologies considering the main drive train equipment and using the principles and equations described previously, which results in an increased efficiency at rated point for the electro-mechanical ASD.

Harmonic filters are not considered necessary as electro-mechanical ASD reduces harmonic impact on the grid as only 15% of power is using a nonlinear load and the ASD uses Active Front End (AFE) regenerative topology which has a lower harmonic content. Modern full-scale ASDs within the discussed power range and by using a multi-winding input transformer may not need harmonic filters on grid or motor side. For higher power range applications a harmonic filter might be required for full-scale ASD. Requirements will however be application specific to the electrical network.

TABLE II
Efficiency comparison vs full-scale ASD

Main component	Full-scale ASD	Electro-mechanical ASD
ASD Transformer	99.0%	99.0%
Harmonic filter	-	-
ASD	98.0%	97.2%
Main Motor	97.4%	97.6%
Gearbox	98.5%	98.1%
Servomotors	-	96.5%
Rated point	**93.1%**	**95.0%**

It must be noted that the individual component efficiencies are dependent on the original equipment manufacturer (OEM), however for the comparison with full-scale ASD its references are taken from: ASD Transformer [7], full-scale ASD [8], main motor (see acknowledgements), full-scale gearbox [9]

Improved efficiencies can be achieved across the driven machine operating speed range of a typical compressor operating range 70-100% (Fig.7)

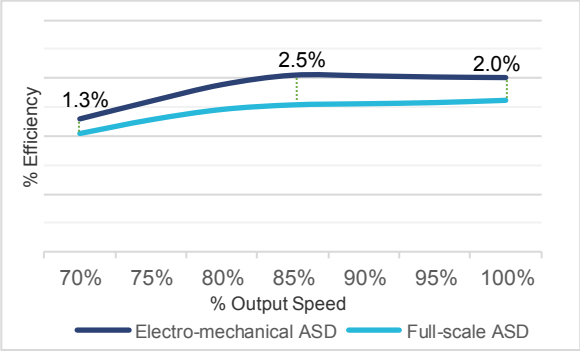

Fig.7 Main drive train efficiency comparison between electro-mechanical ASD and full-scale ASD

B. The impact of auxiliaries

Aside from the main drive train equipment auxiliaries are needed in both solutions and have an influence on efficiencies due to a degree of power consumption, therefore the efficiency comparison can be expanded beyond the drive train equipment itself. Main auxiliaries that could be considered for both solutions include main motor cooling, cooling for the e-room, ASD cooling, and the lube oil pumps (lube oil system itself is not considered as seen as similar for both solutions).

Power consumption for auxiliaries can change depending on the project environment which can be seen in the specific project example later in the paper. For general discussion in this section two differing scenarios described are a Central European climate or a Middle East climate with higher ambient temperatures. The previously mentioned drive equipment efficiency comparison is generalized up to driven equipment of 20MW power however for the auxiliary comparison we choose a specific ~15MW scenario. Therefore, the following will be considered, summarized in Table III

1) *Electro-mechanical ASD*: Cooling is needed for the ASD however due to 15% of control power being used this allows an air cooled ASD to be considered, which has an impact on the electrical room (e-room) HVAC system and its power consumption. For both solutions the main motor cooling could be water cooled where a water-cooling pump is required, or air cooled. Power consumption is slightly less for the constant speed motor due to 85% power contribution. A lube oil pump will be needed therefore a mechanical driven pump is assembled onto the electro-mechanical ASD but considered as a separate auxiliary.

2) *Full-scale ASD:* Typically, air or water cooled ASD would be used but for this power scenario a water cooled ASD will be considered [10] and a liquid-to-liquid system (Fig.8). Loop A is a closed loop circuit with deionized liquid and Loop B is external providing the plant cooling water (sourced from either sea water or cooling towers) which removes the heat. If however their isn`t local cooling water available a specific chiller system may be required which includes a chiller unit and pumping skid that can also include redundancy [11]. Around 10% of the ASD heat loss is dissipated into the e-room so this must also be considered in HVAC power consumption [10]. A lube oil pump is again required which will be considered as a separate power consumption.

TABLE III
Auxiliaries required for both solutions

Auxiliary	Full-scale ASD	Electro-mechanical ASD
Main motor water or air cooled	✓	✓
e-room HVAC	✓	✓
ASD water cooled system	✓	✗
Lube oil pump	✓	✓

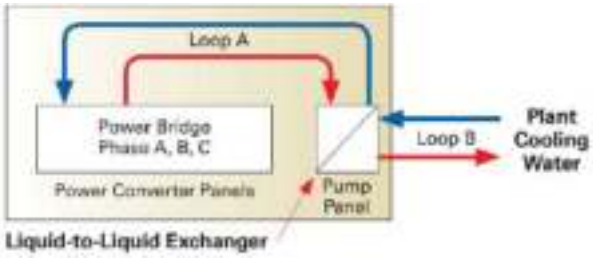

Fig.8 Liquid-to-Liquid ASD cooling system [10]

The auxiliary efficiencies can therefore be calculated using the following equation (3)

$$\eta_{Aux} = (P_{Load} / (P_{Load} + P_{Aux})) \times 100\% \quad (3)$$

where

η_{Aux} Auxiliaries relative efficiency
P_{Load} Driven equipment power
P_{Aux} Auxiliaries power consumption

The two scenarios can now be discussed so that the impact of auxiliaries and therefore total efficiency and energy costs can be observed.

Scenario 1; Central European climate, ambient conditions up to 40°C where cooling water is available within the plant infrastructure. Main motors would be water cooled. The total efficiency comparison is detailed in Table IV and expanded over a compressor operating range (Fig.9)

TABLE IV
Scenario 1 – Total Efficiency comparison of Central European climate

Main System	Full-scale ASD	Electro-mechanical ASD
Main drive train equipment	93.1%	95.0%
Auxiliaries	99.5%	99.6%
Rated point	**92.6%**	**94.7%**

Scenario 2; Middle East environment, ambient conditions up to 55°C, cooling water is not available, and a specific chiller package system is needed (using compressors and pumps). Power consumption would be increased on the e-room HVAC system due to warmer ambient conditions. Main motors would be air cooled.

The total efficiency comparison is detailed in Table V and expanded over a compressor operator range (Fig.10)

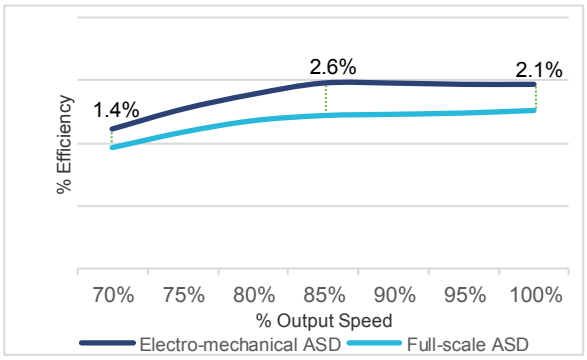

Fig.9 Scenario 1 - Main drive train efficiency plus auxiliaries comparison between electro-mechanical ASD and full-scale ASD

TABLE V
Scenario 2 – Total Efficiency comparison of Middle East Environment

Main System	Full-scale ASD	Electro-mechanical ASD
Main drive train equipment	93.1%	95.0%
Auxiliaries	98.0%	99.5%
Rated point	**91.2%**	**94.5%**

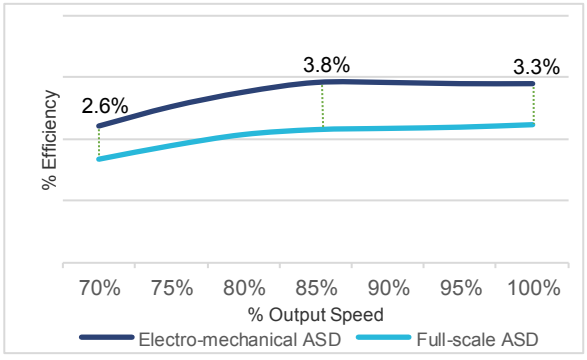

Fig.10 Scenario 2 - Main drive train efficiency plus auxiliaries comparison between electro-mechanical ASD and full-scale ASD

IV. CONSIDERATION TO THE ELECTRIC SUPPLY GRID

When starting high-power variable speed drive trains, the impact to the electrical grid must be considered, here the full-scale ASD has minimal impact to the grid.

Electro-mechanical ASD has two start up possibilities, the first when the main motor is started directly on-line (DOL). Together, the two servomotors increase the speed of the driven equipment smoothly ensuring a short start up time and reduced main motor load. The second and an alternative to DOL start, is a main motor assisted start option, using the servomotors as soft starters, which allows the main motor to be connected to the grid under controlled conditions and large voltage fluctuations are avoided. This is particularly required when large drives are connected to a weak grid [12]

A. Motor Assisted Start

The ESPG when supporting motor assisted start has additional mechanical hydraulic shifting clutches which are engaged at start up. This connects the servomotors with the input shaft of the main motor. The superimposing element of the planetary gear is able to turn with a fixed ratio to the servomotors. (Fig.11).

Fig.11 ESPG hydraulic shifting clutches

On startup (Fig.12) the two servomotors accelerate the main motor (Area 1) while being switched off. Once the main motor reaches its 100% speed the driven machine (i.e compressor) will be typically running at 50% speed (Point 2). The main motor is then switched on and connected to the grid.

If an induction motor is used the rotor will magnetize with a minimal effect to the electrical grid (Fig. 13). After the motor is connected to the grid the servomotors hand over the torque to the main motor and then the hydraulic shifting clutches are disengaged (Point 2). This leads to a direct connection between servomotors and superimposing elements of the gearbox and a disconnection between servomotors and main motor. The servomotors then accelerate the compressor via the planetary gearbox to the desired start up speed (Area 3).

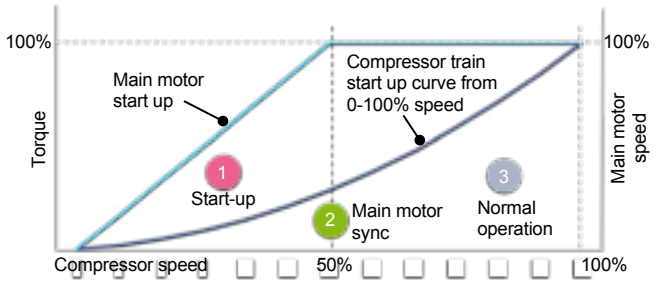

Fig.12 Electro-mechanical ASD main motor assisted start

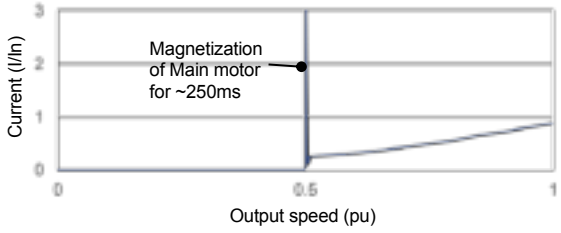

Fig.13 Electro-mechanical ASD induction main motor assisted start showing magnetization

Electro-mechanical ASD motor assisted start therefore reduces the thermal stress of the main motor and power cables, has a short current peak on motor magnetization with a short time ~250ms and the voltage dip observed achieves a tolerable value.

V. RELIABIITY & AVAILABILITY

Full-scale ASD is an established design whilst electro-mechanical ASD uses standard, tried and tested components. MTBF of the individual components in both solutions can be different from manufacturer to manufacturer, as a consequence Table VI can be used to highlight a generalized comparison of MTBF between the two solutions rather than a numerical comparison.

TABLE VI
MTBF Comparison

Main component	Advantage full-scale ASD & gearbox	Advantage electro-mechanical ASD
Transformer		
ASD		
Main motor		
Gearbox		
Servomotors		

When using ASDs in full-scale or electro-mechanical solutions MTBF can be increased and MTTR reduced by implementing redundancy (such as n+1 on power electronics). Additional redundancy is available for electro-mechanical ASD due to the use the two ASDs and two servomotors. If there is a failure of one ASD or servomotor, the electro-mechanical ASD can operate with a reduced power (~80% of rated power) and speed range, which allows for a planned stoppage of the drive train.

Availability illustrates the relationship between system total uptime (MTBF) and unplanned downtime (MTTR), equation (4).

$$\text{Availability} = \text{MTBF} / (\text{MTBF}+\text{MTTR}) \quad (4)$$

Both solutions use existing and well proven components and therefore both benefit from a well-designed overall service concept. Service and maintenance can be optimized to minimize downtime. However, the electro-mechanical ASD solution provides increased availability when compared to full-scale ASD. Both have similar components with equivalent reliability data but the electro-mechanical ASD has the option to operate in a de-rated mode if there is a loss of power to or from one of the servomotors.

VI. TOTEX OVERVIEW

Traditionally projects would only consider operating (OPEX) and capital equipment investment costs (CAPEX) in isolation. Assessment of CAPEX considered the net present value of the project and internal rate of return to gauge a projects individual ranking. OPEX by comparison would largely focus on running costs including periodic planned shutdown maintenance. CAPEX and OPEX budgets are traditionally generated by different parts of an organization reflecting different business drivers and associated behaviors.

The TOTEX by comparison is a more accurate valuation of the life-cycle cost as it considers the weighted average cost of capital (WACC) across the equipment lifetime to provide an annualized CAPEX charge in a given period in addition to the totalized OPEX expenditure, where WACC is effectively the required return to satisfy both debt and equity requirements on the organization allowing for the implicit tax rate. The TOTEX methodology is discussed in more detail by Brosig, Waffenschmidt and Strmpler [13]. Varying parameters within the TOTEX calculation enables a project to understand the sensitivity and relative importance of a parameter on the lifecycle cost and hence a better understanding of the risk for a given commercial scenario.

A. Project Scenario

A gas turbine currently driving a centrifugal compressor with varying operating points has been considered for replacement by an electric motor driven ASD. Energy savings and decarbonization are considered as key reasons to replace the gas turbine. The compressor rated at 6MW with an output speed of 7200rpm (variable speed range down to 5900rpm) is installed in the United Kingdom on a process application, the project scenario will be of a brownfield type. Plant power supply is available 11kV at 50Hz and average ambient operation temperatures are 9°C rising to a peak of 30°C in the summer months. There is limited space for additional electrical equipment in the existing motor control center (MCC) therefore a new e-room is considered. The distance for cabling between the e-room and motors ~100m. The drive train equipment is installed in a hazardous area with ATEX explosion protection required.

Electro-mechanical ASD is compared with full-scale ASD including gearbox with the conceptual solutions defined as follows:

1) *Electro-mechanical ASD (for this section abbreviated EM ASD)*: The drive train consists of a constant speed induction type main motor rated at 6.1 MW 1490rpm IC81W, connected to the existing 11kV 50Hz electrical grid. This is directly connected to the EM ASD superimposing planetary gearbox. A low voltage regenerative ASD controls the two servomotors each rated at 399kW, 690V IC71W. Therefore, the control power for this project is 15% (Fig.3) with specific motor assisted start not required. The ASD has a used power of ~875kW and provides redundancy with independent motor invertors and one infeed system. A separate transformer is installed in the e-room (Fig.14)

2) *Full-scale ASD (for this section abbreviated FS ASD):* The drive train consists of a variable speed induction type main motor rated at 7.5MW IC81W 6.6kV 50Hz connected to a parallel shaft gearbox. This is driven by an air cooled hi-pulse ASD 6.6kV complete with integrated transformer. The cooling was covered by the e-room HVAC system however in the summer months a chiller system is required running for an estimated 500 hours per year, together with the HVAC system.

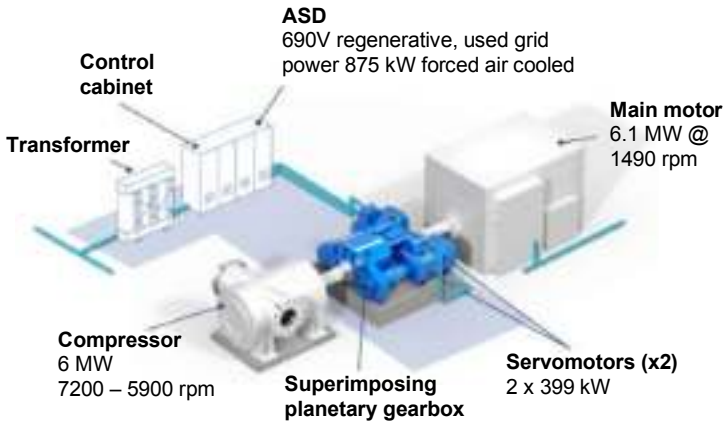

Fig.14 Electro-mechanical ASD 6MW compressor layout

B. CAPEX Comparison

The CAPEX inputs consider all main drive train equipment, auxiliaries and civils required to implement the project and are split into eleven categories, with a final summary of the total noted. General engineering concept to implementation hasn't been considered. Rationale for the main CAPEX inputs (Fig 15 and 16) can be described as follows:

- Main electric motor: EM ASD uses a more economical 6.1MW constant speed motor (85% of compressor output power), FS ASD uses a 7.5MW for variable speed duty, both water-cooled
- Substation: The FS ASD will take the site provided 11kV and with an integral transformer drop the voltage to the required ASD/Motor voltages. The EM ASD will need a transformer to generate the required 690 V for the servomotors. EM ASD require 2 switch-gears, 1 for the fixed speed motor and 1 for the ASD while FS ASD would require only 1 switch-gear for the full system
- Variable speed (VS) main system: Included in EM ASD are all components for the drive package such as ASD, transformer, gearbox (blue highlighted area Fig.14) whereas FS ASD comprises of the ASD and transformer
- Soft starting option: already included in the FS ASD not required for EM ASD
- Gearbox and coupling: Parallel shaft gearbox required for FS ASD and oil free diaphragm couplings for input and high-speed drive shaft connections for both solutions. Planetary gearbox for EM ASD is already included in VS Main System
- Lube oil (LO) system and oil cooler: lube oil system similar for both solutions however overhead run-down oil tank selected for FS ASD while not needed for EM ASD due to the integrated mechanical pump
- Harmonic / grid filters: not required for this project for both solutions
- e-room; For both solutions e-room and auxiliaries are included such as HVAC system. As described previously, the reduction of power on the main electrical equipment for EM ASD allows a reduction on footprint and weight. Therefore, the e-room would have an area of ~22m^2 and volume of ~52m^3 in comparison to the FS ASD with an e-room area of ~80m^2 and volume of ~320m^3. On the drive train skid, for EM ASD the planetary gear with its two servomotors increases the footprint by ~15% and weight by ~10% of the skid, even if on the main motor side a slight reduction is there due to the ~85% power of the main motor
- Cabling; Cables are mainly defined by current and voltage with a great impact of current on the cable section size. With FS ASD system, motor voltages are limited to the ASD output voltage (3kV to 6kV in this case) which is usually lower than the grid input voltage (11kV in this case). For EM ASD, the fixed speed motor is designed for 85% of power and 11kV voltage which result in ~60% less cables. However, EM ASD requires additional cables between its 15% ASD and the servomotors. In total, the FS ASD still requires ~35% more cables compared to EM ASD
- Chiller package: required for FS ASD to cover periodic warmer ambient temperatures, the system works by pump exchanging the heat in the room with a water-to-air cooler. The water is subsequently chilled to below atmospheric temperature using a refrigeration package
- Engineering and Construction: Outside of the core package there is considerable engineering design works to ensure the final package meets site requirements and is safe to operate within the plant. In addition, there is a requirement to complete construction work, isolating and making safe existing gas line, connecting to electrical and control networks, altering civil and structural aspects on site, and managing and planning the entire process

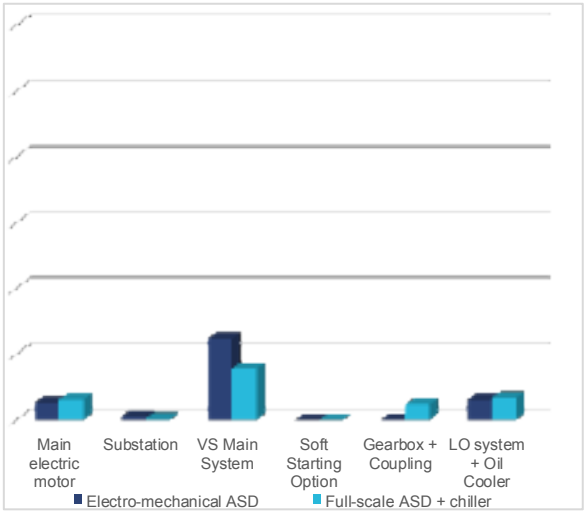

Fig.15 CAPEX comparison of drive train components (first part)

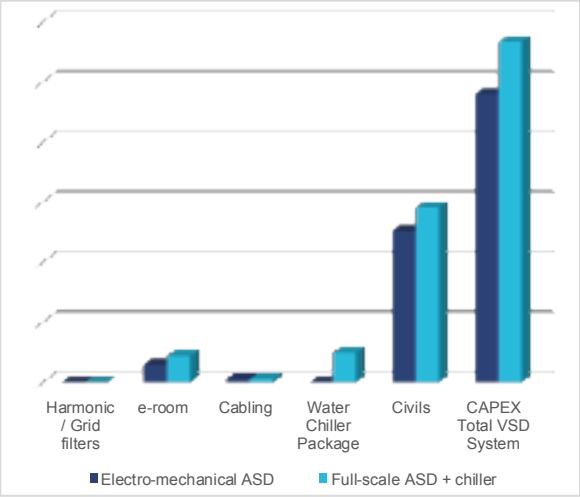

Fig.16 CAPEX comparison of drive train components (second part)

C. *Energy and CO_2 savings*

To calculate energy and CO_2 differences between the two technologies the project efficiencies need to be derived. The main drive train equipment efficiencies are taken from Table II given this project is within the 20MW power range. As noted previously auxiliaries are project specific therefore for this project, FS ASD is utilizing an air cooled ASD with a chiller package being used for 500 hours. The auxiliaries considered are detailed in Table VII, and the efficiencies used are detailed in Table VIII. As the chiller package is being utilized for only 500 hours an additional auxiliary percentage "Auxiliaries (including chiller operating)", 96.5%, is derived for FS ASD.

TABLE VII
Auxiliaries required for both solutions

Auxiliary	Full-scale ASD	Electro-mechanical ASD
Main motor water cooled	✓	✓
e-room HVAC	✓	✓
Chiller package	✓	✘
Lube oil pump	✓	✓

TABLE VIII
Total rated point efficiency comparison

	FS ASD	EM ASD
Main drive train equipment	93.1%	95.0%
Auxiliaries (w/o chiller)	98.5%	99.3%
Total rated point efficiency (w/o chiller)	**91.7%**	**94.4%**
Auxiliaries (including chiller operating)	96.5%	-
Total rated point efficiency (chiller)	**89.8%**	**-**

Dividing the compressor load power (6000 kW) by the total rated point efficiency of the main drive equipment and auxiliaries equates to the total power consumption (kW) of each solution, equation (5). For FS ASD total power consumption is considered with the periodic usage of the chiller package and then without.

$$TPC = P_{Load} / \eta_{Rated} \quad (5)$$

where

TPC Total power consumption
P_{Load} Driven equipment power
η_{Rated} Total rated point efficiency

This study focuses on energy losses per year (MWh/a) not the total energy used, equation (6), therefore for EM ASD 8000 hours are considered and for FS ASD 7500 hours without chiller and 500 hours with chiller is considered.

$$TLO = (TPC - P_{Load}) \times OP / 1000 \quad (6)$$

where

TLO Energy losses per year
OP Operating hours

The energy cost per year is calculated using 0.15 €/kWh [14] as an appropriate UK electricity price at the time of writing this paper multiplying by the calculated TLO. FS ASD considers TLO as the total energy losses with and without chiller operation.

CO_2 emissions and tax on losses can also be calculated using 0.21 kg/kWh [15] and a tax of 53.45 (€/Ton) [16] (Table IX)

The energy savings per year comparing EM ASD with FS ASD are ~235,000 EUR with a saving of 7.4M EUR on energy losses, possible over 25 years including a 2% yearly inflation (Fig. 17). The CO_2 reduction per year comparing EM ASD with FS ASD is 323 Tons with ~440,000 EUR of CO_2 taxes saved over 25 years.

TABLE IX
Energy and CO2 summary*

	FS ASD	EM ASD
Total power consumption (kW)	6543	6356
Total power consumption inc chiller (kW)	6682	-
Energy losses p.a. 7500 & 8000hrs (MWh/a)	4073	2848
Energy losses p.a. inc chiller 500hrs (MWh/a)	341	-
Energy cost p.a (€)	662,100	427,200
CO_2 e Emissions p.a. due to losses (Tons)	926	603
CO_2 tax p.a. due to losses (€/Ton)	49,500	32,000

*all figures rounded

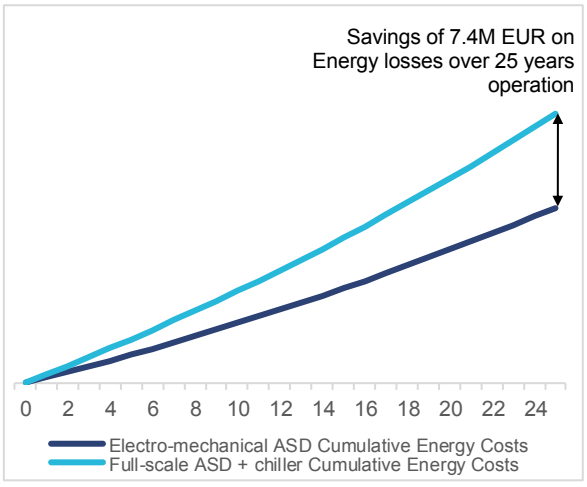

Fig.17 Cumulative energy savings comparison

D. TOTEX (Capital Expenditure + Operational Expenditure)

As previously introduced TOTEX over a 25-year period can be summarized for both solutions (Fig. 18) which includes the CAPEX inputs (Fig. 15 and 16), installation, commissioning and initial project spares, yearly and major maintenance at ~5-year intervals (as a base case) and finally energy costs (Fig.17) per year and CO_2 taxes. In this project scenario EM ASD has a lower initial total project CAPEX input with savings increasing over a 25-year period.

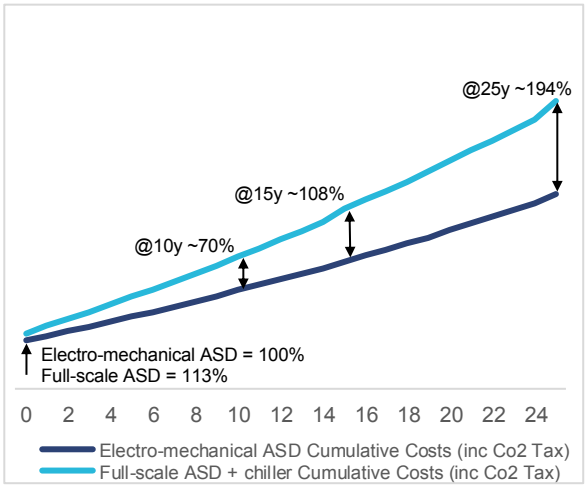

Fig.18 TOTEX comparison

VII. CASE STUDY 5MW PUMP APPLICATION

Electro-mechanical ASDs have been successfully installed and commissioned in 2020 on two boiler water feed pumps at a coal fired power plant in China which were upgrades to the existing variable speed solutions in operation, constant speed electric motor driven hydrodynamic fluid couplings (Fig. 1a). The rated power for each drive is ~4.5MW with output speed of ~5300rpm. The electro-mechanical ASD included a low voltage regenerative ASD with two 500kW servomotors providing the control power (Fig.19). This supported the main aims of the plant to improve overall efficiency long term, reduce energy consumption and greenhouse gas emissions [17]

Fig.19 Electro-mechanical ASD installed on a 4.5MW boiler water feed pump

VIII. CONCLUSIONS

From this paper we established the global and regional context for emissions reductions associated with large mechanical equipment drive trains. The technical requirements of motor drive trains were discussed with the available technologies and their evolution.

A detailed introduction of the electro-mechanical ASD technology was provided, highlighting the principle components, the underlying theory behind the planetary gear box and the power split principle identifying a potential reduction in system complexity for ASD solutions up to 20MW rating.

A comparison of efficiencies between traditional full scale ASD and the electro-mechanical alternative was provided, highlighting efficiency improvements for the electro-mechanical solution of the order of 2.5%. This efficiency gain was complemented by a review of the reduced complexity of ASD auxiliaries associated with the electro-mechanical solution where demands on cooling systems were less. A comparison of the implications of this simplification for both Central European and Middle-East climatic environment was given, reinforcing the advantage of the electromechanical solution over a larger full scale ASD solution.

An assessment of the starting performance requirements for the electromechanical ASD was given, this showed that use of servo motors for an assisted start significantly reduced the magnetizing current impact over a DOL alternative.

The reduction in complexity of the electro-mechanical ASD compared with a full-scale ASD highlighted earlier was seen to have a positive impact on the reliability and availability of the drive train due to greater flexibility to operate under de-rated mode due to loss of a single servomotor.

A detailed evaluation of the TOTEX across the installation lifecycle was provided through evaluation of changing a gas turbine driven centrifugal compressor with an equivalent rated electro-mechanical ASD and full scale ASD. A comparison of CAPEX costs found in favor of the electro-mechanical ASD at the 6MW reference case for the UK. From OPEX perspective energy and CO_2e emissions were evaluated, again showing significant savings for the electro-mechanical ASD. TOTEX comparison was plotted across a 25 year life of installation, integrating CAPEX, OPEX in terms of energy and emissions and OPEX in terms of maintenance charges. Overall, for the reference case a electro-mechanical ASD proved to be significantly more cost effective.

Finally, a real life application of an 4.5MW electro-mechanical ASD retrofit solutions in China on a pump drive train was provided, demonstrating confidence in the technology for the specified application.

In conclusion electro-mechanical ASD can provide a more effective solution to traditional full scale ASD in the power range up to 20MW, particularly when lifecycle benefits are considered. Detailed evaluation on a case-by-case project basis is needed to establish the optimum technology solution, early appraisal of the alternatives is recommended.

IX. ACKNOWLEDGEMENTS

Thanks to Dr. Martin Tilscher (Voith), Bernd Lauter (Voith), Tobias Seeberger (Voith) for general support with this paper and Mark Chisholm (ELIN motors) for motor information.

X. REFERENCES

[1] IEC 61800 series, *Adjustable speed electrical power drive systems*, IEC – SC 22G Dashboard > Projects / Publications: Work programme, Publications, Stability Dates, Project files, accessed 13 December 2021.

[2] NEMA ICS 7 (2020), *Industrial Control and Systems: Adjustable-Speed Drives*, NEMA ICS 7 – Industrial Control and Systems: Adjustable-Speed Drives | Engineering360 (globalspec.com), accessed 13 December 2021.

[3] UNFCCC (2021), *Nationally Determined Contributions*, Nationally Determined Contributions (NDCs) | UNFCCC accessed 03 December 2021.

[4] European Commission (n.d.), *EU Emissions Trading System (EU ETS)*, EU Emissions Trading System (EU ETS) (europa.eu), accessed 03 December 2021.

[5] IEEE Std 958 (2003), IEEE GUIDE FOR THE APPLICATION OF AC ADJUSTABLE-SPEED DRIVES, accessed 10 December 2021

[6] Tilscher, M., Lauter, B., Lindenmaier, J. (2017) "Superimposing planetary gears as variable speed drives for rotating equipment", *46th Turbomachinery & 33rd Pump Symposia 2017*, accessed 08 December 2021

[7] Durantay, L., Van Gemert, D., Lava, J., Spannagel, D. (2021) "A Success Story Of Steam Turbine Replacement By High Speed Electric System Driven Compressor" PCIC paper EUR21_08 Shell & GE, pg2, accessed 31 January 2022

[8] Siemens Perfect Harmony GH180 brochure (2018), *Watercooled-perfectharmony-brochure-june-2018_original.pdf* Siemens | Downloads | Information & Download pg 4, accessed 31 January 2022

[9] RENK high-speed gear units. *Parallel offset and coaxial concepts Renk high speed gear units brochure 2021* RENK | Product & Service, accessed 31 January 2022

[10] TMEIC Application Edge Volume 1, Issue 4 (2019) *Cooling Large Variable frequency drives* TMEIC | Library accessed 1 February 2022.

[11] Bacchetti, L., Batistoni Ferrara, A., Benedini, P., Ramundo, G. (ABB) *Environmental challenges in variable speed drive system (VSDs) applications: design and construction of a water cooling unit facing extreme temperatures and continuous critical duty* World Gas Conference 2012 ABB Library, accessed 1 February 2022.

[12] Voith website (2021) Voith | Variable speed drive | VECO-Drive, accessed 08 December 2021

[13] Brosig, C., Waffenschmidt, E., Strmpler, F., (2018) "Future Economic Efficiency of Gas Distribution Grids," *2018 7th International Energy and Sustainability Conference (IESC)*, 2018, pp. 1-7, doi: 10.1109/IESC.2018.8439977., accessed 3rd February 2022.

[14] Business Electricity Prices (2021) Business *What are the average business electricity prices per kWh in 2021* Electricity Prices | Cost per kWh, accessed 7th February 2022

[15] Greenhouse gas reporting: conversion factors 2021 Business *Conversion factors 2021*, retrieved 7th March 2022, accessed from Greenhouse gas reporting: conversion factors 2021 - GOV.UK (www.gov.uk)

[16] Reuters. S. Twidale (2021) *Britain's carbon market begins trading at higher prices than EU* Reuters | Business | Sustainable Business, accessed 7th February 2022

[17] Voith website, R. Wankerl (2018) Voith | News room, accessed 08 December 2021

XI. VITA

Simon Turnbull graduated from the University of Huddersfield in 2002 with a BSc engineering degree. He has held several positions within the Voith group support topics such as steam turbine control to digitalization. Currently he supports electro-mechanical drive solutions in the Europe region

simon.turnbull@voith.com

Justin Mason is an independent consultant engineer with a 30 year career history in energy, cement and utilities and graduated from the UMIST in 1991 with BEng in Electrical & Electronic Engineering, and a MBA from Lancaster University in 2001. He is currently reading a MSc in Sustainability in Energy Provision and Demand Management at CAT in the UK. He is a Chartered Engineer, a Fellow of the IET and GB national representative for IEC MT18. He has authored and presented at PCIC Europe and he has been a member of PCIC Europe committee since 2012, serving as Vice Chair Technical Chair from 2013-2015 and was elected as the Executive Committee Chair in January 2021.

Justin.mason@trydanolenergy.solutions

Michael Rimmer is a Chartered Mechanical Engineer working as a machinery engineer in Costain's front end / consultancy group. He has 10 years' experience in the oil and gas industry matching user, machinery and system requirements to minimise capital expenditure and environmental impact, improving project economics and viability. He has worked on gas processing projects on 6 continents ranging from production to transmission and covering NGL extraction, liquefaction and storage.

michael.rimmer@costain.com

Wissam Moubarak has 15 years experience with electrical systems in the Energy and Oil & Gas industry, specifically with power conversion, MV VFDs and motors. He graduated from INSA – Rennes – France in 2007 with “Diplome d’Ingénieur” (Master’s Degree) in Electronic & Computer Engineering. He has worked through different technical, R&D and Sales related roles before his current assignment at VOITH supporting the company’s business development activities for electro-mechanical drive solutions.

wissam.moubarak@voith.com

DIGITAL DESIGN PROCESS FOR TRACE HEATING SYSTEMS

Paper No. PCIC Europe 22_10

Ben Johnson
Thermon Industries
USA

Lamont Lewis
Thermon Industries
Austin, TX
USA

Daniel Ridsdale
Thermon Industries
Gateshead Tyne & Wear
UK

Abstract - Large capital projects are now designed using fully digital 3D modeling systems. Leveraging the digital plant model and digital data to engage the supply chain in the most efficient and accurate manner can yield cost savings to the user/operator and EPC. A case study is presented showing the efficiency of exchanging digital model data for piping and trace heater design information as opposed to relying entirely on drawings. Techniques and best practices are discussed for exchanging piping and trace heating data in both directions between the EPC and heat trace supplier. The benefits of a fully digital workflow for the project design teams are described.

Index Terms — PCF Files, 3D Modeling Packages.

I. INTRODUCTION

Traditional trace heating design processes involve many man hours of manual file sorting, document control, data transfer and drawing generation, review and approval for release. Even though the input to the process has evolved to digital drawings in pdf files and line designation tables in spreadsheets, the process itself has changed very little.

EPC firms now utilize modern 3D modeling packages for plant design. These systems can provide all the information needed to design heat tracing systems in a digital format that can be consumed by other systems to recreate the piping geometries. This is the basis for a fully digital design process that reduces project execution time, assures data integrity, and improves document control and change management as well as allow 24/7 file exchange with offices located around the world. This paper will compare a system that allows heat trace designers to work in the 3D space defined by the customer's model with the traditional manual design process.

II. MANUAL VS DIGITAL HEAT TRACING DESIGN

A. *Manual Design Process*

Manual heat trace design practices date back to the days of analog data in the form of hand drawn drawings and hand generated lists. The documents that feed the process have evolved to a digital form but the basic steps remain essentially unchanged. The traditional documents from the EPC consists of:

- P&ID Drawings
- Pipe Spool Drawings
- Plot Plans
- Area Classification Drawings
- Equipment drawings
- Line Designation Table

The primary deliverable from the trace heating design process is the heat tracing isometric. This document conveys the trace heat routing on pipe and equipment, materials list for the trace heating circuit, the electrical loading information for the circuit and any other installation instructions needed for the design. Additional documents can include the trace heating line list, summary bill of materials, loading calculations for transformer and panel sizing as well as load balancing and power distribution. The manual process consists of multiple steps performed by hand to create the trace heating isometric and other deliverable documents. These steps are:

1) Sort piping spool drawings to separate the lines and equipment to be heated from non-heated pipe and equipment...
2) Sort Revisions to separate unchanged drawings from revised and unchanged drawings.
3) Sort drawings by area, work package or module.
4) Do manual sketch combining the spool piece drawings so heat tracing circuits can be designed.
5) Sketch routing of trace heating on take-offs.
6) Use trace heating vendor's design software to confirm layout is proper, calculate electrical loading and generate a materials list for the circuit.
7) Manually enter design data into a spreadsheet format.
8) Create trace heating line list.
9) Create load calculation list.
10) Manually create power connection, temperature sensor and end termination location list for layout drawing/plot plan.
11) Create isometric from sketch of trace heating routing on take-off.
12) Manually enter circuit design data and add installation details to the isometric.

Several of these steps can be iterative. The trace heating designer will provide the CAD operator with the trace heating routing on the take-off. The CAD operator will generate the trace heating isometric. The isometric will be returned to the designer for review. The result of the review could be a sign off or return to the CAD group for modifications.

The manual tracking of the drawing and document status requires additional manpower. When a subsequent document package is received the manual sorting process would have to be repeated for the entire package. The drawings representing heated lines would then be submitted to the designer who would then have to determine if the lines had any changes affecting the trace heating design and if so, whether trace heating isometrics had already been created for those lines. If the isometric exists for this line then there is a means of tracking the document and updating it. If the line has not been designed yet then locating and comparing the new

drawing to the previous revision can be very time consuming. This workflow is depicted in Figure 1.

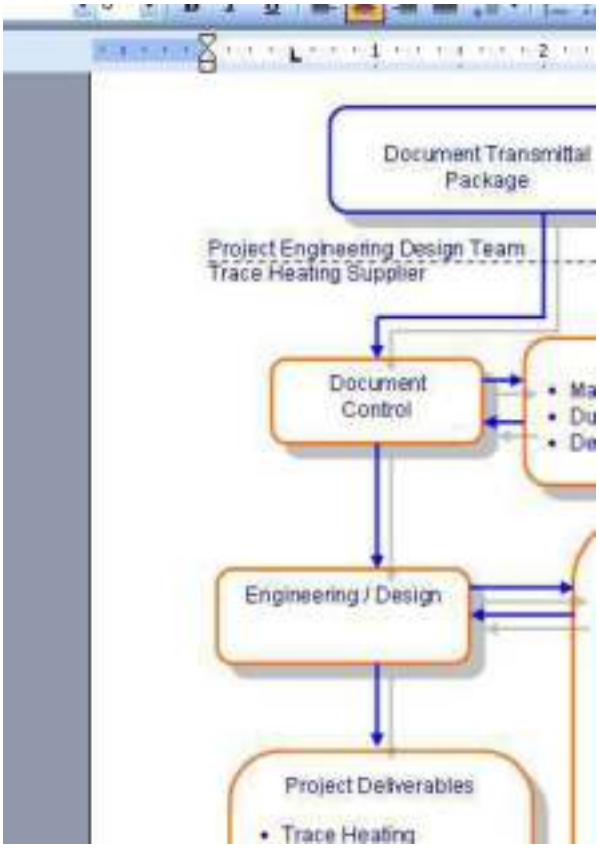

Figure 1: Typical workflow in manual design process

B. Digital Design Process

With EPCs now utilizing digital 3D modeling systems to drive the design and construction of new facilities, there are opportunities to dramatically improve the trace heating design process. All 3D modeling systems in common use today have the ability to export the geometric pipe information in the form of either an intermediate data format (idf) or piping component file (pcf) file. These files contain the information necessary to recreate the piping configuration in the plant model on another system. Utilizing these files and other data available digitally, the overall design process for trace heating can be significantly improved. The process involves a suite of software tools that consists of:

- File Sorting Utility
- Trace Heating Manufacturer's Recommended Design Software
- 3D Modeling Software
- Trace Heating 3-D Design Software

The structure of idf and pcf file include an attribute to indicate whether or not the pipe in the file is to be heated. A utility can interrogate the files and determine whether or not the pipes require heating. This utility can evaluate all the pcf files in a selected folder and sort them according to this attribute. The utility can be used to select and move the files with heated lines to a folder for processing and the un-heated lines to a separate folder. This can take a manual task that requires hours and complete it in a matter of seconds.

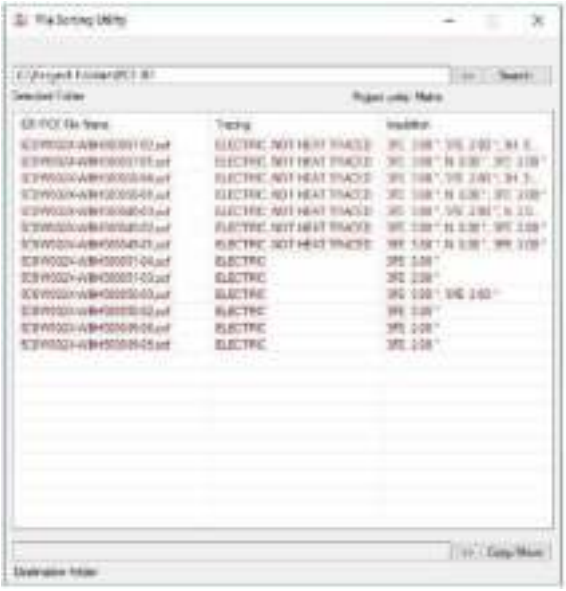

Figure 2: File sorting utility

The model files containing lines to be heated can be imported into 3D modeling software to recreate the pipe configuration from the original model. These files will all be imported into the main model to provide a project wide view to the lead trace heating designer or supervisors.

Figure 3: Line groups imported into 3D modeling package

The 3D design software incorporated into the 3D modeling package captures the meaningful metadata for each line group imported into the model. This provides the lead designer with revision number, quantity of valves, flanges, supports and overall length for each line group. This same view indicates the design status for each line group. A report can be generated with this information so it can be shared.

Figure 4: Main compare window showing metadata

Once the piping model is recreated, it can be divided into logical subgroups for trace heating design. These divisions are often by area, work package or module but can be based on any project requirement. The various line groups can be assigned to a team of designers to route the trace heating and generate the deliverable documents.

When a package is assigned to a designer, the line groups are copied to a separate model utilized by that specific designer (Design Model). The designer will route the trace heating on the design model and verify the design using the trace heating manufacturer's software.

The designer can import the pipe configuration along with valves, flanges, and supports directly into the design program database from within the 3D model environment. During this import, the designer can select from preconfigured templates in the design program that contain the design parameters such as insulation type and thickness, voltage, area classification, exposure temperatures and others so they do not have to be entered for each design. This improves data integrity and saves time during project execution.

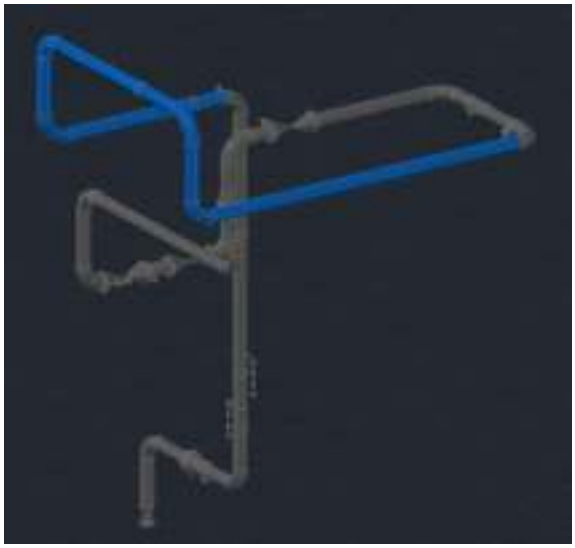

Figure 5: Designer model with color coding indicating traced and untraced pipe

The trace heating software integrated within the 3D environment allows system optimizations. Trace heating designs can be optimized through rapid iterations to maximize circuit length and minimize power points.

With the trace heating optimized, the designer can generate the heat tracing isometric without leaving the design model. Once the trace heating manufacturer's software has calculated the loading and bill of materials, the designer clicks a button on the designer palette within the 3D environment and the trace heating isometric is generated.

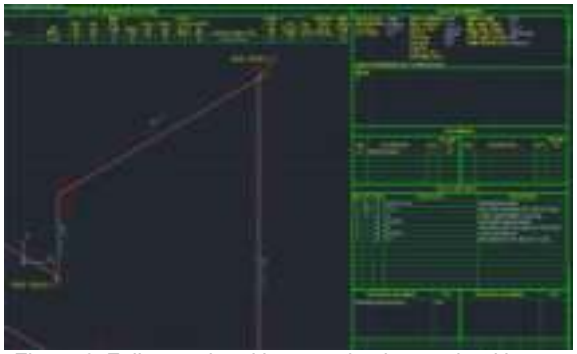

Figure 6: Fully populated heat tracing isometric with heater routing, electrical loading and material take off

When subsequent document packages are received from the customer, the idf or pcf files are sorted and imported to the 3D environment. If a file has changed, the new entry appears as a sub row under the existing file reference. A caret appears next to the row indicating the presence of a revision. The designer can review the metadata associated with the revision against the existing file to determine if anything material to heat tracing has changed.

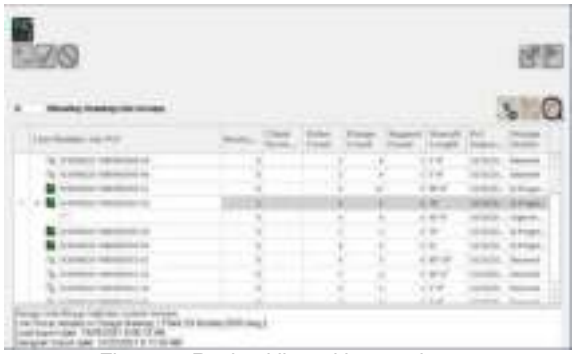

Figure 7: Revised line with metadata

The designer can also select both the existing row and new revision and compare the pipe configurations in the 3D environment to see the impact of the change. The new configuration appears offset from the original routing with color coding to indicate what is new, revised or deleted. If the revised file is accepted, the designer model will be notified that a change to a line group in the model needs to be imported. If the trace heating on that line group has already been routed and the isometric created, then the layout and isometric will be updated to reflect the changes. All of this is done within the model.

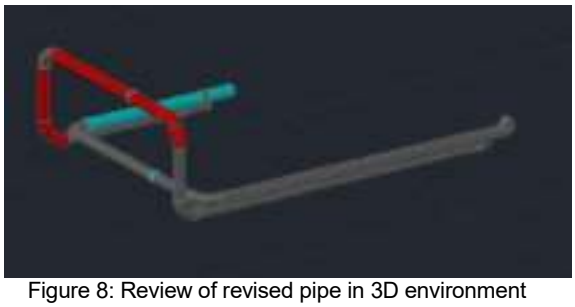

Figure 8: Review of revised pipe in 3D environment

With the 3D modeling package and trace heater manufacturer's software running on a wide area network (WAN), the designers can be located anywhere globally. This allows the designers to be positioned in low cost engineering centers while project managers or project leads are located locally providing direct availability for the client and construction teams.

The workflow for the digital process is depicted in Figure 9.

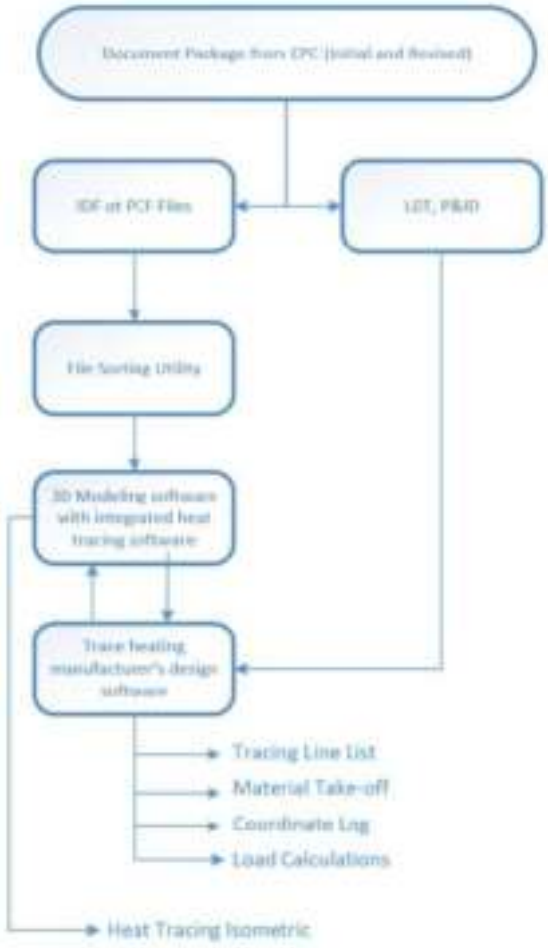

Figure 9: Digital Design Workflow

Experience with projects using the digital design tools has shown an overall reduction of man hour requirements for both the heat tracing vendor and their clients. The following represents a petro-chemical project consisting of 425 trace heating circuits and approximately 16,000 meters of trace heating.

For the client's project engineering team, the man-hour reductions come from:

- 3D model administrator extracts piping spool files from the plant model for pipe fabricators. These same files can be used by the trace heating 3D design software. No separate drawing extraction needed.
- Electronic document transmittal

This resulted in a reduction in client man-hours of approximately 60%.

The trace heating supplier experienced a reduction in man-hours due to:

- Improved document control
- Automated process for sorting heated and non-heated line groups
- Automated change management
- Automated trace heating design process
- Automated generation of trace heating deliverable documents
- Electronic document transmittal

This resulted in a reduction of man-hours by approximately 50%.

To optimize the power connection location for power distribution or control panels it is necessary to generate a plot plan. The manual process for creating a plot plan, to show the location of all power connections, temperature sensors and trace heating terminations, involve the CAD operators adding each coordinate and tag by hand. The digital design process can automatically capture the coordinates and automatically generate a plot of each location. This allows the trace heating vendor to quickly optimize the location of power distribution and control panels along with transformers, cable tray, tray loading and routing. The coordinates and tags can be presented in a report that can also be provided as a deliverable to the client's model administrator. The report can be used to import the locations into their 3D model.

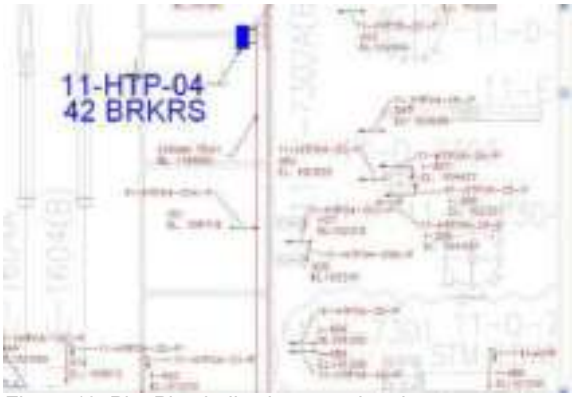

Figure 10: Plot Plan indicating trace heating component locations.

The utilization of the digital design process clearly improves the delivery of the heat tracing engineering design package. The benefits extend to materials management as well. The lead trace heating designer can separate line groups into design models based on:

- Work Package
- Area
- Module
- Process
- Priority or Critical lines
- Other requirements

On-time delivery of materials is crucial to the success of the trace heating project. The digital design process facilitates streamlined communication and coordination between the trace heating supplier and the construction teams. This provides the ability to coordinate the delivery of the trace heaters, or trace heater sets, along with the required system accessories with the construction schedule for specific areas of the project. Utilizing these tools greatly increases efficiency of construction labor and warehousing materials. This contributes to an on-time commissioning, start-up and turn-over process with as-built drawings for the trace heating system.

III. CONCLUSIONS

Utilizing a fully digital design process provides many benefits over the manual execution of a trace heating project. The process is more efficient for both the client's engineering team as well as the trace heating vendor. The data integrity is improved throughout the process by dramatically reducing the amount of manual data entry. Automatic model generation reduces time and improves data integrity over manually drawn take-offs. The ability to automatically identify changes in revised files and visualize those changes provides a significant improvement in the change management process. The accelerated design process supports early panel sizing and location. This greatly improves the ability to maintain schedule as these are typically long lead items. Materials management through timely project execution and coordinating material delivery with construction schedules reduces construction labor and warehousing costs. The benefits of utilizing the continued improvements in digital data and processes are realized by the EPC, construction contractor, trace heating vendor and the end user.

VITA

Ben C Johnson is a Senior Consultant for Thermon, Inc.His career includes more than 52 years with Thermon and eight years prior in the petrochemical industry. He holds eight patents and has authored or co-authored 27 papers for various societies. He is the convener for TC31 Maintenance Team 60079-30, Electrical Equipment in Flammable Atmospheres, Electrical Resistance Trace Heating and the US technical advisor for IEC TC27, Safety in Electroheat Installations. Mr. Johnson is a Life Fellow of the IEEE, is Past President of the IEEE Standards Association, Past Chair of the IEEE IAS Petroleum and Chemical Industry Committee, and was co-chair of the IEEE/NFPA Collaboration on Arc Flash Phenomenon Research.
After two years at Lamar University and San Jacinto College, Mr. Johnson enlisted in the U.S. Navy and served as a member of the submarine service for 6 years.

Lamont Lewis is the Global Product Manager of Software for Thermon Inc. He has served in several capacities during his 37 year career with Thermon, including product testing and certification, system engineering and design. The last 23 years have been dedicated to managing the development of design software. He has a BSME from the University of Texas at Austin.

Daniel Ridsdale is a Design Engineer at Thermon Industries, based in the UK. He has worked for Thermon for 9 years, providing expertise for both electric and steam heat tracing projects of varying size and complexity. Daniel has had significant involvement with heat tracing design solutions using 3D software.

SELECTION AND RETURN OF EXPERIENCE OF INTEGRATED MOTO-COMPRESSORS ON TWO OIL & GAS SITES

Paper No. PCIC Europe EUR22_11

Lionel DURANTAY
GE Power Conversion
442, Rue de la Rompure
54250 Champigneulles
France

Olivier PELLERIN
Baker Hugues
480 Allée Gustave Eiffel
71200 Le Creusot
France

Alexandre BOUTEILLE
TotalEnergies
ZI portuaire du Havre - BP27
76700 Harfleur
France

Laurent GARAUDEE
TotalEnergies
ZI portuaire du Havre - BP27
76700 Harfleur
France

Sebastien BOUYSSOU
TotalEnergies
Avenue Larribau
64018 Pau
France

Edouard THIBAUT
TotalEnergies
2, Place Jean Millier
92078 Paris
France

Abstract – With the development of high-speed motors and active magnetic bearings, integrated moto-compressors (seal less, oil free, centrifugal compressor driven by variable speed drive system) using process gas to cool the motor have been developed as an alternative solution to conventional compression trains using either turbines or low speed motor associated with gearbox.
The first part of the paper presents and describes the integrated moto-compressors and variable speed drive technologies used on two Oil & Gas sites in Europe and South America. The second part of the paper explains and gives the reasons of the selection of integrated moto-compressors for these two Oil & Gas sites. Finally, the last part of the paper provides the site operator and manufacturer return of experience of these integrated moto-compressors.

Index Terms — High-speed motor, integrated moto-compressor, magnetic bearings, VSD.

I. INTRODUCTION

With the development of high-speed motors and active magnetic bearings, integrated moto-compressors (seal less, oil free, centrifugal compressor driven by variable speed drive system) using process gas to cool the motor have been developed as an alternative solution to conventional compression trains using either turbines or low speed motor associated with gearbox. The first part of the paper presents and describes the integrated moto-compressors and variable speed drive technologies used on two Oil & Gas sites in Europe and South America. The second part of the paper explains and gives the reasons of the selection of integrated moto-compressors for these two Oil & Gas sites. Finally, the last part of the paper provides the site operator and manufacturer return of experience of these integrated moto-compressors.

II. INTEGRATED MOTO-COMPRESSORS AND VARIABLE SPEED DRIVE TECHNOLOGIES

A. Integrated moto-compressors

In a conventional electric motor driven compressor package, the compressor is directly driven by a 4-pole air cooled induction motor fed by the VSD, through a gearbox, and the complete shaft line is supported by oil lubricated bearings. Thanks to the development of the high-speed asynchronous atmospheric motors and the AMBs technologies, high speed and oil free motor driven compressor became available in the 90s. The high-speed motor technology allowed getting rid of the speed increaser oil lubricated gearbox to drive the compressor. The latter being supported by active magnetic bearings allowed getting completely rid of lube oil systems. Directly connecting the motor and the compressor in a hermetic pressure casing, in which both high-sped motor and AMBs are cooled by the process gas, allowed getting rid of the dry gas seals and the associated conditioning system. The gas processed in upstream conditions is containing a large percentage of methane which is a better dielectric insulator than air, with thermal conductivity 4 times higher than air, which improves the cooling and compactness of the motor [1].

Fig.1. Gearbox Conventional Architecture vs Integrated Multi-Stage Architecture Layout

Compared to conventional electric compression, the integrated motor technology has the following main advantages (Fig.1):

- Strong reduction of weight and footprint,
- No more gear box, no more lube oil system, no more dry gas seal systems,
- No cooling water, no lubricating oil, no instrument air, no nitrogen,
- Only few remaining instruments,
- No direct emission (no gas leakage to the flare, no oil vapor) and low noise,
- Reduced maintenance (no DGS),
- Reduction of commissioning time and start-up operations,
- Reduction of integrated CAPEX and low OPEX.

When pressure ratio is lower than 1.6:1 the moto-compressor architecture can be simplified with a unique impeller generating the requested head to increase the pressure. Consequently, this impeller can be directly mounted on the motor shaft, saving the requirement of a separated compressor shaft and associated set of magnetic bearing. This simple architecture keeps the rigid shaft rotodynamic (Fig.2).

To keep the highest efficiency and avoid having the cooling flow recirculating on the complete compressor head, the electrical motor and AMB cooling is generated by a small fan (a small centrifugal stage) mounted on the opposite side of the main compression impeller (Fig.3). This small fan picks the fresh gas upstream the compressor flange, generate just enough head to ensure a safe and reliable cooling flow on the complete operating range, while the hot gas is re injected between the inlet flange of the compressor and the cooling flow supply. Specific distance between the various connection avoids unwanted recirculation.

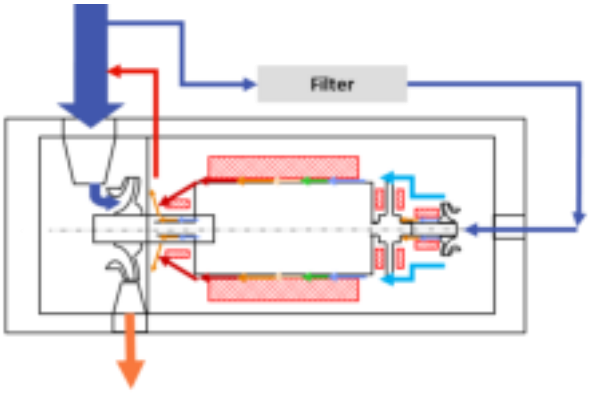

Fig.2. Integrated Single-Stage Architecture

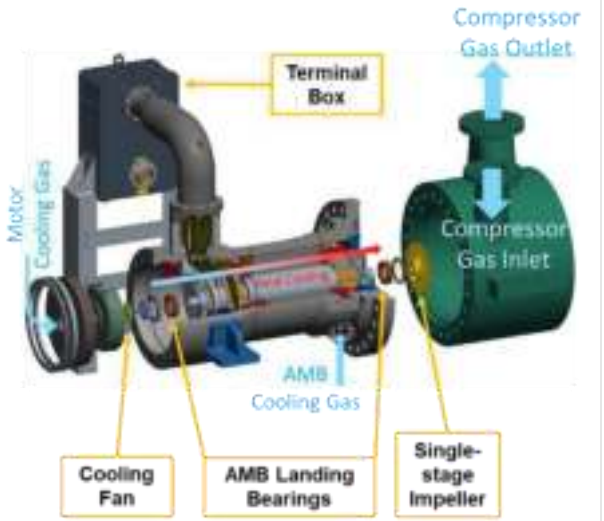

Fig.3. Integrated Single-Stage CAD View

The integrated architecture using a multi-stage compressor is adapted to the large compression ratio (Fig.4). This architecture uses a flexible coupling between motor and compressor, like couplings used for conventional compressor packages [2].

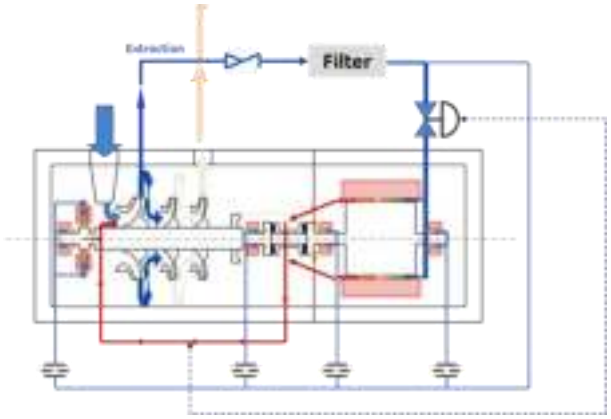

Fig.4. Integrated Multi-Stage Architecture

The squirrel cage rotor of the motor is adapted for high-speed conditions and comprises a steel lamination assembly compressed by tie rods between two end rings and two shaft ends (Fig. 5). The cage bars can expand axially through the end ring. The copper bars are inserted in the slots between the two end rings to form the squirrel cage. The laminated technology allows high efficiency, and high rotor peripheral speed up to 270 m/s.

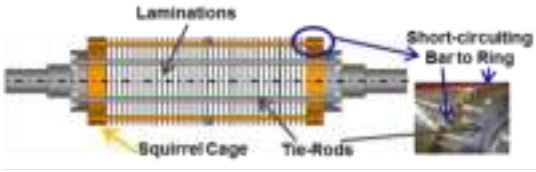

Fig.5 Laminated Induction Rotor Technology

For its dynamic behavior, the rotor of the motor operates in subcritical free-free mode when using magnetic bearings, meaning that the first bending mode is above operating speed with sufficient separation margin.

In 2007, and after a long qualification process, integrated compression system was validated for “Clean and Dry” natural gas applications with low contaminants such as H_2S (< 15 ppm) and with some limitation in terms of pressure, speed, and power [3]. Except for high H_2S & CO_2 (Acid) and Ammoniac contents, cracked gas, and high discharge pressure above 300 bar, the integrated compression can be used for all other types of gas whose process conditions change over time:

- Mid & Upstream: Natural Gas and Associated gas (Sweet and Sour),
- LNG: Mix-refrigerant, Boil of Gas,
- Downstream: Ethylene, Propane, Butene, H_2 …

The integrated motor (Fig.6) is designed for the following conditions [1]:

- Up to 15 bar partial pressure CO_2,
- Up to 15 mbar partial pressure of Wet H_2S,
- Up to 150 mbar partial pressure of Dry H_2S,
- Up to 200 bar SOP,
- Up to 100% relative humidity at suction,
- RGD < 30 bars/min.

The gas outlet temperature of the motor is limited and controlled to avoid any risk of gas fouling which can clog the end-windings and the ventilation ducts of the stator.

Fig.6. Single-Stage Motor-Compressor during string test

B. Variable speed drive

The Variable Speed Drive is a Voltage Source Inverter (VSI) commonly used to drive integrated electric compression train (Fig.7) since it allows to control high speed induction motor at a requested power factor, maximizing the torque generation by an optimum vector control. This technology is applied to many low speed and high-speed applications in a wider range of power.

The rectifier is a Diode Front End selected in 24-pulse configuration to minimize current harmonic emission in the upstream electrical grid [1]. It combines two parallel 12-pulse rectifiers arrangement with one primary Star circuit (RY) & one primary Delta circuit (RΔ) with 4 secondaries circuits (R1), (R2), (R3), (R4) producing a 15-degree phase lag (Fig.8).

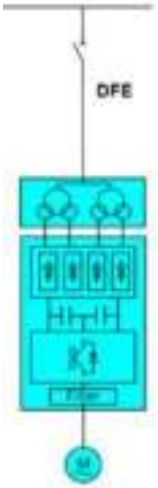

Fig.7. 24-Pulse-DFE NPP-Inverter

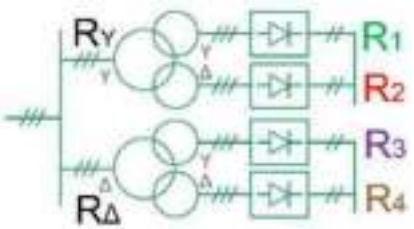

Fig.8. 24-pulse Rectifier

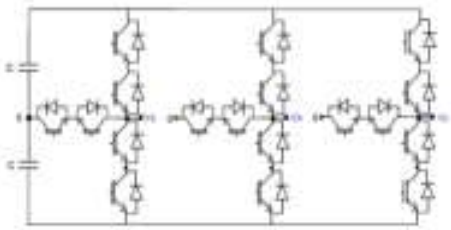

Fig.9. NPP VSI Inverter Topology

The inverter is a NPP PWM VSI inverter where the clamping diode valves of an NPC inverter (Fig.10) are replaced here by an IEGT valve giving additional controllability (Fig.11). With such a topology, each valve commutates with only half the DC bus voltage, reducing the devices commutation losses by three (see Table I) [4]. The output voltage is increased proportionally to the number of power switches per valve, each device being operated with the same current and sharing the same voltage (Fig.9).

TABLE I
NPC vs NPP Comparison

Converter Type	NPC	NPP
Level #	+	+
IGBT #	++	+
Diodes #	+	+
Output Voltage THD	+	+
Max commutation voltage	+	++
Rotor Max Voltage	+	++
Rotor Max Current	+	++
Max commutation frequency	+	++
Max current	+	+
(N+1) redundancy	-	+

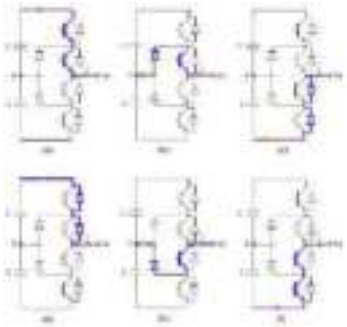

Fig.10. NPC Commutations

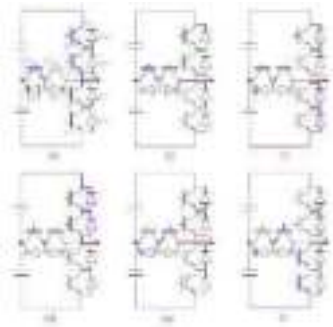

Fig.11. NPP Commutations

Due to the high-speed motor, the VSI inverter operates at fundamental frequencies above 90 Hz therefore there is a power derating of the inverter due to the significant switching losses of power semiconductors. A VSI output sine filter would have been normally used to feed the high-speed motor but by controlling the semiconductors of the inverter with a pulse synchronous control there is a significant reduction of the harmonics of currents fed into the motor, limiting the stator Joule losses and the torque pulsations (Fig.12).

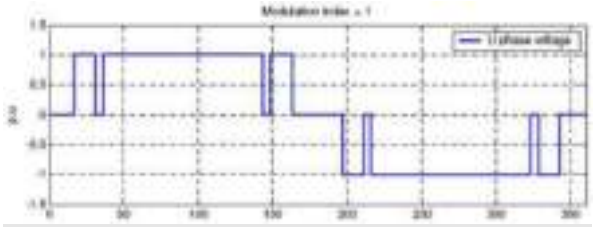

Fig.12 Example of pulse synchronous control

Therefore, due to this thermal margin, sine filter is not used and is replaced by a 3 times lighter LLC filter which is nevertheless necessary to avoid risk of reflected wave and voltage overshoot at motor terminal (Fig.13).

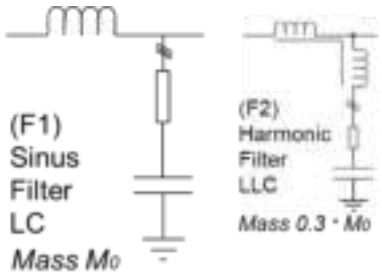

Fig.13. Inverter Sinus and LLC Filters

III. REASONS OF THE SELECTION OF INTEGRATED MOTO-COMPRESSORS

The two business cases, respectively named BC#1 and BC#2, are presented below (see Table II):

TABLE II
Business Cases Characteristics

Parameters	BC #1	BC #2
Location	France	Bolivia
Process	Downstream	Export compression
Process Gas	Ethylene	Natural gas
Compressor Architecture	Multi-Stage	Single-Stage
Unit #	1	2
Commissioning	2015	2016
Gas Flow	0.77 MSm^3/day	7.5 MSm^3/day
Pressure	13 to 97 bars	73 to 106 bars
Motor Voltage	2.4 kV	2.8kV
Motor Power	3.2MW	4.7MW
Rated Speed	11,617 rpm	11,553 rpm
Inverter	3-Level	3-Level
Rectifier	DFE	DFE

A. BC#1 - European site

From the Northeast to the South of France, several ethylene production plants delivered their product to the chemical customers through a common pipeline. Ethylene stream was either from North to South or from South to North depending on the production available or the storage capacity level. Decision was taken to stop the ethylene production plant located at the Northeast and to increase the flow rate from the South to the North. To reach the new duty, one existing compression station composed with two redundant reciprocating compressors had to be upgraded. The main design criteria were the ethylene flow demand and temperature fluctuations, the start-up conditions including a large differential pressure range and the possibility to not depressurize the compressor while is stopped for a long period. Three scenarios were considered:

- Revamp and upgrade of the two existing reciprocating compressors.
- New conventional motor driven centrifugal compressor
- New integrated moto-compressor

Integrated double stage moto-compression has been selected for the following main reasons (Fig.14 & 15):

Fig.14. Ethylene Integrated Compression

- A product dedicated to the pipeline applications and continuously improved with the return of experience
- A fully hermetic moto-compressor package enabling zero emission released to the atmosphere.
- A high level of availability due to the 6 years in between servicing. The maintenance activity was also supposed to be simplified because of the few mechanical components (no gearbox, no piston/cylinder) and the use of magnetic bearings.
- A reduced footprint of the overall process unit.
- A possible remote control of the compressor.

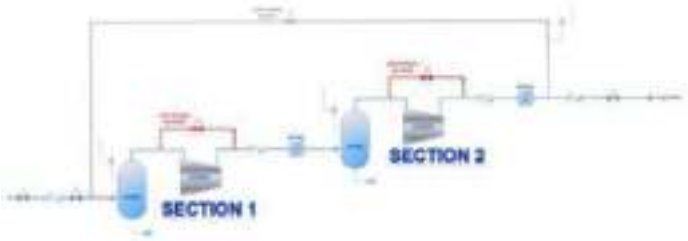

Fig.15. Process Flow Diagram

B. BC#2 - South America site

This solution is in a very remote location, at more than 1000-meter altitude. Natural gas streams coming from various well pads are gathered in a central processing facility where the gas is treated, including dehydration, to reach Customer specification. The integrated moto-compression located in this central facility is used to boost gas in a long export pipeline after treatment (Fig.16).

Fig.16. Export Integrated Compression

The operating mode of the integrated moto-compression is continuous with seasonal variations in export flow demand. Hence, maximum availability is required for this duty. Integrated moto-compression has been selected for the following main reasons:

- Being a relatively low-pressure ratio service, compression could be achieved with a single stage/impeller configuration, for which a conventional arrangement with low-speed motor plus gearbox plus compressor would have been significantly more complex than the overhung impeller integrated moto-compressor which has been selected (only two bearings versus eight bearings for a conventional solution). The latter arrangement eliminated the auxiliaries usually needed for a conventional package (e.g., no nitrogen needed for dry gas seals, thus simplifying the installation) and significantly reduced the amount of remaining instrumentation for a simplified maintenance in operation.

- The central processing facility accessibility was reduced, and the integrated moto-compression drastically simplified the packages transportation.

IV. REX OF INTEGRATED MOTO-COMPRESSORS

A. REX Operators

1. BC#1 - European site

This project has been an opportunity to develop the first ethylene integrated moto-compression. According to the pressure and temperature, ethylene becomes either a gas or a supercritical fluid which makes the process control and regulation complex. The development and commissioning of this new process control were probably the main difficulties faced by the project team. Here below are the main lessons learned:

- Starting conditions at Settle Out Pressure (SOP) and process transient conditions shall be properly studied to avoid issues during commissioning and at later stage during normal operations.
- Good communication between the compressor, motor and VSD manufacturer is key to properly tune the VSD software and save time during commissioning.
- Cabling shall be thoroughly checked after construction to secure the commissioning planning.
- Kinetic support used to mitigate voltage dips shall be properly tuned to avoid spurious trip by having the compressor going into surge area.
- Compressor load flow controller shall use a PID regulation instead of an on/off control to avoid gas flow fluctuation.
- Lightning EMC disturbance mitigation shall not be overlooked to avoid power control board failure.

When issues and tuning were made, without any delay, the compression unit had started in 2015 and the first servicing held in 2021 without any major issue discovered.

2. BC#2 - South America site

The integrated moto-compressors were commissioned between the end of 2016 and the beginning of 2017. At the compressors level, commissioning has been essentially slowed down by connections issues at the high voltage junction boxes and by control system issues. From a construction standpoint, it was observed that high frequency motor and VSD require a special attention with regards to cable installation (Fig.17), screen earthing and earth mesh grid. The latter shall not be underestimated as it can produce EMC issues leading to spurious trip of the VSD.

Operational experience also demonstrated that VSD internal cabling must be properly verified at converter factory and that any modification, upgrade or cabling modification on site be properly monitored to ensure proper reliability/availability of the VSD. Ethernet connection switches are not equivalent, they shall be extensively tested before site implementation to ensure compatibility and proper integration within the site ethernet network.

Fig.17. Shield burnt by high current circulation

At the end of summer 2021, each integrated moto-compressor cumulated more than 17,000 and 19,000 hours. While the compressor part (motor plus compressor) exhibited very good mechanical and thermodynamic performances, several upsets were encountered with the VSD, leading to a reduced availability of the overall compression system. This was due to a lack of feedback from the new control architecture that had been implemented for this project. The hardware was sensitive to EMC disturbances (Fig.18) which generated premature and spurious trips originated by the VSD control system.

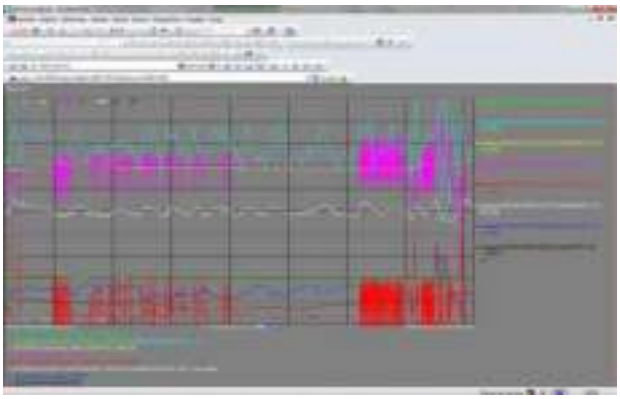

Fig.18. Export fluctuations

However, despite the previously mentioned issues which have been resolved by the VSD supplier, the integrated moto-compression is viewed as a flexible system by the operators of the facility. This REX enabled the VSD supplier to integrate a whole series of tests into its Real-Time Control Simulator platform, making the robustness of the system more reliable.

B. Manufacturers REX and Challenges

1. Moto-compressor Platforming

Since this moto-compressor introduction in 2007, the compressor and motor manufacturers have implemented some upgrade on the initial design of the unit.

The coupling chamber access was originally a square bolted trapper (Fig.19), it is now a standard RF flange with associated counter flange. Because the change is only the drilling geometry, the round shape does not change the compressor casing design, neither the accessibility of the coupling while using the standard flange design facilitated a lot the maintenance (Fig.20).

Fig.19. Coupling access square shaped

Fig.20. Coupling access standard RTJ flange

The motor casing was initially a welded casing with bolted cover. The AMB connector on the motor were different and using different mounting method from the compressor ones (Fig.21). The new motor casing is now using a design like the compressor one, i.e., using bolted flange and full machined design with a motor cover closed with shear ring. Electric motor casing is identical for both single-stage and multi-stage compressor arrangements (Fig.22). Regarding the AMB connector, it is now using the same design as the compressor casing. It simplifies the moto-compressor assembly during manufacturing and the maintenance operation.

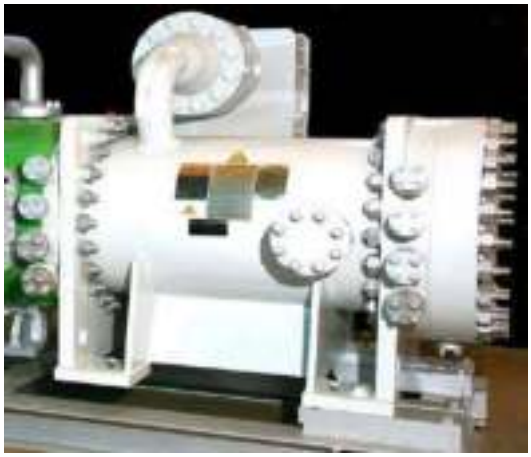

Fig.21. Original welded motor casing

Fig.22. Full machined motor casing

2. BC#2

On the BC#2 project, the compressor manufacturer introduces a simplified version of the multi-stage arrangement to match the low-pressure ratio requirement below 1.6:1.

The first challenge was to manage the axial thrust on the unit. It is important to predict and compensate properly the axial thrust as magnetic thrust bearing has a lower capacity compared to oil thrust bearing. In the single stage arrangement, the axial thrust is a combination of thrust generated by the variation of gas momentum (so-called dynamic axial forces) and the differential pressure across the impeller and across the balance piston (so-called static axial forces) [5]. Usually, static axial force of the impeller is mainly compensated by axial force of balance drum and the remaining by the thrust bearing, keeping some capabilities for dynamics axial forces (Fig.23). The compressor manufacturer developed and patented [6] a dynamics axial thrust compensation device to avoid reaching the limit of magnetic bearing thrust capacity without limiting the operating range of the unit (i.e., limiting dynamics axial thrust). This device allows compensating the variation of gas momentum across the impeller, especially when operating in large flow (close to choke flow) thus expanding the operability of the unit.

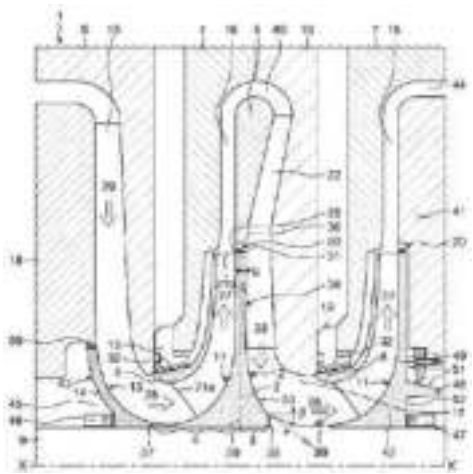

Fig.23. Dynamics Thrust compensation device

The second challenge was to validate the new cooling flow schematic with a fan. On multistage arrangement, the cooling gas is extracted from the 1st impeller discharge, generating a recirculation of gas on a fraction of the total head generated by the compressor. Using such a configuration on a single impeller compressor generates a recirculation on the total head generated by the compressor and thus affects more the performance. To maximize efficiency, it has been decided to install a cooling fan on the non-driving end of the motor to ensure the cooling of the complete unit (Fig.24). The general principle of the cooling circuit of a single stage overhung integrated machine is shown in figure below

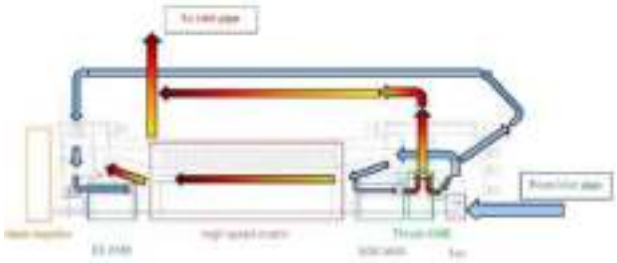

Fig.24. Single stage overhung integrated compressor cooling scheme

The system is fully autonomous and passive. No active regulating device is used. The flow delivered by the fan is split in four main branches, corresponding to the elements to be cooled:

- Thrust bearing outboard,
- NDE radial AMB + inboard thrust bearing,
- Motor stator and rotor,
- DE radial AMB.

Main challenge was to ensure a safe and reliable cooling of each electrical component on the complete operating range without any active regulation. As much as possible, mastering the cooling system requires having knowledge of the pressure, temperature and flows that goes through the different branches of the circuit A cooling model based on the multistage one has been developed to have a simulation tool to prove the safe behavior on the complete operating range and to validate the passive cooling method [7]. Pressure drops across the various component to be cooled by the process gas are well known thank to the multistage experience, and a dedicated 1D pressure drop & cooling model validate the principle of passive cooling.

Main challenge was the proper calibration of the cooling flow to ensure the reliability of the modeling. The 1D pressure drop model (Fig. 25) validated the principle of passive cooling.

BC#2 was the first single stage arrangement manufactured. To validate modeling, extensive instrumentation and measure has been recorded during the test of the unit and the orifice that usually distribute the flow in the various branch of cooling have been replaced by manual lockable valves to fine tune the flow distribution (Fig.26).

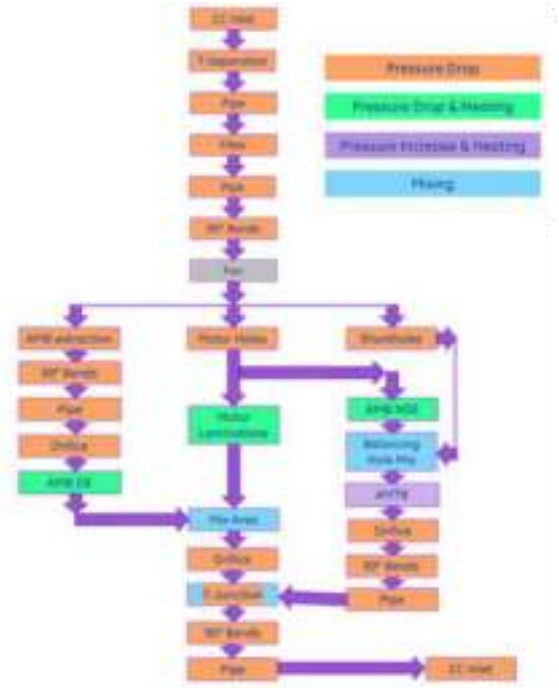

Fig.25. Schematic cooling network

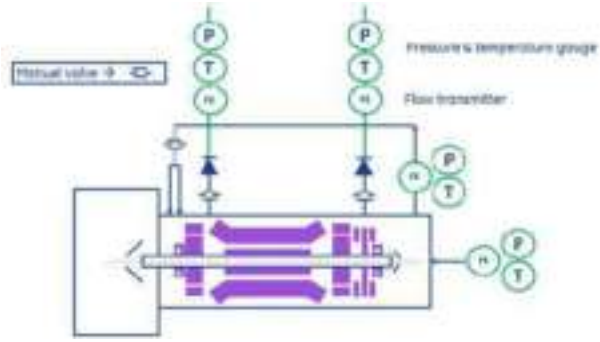

Fig.26. Additional instrumentation for cooling validation

The test sequence includes a simulate test (PTC 10 type II) to characterize the behavior of the reliability of the model. Regarding the fan, performances are determined thanks to the special instrumentation installed around it. While the fan pressure ratio was properly predicted, the efficiency was over predicted. The experimental efficiency must be considered carefully as the temperature increase through the fan is very low (~5 °C). The value of efficiency is of low importance as the power absorbed by the fan is very small with respect to the full system power. The experimental pressure drop characteristics of the different elements are re-injected in the simulation tool.

The application of the calibrated simulation tool allows determining the real cooling circuit characteristic. it appears than the achieved pressure drop is about half the initial estimated one. Therefore, the fan would work in the stone wall region. On the first unit, thanks to a manual valve upstream the fan, an artificial pressure drop has been created to have a better matching between the selected fan and the circuit characteristic. Once calibrated, the cooling repartition model match well the experimental result (Fig.27).

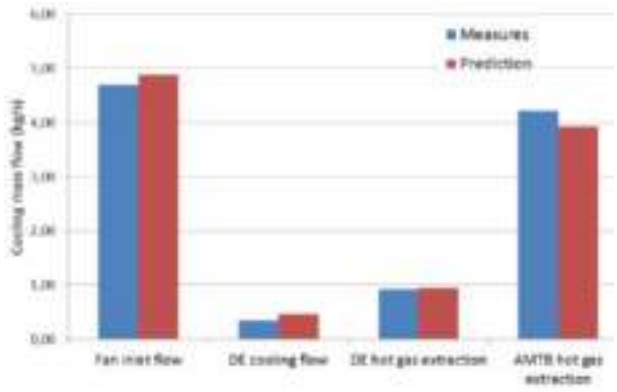

Fig.27. Flow repartition comparison during type II test

Seven different stable points executed during the type I tests have been analyzed to validate the model in a much wider range. The predicted and measured values are compared in the figures (Fig.28).

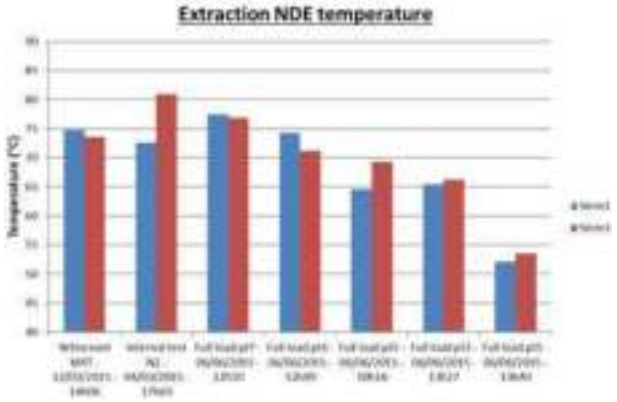

Fig.28. Comparison of predicted and measured cooling parameters during type I test

In general, a very good agreement is observed, meaning that both the flow repartition and the system losses are well modelled. The global mass flows are within 5% and the discharge temperatures are within 5°C, except for the point with Nitrogen N_2.

At the light of these results, the system was considered qualified, and the prediction tool now used on any case to design an optimum fan for each application.

V. CONCLUSIONS

The integrated moto-compressors line is a mature and proven solution with many references, bringing several advantages compared to conventional solution: no shaft end seal leakage, no restriction in long term pressurization for dry gas, improved availability thanks to dry gas seal absence. The overall casing of the motor-compressor has been improved and structured to facilitate assembly and maintenance operations for the two types of single-stage and multi-stage compressors and the range of associated asynchronous motors.

On the VSD side, there is still the need having a standard product approach which is not the case today where the VSD is customized for each project. Return of experience has shown that a special focus shall be put on the VSD and compressor control software's to configure it and debug it prior to the commissioning. Field Service Engineer (FSE) training shall be improved to secure the commissioning and improve the resolution of issues at site before production start-up.

VI. ACKNOWLEDGEMENTS

Special thanks to Thomas Alban (Engineering Director of Baker Hughes Thermodyn) and Sylvain Guillemin (R&D Principal Engineer of Baker Hughes Thermodyn) for their support for this paper.

VII. REFERENCES

[1]. L. Durantay, A. Gelin, E. Thibaut, Y. Vidalenc, "Integrated Moto-compression versus Conventional Solution ", in PCIC Europe proc., Paris, May 2019.
[2]. J.M. Pugnet, P. Friez, P. Laboube, "Centrifugal Compressor Having a Flexible Coupling, US Patent 2006/7144226, Dec 5, 2006.
[3]. J. F. Grignard, M. Poerner, L. Durantay, S. Galioto, J. Krahn, "Corrosion Testing of a Subsea Motor and Stator Winding Insulation," in *ASME Turbo Expo*, June 2015.
[4]. V. Guennegues, "Contribution to the study of multilevel converters for high-speed motor applications", PhD, Institut National Polytechnique de Lorraine, Dec 2009.
[5]. L. Baldassarre, A. Bernocchi, E. Rizzo, M. Fontana, F. Maiuolo, "Axial Thrust in High Pressure Centrifugal Compressors: Description of a Calculation Model Validated by Experimental Data from Full Load Test, *TPS Conference Record*, 2015, Houston TX.
[6]. Patent WO 2014/102125 Al.
[7]. Th. Alban, O. Pellerin, P. Laboube, B. Quoix, A. Gelin, M. Oliva, "Mechanical and Performance Testing Method of an Integrated High-speed Motor Compressor", in *TPS Conference Record*, 2009, Houston TX.

VIII. NOMENCLATURE

AMB	Active Magnetic Bearing
CAPEX	CAPital Expenditure
DC	Direct Current
DE	Driven End
DFE	Diode Front End
DGS	Dry Gas Seal.
EMC	ElectroMagnetic Compatibility
FSE	Field Service Engineer
IEGT	Injection Enhanced Gate Transistor
HGBP	Hot Gas ByPass
NDE	Non-Driven End
NPC	Neutral Point Clamped
NPP	Neutral Point Piloted.
OPEX	OPerational EXpenditure
PWM	Pulse Width Modulation
REX	Return Of Experience
SOP	Settle Out Pressure
VPI	Vacuum Pressure Impregnation
VSD	Variable Speed Drive
VSI	Voltage Source Inverter

IX. VITA

Lionel DURANTAY is graduated from the ENSEM of Nancy, France (Ecole Nationale Supérieure d'Electricité et de Mécanique) with an engineering degree in 1989 then passed PhD in 1993. As R&D Leader, he has developed innovative variable speed motors & generators solutions for Oil & Gas, Renewable and Marine businesses. He has authored or coauthored 40+ technical papers. He presently holds 15+ patents. He is currently Chief Technology Leader in GE Power Conversion.
lionel.durantay@ge.com

Olivier PELLERIN is graduated from Ecole Nationale Supérieure de Mécanique & Aéronautique (ENSMA) in Poitiers France. After starting is career in 1999 as Compressor Design Engineer in Thermodyn Le Creusot, he was application engineer for integrally geared centrifugal compressor in Sundyne. Back in Thermodyn since 2007 as product leader in charge of the expansion of the ICL product line. Since 2014 he is commercial & marketing manager for Thermodyn product. He has coauthored 3 technical papers about centrifugal compressor technologies.
Olivier.pellerin@bakerhughes.com

Alexandre BOUTEILLE is graduated as an electrical engineer from the Ecole Nationale Supérieure d'Ingénieurs Electriciens de Grenoble (ENSIEG) in 2001. He joined TotalEnergies in 2011 and participated to several onshore petrochemical projects in Europe with a position of electrical engineering and commissioning leader. He is currently electrical specialist in TotalEnergies and involved in various projects or technical support to the assets.
alexandre.bouteille@totalenergies.com

Laurent GARAUDEE is graduated from the ENSAM (Ecole Nationale Supérieure d'Arts et Métiers). He works 7 years for DRESSER-RAND as technical support and commissioning/start-up engineer. He joined TotalEnergies in 2015 as rotating specialist.
laurent.garaudee@totalenergies.com

Sebastien BOUYSSOU is graduated from ENSAM (Ecole Nationale Supérieure d'Arts et Métiers). He worked 8 years for Thermodyn, Le Creusot, as compressor design engineer, project engineer and project engineer's leader. He joined TotalEnergies in 2009 as rotating equipment specialist.
sebastien.bouyssou@totalenergies.com

Edouard THIBAUT graduated as an electrical engineer from the Ecole Supérieure d'Ingénieurs en Electronique et Electrotechnique (ESIEE). Before joining TotalEnergies in 2009, he worked eleven years for Alstom Power Conversion and then Converteam. He held several positions as Variable Speed Drive Systems design and commissioning engineer in several major international projects both Onshore and Offshore in Europe, Asia and North America. He has authored or coauthored 22 technical papers. He presently holds 3 patents. He is currently electrical specialist for various projects within TotalEnergies.
edouard.thibaut@totalenergies.com

NEW NON-METALLIC CABLE SUPPORT SYSTEMS FOR HARSH ENVIRONMENTS

APPLICATION IN EX ZONES

Paper No. PCIC Europe EUR22_12

Lead Author:
Mr. Jose Antonio Mostazo
Barcelona
Spain

Author B:
Mr. Marc Serra
Lyon
France

Author C:
Mr. Albert Casas
Barcelona
Spain

Author D:
Ms. Elena de la Cruz
Barcelona
Spain

Abstract - One of the trends for future developments, including those offshore and harsh environments, is for modular construction minimizing site assembly.
Size, weight and availability of complete range of fittings are key factors for modulator construction, and all elements are considered including cable support systems.
This paper will explore the use of non-metallic cable support systems, particularly for harsh environmental conditions.
Work done to determine the acceptability, according to IEC 60079-32-1, for use of new non-metallic cable support systems in hazardous areas will be presented and compared with the use of traditional metallic and non-metallic cable support systems.
Practical measures for mitigation of issues of electromagnetic compatibility will be addressed.

I. INTRODUCTION

Traditionally cable support systems such as cable trays and ladders have been made of metals. Over the past years, new thermoplastic formulations which can provide the required mechanical capabilities of cable support systems have been developed. They greatly enhance resistance to corrosion in harsh environments, increasing durability. Being non-metallic, they also help to improve electrical safety.

Cable trays, regardless of the material of which they are made, are not within the scope of ATEX Directive 2014/34/EU, as they do not have autonomous function; are not essential for a safe functioning of ATEX equipment or protective system, and have no own source of ignition (See Annex II in the Application Guideline of the Directive 94/9/EC. Borderline-List. ATEX products).

The Notified Bodies cannot certify products beyond the scope of the mentioned Directive, but the products can be analyzed to elaborate a report about the safe use of the product in Ex Zones (Risk Analysis), according to the current status and the relevant guidelines in this field.

This paper is a new approach following the IEC ATEX standards to consider the second way to analyze the use of cable trays in Ex Zones.

Historically the consideration has been to use a conductive material with an earthing resistance <1Mohm, or by limiting the surface of insulating materials which cannot fulfil that resistance. But the option to make a Risk Analysis has been long overlooked.

This document shows the conclusions of the study about the use of non-metallic thermoplastic cable trays in ATEX areas, which serves as a Risk Analysis.

II. MATERIALS USED TO MANUFACTURE CABLE TRAYS

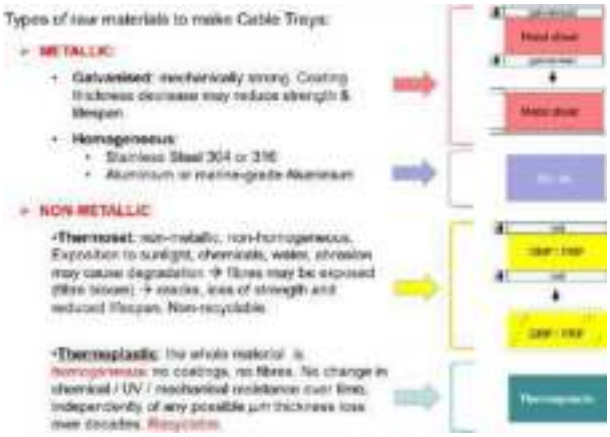

Galvanized systems have limited lifespan in harsh environments:

Table I: Annex K of IEC/EN BS 61537
Environmental categories and corrosion rates for zinc only galvanising

Environment	Corrosion rate in µm per year of coating deposited
Interior: dry	< 0.1
Interior: occasional condensation Exterior: rural	0.1 → 0.7
Interior: high humidity, some air pollution Exterior: urban, inland or mild coastal	0.7 → 2
Interior: swimming pools, chemical plants Exterior: industrial inland or urban coastal	2 → 4
Exterior: industrial with high humidity or high salinity coastal	4 → 8

Table 2: Table of IEC/EN BS 61537
Corrosion classes for metallic materials (Steel).

Class	Material and coating	Coating standard	Minimum coating thickness (µm)	Hours to Salina Mist Test (ISO 9227)	Years to visually rusted surface
1	Steel S235 prepainted	EN 10327 EN 10169	10	120	2.5
2	Steel S350 prepainted		14	480	3.1
3	Hot dip galvanized	ISO 1461	45	480	7.5
4	Hot dip galvanized		55	600	9.1
5	Hot dip galvanized		70	720	10.8
6	Hot dip galvanized		85	840	14.7
7	Steel	EN 10084	–	–	–

NOTE: IEC/EN BS 61537 Corrosion classes are based only on humid and saline corrosion tests ISO 9227. Other relevant types of corrosion are currently under consideration by the IEC/EN BS 61537.

Thermoset products lose effectiveness when subject to weathering and/or chemicals. Moreover, some of these thermoset products add conductive additives to comply with the <1 Mohm requirement. That requires installing earthing connections, ensuring that the corrosion caused by those harsh environments does not affect them and they can maintain conductivity.

Maintenance of conductivity of the earthing systems for metallic systems is alterable. I.e. it depends on maintenance and upkeeping activities, making them dependable on human factor.

One of the advantages of a thermoplastic solution is that features are unalterable over time. The same reaction can be expected on the day of commission vs some decades later.

III. RELEVANT IGNITION SOURCES FOR CABLE TRAYS

Table 3: Preliminary Risk Analysis comparing insulating and metallic cable trays use in hazardous areas
(by TÜV SUD Process Safety).

IV. CHARGE AND DISCHARGE MECHANISMS

Unlike metallic bodies, which can be charged by contact, induction and friction, insulating bodies can only be charged by friction:

Table 4: Electrostatic charge and discharge Mechanisms (by TÜV SUD Process Safety)

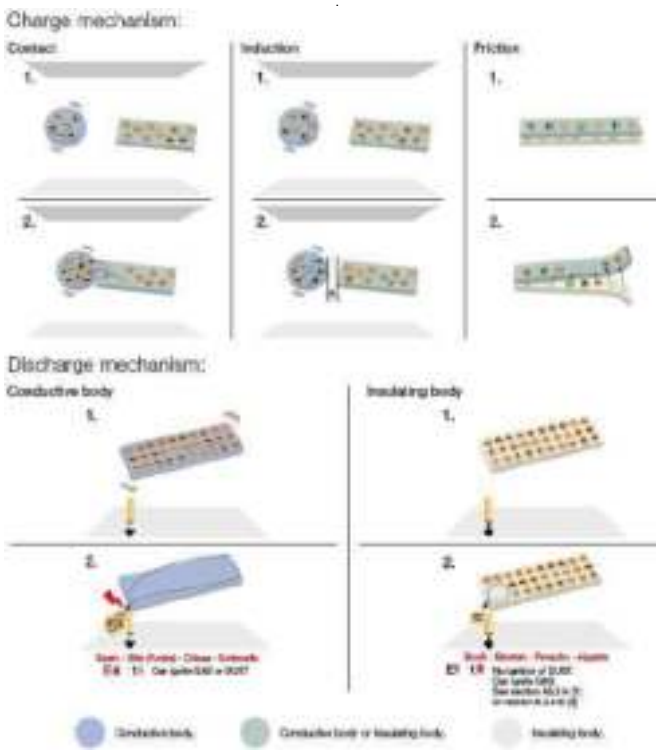

A possible discharge in a conductive body may have much higher energy and for a longer time compared to a discharge in an insulating body.

V. USAGE CRITERIA

a) Preliminary definitions:

• Singular operations: Operations such as installation, unpacking, handling, mounting, feeding cables, feeding pipes, etc. are considered within this point. These operations are considered singular as they are not continuously performed and have a clear start and end point.

• Normal use: All operations and conditions present under intended use of the facilities.

b) Table of acceptance criteria for a safe application of thermoplastic Cable Trays:

Table 5: Acceptance criteria for safe application of thermoplastic cable trays in hazardous areas
(by TÜV SUD Process Safety based on Risk Analysis and IEC/TS 60079-32-1:2013).

(1) Singular operations in this zone require issuing a fire permit. A work permit should be issued in classified areas to perform maintenance operations regardless the material of the cable trays. After performing installation in classified areas with insulating cable trays, a short waiting time (about 30 minutes) must be given before resuming normal operation. Metallic trays will discharge immediately when earthed*.

(2) No installation allowed due to the fact that normal use is not allowed in this zone. The reason is that effective electrostatic discharges cannot be excluded according to the zone requirements in terms of maximum insulating surface limitation when considering very rare malfunctions.

Nevertheless, cable trays are typically not installed in Zone 0.

(3) Due to the ignition sensitivity of gases for Explosion Group IIC, the same criteria as in note 2 is applied in Zone 1 for substances of this group.

(4) In Zone 20, there is no effective limitation of the maximum non-conductive surface. Nevertheless, cable trays are typically not installed in Zone 20.
Use of cable trays in Zone 20 has not been considered.

(5) According to section 3.3.3 of IEC/TS 60079-32-1:2013 [3], and the table describing the classification of zones, metallic parts with a capacity of more than the following values must be earthed:

a) 10 pF for: Zone 21 with MIE > 10 mJ or Zone 2

b) 6 pF for: Group IIA in Zone 1 and Zone 21 with MIE < 10 mJ

c) 3 pF for: Group IIB in Zone 1

(6) Spare parts (screws and mounting axes) used in assembling of these thermoplastic cable trays do not need to be earthed due to the fact that their capacity is below the limits defined and the considerations mentioned in note 5.

(7) Use of thermoplastic cable trays in Zone 1 (including substances of explosion Group IIA and IIB, but excluding substances of Group IIC) may be acceptable if normal operation does not cause the presence of charge build-up on the trays. Meaning that, under normal operation, tasks and actions performed do not cause friction or separation processes on them.

Where the presence of processes generating charge built-up on the trays may be prevented by:

· Keeping cable trays away from the source of charge built-up (e.g. make them not normally accessible by the operators, for instance by placing them underneath the ceilings, etc.)

· Or Placing a physical barrier between cable trays and the source of charge built-up.
In Zone 1 it is recommended to issue a work permit for specific operations which can generate charge built-up, i.e. cleaning operations by friction or water jets, placing or removing cables on the trays, etc.

(8) Metal and other conductive or dissipative material should be connected to earth with the exception of very small items (capacity below the limits on note 5).

(9) As a general rule to prevent electrostatic risks, cable trays must not be installed in the path of a filter exhaust stream, since in case of filter failure the high solid density in the gas stream could generate a significant charge by friction in the tray.

* Attention must be paid to the presence of painting layers on these pieces. Painting layers may cause conductive parts to become isolated. Caution with paint layers isolating conductive objects is a general rule to prevent electrostatic risk.

** Cleaning by friction (wiping) or by blowing air to remove dust is strongly not recommended.

*** In ATEX Zones, cable connections must be done inside Ex certified enclosures.

NOTE: Under hybrid mixtures (gas+dust) the usage criteria of gases must be taken as critical safety elements, regardless of the cable tray material.

VI. OTHER CONSIDERATIONS

(1) Rain as a significant charging mechanism for insulating cable trays.

Water droplets may get charged while slipping over dry insulating surfaces, nevertheless, in case of rain charge generation is low and the presence of wet surfaces easily helps to dissipate the charge. Therefore, criteria described in table in section IV are valid even if rain can be present in the facility.

(2) Wind as a significant charging mechanism for insulating cable trays.

Clean gases do not generate electrostatic charges. Charge may be generated by gas streams with a high solid particle density. Charging mechanism due to particles present in atmospheric wind is not significant due to the low solid particle density. For process streams with presence of solid particles note (9) above must be considered.

(3) Vibration.

A clear vibration which can be noticed while touching the tray may continuously generate charges due to the constant movement and separation of the trays and cables supported. Therefore, it would be considered as a continuous charge generation and is not allowed. In such a situation, the charge generation and charge accumulation should be carefully assessed regardless of the material of the tray since other insulating surfaces, such as cables, could also be present.

VII. CONCLUSIONS

Risk Analysis on insulating Cable Trays in Ex Zones shows:

- Thermoplastic Cable Trays have fewer sources of ignition than Metallic Cable Trays (1 vs 3).
- Thermoplastic Cable Trays have fewer charging mechanisms than Metallic Cable Trays (1 vs 3).
- A possible discharge in a conductive Cable Tray may have much higher energy (higher risk of spark) and for a longer time compared to a discharge in a thermoplastic Cable Tray. While an earthing system should prevent that, it all depends on its condition and status of maintenance.
- Thermoplastic Cable Trays cannot be used in 0/20 Zones, but they can be used in most 1/21 and 2/22 Zones.
- A Risk Analysis according to the current status and the relevant guidelines is a valid instrument to determine the suitability of thermoplastic Cable Trays in Ex Zones.

VIII. VITA

Jose Antonio Mostazo graduated from the ETSEIB-UPC Engineering school in 2000 with a degree in mechanical engineering. He has been a Product Quality Manager for the Unex Group since 1999 to 2004 and Support Systems Technical Manager since 2004.
jamostazo@unex.net

Marc Serra graduated from the ENSMM Engineering school in 2000 with a master's degree in mechanical engineering. He has been a Technical Product Engineer for the Unex Group since 2007 and France Technical Product Manager since 2020. He is a member of the AFNOR standards U15 committee.
mserra@unex.fr

Albert Casas graduated from the UPC - Polytechnical University of Catalonia in 2001 with a degree in Electronics Engineering, and from the Northumbria University (UK) in 2003 with a Bachelor's Degree in Electronics and Communications Engineering. He has been a Sales Area Manager for the Unex Group since 2009 for the International Department.
acasas@unex.net

Elena De La Cruz graduated from the EHU/UPV - University of the Basque Country in 2004 with a degree in Macroeconomics and from the ICEX-CECO in 2005 a Master's degree in Foreign Trade. She has been a Sales Area Manager for the Unex Group since 2006 for the International Department.
edelacruz@unex.net

IX. REFERENCES

Reference documents for the elaboration of the usage criteria table:

[1] TRBS 2153: 2009 Technische Regeln für Betriebssicherheit. Vermeidung von Zündgefahren infolge elektrostatischer Aufladungen.

[2] CENELEC CLC/ TR 50404: 2003 "Electrostatics - Code of practice for the avoidance of hazards due to static electricity".

[3] IEC/TS 60079-32-1: 2013, Technical Specification EXPLOSIVE ATMOSPHERES – Part 32-1: Electrostatic hazards, Guidance, Edition 1.0.

[4] BGR 104: 2005 BG-Regel Explosionsschutz-Regeln für das Vermeiden der Gefahren durch explosionsfähige Atmosphäre mit Beispielsammlung.

[5] SUVA Merkblatt 2153. Explosionsschutz. Gründsatze Mindstvorschriften Zonen.

[6] ESCIS (Expert Commission for Safety in the Swiss Chemical Industry). Static Electricity, rules for plant safety. 1988.

[7] Directive 2014/34/EU on the harmonisation of the laws of the Member States relating to equipment and protective systems intended for use in potentially explosive atmospheres.

[8] Directive 1999/92/EC on minimum requirements for improving the safety and health protection of workers potentially at risk from explosive atmospheres.

[9] EN 1127-1: 2011. Explosive atmospheres – Explosion prevention and protection – Part 1: Basic concepts and methodology.

[10] IEC 60079-10-1: 2008. Classification of areas. Explosive gas atmospheres.

[11] IEC 60079-10-2: 2009. Classification of areas. Combustible dust atmospheres.

[12] IEC 60079-14: 2007 Explosive atmospheres. Part 14: Electrical installations design, selection and erection.

[13] M. Glor, A. Pey; Modelling of electrostatic ignition hazards in industry examples of improvements of hazard assessment and incident investigation. Journal of electrostatics 71 (2013) 362-367

X ACKNOWLEDGMENTS

Mr. ALEXYS PEY from TÜV SÜD PROCESS SAFETY for helping in writing the report on RISK ANALYSIS.

REPLACEMENT OF STEAM AND GAS TURBINES WITH ELECTRICAL HIGH-SPEED DRIVE SYSTEMS FOR CO2 REDUCTION

Paper No. PCIC Europe EUR22_13

Hartmut Walter
Siemens AG
Berlin
Gemany
Ht.Walter@siemens.com

Bart Sauer
Senior Member IEEE
Siemens
Cincinnati, Ohio, USA
Bart.sauer@siemens.com

Gijs van Maanen
Siemens AG
Nuremberg
Germany
Gijs.van.Maanen@siemens.com

Abstract - Regulations on Co2 emission reductions, as well as potential taxation on Co2 production are coming in place worldwide. There are many possible ways to reduce Co2 emissions in Chemical and Petrochemical plants. One is to replace Steam Turbine (ST) or Gas Turbine (GT) equipment drives with electrical drivers. This can be done for new plants, as well as for existing plants, however, the requirements can be very different.

Index Terms — Turbine Replacement, Gas Turbine, Steam Turbine, Electrification, Co2 emission Reduction, Emission Reduction, Emission Tax

I. INTRODUCTION

This paper builds on a PCIC-2015-xx paper [1] that presented high speed (HS) solutions for turbine replacements with a focus on a Pacific Island refinery installation.

Now presented are more details related to current environmental and sustainability issues, including Co2 emission reductions, while diving into the latest electrical driver technology advances and the realm of challenges faced in production plants with turbine replacements

The international treaty on climate change, the Paris Climate Accords adopted in 2015 has led to many new and upcoming regulations in different regions around the world related to Co2 reduction. Countries, carbon energy producing companies, carbon refiners, carbon using manufacturers and major suppliers to the petroleum and chemical market have all had to make adjustments. Terms like “net carbon neutral”, “green energy” and “sustainability” are now commonplace in stockholder meetings and reports.

Natural gas turbines and steam turbines (coupled with their power plant sources of steam) are prime targets of refineries, chemical plants and pipelines for reduction of Co2, with the added benefit of overall energy efficiency and reduced operational costs.

Both “green field” (new installations) and “brown field” (replacement of existing equipment) are addressed, including the most current and reliable technology in motors, variable speed electric drives and monitoring to service these applications. It should be noted that existing turbine installations often are central to plant operations and without redundancy. 100% availability is very commonly demanded.

This paper will not try to present financial case studies related to efficiencies or emissions type penalties due to the wide range of efficiencies and emission levels to be considered, but rather address the replacements themselves.

A Check Sheet to aid owners of turbine in the evaluation of turbine replacements with electrical drives and lastly field examples are provided.

Efficiency and Emission Footprint

The turbine replacement support on two fields: efficiency improvement and emission footprint reduction.

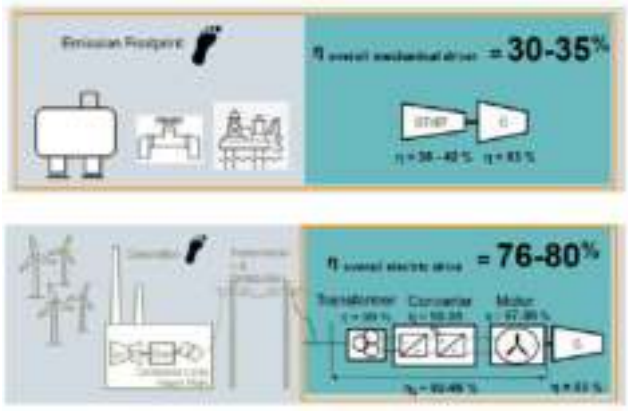

Fig. 1: Efficiency and Emission Comparisons

Fig. 1 describes the efficiency improvement and emission footprint reduction. The frame symbolizes the plant borders.

The efficiency roughly doubles when comparing a turbine mechanical drive to an electrical drive. As these applications are often in a high power range (> 1 MW), this improvement can have a significant, long-term operating cost impact.

While the reduction of the emission footprint within the plant for this application may decrease to zero, the energy consumed by an electrical driver must still be produced. That source may still result in CO2 emission footprint. Alternatively, the electricity might be produced in wind farms or another green energy production. Another possibility is a modern combined cycle power plant which could provide the electricity and help to reduce the overall emissions.

Field of turbine replacement affects two types of turbines typically used as compressor driver: gas turbines and steam turbines. As for the gas turbine the emission is directly related to the function of the turbine, however for the steam turbine, the emission is related to the steam production process in a boiler. In both cases the fuel to drive the turbine is available "anyway" and in case of the steam turbines in chemical or petrochemical plants a necessary product for the process or a byproduct of the process. By installing bigger boilers, the necessary amount of steam could be made available.

As this "anyway" with the new boundary conditions and regulations comes with a surcharge, therefore it is worth the effort to explore the benefits of replacing the turbines with electrical drivers and to balance the benefits of lower environmental taxes, higher efficiency and/or a more flexible process with the challenges to exchange turbines in existing plants; turbines which are running and earning profit.

We will have a look at the gas turbines and steam turbines separately.

Gas Turbines

Gas turbines are mainly installed at pipeline stations and on offshore production platforms and Floating Production Storage and Offloading facilities (FPSO). Here gas is available out of the pipeline or out of the production. Usually pipelines or platforms have no strong electrical grid available, so the use of gas turbines as driver was the best choice. Already due to noise and exhaust constrains, some pipeline stations near populated areas were equipped with electrical drivers where grid connection was possible without greater investment.

On offshore platforms electricity to run the platform is produced with gas turbine driven generators. However, this amount of electricity available or the island network capacity is not enough to run the main compressors or pumps with electrical drives. So also here, gas from the production is used to run gas turbines as mechanical drivers.

The gas turbines generally follow a kind of standardized power and speed combination, which is very similar for all manufacturers.

TABLE 1: TYPICAL POWER AND SPEED COMBINATIONS FOR GAS TURBINES

Power [MW]	Speed [rpm]	Manufacturer Type
5	14000	A
10	12000	B
12,5	9500	C
15	8500	D
28	6000	E
...	...	...

This might ease the exchange, as for the electrical driver motors with this power and speed range can be designed and used multiple times regardless the turbine manufacturer that is replaced. This is important, as the standard approach have a significant impact on the initial cost of the drive system and therefore on the capital expense (CAPEX) of the exchange project.

As the gas turbines has a very high power density, the power related to the speed is comparable high to an electric motor capability.

The motor has much larger diameters at the shaft and a heavier shaft than the turbine, so mostly the power speed combination may create a challenge to the electrical driver in terms of rotor dynamics and maximum speed.

Today it has become more common to see studies about how to electrify platforms or FPSOs, with floating wind farms or onshore grid connection. As those studies and the following electrification still need time, the first turbine replacements will continue happen on the steam turbine side.

Steam Turbines

The steam turbines are commonly installed in Chemical or Petrochemical plants and refineries, where steam is a necessary base product needed in the production and sometimes also is a by-product of the process, so it was obvious to design plants with boilers enough steam to run the plant process plus those steam turbines to be installed on the bigger compressors. As those main compressors require reliable drivers, a steam turbine was a good choice.

Now also here with the need for efficiency increase and emission reduction, the balance of the benefit with the challenges of process changes and driver changes in profit earning plants leans towards an exchange.

As steam turbines are typically installed on an elevated table foundation, the available space after removing the turbine is often very limited. See Fig. 2. The new electric motor design must be able to provide the needed power@speed combination with minimal size and weight.

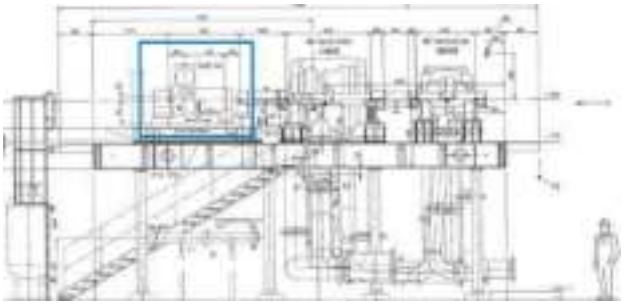

Fig. 2: Typical Installation of a steam turbine on an elevated table foundation

Another common attribute of steam turbines is that they are usually customized in power and speed to match the specific, sometime very unique mechanical driver (i.e., compressor). This leads to a large combination of power and speed

combinations required for the electrical drivers. Fig. 3 provides a graphical representation of speed and power combinations considered in turbine replacement studies.

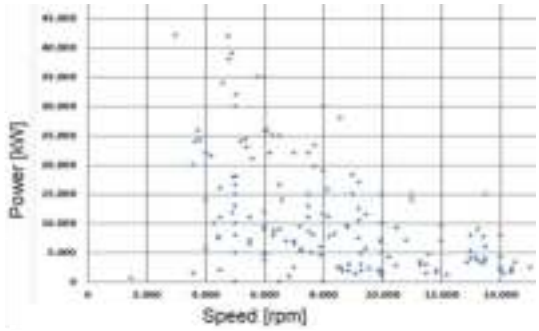

Fig. 3: Power and Speed Distributions for ST Replacement Studies Received in 2019 and 2020

II. TURBINE REPLACEMENT MODELS

As the turbine replacement is an upcoming task, the established business and project execution are not yet set up as for new plants, with the End User using a process license, place the order for a turn-key solution to an EPC, the EPC procure at OEMs, they at vendors.

The involved parties in the turbine replacement are also the end users, but in a different role. They are now already owner of the plant and the equipment. Changes on the equipment such as a driver change and civil work on foundations are on the risk of the End User. The end user might involve an EPC to do the exchange, but those EPC's might not be the ones doing turn-key solutions for new plants, it might be smaller offices, located close to the site and maybe already have established relation with the End User doing service work and repairs.

The compressor OEM will be only involved if the compressor is refurbished or renewed. The vendors for the electrical driver solution might be directly contacted through the End User or EPC. In case of a refurbishment or new compressor, the OEM service department or Department for new equipment will be involved, contacting the vendor for the electrical drive system. In this case, the structure of the set up becomes close to the known set up for new plants.

Brown Field

Turbine replacement in the brown field refers to the exchange of turbines in existing plants. Those turbines might run already for many years or decades and the production is stable. As the steam turbine is very compact and usually sit on an elevated table foundation a replacement with a direct driven high speed motor system is necessary in most of the cases.

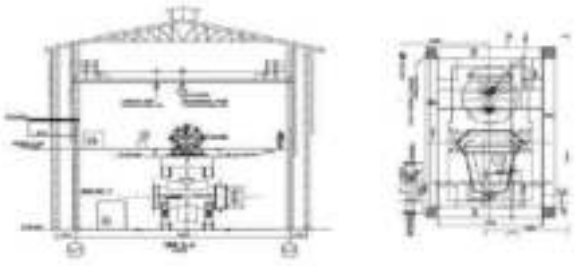

Fig. 4: Typical Steam Turbine Layout on Elevated Table Foundation

There are three different levels of replacement scope:

1. The ST is exchanged with an electrical driver, the compressor with a new compressor.
2. The ST is exchanged with an electrical driver and the existing compressor refurbished.
3. The ST is exchanged with an electrical drive and the compressor stay unchanged.

Fig. 5: Replacement Scope Sketch Cases 1~3

As for case one, the compressor OEM is involved, and the scope of work and responsibilities are very similar to new plants. Different is, that the new compressor train needs to fit I the existing foundation. This can be achieved by mounting a ready skid, bearing the new compressor and driver on the existing foundation.

For the interfaces between driver and compressor the compressor OEM take care as usual.

In case two, the service group of the OEM is involved, and here the scope of work and responsibilities are very similar to new plants. The adjustment to the existing foundation needs to be done only for the motor. The intermediate based plate might be the scope of the electric drive vendor, the responsibility for the foundation will lie within the compressor OEM.

The major difference for all involved parties is case three. As here the compressor OEM who usually cares about the coupling and the string analysis is not involved, therefore this scope must be assigned to one of the remaining parties, the End user, the EPC or the electrical driver vendor. As all of them are not specialized in such a task maybe the involvement of a third party, e.g., an engineering office, specialized in such analysis and coupling selections might be the best choice.

With an electrical not only the 1x and 2x excitation must be considered. Additional torsional excitation and the short circuit

excitations in case of a two or three phase sort circuit as well as the VFD related torsional excitations must be considered.

The torsional analysis for the new string must be done. For the details of the calculation refer to API 684 recommended practice [1] and PCIC-2019-30 paper on torsional analysis of electric driven compressor trains [2].

Regardless of which parties will do the analysis the steps are same:

1. Examine the existing torsional analysis and recalculate with the tool to be used for the analysis and make sure to get the same results
2. Check the coupling data sheet and properties of the existing coupling
3. Exchange the steam turbine model with the motor model and recalculate
4. Check the new eigenfrequencies with the 1x, 2x and VFD excitations in the Campbell diagram
5. If no excitation is within the specified speed range, add the short circuit excitation
6. Here the safety concept must be decided and agreed to either let the coupling slip, break, or withstand
7. If the agreed safety concept fits with the existing coupling the coupling can be used
8. In case there are excitations within the specified speed range either the stiffness or damping parameters need to be adjusted or a new coupling with the required parameters are selected. In case of selection of a new coupling it must not to change the weight of the half coupling on the compressor side, as this will change the lateral dynamics on the compressor side. Also, the coupling hub at the compressor side must remain on the compressor shaft.
9. After selection of a suitable new coupling also the safety for the short circuit excitation must be checked

Green Field

Turbine replacement in the green field refers to the installation of electrical drivers instead of steam turbines when designing a new plant and/or to integrate electrical drivers in the standard compressor skids offered by compressor OEMs.

Generally, for new plants there is no space restrictions so the selection of the electrical drive can be a 4-pole (1800 RPM / 60 Hz) motor plus gear box or a high-speed motor with VFD. See Fig. 6.

Note, while the gear box solution can possibly provide a lower initial cost, the high-speed gearless solution provides a smaller footprint and weight plus:

1. Higher system efficiency
2. Variable speed control
3. Elimination of the gearbox
4. Elimination of coupling
5. Smaller footprint & weight
6. Reduced lube oil requirements

All these result in in lower operating costs.

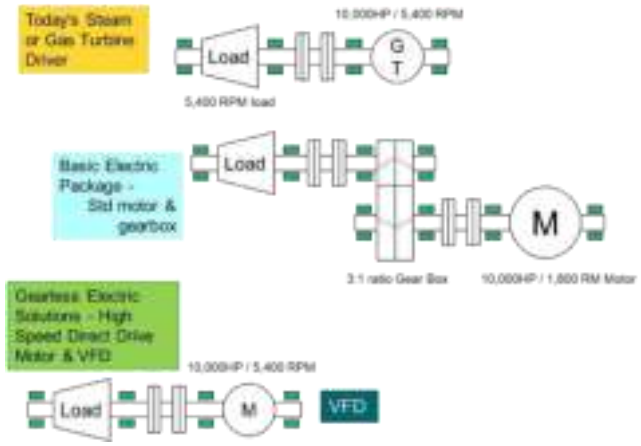

Fig. 6: Typical Electric Drive Options

III. TECHNOLOGY

For all the characteristics a steam turbine provides as a driver the electrical system need to have a fitting design. What are the most important points to meet?

Steam turbines are very compact and usually sit on an elevated table foundation. To keep the existing foundation a high-speed motor for direct coupling optimizes in size and weight is necessary.

As the steam turbines are customized and comes in many different power and speed combinations the motor design must be flexible to meet those.

The steam turbines are used at critical services and often run three to five years uninterrupted. So, the motor must be highly available and reliable in the design.

Additionally the time frame for the replacement might be limited to the usual scheduled service downtime of a plant after a lets say 5 year running period. To keep the plant profitable, the replacement should be done within four to six weeks.

This requires a more or less plug and play solution, properly pretested and suitable to be started and run up without for exampled field balancing actions.

The electrical system for the replacement basically consist of the motor, a variable frequency drive, as we run above line frequency, and transformers.

For the variable frequency drive and the transformers the established products for Oil & Gas applications will be used. The higher output frequency affect obviously much more the motor design, as you can imagine, as here we have the shaft running now at much higher speeds.

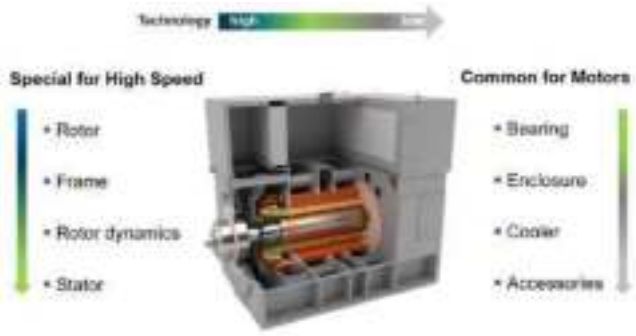

Fig. 7: Motor components for High-Speed Motors

Fig. 7 shows the components of a high-speed motor with a ranking from high technology parts special for high-speed motors to low technology parts, common for all motors.

The difference to a standard motor is the speed or frequency. Steam turbines run up to 16.000rpm, so we need a motor capable the same.

The part of the motor most affected of this difference is the shaft, and second is the frame, what needs to hold the shaft.

Let's have a closer look at the influence of the high speed or frequency on the shaft.

Rotor

Fig. 8: Areas of Influence of High Rotational Speed on the Shaft

Fig. 8 shows the sketch of a cross section of the active part of a shaft. We see the shaft and copper bars depicted. The diameter can be from 300mm onwards, depending on the necessary output power of the motor. Now, we imagine, this section rotates with let's say at a speed up to 16,000rpm.

The first what may come in mind is the centrifugal force, pulling on the bars and the shaft material. The centrifugal force is a function of the radius and the square of the speed, so it grows significant when we move from a 2p/60Hz/3,600rpm design to a 2p/266Hz/16,000rpm design.

As a picture to imagine the force we can think about a small truck hanging at each copper bar and rotating with the shaft. We must ensure, that our material can handle this force and that no part of the shaft is moving due to the centrifugal force.

The next we must consider is the surface speed. It can reach levels as high as 290m/s. This is close to supersonic speed. Here we must consider the air friction losses. They are accountable for a major part of the losses in a high-speed motor. To keep them on a minimum and also to avoid additional noise due to turbulence, the rotor surface should be as smooth as possible.

Lastly, we need to consider our balancing situation. The residual unbalance can be expressed as an eccentricity between the center of mass and the center of rotation of the shaft. To fulfill the vibration requirements of common specifications like ISO or API, a residual unbalance with an eccentricity of around 10 micrometers must be achieved and, very important, kept over the lifetime of the motor [5], [6], [7]. That means, no moving parts, even in the fraction of micrometers during all operating conditions, such as hot/cold, or start/stop condition. A human hair has a thickness of around 25micrometer, double the size of the required unbalance eccentricity.

There are many different designs possible for a shaft. Existing designs from smaller high-speed motor in the kW range such as PEM low-voltage designs can be examined. As the required power of the steam turbines go up to 20MW, this design might not be the suitable one.

Fig. 9: Example of a Laminated Shaft Design with Laminations Shrunk on the Rotor

Also, the standard laminated design used for two pole motors might be expanded to but just at higher speeds. Here the lamination shrunk on the shaft is very much limited in speed due to the limitations of the shrink fit of the sleeves. Additionally, these types of rotors have multiple parts that are fitted together, hence that pieces what can move will be moving, with greater magnitude as the speed increases. So we might think about other designs.

Instead of using existing designs and try to use them in an expanded way it might be worth to do it the other way round: which shaft would fit best the requirements and then find out how to produce it. The best would be a massive shaft, made of one piece.

We have two ways here to go: Find a way to connect copper and steel to create an induction motor with a copper cage to have lowest electrical losses or use just a steel body with open slots (a so-called Reluctance motor).

Fig. 10: Example of a Synchronous Reluctance Rotor

As the premium is a massive shaft with coper cage, we should investigate the possible technology to manufacture such a shaft.

There are many ways to connect copper and steel: Brazing, Soldering, Galvanic Deposition, Cold Spray, diffusion welding, and so on.

The diffusion welding using the High Isostatic Pressure (HIP) method is the best suitable method to produce such a massive shaft in a commercially attractive way and high quality.

What is diffusion welding? Here, the atomic properties of copper, a steel alloy and a bonding material are used. The chosen materials intend to exchange electrons and to diffuse into each other naturally by the time. Naturally this process would need a very long time. it can be speed up and done in a controlled way by expose the material to 1,000 bar and 1,000 Degree Celsius environment, and after around one hour, the bonding is achieved.

Fig. 11: Examples of a Massive Shaft Design Produced Using the HIP Technology

Such a massive squirrel cage induction motor rotor, has exactly the properties needed for high speed operation.

1. 100% bonding between Copper and Steel body
2. No moving parts
3. Smooth surface
4. Minimal thermal influence
5. Unlimited lifetime

Such shafts are in production and operation for nearly 20 years and are proven in more than 80 customer applications.

Balancing and overspeed testing

Rotor balance and overspeed testing are vital for high-speed motors. The balancing will be done according to the ISO standards [4] [5]. API 541 [6] refers also to this standard. In any case, in the balancing machine the residual unbalance will be checked at the rated speed points.

The overspeed test will be done according to the relevant project specification and vary between 10% and 20% overspeed. As some power and speed combinations are very challenging, sometimes a lower overspeed is agreed between the parties.

Fig. 12: Set up of a High-Speed Rotor for Balancing

In the balancing machine the required residual unbalance to later fulfill the vibration requirements will be achieved.

For a massive shaft with no moving parts, also the handling after balancing, the vibrations and impacts on the shaft and motor during assembly, transport and installation will not change the residual unbalance situation. The vibration results achieved in the customer FAT will be kept.

This is crucial for the Turbine replacement market as the short installation and commissioning window does not allow surprises and for example additional time for field balancing.

Variable frequency drive (VFD)

For the VFD and transformers the established product lines used in the Oil&Gas industry can be used. Sure, it must be checked that the motor is specified for inverter duty, for example regarding the insulation system, but this is not a topic only for high-speed systems but generally for VFD applications. Furthermore, specifically for high-speed systems, the output frequency has to be considered because it might cause some de-rating of the power electronics, in order to keep the required reliability, when going up to typical (very) high speeds like 16,000 rpm.

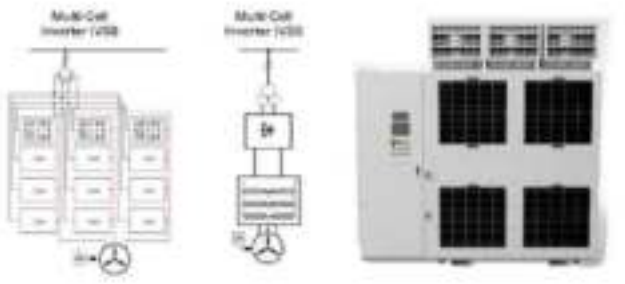

Fig. 13: VFD Topology with Multi-Cell Layout

When replacing a Steam Turbine, the motor replaces the turbine as the driver. As discussed before, the reliability and availability level of the Steam turbine can be reached with the motor, if the motor is designed properly.

The VFD (and possibly a transformer) is an additional component that is added to the system compared to a mechanical driver. It has to be made sure, that the electrical drive components (VFD, transformer and motor) is as reliable and available as the steam turbine.

VFD reliability can be enhanced with cell bypass technology, redundant auxiliary systems, and/or semiconductor redundancy. Alternatively complete cell redundancy, including not only the semiconductors, but control electronics, power supplies, and capacitors can be added.

Digital System Control

Although not covered in detail for this exposition, digitalization of assets is a hot topic nowadays, providing operators real benefits on major topics, like reliability, availability and other OPEX related improvement. Also this topic is not specifically for turbine replacement projects, but applies to rest of the drive equipment on site or even complete site also. Nevertheless, since digitalization can provide real benefits regarding important topics for turbine replacement projects, digitalization topics are shortly referred to.

Making assets just digital without digitalization strategy misses an enhancement opportunity. However, once digitalized full benefits can be explored, like:

- Optimization of drive train performance by analyzing and combining process and drive data
- Further optimization of the reliability and availability by pro-active response
- Remote assistance options, both proactive and, eventually, reactive.

The opportunity to avoid any shutdowns has taken additional steps forward with available systems today

IV. CHECK SHEET

Appendix A shows a check sheet, describing the main steps towards a steam turbine exchange.

The check starts with an inventory of the potential steam turbines to be replaced by the end user. The inventory should cover the power and speed combinations of the turbines, the expected date for exchange, the foundation information as a minimum. As the timeline from identifying the turbines until start of exchange is around three years, the steam turbines with the potential for the first upcoming exchange can be identified. As explained above, the steam turbines are customized design, but maybe there are several turbines with similar torque requirements, so that maybe one motor design can be used to exchange different steam turbines. This might have an impact on the CAPEX of the exchange project.

To go ahead with a firm study an EPC need to be involved. For the electrical driver now more detailed information on the existing string, such as the torsional analysis or the oil supply data need to be collected.

From here, the discussion and decision on the scope for each supplier need to be done. After that, the EPC or end user will collect all commercial data and eventually kick of the project.

V. FIELD EXAMPLES

This field example is about the replacement of a steam turbine with an 8,250kW / 5,855rpm VFD driven electrical motor in a refinery in Spain.

The steam turbine was placed on an elevated table foundation. To adjust the shaft height to the compressor a intermediate base plate was used. This base plate also adjusts the anchor bolts between the foundation and the motor fixation points.

Fig. 14: Table Foundation and Motor with Intermediate Base Plate

The motor was set up on the foundation and the connections for the main cables, auxiliaries as well as the purge system prepared prior to the commissioning start of the motor vendor.

The commissioning then included the check of all connections and accessories and the purge system.

In the next step, the motor was run up to operational speed in an uncoupled condition. The vibration and shaft velocity were on a very low level.

Fig. 15: Bearing Velocity at Uncoupled Solo Run of the Motor at 5,867 rpm

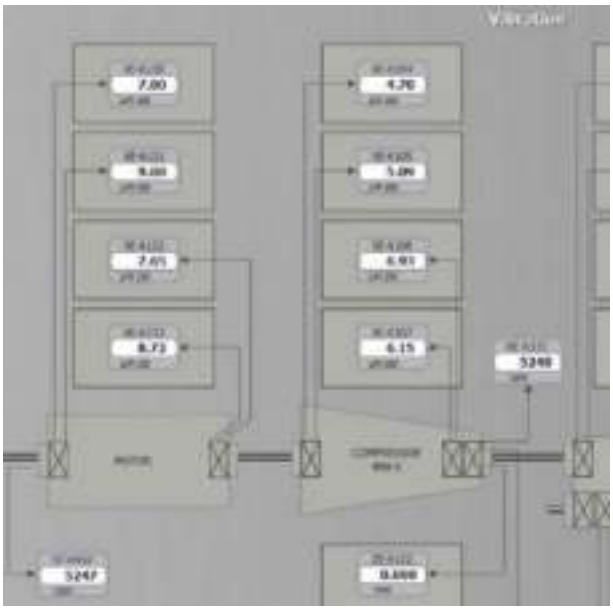

Fig. 16: Shaft Displacement after 12-hour Load Run at 5,247rpm

Also, the bearing temperatures, winding temperatures and bearing vibration were very satisfying after the 12-hour load run.

Fig. 17: Bearing velocity at load run after 12 hour running time 5866 rpm

The complete commissioning was done within 3 weeks, well inside the scheduled time frame. The work on the exchange could continue and eventually the plant could be started at the planned time.

Another reference for a brown field steam turbine replacement is with a 3,700kW / 5,700rpm VFD driven electrical motor in a refinery in Hawaii. Also here, the motor needed to fit within the existing foundation. In this case, the space was very limited. The motor is located on an overhung structure.

As this structure is flexible compared to the requirements of API 541for a stiff foundation, an analysis of the foundation was done. Details can be found in the PCIC-2015-xx paper [3].

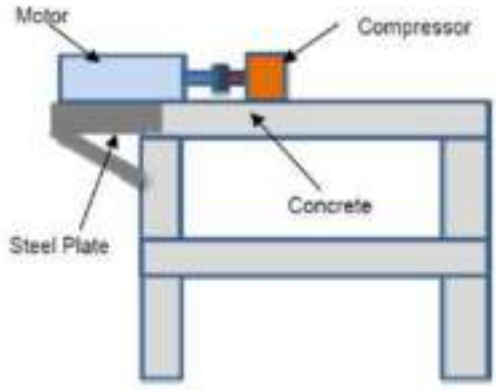

Fig. 18: Schematic of the Foundation with the Motor Partially Sitting on an Overhung Structure

With the excitation of the expected residual unbalance into the foundation analysis model, the expected response was precalculated and the structure adjusted to reach vibration levels within the specified API limits.

Fig. 19: Installation of the Motor on Site

Also in this reference, the vibration on site is very low and stable over the time. This predictable behavior is a very big asset for the massive shaft design for steam turbine replacements.

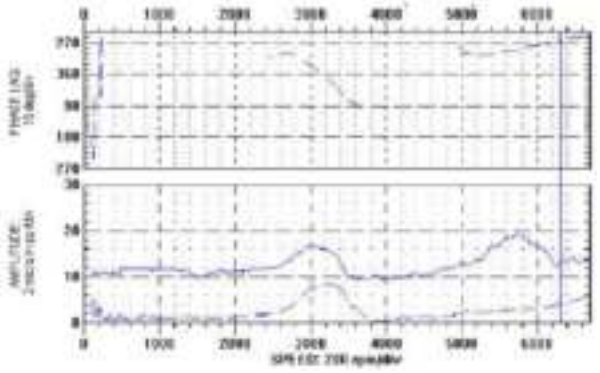

Fig. 20: Measured Shaft Vibration at Factory Acceptance Test with Maximum Vibration Below API Specification

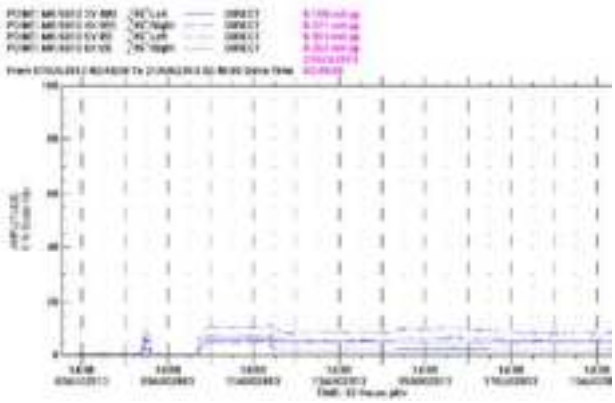

Fig. 21: Five Days Vibration Trend at Commissioning with Maximum Vibration Well Below API Specification

VI. CONCLUSION

While the design changes and implementation challenges exist to replace the common gas turbine and steam turbine installations on new and existing installations, the push for increased operating efficiency and decreased emissions of CO2 are leading more and more to the option of electrical drivers for mechanical equipment in the Petrochemical industry.

Today, more than ever before, the advanced electrical systems with field-verified motor designs with single-piece rotor cages, high availability variable speed drives with built-in redundancy and digital system control and monitoring provide the reliability demanded by these applications plus, operating expense reduction and lower CO2.

VII. REFERENCES

[1] S. Dixon,T. Salazar, S. Singhal "Electrification of Alkylation process with high-speed motor drive systems in a refinery", *PCIC-2015-xx*

[2] API recommended practice 684, Second Edition, August 2004 on torsional Analysis

[3] B.Venkataram, R. Kurz, M. Vagani, J. Mistry, G.- J. Cole "Torsional Vibrations in Electric Motor Driven Compressor Trains", *PCIC-2019-30*

[4 ISO 1940-1, Mechanical vibration — Balance quality requirements for rotors in a constant (rigid) state — Part 1: Specification and verification of balance tolerances

[5] ISO 11342, Mechanical vibration — Methods and criteria for the mechanical balancing of flexible rotors

[6] API 541, Form-wound squirrel-cage induction motors — 500 horsepower and larger

VIII. NOMENCLATURE AND APPREVIATIONS

Q	Balancing Grade acc DIN ISO 1940
ω	Angular velocity
ε	Distance between geometric center and center of Gravity
VFD	Variable Frequency Drive
FAT	Factory acceptance test
FPSO	Floating Production Storage and Offloading Vessel
HIP	High Isostatic Pressure
1x 2x	one time and two times speed/frequency

IX. VITA

Hartmut Walter graduated from the Technical University in Berlin in 1996 with a master's degree in engineering science. After graduation he joined Siemens Large Drives facilities in Nuremberg/Germany responsible for vibration and acoustic aspects in the R&D department. After a period as technical adviser in the Siemens sales office in Tokyo/Japan, he joined Siemens Large Drives facilities in Berlin/Germany. There he was responsible manager for the development of highly innovative products such as large High-Speed Motors and Active Magnetic Bearing Systems. From 2010 to 2018 he represented Siemens General Manager for Siemens Large Drives in Tokyo/Japan. Since 2018 he is working on developing solutions for turbine replacements.

Bart Sauer graduated from Case Western Reserve University in 1989 with a Bachelor of Science degree in Mechanical Engineering. He has been an employee of Siemens at the ANEMA motor plant in Norwood, OH, since 1990, serving in roles as a Mechanical Product Engineer, Sales Application Engineer, and his current role as Oil & Gas Market Segment Manager 2009. He has been an author on four previous IEEE papers and is currently a member of the IEEE / API 541/546/547 committee.

Gijs van Maanen graduated from The Hague University of Applied Sciences in 1995 with a bachelor's degree in electrical Drive Systems Technology. After graduation, he joined Siemens Large Drives in the Netherlands, starting as commissioning and service engineer for global large drive projects. After this period, he was responsible for site- and project management in the Netherlands from 2005 – 2016. He joined Large Drive facility in Berlin in sales department, especially for high-speed motors and magnetic bearing systems. In his current role, he is responsible for Global Project Development.

APPENDIX A:
CHECK SHEET ON TURBINE REPLACEMENT

TABLE A-I

	Item	Comment	Effect	Involved parties	Remaining time to next scheduled shut down
1	identify the potential turbines to be exchanged in the plants including the remaining time for the next overhaul window	identify exchange schedule	Overview	End User	any time
		identify Potential Investment & Savings	Overview		
		Turbines with similar torque requirement might be served by same motor design	cost savings		
2	Bundle the potential turbines acc. the exchange			End User	
3	Compile the necessary information for an initial budget and technical feasability check at the motor vendor. Data base - Documentation on existing plant/skring	Rated power and speed		End User / potential EPC	
		Maximum continuous operating speed			
		Cooling medium inlet temperature			
		Foundation maximum available length and width			
		Foundation static load capability			
		Foundation dynamic load capability			
		Existing turbine bearing oil supply (flowrate, inlet temperature, oil type)			
		Coupling data and drawing			
		Torsional Analysis existing train			
4	Optional select one for a prototype exchange study			End User	36 months
	Do an exchange study on a bundle				
5	Share the data of the selected bundle or exchange prototype with the electrical drive vendor	get a initial and fast feasability check and budget cost	Overview for Invest	End User / E-Vendor / EPC	30 months
6	Firm study with electrical drive vendor	get firm designs and cost for the exchange		End User / E-Vendor / EPC	30 months
		decide on scope of supply especially for base plate, coupling and torsional analysis, oil supply, grid connection		End User / E-Vendor / EPC / Engineering Company	
7	Kick off the turbine exchange	lead times with delivery on site might be up to 15 to 18 months depending on included tests, site location		End User / E-Vendor / EPC / Engineering Company	24 to 30 months
8	Equipment on site				2 to 1 month
9	Installation and commissioning				0 month
10	Start up				- 1,5 to 2 months

Good practices to design LV switchgear to reduce footprint, costs, and CO2 footprint

Paper No. PCIC Europe EUR22_14

Laurent Bloch
Schneider Electric
Grenoble
France

Philippe Angays
Technip Energies
Paris
France

Victor Ascher
Technip Energies
Paris
France

Jean-Philippe Herpin
Schneider Electric
Grenoble
France

Mathieu Guillot
Schneider Electric
Grenoble
France

Benoît Stefanski
Schneider Electric
Grenoble
France

Abstract - Optimization for electrical equipment has been a constant interest for O&G and Petrochem operators, as well as to EPCs. A special attention shall be paid to LV switchgear as end users, specifiers and designers can select many alternatives, which may significantly impact the outcome. This paper will discuss some key design choices and present good practices to reduce footprint and costs as well as to reduce CO2 footprint, as part of Operators sustainability agenda. It will focus on the impacts of circuit breaker/fuses choice at switchboard level, complementing the paper presented at PCIC Europe 2013 [1], nominal voltage selection and some other design proposals enabling to reduce LV switchgear footprint, costs, and CO2 footprint.

Circuit breaker/fuses choice: fuses are often perceived as a cheaper alternative to circuit breakers. That could be challenged from a TCO or Totex perspective, but the experience gained in supporting end-user projects clearly shows that MCC footprint is smaller with circuit breakers when dealing with mid to large size MCCs. This is leading to up to 10% cost reduction, not to mention lower electrical rooms costs and reduced CO2 emissions.

Nominal voltage selection: combined with appropriate product selection, shifting from 400V to 690V nominal voltage can bring significant optimizations, as demonstrated by relevant case studies.

Digitization and IED enhancement also lead to save on footprint and costs, both at construction and during operations.

As a conclusion, the CO2 footprint assessment is presented for the main LV switchgear design improvement suggested in this paper.

Index Terms — LV switchgear, design practices circuit breakers, footprint, costs, carbon emissions

I. INTRODUCTION

Optimization for electrical equipment has been a constant interest for O&G and Petrochem operators, as well as to EPCs. A special attention shall be paid to LV switchgear as end users, specifiers and designers can select many alternatives, which may significantly impact the outcome. This paper will discuss some key design choices and present good practices to reduce footprint and costs as well as reduce CO2 footprint, as part of Operators sustainability agenda. It will focus on the impacts of circuit breaker/fuses choice at switchboard level, complementing the paper presented at PCIC Europe 2013 [1], nominal voltage selection and some other design proposals enabling to reduce LV switchgear footprint, costs, and CO2 footprint.
This paper reviews practices for IEC switchgear, but conclusions would also make sense qualitatively for other geographies and standards, even though voltages and ratings as well as quantitative estimations will differ.

II. MOTOR CONTROL CENTERS (MCC): REDUCE FOOTPRINT AND COSTS UP TO 10% BY SWITCHING FROM FUSES TO CIRCUIT BREAKERS

Circuit breakers enable O&G and Chemicals Operators to benefit from smaller switchboards and to digitize their power system, yet ensuring similar or superior protection level as fuses.
Fuses are the legacy design with good performances for overload and short circuit protection.
Circuit breaker design and performances have been drastically improved since MCCB introduction on the market, reaching similar and sometimes better electrical performances than fuses.
In addition to performing protection, circuit breakers are fully part of electrical digital systems

- Breaker health and status monitoring
- Metering
- Power system monitoring
- Advanced protection and alarming

Note: in this document, MCCB refers to a limiter circuit breaker selectivity category A according to IEC/EN 60947-2 or 4-1.

2.1 Fuse switch and circuit breaker alternatives: designer choices

2.1.1 Low voltage installation rules

Low voltage circuits shall be protected against overcurrent such as overload or short-circuit. In addition, most common protective measure against electric shock - automatic disconnection of the supply - relies also on an overcurrent protection in particular in TN system. IEC 60364 series “Low voltage electrical installations”, and

related national electric codes recognize equally circuit-breakers according to IEC/EN 60947 or IEC/EN 60898, and fuses according to IEC/EN 60269 series to perform such overcurrent protection. Nevertheless, both solutions are not equivalent.

The aim of this paper is not to re-open the debate between Fuse and Circuit-breakers as products. Differences are known and explained, see for example [1]

But we would like to complete this comparison with additional criteria such as switchboard footprint, costs and sustainability, as well as to clarify some misperceptions.

2.1.2 Cable Protection and cable sizing

First common false idea is that fuses allow smaller cross section for cables.

According to IEC 60364-4-43 and related national rules, cables shall be protected against overload and short-circuit. Cable cross section and its related current carrying capacity and overcurrent protection characteristics shall satisfy the following rules:

For overload:

$I_n \leq I_Z$ — I_Z is the continuous current-carrying capacity of the cable

I_n is the rated current of the protective device

NOTE 1 For adjustable protective devices, the rated current I_n is the current setting selected.

$I_2 \leq 1{,}45\ I_Z$ — I_2 is the current ensuring effective operation in the conventional time of the protective device. The current $I2$ ensuring effective operation of the protective device shall be provided by the manufacturer or as given in the product standard.

For short-circuit:

$LT \leq K^2 S^2$ — S is the cross-sectional area, in mm².
K is a factor taking account of the resistivity, temperature coefficient and heat capacity of the conductor material, and the appropriate initial and final temperatures. For common conductor insulation, the values of k for line conductors are shown in IEC 60364-4-43 Table 43A.
LT: the let through energy (I^2t) quoted by the manufacturer of the protective device for the maximum short-circuit current

The main difference between fuses and circuit breaker according to IEC/EN 60947-2 is that

- I_2 for fuse = 1,6 In
- I_2 for circuit breaker = 1,3 Ir
  (even 1,2 for electronic release)

In other words, the accuracy of overload tripping characteristics of the circuit breaker is better than fuse allowing a cable current carrying capacity closer to the circuit breaker rating compared to the fuse rating (see Fig.1).

Let's consider a 3 phases circuit supplying a 150A load.

The circuit is a made of 3 Cooper single core conductors PVC 70°C on perforated tray: IEC 60364-5-52 Table B52-10 Column 6 Method of installation 31-F
Cross section area of such a circuit protected by a 160A circuit breaker can be 50 mm2 Cu (Iz = 174).
Cross section area of such a circuit protected by a 160A fuse shall be 70 mm2 Cu (Iz = 225).

When considering short-circuit protection : for such a cable K = 115 so the maximum let thrgough energy for MCCB shall be lower than $50^2 * 115^2 = 3.3\ 10^7\ A^2S$.

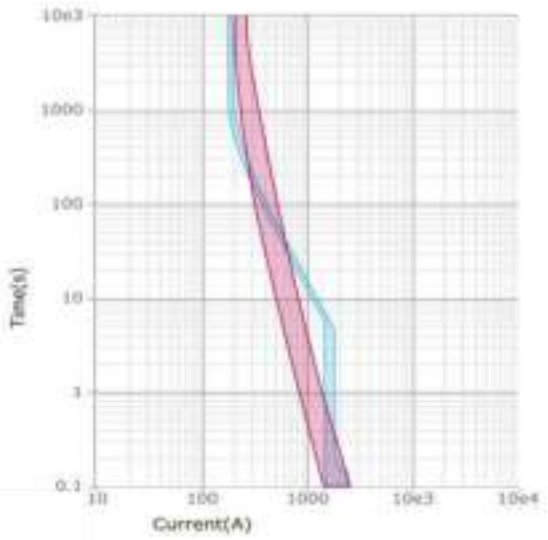

Fig. 1: gG160 fuse time versus current curve (red) compare to 160A MCCB with electronic trip unit (blue)

160A MCCB frame will limit the energy far below this value. See Fig. 2 providing let through energy curves from three different manufacturers for 160A MCCB frame (2021 IEC catalogs), they are all below $1.10^6\ A^2S$ so far below = $3.3\ 10^7\ A^2S$ calculated for 50mm2 Cu PVC cable.

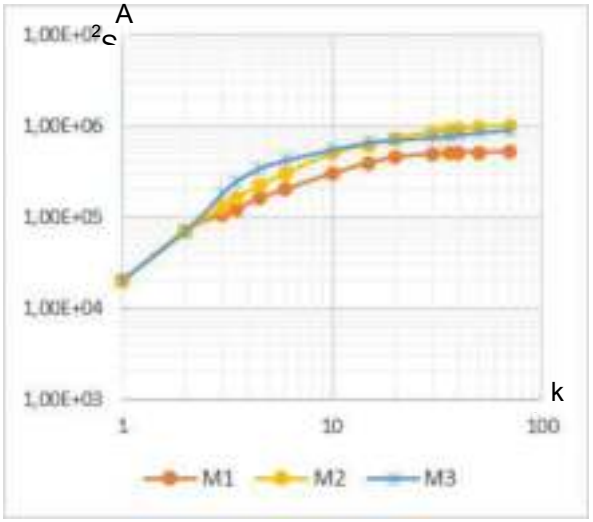

Fig. 2: I^2 t limitation curve 400Vac for 160A MCCB from several manufacturers

MCCBs are protecting properly cables against short-circuit, the only point of attention is for low trip unit rating compare to the MCCB frame rating.

Main MCCB manufacturers are now using double breaking technology for frame higher than 100A, providing high level of current limitation. The two contacts and two arc chambers of the double breaking capacity reduce significantly the let through current and let through energy.

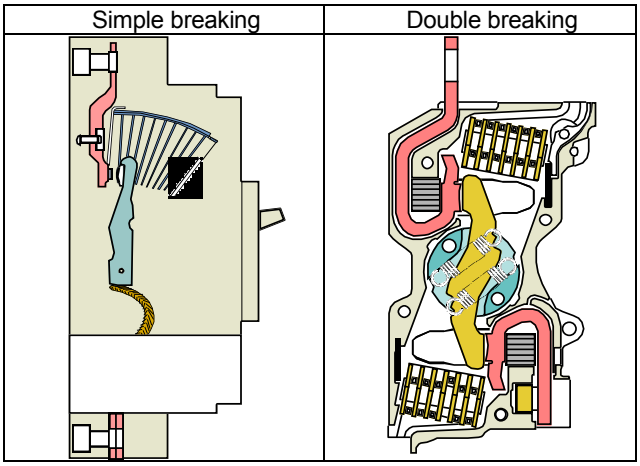

Fig. 3: illustration of single breaking principle versus double breaking principle for MCCB.

For smaller rating like 32A or 63A motor MCCB, single breaking capacity and internal impedance provide enough limitation to protect properly cables associated to the ratings.

If both solutions are recognized equally for protection of cables against overcurrent, thanks to accuracy of its overload protection, circuit-breaker will allow a smaller cross section, or for a given cross section a better overload protection of circuits, helping to reduce cable damages and fire risk.

2.1.3 Selectivity and coordination performances

Second false idea is that fuses are providing better selectivity and/or coordination with contactors

Let through current and energy limitation performances are also linked to selectivity and coordination between short-circuit protection and switching devices like contactor or switch disconnector. These performances are covered by IEC/EN 60947 series of standards:

- IEC 60947-2 Annex A for Selectivity,
- IEC 60947-4-1 for coordination between overcurrent protection and contactor and overload relay for motor starter,
- IEC 60947-3 for coordination between overcurrent protection and switch disconnector.

These standards do not make differences between overcurrent protection provided by fuses or circuit breakers.

Main manufacturers of MCCB propose solutions for full selectivity based on energetic coordination for high short-circuit current between MCCBs frame. Additionally, electronic trip units allow fine adjustment and time delays to cover long cable or weak short-circuit current situation.

Type 2 coordination for motor starter based on MCCB is also proposed and achieved with optimized size of devices. If fuse may be better to protect motor starter at maximum short-circuit capacity of the fuse, MCCB is often better to protect the contactor for the second test required by IEC/EN 60947-4-1 at “Prospective short-circuit current Ir”

Manufacturers are providing such information in coordination guide [2] and are embedded in electrical design software such as ETAP, Caneco BT and others.

However, in term of integration, some of those data being manufacturer dependent, it can be difficult for an EPC contractor or final user to manage coordination when different suppliers are involved. This is an issue difficult to address, as data result from product tests. Hence it can be time consuming within a project execution, especially when the classification company requires justification.
But including tripping curves, limitation curves and coordination performances in product description standards (such as ECLASS ADVANCED or IEC 62683-1 Low-voltage switchgear and controlgear/Product data and properties for information exchange) would be a step forward for EPC tools and detailed engineering phases.

2.1.4 Reliability and maintenance

Third common false idea is that fuses are more reliable and installations with fuses are easier to maintain.

Comparison of operation of fuses versus circuit breaker is always considered from the “overcurrent” function perspective. But this event is very rare, and even will never happen for a significant number of circuits. Where all circuits will have to carry current without excessive temperature rise, will have to be opened/closed/padlocked, etc. Analysis for field return of MCCB and switch fuse demonstrate that the global failure rates are quite similar, but with different failure modes (See Fig. 4). Probability of dangerous failure (no trip on fault) are in both cases very small but other failure modes are present requiring maintenance and care for both solutions. For example, switch-fuse solution shows a higher probability of mechanical issue (failure to close, failure to open) that could disturb daily operations.

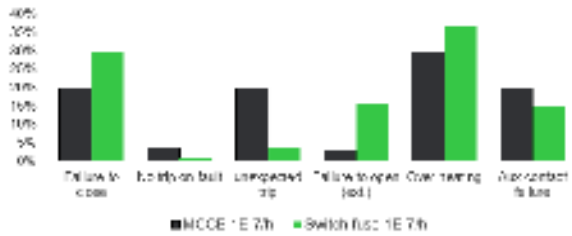

Fig. 4: Split of failure rate by failure modes for switch fuse solution and MCCB

So, both solutions need a minimum of maintenance to ensure proper functioning during all expected life of the installation. Advanced diagnosis function in electronic trip unit of most recent circuit breakers allow now to estimate contact wear due to current breaking. That trend towards

ageing information built in circuit breakers will prove powerful for maintenance scheduling and remove concerns from operators (See also 4.3 below).

2.1.5 Operation in IT system

Fourth common false idea is that fuses are more suitable for IT type of system earthing.

Fuse based solution is inherently designed and tested with a "single pole" approach. So, short-circuit breaking performances are based on a single fuse-link for a rated voltage. Then in 3 phase system, the fuse-link are installed for one circuit, each of them able to handle any type of short-circuits. A 3 or 4 Poles MCCB short-circuit breaking performances are based on the more demanding situation that is a 3 phases short-circuit in a 3-phase system supply. In that case, the rated voltage is the line-to-line voltage and each breaking pole is operating under line to neutral voltage. This breaking capacity test is perfectly relevant for all short-circuit situations between phases (or Neutral if any) and between a phase and earth for all types of system earthing (TN, TT or IT). IT system being a particular situation as there is no significant overcurrent caused by a phase to earth fault, so no overcurrent protective device will trip in that case.

But this operating mode of IT system lead to a new situation unknown in TT or TN that is called "double earth fault". Meaning a first line to earth fault occurs somewhere in the installation. This fault is not cleared and a second line to earth fault occurs later on another line in another circuit.
In such a situation a circuit breaker may have to break a current with only one pole under the line-to-line voltage. If a fuse-linked test covers this situation, it is true that a standard breaking capacity test ("Icu/Ics"of a 3P/4P circuit breaker) is not relevant.
LV circuit breaker standard cover this situation by a test described in IEC/EN 60947-2 Annex H: Test sequence for circuit breakers for IT systems. Introduction of this annex states: "This test sequence is intended to cover the case of a second fault to earth in presence of a first fault on the opposite side of a circuit breaker when installed in IT systems".
Low Voltage installation rules such as IEC 60364 requires circuit breaker compliant to this IEC/EN 60947-2 Annex H. Some national regulations may have additional requirements.
There is no short-circuit calculation standard (not covered by IEC 60909-0 for example) giving rules to estimate the minimum and maximum current for such situation.
So, the breaking performances of overcurrent protective devices is not clearly specified by most common codes for this special situation of IT system.

That being said, the two main benefits of IT system

- no automatic disconnection in case of earth fault, and
- very low earth fault current (hundreds of mA, few Amps maximum)

are lost when a first line to earth fault is present in the system. Consequently, it is mandatory to locate and clear this first fault in a reasonable time to keep the system performance and up time. This point is enforced in standards, with the obligation when using IT system to have an onsite maintenance team to correct faults. And depending on the prospective time of fault clearance, even over insulation of equipment can be required. It is therefore strongly recommended to instal insulation fault locator on feeders. If a second fault occurs, event with a very low probability to happen, two overcurrent protective devices are always involved. This will limit the consequences if any.

2.1.6 Power losses

It is commonly admitted that power losses of fuse-based solution are higher than circuit breaker solution. [1] provide detailed information of power losses comparison. When it comes to power dissipation, there is no general rule and complete functional unit power dissipation should always be evaluated in particular for motor starters with various type of starting. A simple device to device comparison is not always fair nor relevant, and a complete view should be preferred (See case study below). However, a fuse switch disconnector solution in the range of 100A to 630A will dissipate around 2 times more than an MCCB with electronic trip unit.

From an EPC point of view, this can have major impact on the HVAC system, which is one of the most demanding power consumers in a substation. It also impacts the operation under emergency conditions, where HVAC can be switched off, and temperature inside emergency switchboard can rise in very short time counted in minutes, sometimes lower than the required time for the evacuation of an offshore platform for example. So, thermal dissipation of equipment is a major concern for the safe operation of a plant.

2.1.7 Features

Circuit breakers, in particular with electronic trip units, embed in the same footprint more features: they allow digitization thanks to metering, monitoring, communication, and also additional protection (See Fig.5)

Features ■ Standard □ Optional	Circuit breaker	Fuse Switch-Disconnector
Isolation	■	■
Manual control	■	■
Remote Control	□	
Overcurrent	■	■
Earth leakage / Ground fault	□	
Signaling (O/C/trip status)	■	■
Metering	□	
Diagnosis (trip history, contact wear…)	□	
Communication	□	

Fig. 5: Features provided by circuit breakers and fuse switch disconnector

2.2 LV switchgear footprint and costs

The width of a circuit breaker is in most of the cases smaller than for the fuse switch having the same rating. Particularly, above 15kW, drawers with circuit breakers become more compact than with fuses switches. The reduction is usually between 50 to 100 mm, for PCC or MCC feeders.
The next example is for a 30kW motor, the typical size with a fuse switch is 200mm, and can be reduced to 150mm using a circuit breaker

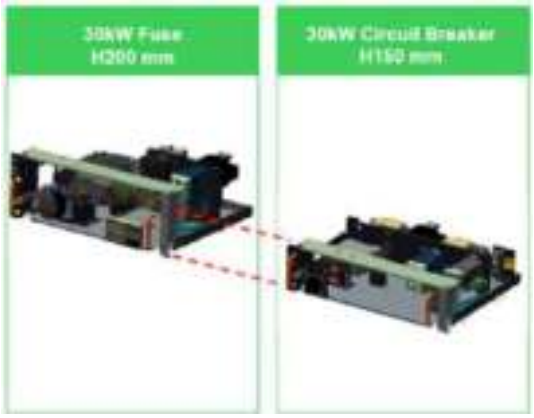

In the following table, we can see that a fuse drawer is from 16% to 100% higher than the equivalent one with a circuit breaker, except for motors below 15kW. Even though small motors make up most of load lists, the assessment at switchboard level will show footprint advantage remain to circuit breakers.

Above values have a significant impact at the level of the switchboard, as demonstrated with below comparison.
The following example is based on a switchboard with 2 sections, 2 incomers 3200A and a bus-tie 3200A, having on each side 45 feeders
Configuration A is for Fuse Switch

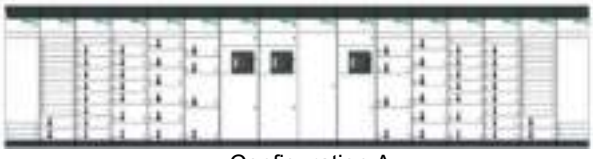

Configuration A

To accommodate the different feeders, 12 feeder cubicles are needed with fuse switch.
The configuration B is with the same feeders, using circuit breakers.

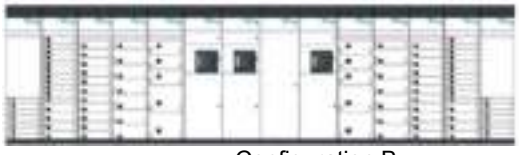

Configuration B

In this case, only 10 feeder cubicles are needed for the very same load list

The length of the switchboard decreases from 9.8m to 8.6m (1.2 meter, corresponding to 12%), moving from 12 feeder cubicles to 10 cubicles. It is a significant saving for the sheet metal, but also for the copper of the horizontal busbar and of the vertical busbar in 2 cubicles.
The cost of the switchboard can hence be reduced up to 10%

It could be challenged whether those drawers or switchboard assessments really translate in similar figures for a complete facility, as many factors could modify those conclusions at drawer level, and make it more or less true facility wide. That comparison has been made for an actual project, for an LNG train facility, with an LV scope of 15 switchboards, corresponding to 250 LV cubicles.

Needless to say, footprint and cost differences significantly varied from switchboard to switchboard, but selecting fuses instead of circuit breakers led to switchboards 12% bigger and 8% more costly for the total project.

As a conclusion, the optimizations circuit breakers allow at drawer level effectively translate into tangible m² saved for the electrical rooms as well as a significantly lower procurement cost.

III. SELECT THE MOST SUITABLE LV VOLTAGE LEVEL

The use of a higher low voltage level as 690V instead of 400V has benefits and advantages, mainly in term of cost saving, footprint saving, weight saving as well as network efficiency and carbon emission reduction.
To confirm the above statement, the following detailed analyze has been performed by using a real case example from O&G industry.
The target was to assess the convenience of the 690 V for the Low Voltage electrical networks, vs 400V. The analysis includes transfer of medium size motors (from 200kW to 400kW) from 6.6kV to 690V, which becomes possible thanks to this higher voltage level.

The below detailed comparison between the two alternative solutions has been performed focusing on the following items:
- Low Voltage switchboards
- Upstream Medium Voltage switchboard
- Distribution transformers
- Cables
- Induction motors

Costs, footprint, and weight comparison will be highlighted in percentage whereas carbon footprint saving will be also highlighted in kgCO2e.

This analysis is limited to the section of the electrical architecture presented below, which is the relevant part of

the complete system.

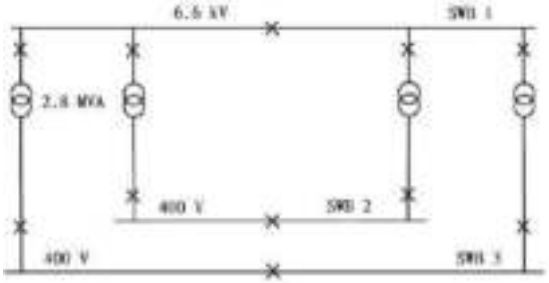

Alternative 1: 400V design

400V key design parameters and characteristics which have been considered:
- 1 x Medium Voltage switchboard 6.6kV, 1250A, 25kA
- 2 x Low Voltage switchboards 400V, 4000A, 65kA (with circuit breakers)
- 4 x Dry type Distribution transformers 2800kVA, 6600V/420V
- Load list as below

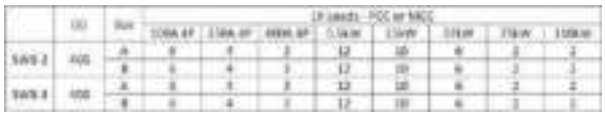

Small non process loads typically below 5.5kW (heating and lighting as an example) are considered powered through 400V distribution boards.

690V key design parameters (Alternative 2):

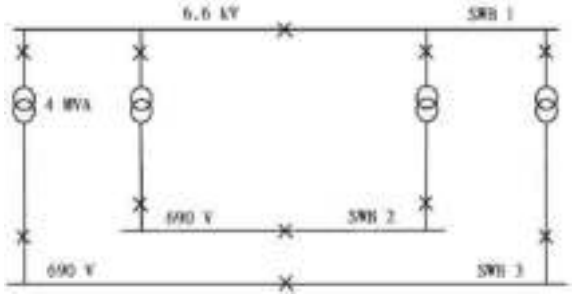

Alternative 2: 690V design

Following characteristics have been considered:
- 1 x Medium Voltage switchboard 6.6kV, 1250A, 25kA
- 2 x Low Voltage switchboards 690V, 4000A, 65kA (with circuit breakers)
- 4 x Dry type Distribution transformers 4000kVA, 6600V/720V
- Load list as below

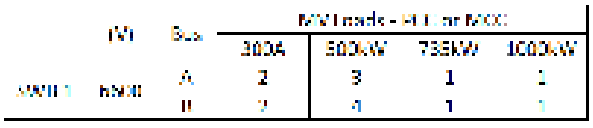

3.1 Medium Voltage Switchboards comparison between Alternative 1 and 2

Transferring the nine (9) smallest MV motors to 690V low voltage switchboard will lead to the following savings:
Cost saving: 32%
Weight saving: 31%
Footprint saving: 32%

Alternative 1 / Front face of 6,6kV medium voltage switchboard with a total length of 18,2m

Alternative 2 / Front face of 6,6kV medium voltage switchboard with a total length of 12,35m.

3.2 Low Voltage Switchboards comparison between Alternative 1 and 2

By the transfer of MV motors (9 in total), 690V low voltage switchboard has increased in size of two (2) columns. The additional length is 1,2m. It is worth noting that without the transfer of MV motors to 690V, the 690V switchboard would have had the same size as its equivalent 400V switchboard.

Overall impact on the low voltage switchboards is the following:
Costs increase: +27%
Weight increase: +15%
Footprint increase:+15%

Front face of 400V low voltage switchboard (7,95m total length)

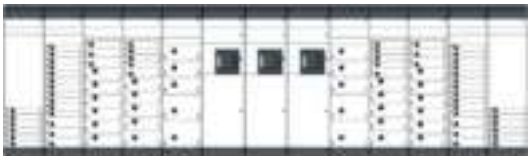

Front face of 690V low voltage switchboard with additional motors (9,15m total length)

If there would have been no transfer of motors from 6,6kV to low voltage, impact on switchboards by using 690V instead of 400V would be as below:
Costs saving: 7%
Weight saving: 15%
Footprint saving: 15%

Note: in case of 690V (without additional motors originally MV), cubicle quantity is reduced thanks to short-circuit reduction below 50kA and incomers and main busbar rating reduction below 2500A.

3.3 Impact on Distribution Transformers

Transfer of MV motors to 690V impacts distribution transformer sizing. The 2,8 MVA 6600/420V Dry type transformers proposed in the alternative 1 would then become 4 MVA 6600/720V, with following impacts:
Costs increase: +44%
Weight increase: +46%
Footprint increase: +33%

3.4 Impact on induction motors

With alternative 2, i.e., 690V instead of 400V for low voltage and nine (9) motors transferred from medium voltage 6,6kV to low voltage, costs and weight savings are the following:
Costs saving of 15%
Weight saving of 2,4% (2,28 t)

3.5 Impact on MV and LV power cables

To assess impacts on power cables, induction motors are considered at 200 meters from switchboards in average.
Sizing of MV and LV cables has been done according to the recommendations from the Standards.
Costs saving associated to alternative 2 is 17%
Weight increases is 2,4% (~1 t)

3.6 Carbon footprint during construction phase (CAPEX)

The below analysis addresses impact on sustainability Scope 1 and 2 which are the direct and indirect emissions linked to the manufacturing of product/equipment and the energy used for operations.

By the integration of 690V instead of 400V as well as transfer of small 6,6kV motors to Low Voltage, carbon footprint savings/impacts concerning manufacturing of electrical equipment and induction motors are the following:

- Medium and low voltage switchboards : -18% (~19tCO2e)
- Medium and low voltage induction motors : -3% (~10tCO2e)
- Distribution Transformers (increase of power) : +20% (~16tCO2e)
- Medium and low voltage cables: -6% (~7tCO2e)

So, the total carbon footprint saving for the construction phase (CAPEX phase) is -3%, corresponding to ~20tCO2e.

3.7 Carbon footprint during operations phase (OPEX)

In order to quantify impact on Carbon footprint during operations, the following key considerations on MV and LV respective motors efficiencies have been selected:
• For small MV motors energized at 6,6kV level (250kW, 280kW, and 315kW motors), the efficiency considered is 94,5% (motors close to their nominal load).
• If those motors are transferred to 690V level, the efficiency will become 96% (under similar conditions) considering IE3 low voltage motors.
• All others low voltage motors of this analysis are assumed IE3 motors, with below efficiency ratios:

5,5kW	15kW	37kW	75kW	110kW
89,6%	92,1%	93,9%	95%	95,4%

OPEX carbon footprint savings associated to the implementation of Alternative 2 are based on 8000 hours/year operation time (90%, during 5 years operation between 2 turnarounds)

Results of the analysis based on new efficiencies and losses:

- Medium and low voltage induction motors: -5% (~90tCO2e)
- Distribution Transformers (increase of power): +30% (~22tCO2e)
- Medium and low voltage cables: +10% (~34tCO2e)

So, the total carbon footprint saving for OPEX is -2%, corresponding to ~34tCO2e.

3.8 Conclusion

This analysis demonstrates the benefits of the use of 690V with transfer of small Medium Voltage motors to Low Voltage. In that case, the total costs savings are 11%.

If we would limit the analyze to the replacement of 400V by 690V (excluding transfer of small MV motors to 690V), then the total cost savings would be limited to 7%.

As demonstrated in paragraphs *3.6* and *3.7*, carbon footprint savings of the 690V electrical architecture is ~3% for CAPEX and ~2% for OPEX.
By excluding transfer of small Medium Voltage motors to Low Voltage, savings would be slightly lower.

In addition to move to 690V instead of 400V, the recommendation is to transfer small MV motors to LV. This transfer should be limited to approximatively 280kW. This limitation enables to take advantage of the benefits, without increasing too significantly the distribution transformer rated power and LV cable cross sections.

IV. OTHER DESIGN PRACTICES

4.1 ACB integrated control units

For process industry such as O&G, the typical legacy solution to control incomer and bus-tie circuit breakers has been to select unprotected breakers associated to external protection relays.
There have been 2 main reasons leading to this design:
• Protection features requirements beyond what Air Circuit Breakers (ACB) control units could typically support
• IEC 61850 communication protocol not supported by LV ACBs

Recent Air Circuit Breaker technology is changing the game and is enabling footprint and costs savings, thanks to extended protection features and IEC 61850 capability

Protection plans for O&G facilities are often complex, and sometimes unnecessarily complex. Tailoring the

protection requirements to just enough feature will allow not only to use ACB integrated trip units but also reduce engineering, commissioning and troubleshooting time. Not to speak of tripping consequences because of non-adapted settings and implementation.

Typically, designer could select, in most cases, the following short circuit and overload protections:

- ANSI 50/51 Instantaneous Overcurrent
- ANSI 50N/51N Earth/Ground Fault
- ANSI 86 Lockout

And if transformer monitoring is required

- ANSI 63 Transformer pressure
- ANSI 49 Transformer Thermal

This circuit breaker based solution should be complemented with a PLC to perform ATS to manage change-over for incomers and bus-tie, based on the following complementary protections:

- ANSI 25 Synchro Check
- ANSI 27 Undervoltage
- ANSI 27R Residual Undervoltage

As ACB control unit is integrated into the circuit breaker, footprint for the external relay is saved.
It can also enable to have 2 ACB in the same cubicle or to leverage that space for other devices such as Arc Flash relay, ATS PLC, etc.

In addition, often Customers require to install the external relay in an adjacent cubicle to the ACB cubicle. This is a common practice for O&G, leading to additional footprint.

For an O&G double radial typical switchboard with 2 incomers and a bus-tie, it generally leads to 2 additional cubicles (one for each incomer)
The external relay for bus-tie can often be installed without additional cubicle, above the circuit breaker.

Fig. 6: example of footprint savings

Cost savings for that design:
Leveraging ACB control unit is leaner than external relay, typically MV protection relay
• LV ACB control unit is cheaper than the external relay
• There is no need for external CTs nor VTs.
• Saving on the footprint and removing a couple of cubicles will make significant savings

Those savings are related to the incomers/bus-tie section, and are not related to the number of feeders and motor control units
Nevertheless, cost savings typically represent 5 to 8% of the switchgear cost, which is worth challenging the protection plan

4.2 LV switchgear and MV/LV transformers close coupling

Footprint of low voltage system must sometime be regarded as a whole, integrating step down transformer, busduct and switchboard in a single design thinking. In congested location such as offshore application where additional space in electrical room can be very expensive, it is key design factor. But this should also be considered for onshore as more and more modular design is required to reduce the construction time and people at site.
Reduction of rooms size is not the only target, even if always an interesting option. Better use of space can also be a factor of optimization when taking in account all constraints such as space around switchboards, interferences with HVAC duct on ceiling, cable routing in cable vault, …

Below is an example of optimization on a floating unit.

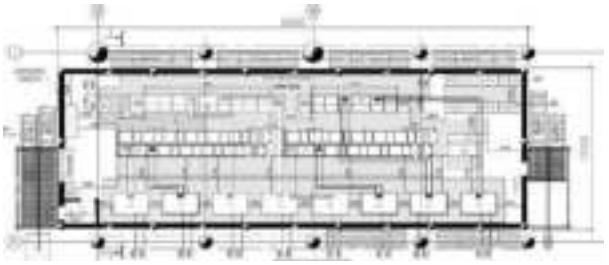

FEED design

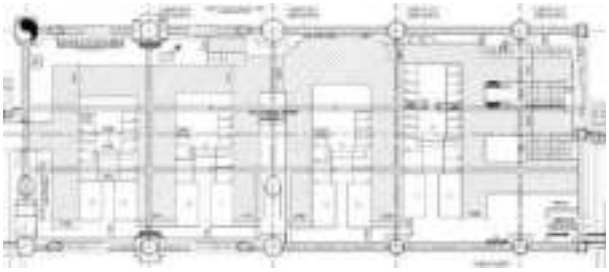

EPC Design

Overall dimensions of the rooms are the same, 35 by 12 meters. So, the new arrangement does not reduce square meters. But during detailed design, structural calculation showed that a main beam needed to pass in the middle of the room, leading to an impossible arrangement of switchboards as per FEED. Maintaining this configuration should require to increase room size, which was impossible.

It was decided to make two main changes :
*Not using back to back configuration to reduce switchboards depth
*Joining transformers in line with switchboards to eliminate the need of big busbars crossing the room (to the exception of the much smaller ones, interconnecting section A and B of each switchboard).
So even if square meters to be build were not drastically saved, a much better use of the available space was made. It also allowed to reducing congestion in ceiling arrangement, to also ease the installation of HVAC and

other equipment required to be fixed there.
In addition, this design allowed to reduce the design manhours for busducts, as well as the risk of rework during construction phase, and to reduce the cost of the copper bars required.

4.3 More digital for more efficient operation and maintenance

Digitization is on top of the agenda for all parties within our Industry, Operators and Owners, EPCs, Vendors, and we presently just see the tip of the iceberg for LV switchboards. To mention a few revolutions ahead of us: augmented and virtual reality to support Operation & Maintenance, moving from monitoring and control devices (appliances) to virtualized applications and data hubs.
Within this paper, we will be focusing on two topics: Operations & Maintenance support within smart circuit breakers and remote operations, with the trend to unmanned operations.

Within all circuit breakers from typical O&G switchgear, incomers and bus tie circuit breakers are especially important to the energy availability and continuity of the process.
Those Air Circuit Breaker and their electronic trip units have been providing basic monitoring and communication features since early 2000s. With the conjunction of microcontrollers ever increasing capabilities and more powerful algorithms, new features are now made possible. Among others those features will contribute to a better maintenance and less downtime.

As all O&G and Chemical operators expect to keep maintenance and product retrofitting for the turnaround typically planned every 4 to 6 years, understanding the ageing of main devices is key.
Operation counters have often been implemented, but they poorly reflect the actual ageing of ACBs. ACB control units can integrate those operations counters as well as algorithms to assess the actual ageing of the circuit breakers and the control units itself. Those algorithms need to be based on assessment campaign on the devices, then engineered and developed to provide accurate support to Operators. To name few such parameters: load profile, number of trips in operation, contact wear, coils diagnostics (MN, MX, …), remaining service estimation, maintenance scheduling information. Those data and indicators can be displayed on the control unit HMI, or more conveniently on a handheld device for nearby operations, and communicated to any asset management solution.
Operators can either rely on the alarms and recommendations provided by the ACB manufacturer or leverage the data for their own assessment.
In addition, those ACBs have become events logger: tripping events, operations, settings modifications, exceeding thresholds (alarming), etc.

4.4 Remote operations, trend to unmanned

Depending on many factors, operations of an oil and gas plant can be a complex combination of procedures for anticipated situations but also people competences that are key in unplanned situations. And it is well known that our friend Murphy and its law is a universal constant.

Thanks to digitization, lots of information are now available and process systems already integrate a number of algorithms to ensure safe and reliable control of processes. But the increasing amount of data make their analysis quite complex and this complexity is increasing exponentially with the number of data to be treated.

There is a huge interest to improve the use of those data to either control remotely, and even make the installation autonomous without need of an operation crew. This is a trend for offshore platform or plant in remote locations.

First projects came to life: possibility of remote operation for a FPSO, autonomous operation for an offshore well platform, automated inspection made by autonomous robots, control of subsea applications (obviously from remote), … But all those experiences show that sometimes human and its experience is still the most efficient safety barrier when Murphy knocks on the door.

Remote operation is taking more and more place in control strategies for plant operation, allowing for example to mutualize the high-level troubleshooting teams in a central location, supporting different plant operators around the world thanks to digitization and digital twins technology.

But the totally unmanned plant will remain a long-term objective for a significant amount of time due to the high number of the decision scenario to be managed and their complexity, but also due to numerous regulations in place around the world dealing with operations, safety and environment. To use an image: with autopilot devices, most of the modern planes could take off, fly and land without intervention of the pilot in 99% of the situations. But regulation will prevent this to happen because of this 1% time where a correctly trained human being is still the most efficient safety device.

Those examples highlight the concrete benefits operators will get from the current digitization trend, with major evolutions and benefits in the coming years.

V. CONCLUSIONS

In this paper, some design practices have been shared which enable EPCs and Operators to reduce footprint and costs:
*use of circuit breakers instead of fuses, which can typically reduce footprint and costs in the order of magnitude of 10%
*shift from 400V to 690V and transfer “small” Medium Voltage motors to 690V motors, up to 280kW
*new features embedded in circuit breaker digital control units

In addition to those economical benefits, some of those design practices, especially the move to 690V, contribute to reduce the environmental impact: 3% carbon footprint savings for construction and 2% for operations (for the scope considered in the case study).

VI. REFERENCES

[1] PCIC IS-22 2013: FUSES OR MOLDED CASE CIRCUIT BREAKERS What are benefits and disadvantages of MCCB or fuse for “in line” protection?

[2] Selectivity Cascading and Coordination Guide Schneider Electric 2021
https://www.se.com/ww/en/download/document/LVPED318033EN/

[3] PCIC Europe 2017: FPSO electrical network optimization for significant savings: where lies the cost?

VII. VITA

Laurent Bloch received his Engineering Degree in 1985 with a specialization in Mechanical and systems Engineering. After a first experience at L’Air Liquide Engineering Division, he joined Schneider Electric in 1989. He worked for Schneider Electric Contracting Division in France and abroad, then moved to different marketing positions related to electrical distribution and energy management solutions. He has been supporting O&G and Chemical business for LV solutions for last 5 years.

Philippe Angays has a master in Electronics and Electrical Engineering and a specialization in Robotics at the University of Science of Lyon in 1984. He worked as engineer for industrial robotic
applications. In 1991, he joined 2H Energy, a major gensets builder in Oil & Gas applications. He managed the design department for special applications, like black-start and emergency electrical systems for installations such as FPSO or offshore platforms. He joined the electrical department of Technip in 2005 as expert engineer for power plant applications. He his now a Technology Expert Fellow for electrical matters for Technip Energies worldwide.

Victor Ascher is head of electrical equipment section in Technip Energies Paris office. He previously acts as lead electrical engineer in major onshore and offshore projects in particular Arctic LNG 2 for Novatek and ZapSibNeftekhim for Sibur

Jean-Philippe Herpin is a LV equipment expert, supporting the main customer projects of Schneider. During his carrier with this company, he has been part of the development of circuit breakers like Masterpact and the LV equipments like Prisma or Okken. Jean-Philippe HERPIN is graduated from CENTRALE Lyon engineering school in 1987

Mathieu Guillot is a power system expert in charge of LV power products application marketing. He has held various positions in MV R&D, in Solution and Services for MV and LV and LV circuit breakers marketing for Schneider Electric. He is also member of the IEC TC64/MT2 working group, in charge of overcurrent protection and thermal effects in the IEC 60364 series. Mathieu Guillot is a graduate of CENTRALE-SUPELEC engineering school in Paris. France (1994).

Benoit Stefanski is a Power system architect in charge of proposing Electrical architecture and equipment optimizations in early phase of O&G projects. In 2005, he joined Schneider Electric as Medium Voltage Technical manager in R&D. Afterward, he moved to Medium Voltage Tendering then joined the Grenoble Project & Engineering Center for projects Tendering and Execution.

ELECTRIC DISCHARGES IN BALL BEARINGS OF A 3.9 MW DOUBLE FED INDUCTION GENERATOR POWERED BY A 2-LEVEL VSI

Paper No. PCIC Europe EUR22_15

Dr. Lionel Durantay
Senior Member, IEEE
GE Power Conversion
442, rue de la Rompure
54250 Champigneulles
France
lionel.durantay@ge.com

Dr. Kum-Kang Huh
GE Global Research Center
1 Research Circle
12309 Niskayuna, NY
USA
huhk@ge.com

Christophe Grosselin
GE Power Conversion
442, rue de la Rompure
54250 Champigneulles
France
christophe.grosselin@ge.com

Gaëtan Miclo
GE Power Conversion
442, rue de la Rompure
54250 Champigneulles
France
gaetan.miclo@ge.com

Abstract – The Double Fed Induction Generator (DFIG) with a rotor fed by PWM converter through a slip ring is the most common architecture used for onshore windmills. Compared to motors fed by power electronic through the stator, this configuration is more severe for the electrical stresses in the ball bearings. The first part of this paper describes two architectures of variable speed asynchronous machines including a 3.95MW DFIG system powered by a 2-level voltage source inverter. The second part overviews the common mode voltage mechanisms from the drive inducing high frequencies currents in the bearings. A new indicator of bearing electric discharges is presented and completed by two others existing indicators for bearings electric lifetime. The last part focuses on comparison of two mitigation techniques on bearings currents based on experimental measurements and lifetime prediction using the three indicators.

Index – Power Electronics, Common Modes Voltage, Ball Bearings, Double Fed Induction Generator, Earthing, Insulation.

I. INTRODUCTION

The use of variable speed motors or generators is more and more widespread in the industrial world, in oil & gas compression, marine propulsion and intermittent renewable energy generation. Electrical systems make a variable frequency converter interact with an electrical machine. The speed variation allows a real-time optimization of the performance of the system as well as a reduction in consumption of energy combined with a reduction in the generation of greenhouse gases. Power converters are real time controlled with rapid switching of the IGBTs arms, connected to the different phases of the electrical system.

Unlike a three-phase DOL grid which generates almost no unbalance between the phases varying in a purely sinusoidal manner, a PWM control of the voltage switches generates zero-sequence voltage imbalances, called common mode voltage (V_{cm}), which, through the leakage impedance of the system grounding, induces a non-negligible amount of high-frequency leakage currents, especially in the bearings of the electrical machine.

These leakage currents are generated by capacitive electric discharge mechanisms in the lubricants of anti-friction bearings (ball or roller) or hydrodynamic lubricated bearings. The accumulation of these discharges over time will erode and deteriorate the bearing surfaces and pollute the lubricants (grease or oil) with vaporized metallic debris and ultimately destroy the bearings, stopping production and requiring unscheduled replacement of defective parts.

Analyze of components failure data for wind power generators greater than 2MW shows that it is mainly the bearings that fail with a percentage of occurrence of 58% far ahead of stator or rotor failures (fig.1) [1]. A large part of these bearing failure faults is due to stray currents, the physics of which need to be understood and controlled.

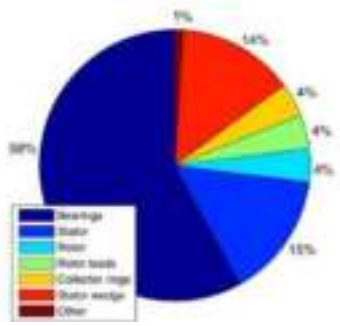

Fig.1. Failures distribution in WT generators > 2MW

The objectives of this publication are:

- to explain these discharge mechanisms,
- to describe three useful indicators making it possible to quantify these phenomena of electrical erosion,
- to compare two electrical arrangements in order to reduce the occurrences of discharge and to increase the electric lifetime of the bearings and the availability rate of the full system.

II. THE PHYSICS OF VSI-POWERED SYSTEMS

A. Stator or Rotor VSI-Fed machines Systems

Electrical machines with a power greater than 1MW are usually supported by roller (anti-friction) bearings or sleeve (journal) bearings. The physics of oil-lubricated journal bearings will not be covered in this publication. The EDMs are less severe there because of their lubricated airgap of the order of a few hundredths of a millimeter compared to roller bearings whose lubricant contact thicknesses are less than a hundredth of a millimeter.

In the case of a VSI-powered stator, the 3-phase stator windings create a rotating magnetic field. Its frequency of rotation is called the synchronism frequency. The rotor consists of copper bars not insulated, short-circuited at their end by two conductive rings and constitute a "squirrel cage" (fig.8). The cage is swept by the rotating magnetic field. When a resistant torque is applied on the shaft by the load, it induces a rotor slippage (Ω_{rs}) with a rotor pulsation (Ω) a bit lower than the stator pulsation (ω_{drive}) which is fixed by the control of the inverter:

$$\Omega(\text{shaft}) + \Omega_{rs}(\text{Variable Load}) = \omega_{drive}/p \quad (1)$$

The slippage speed (Ω_{rs}), of the order of a few revolutions per minute (some % of stator pulsation / p), interacting with the variable frequency induction field of the stator, induces by Lorentz's Force a rotor current into the cage. This rotor current, interacting with the stator induction, induces by Laplace's Force a torque generation in opposite to the resistant (load) torque. Figure 2 describes this motor power supply configuration by the stator where the drive is sized to transit 100% of the system power, from the network to the motor. This configuration of variable speed system is for example used for the electric propulsion of icebreakers using azimuthal squirrel cage induction motors, called POD (fig.2 & 3). The stator is built with a medium voltage winding, for phase-to-phase voltages above 3kV (fig.4).

Fig.2. 2 x 7.5MW "Pod" Propulsion for Ice Breaker

Fig. 3. "Pod" 3-phase Stator

Fig. 4. "Pod" Squirrel Cage Induction Rotor

In the case of a VSI-powered rotor, the rotor consists of a low voltage three-phase winding (fig.6) and the stator of a medium voltage three-phase winding. This kind of system is used in power generation (fig.9), in particular for on-shore wind turbines using a gearbox between the low-speed turbine and the medium-speed generator, which is generally a 4-pole induction machine having a synchronous speed of 1500rpm to output on a 50Hz grid or 1800rpm to output on a 60Hz grid. This machine is called Double Fed Induction Generator (DFIG) (fig.5).

Fig.5. 3.95MW 4-pole DFIG

Depending on the wind speed which modifies the rotation speed of the generator shaft, the drive adapts its frequency to generate the network frequency at the stator terminals.

$$\Omega(\text{geared wind turbine}) + \Omega_{rs}(\text{drive}) = \omega_{grid}/p \quad (2)$$

The slippage speed (Ω_{rs}) reaches a few hundred revolutions per minute (a few tens of % of stator pulsation / p) and depends on the speed range of the wind turbine:

$$\text{slippage}\ (\%) = 100 * p * \Omega_{rs}(\text{drive})/\omega_{grid} \quad (3)$$

The drive must be able to inject up to 30% of the power produced by the stator. The advantage of this solution is to reduce the size and voltage of the drive compared to a fully fed powered stator. This technology requires inserting a slip ring between the 3-phase wound rotor and the fixed drive (fig.7).

Fig.6. DFIG 3-phase Low Voltage Rotor

Fig.7. Slip Ring

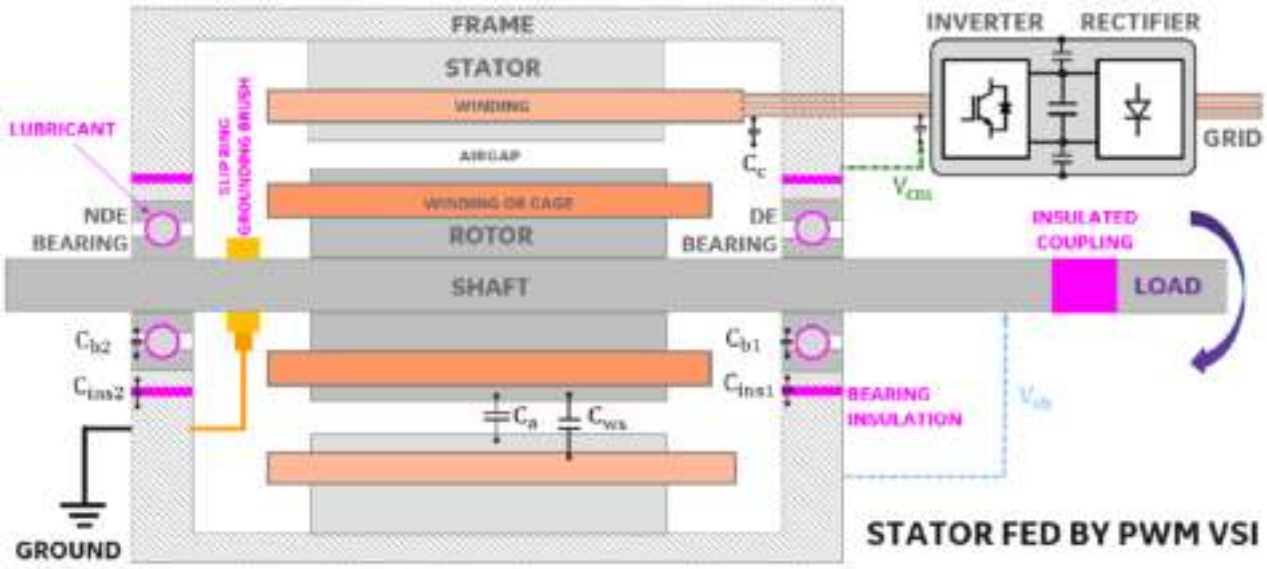

Fig.8. Wound Stator fed by Medium Voltage VSI (Variable Speed Motor System)

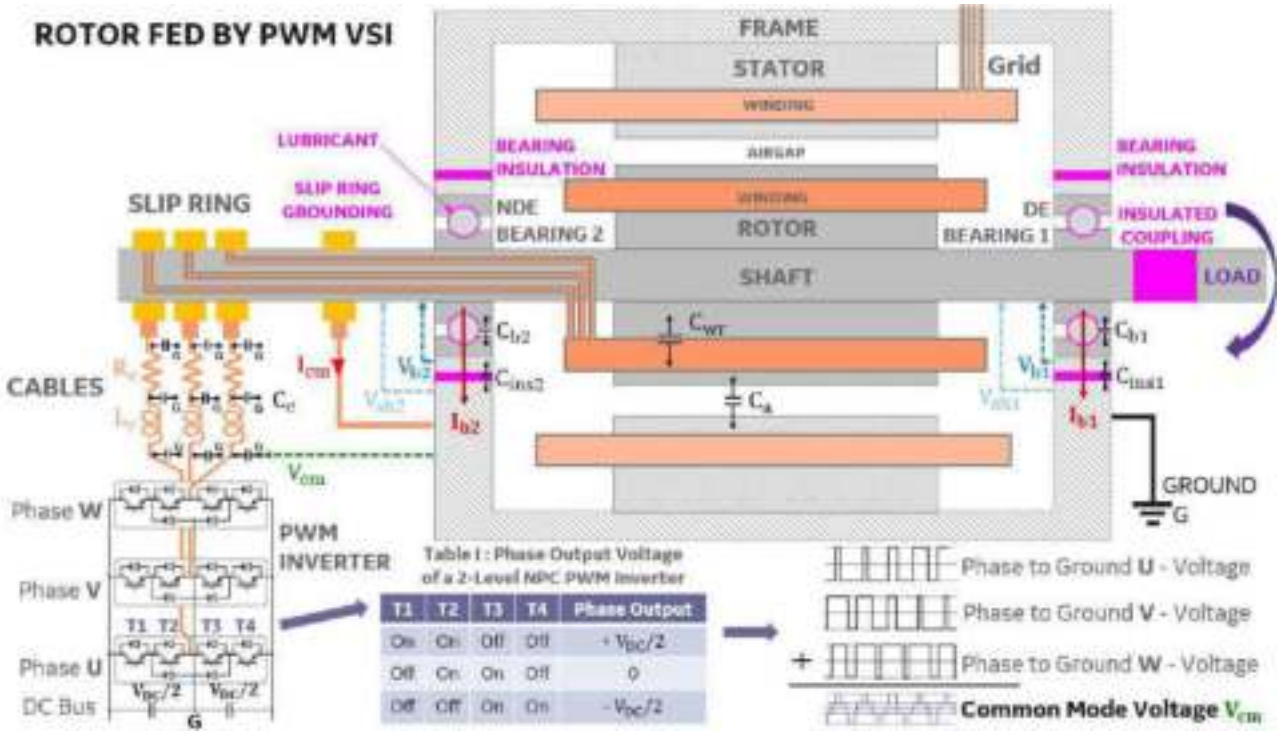

Fig.9. Wound Induction Rotor fed by Low Voltage 2-Level VSI (DFIG System)

B. PWM-Control of VSI

Unlike power diodes whose electrical conduction cannot be stopped by a trigger, power transistors (IGBT, IEGT…) have a trigger that allows control of the opening and closing of electrical conduction, like a switch. Connected to a DC voltage bus, generally stabilized by capacitors, the arrangement of these power transistors makes it possible to generate three-phase voltage waves at variable frequency inducing currents having the same fundamental frequency in electrical machines.

A control of these inverter arms, called Voltage-Source-Inverter (VSI), by Pulse-Width-Modulation (PWM) makes it possible to reduce the average power delivered by an electrical signal, by effectively chopping it up into discrete parts. The average value of voltage (and current) fed to the load is controlled by turning the switch between supply and load on and off at a fast rate, around a few kilo Hertz (kHz) for an electric machine fed by the drive. The PWM algorithm allows rapid and optimal control of the electric machine according to the needs of the load.

However, it has two disadvantages which must be quantified and reduced which are the common mode voltages and the {R-L-C} circuit resonance.

1. Common Mode Voltages

In a three-phase machine fed by three sinusoidal voltage waves of same amplitude and same frequency, phase shifted between them by 120°, the instantaneous sum of the three voltages is always equal to zero, or very close to zero due to grid imbalance. This is not the case in a three-phase system (U-V-W) controlled by PWM inverter because the switches do not conduct simultaneously on the three phases (fig.10). This results in instantaneous voltage imbalances at the switching frequency of the signal, the amplitudes of which depend on the control method (toggle, synchronous or asynchronous, etc.) and the number of voltage levels [2].

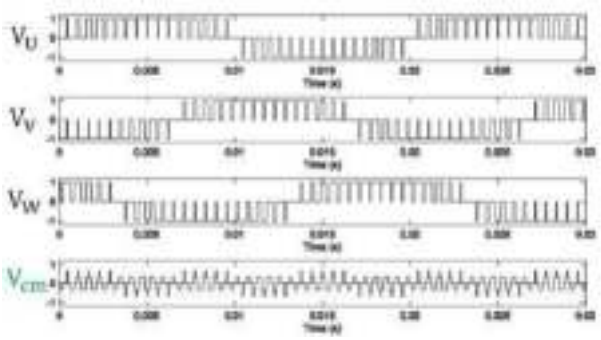

Fig.10. Phase-to-Ground and Common Modes PWM Voltages Patterns

For a 2-level inverter, the common mode voltage (V_{cm}) amplitudes, at the inverter terminals, are given by the following formula:

$$V_{cm} = \frac{V_V + V_U + V_W}{3} = \pm \frac{V_{DC}}{2}, \pm \frac{V_{DC}}{6} \qquad (4)$$

This common mode voltage generates leakage currents to the ground all around the system. These currents will be limited by the insulation capacitances of the various system components in contact to the ground: cables, rotor windings to ground (C_{wr}), stator windings to rotor ground (C_{ws}), air gap between the stator ground and the rotor ground (C_a) (usually bearing seals airgap), bearing lubricant (C_b), bearing insulation (C_{ins}).

For a VSI-fed stator, the shaft voltage $(V_{sh,s})$ near the bearings, proportional to (Vcm_s) at the stator terminals, is given by the following formula:

$$SVR_s = \frac{V_{sh,s}}{Vcm_s} = \frac{C_{ws}}{C_{ws} + C_a + 2.C_{eq}} \qquad (5)$$

- where (C_{eq}) is the equivalent capacitance of one bearing:

$$C_{eq} = \frac{C_{ins}\ C_b}{C_{ins} + C_b} \qquad (6)$$

For a VSI-fed rotor, the shaft voltage $(V_{sh,r})$ near the bearings, proportional to (Vcm_r) at the rotor terminals, is given by the following formula:

$$SVR_r = \frac{V_{sh,r}}{Vcm_r} = \frac{C_{wr}}{C_{wr} + C_a + 2.C_{eq}} \qquad (7)$$

A large Shaft-Voltage-Ratio SVR induces a high residual voltage of the bearings. The capacitance of the motor windings has a first order impact on the shaft voltage ratio. This capacitance is inversely proportional to the thickness of the insulation of the coils (strand insulation + ground wall insulation) (fig.11) which is proportional to the phase-to-ground voltage applied at the machine terminals.

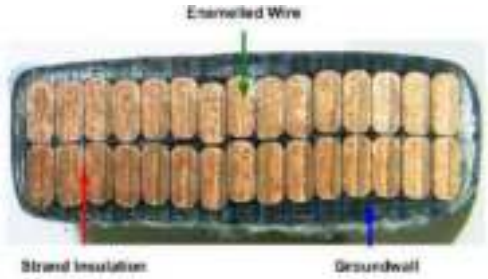

Fig.11. Cross Section of a Multi-turn Form-wound Coil [3]

A low voltage winding has an insulation thickness of less than a millimeter while a medium voltage winding has a thickness of a few millimeters. Viewed from the bearings through the rotor, the capacitance of the stator winding is significantly reduced by the main air gap of the motor. So, a low voltage rotor has a much higher shaft voltage than a medium voltage stator:

$$C_{ws} < C_{wr} \Rightarrow SVR_S < SVR_r \Rightarrow V_{sh,s} < V_{sh,r} \qquad (8)$$

The shaft voltage fed by low voltage rotor $(V_{sh,r})$ can be a few tens of volts, more than 10 times higher than the shaft voltage fed by medium voltage $(V_{sh,s})$.

2. System {R-L-C} Resonance

The switching transient of the power transistors generates dV/dt voltage gradients which are generally limited to 1kV/µs so as not to prematurely damage the insulation of the coils of the machine [3]. The frequency excitation bandwidth of a voltage gradient is inversely proportional to the switching time (fig.12 & 13). For low voltage amplitudes of a few hundred volts $(V_2\text{-}V_1)$, the excitation cutoff frequency (f_1), resulting from a gradient of 1 kV/µs (a) is of the order of a few kilo Hertz (kHz).

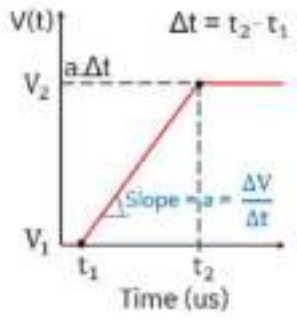

Fig.12. Time Signal of a Voltage Gradient

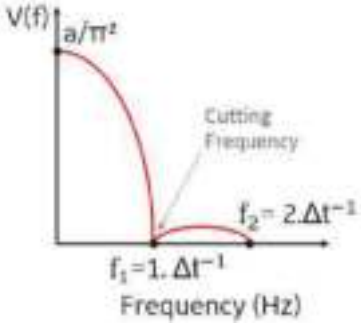

Fig.13. Frequency spectrum of a Voltage Gradient

$$V(f) = (V_2 - V_1) * \left(\frac{\sin(\pi.\Delta t)}{\pi.\Delta t}\right)^2 \qquad (9)$$

This voltage excitation interacts with the leakage impedance resulting from the connections between the various resistors, inductances and capacitances of the system which can be modeled by an equivalent {R-L-C} circuit. This {R-L-C} circuit has an electrical resonant pulsation given by the following equations which is excited by the dV/dt bandwidth. This results in a common mode resonant current (I_{cm}), the amplitude of which is damped by the equivalent resistance of the circuit (R), and which can reach a few tens of amperes [4]:

$$I_{cm}(t) = \frac{V_{cm}}{Z_0 \cdot \sqrt{1-\zeta^2}} . e^{-\zeta \omega_n t} . \sin(\sqrt{1-\zeta^2}\ \omega_n t) \quad (10)$$

- where:

$$\omega_n = \frac{1}{\sqrt{LC}} \text{ and } \zeta = \frac{R}{2}\sqrt{\frac{C}{L}} \text{ and } Z_0 = \sqrt{\frac{L}{C}} \quad (11)$$

The addition of a filter reducing the slope of the dV/dt making it possible to lower the cut-off frequency below the resonance frequency of the circuit. This type of filter is usually integrated at the output of the inverter with shielded cables for medium voltage motors, with an acceptable over-cost. It is also necessary to add a rotor grounding circuit via brushes, to drain these common mode currents by bypassing the bearings. This grounding track is integrated in the slip ring of the DFIG generator in addition to the 3-phase tracks.

III. BEARINGS ELECTRIC DISCHARGES

A. Discharge Mechanisms Inside Bearings

In rolling bearings, Electric Discharge Mechanisms (EDM) appear in between the outer racetrack and rolling elements, or the inner racetrack and the rolling elements, lubricated by a dielectric fluid (fig.14). During the dV/dt commutations having duration around micro-seconds, the increase of a few volts in the voltage between the two surfaces behaving like electrodes, combined with a reduced air gap of a few micrometers generates an electric field sufficient to ionize the lubricant. The recombination of electrons with the ions radiates photons, when the electric field reaches its critical breakdown value, named Lubricant Electric Strength (E_{th_lub}) which depends on temperature (T), bearing leakage current (I_b), and electric conductive debris.

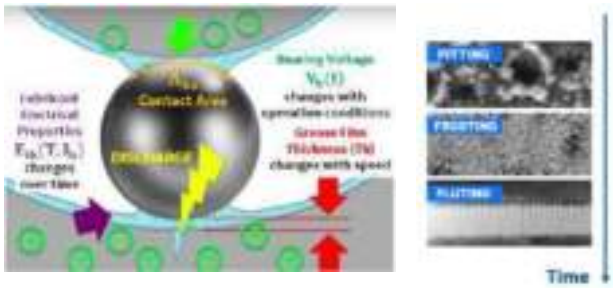

Fig.14. Micro Electric Discharges Mechanism

The leakage current of the bearings is given by the following formula where (C_b) is the electrical capacitance of the lubricant at the level of the rolling element:

$$I_b = C_b * \frac{dV_b}{dt} \quad (12)$$

where: $$C_b = K_{cur} * \frac{\varepsilon_0 * \varepsilon_{r,lub} * A_{hz}}{2\ h_{lub}} \quad (13)$$

When the voltage reaches the breakdown threshold voltage (V_{th}), the capacitive energy stored in the system (En_D), of the order of tens of micro-joules, is discharged via a glow-to-arc transition (fig.15):

$$V_{th} = Th_{lub} * \ (\ 2 * E_{th\_lub}(T, I_b, Debris)\ ) \quad (14)$$

$$En_D = 0.5 * C_b * V_{Th}^2 \quad (15)$$

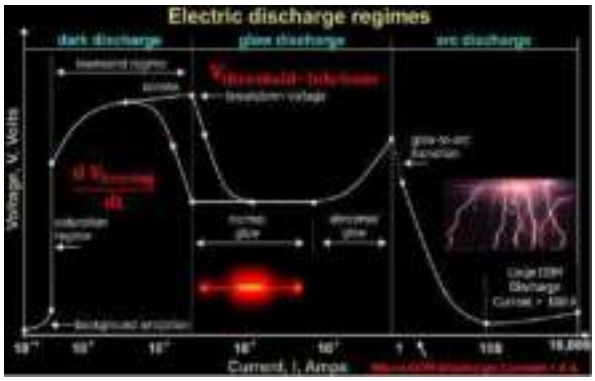

Fig.15. Electric Discharges Regimes

We speak of micro-EDM when the average discharge currents are below the order of a few amperes, which is the case for anti-friction bearings. The electric arc is a few nanometers cross-section and reaches a temperature above 5,000K. Its impact locally sublimates the material which is instantaneously transformed into micro metallic debris. During the discharge, the lubricant moves from a capacitive state of a few micro farads to a conductive state having an equivalent discharge resistance (R_D) of the order of a few ohms. Experimental studies in titanium micromachining show that it is possible to measure the size of craters of the order of a few micrometers as a function of the discharge energy (fig.16 & 17) [5].

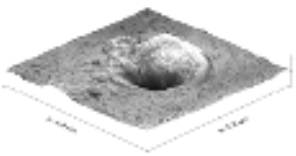

Fig.16. Crater 3D AFM Picture (Titanium) @ 0.1 uJ Discharge

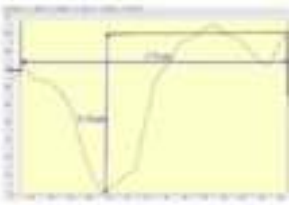

Fig.17. Crater Dimensions (Titanium) @ 0.1 uJ Discharge

The accumulation of these discharges over time will deteriorate the kinematic contact surfaces of the raceways and the rolling elements of the bearing through three states: an initial pitting, a transient frosting, and a final fluting (fig.14 & 18) destroying the bearing by thermal effects and shocks.

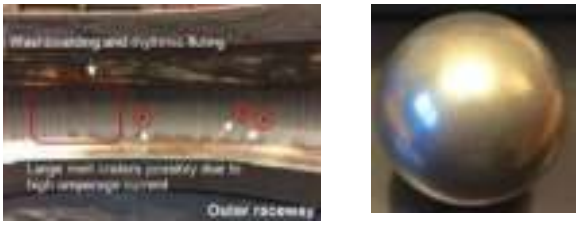

Fig.18. Fluting of Outer Race Way and Balls. [2]

B. State of the Art for Bearing Insulation

Voltage criteria between shaft and ground, based on feedback from DOL electrical machines, are proposed in the literature and certain standards such as **NEMA MG1** which recommend a voltage lower than **1Vrms**. This criterion is even more difficult to satisfy knowing that the shaft voltage increases as the power to the cube of the machine size for a DOL machine [6]:

$$V_{sh} \alpha (\text{Machine Size})^3 \quad (16)$$

To prevent electrical erosion of the bearings, it is recommended to insulate the DE and NDE bearings of large machines. This insulation can be made with ceramic bearings which are however limited in size for manufacturing reasons. The other solution consists in inserting between the bearing and the frame an insulation made with an electrically and magnetically inert composite material. For a maximum admissible dV/dt level at the drive terminal, the capacitance of this insulation must generate an Apparent Leakage Current Density (J) in the bearing lower than [7]:

- $J < 0.1 \frac{A_{pk}}{mm^2}$ @ 60 Hz Direct-On-Line (17)
  If not forced lubrication
- $J < 0.8 \frac{A_{pk}}{mm^2}$ @ 60 Hz Direct-On-Line (18)
  If forced lubrication

where: $J = I_b / A_{hz}$ (19)

The bearing residual voltage (V_b) is lower than the shaft voltage (V_{sh}) and proportional to the capacitive bridge ratio between the bearing and its insulation:

$$V_b = \frac{C_{ins}}{C_{ins} + C_b} * V_{sh} \quad (20)$$

where: $C_{ins} = J * A_{hz} / \frac{dV_{drive}}{dt}$ (21)

It is possible to reduce the capacitance by increasing the thickness of the insulation, but care must be taken to control the mechanical stiffness of these insulations supporting the shaft-line to avoid risks of vibrations and mechanical resonance.

C. Electro-erosion Indicators

It is important to quantify the electro-erosion risks of machines powered by VSI inverter. Based on a bibliographic search and specific research work, three useful indicators are proposed.

The first indicator (L_{e_fD}) is a lifetime prediction for a VSI-fed machine. It is deduced from a statistical indicator ($L_{e\_60\,hz}$) of electrical life of the rolling bearing [4], interpolated on measurements of apparent current density (J) for machines powered by a DOL network, by linearly correcting the frequency of occurrence of discharge between the frequency of a 60Hz DOL grid and the measured discharge frequency (f_D) with the converter (close to the PWM carrier frequency):

$$L_{e\_60\,hz} = 7{,}867{,}204 * 10^{-(2.17*J)} \quad (22)$$

$$L_{e\_fD} = 60\ \text{Hz}/f_D * L_{e\_60\,hz} \quad (23)$$

The second indicator is the Bearing Electric Stress (W_{es}) considering the bearing current (I_b) is proportional to the arc current (I_{arc}), itself proportional to the product of apparent bearing current density (J) and the Hertzian contact area, and increasing linearly with the discharge frequency (f_D) (close to PWM switching frequency) and the time of operation (t_{op}) [6]:

$$W_{es} = J * t_{op} * f_D \quad (24)$$

Based on the research of A. Muetze, it is possible to determine the threshold levels of electric erosion patterns for a rolling bearing:

- Races Pitting if $W_{es} \leq 10^{+9}$ A/mm²
- Races Melting-Frosting if $10^{+9} < W_{es} \leq 10^{+10}$ A/mm²
- Races Fluting if $W_{es} > 10^{+10}$ A/mm²

In addition, we have also developed a new indicator to quantify the electrical eroded thickness over time (Th_{er}). It is possible for a given metal to determine the volume of sublimated matter of a crater after arcing as a function of the discharge energy by the function ($Vol_{crater}(En_D)$). The total volume of material sublimated over the time is proportional to the discharge frequency (f_D) (close to PWM switching frequency) and the time of operation (t_{op}) and a metal coefficient (K_{metal}):

$$Vol_{er} = K_{metal} * t_{op} * f_D * Vol_{crater}(En_D) \quad (25)$$

Knowing from the supplier of bearings the width (L_T) and the average diameter (D_T) of contact on the tracks, it is possible to calculate the thickness eroded over time (Th_{er}):

$$Th_{er} = 0.5\ [D_T - \sqrt{D_T^2 - \{4 * Vol_{re}/(\pi * L_T)\}}] \quad (26)$$

We propose as acceptance criteria a maximum erosion threshold equal to the roughness of the rolling tracks.

IV. MEASUREMENTS ON TWO ARRANGEMENTS

A. Tests Description

The machine tested is a large DFIG powered by its low voltage drive with a power of around 4 MW (fig.5):

TABLE I
Double Fed Induction Generator Characteristics

Parameter	Value
Power	3.95 MW
Grid Frequency	50 Hz
Polarity	4
Speed Range	1000 rpm to 2000 rpm
Stator Voltage	6 kV
Rotor Max Voltage	850 V rms
Rotor Max Current	1700 A rms
Bearings	Balls
Coupling	Insulated
Lubricant	Grease
PWM Converter	2-level

The generator is instrumented with voltage and current measurement probes having a very wide bandwidth making it possible not to filter the signals dynamic, during switching transients of the power transistors. As described in Figure 9, shaft voltage ($V_{b\,i}$), bearing voltages ($V_{b\,i}$), bearing current ($I_{c\,i}$) and ground brush current (I_{cm}) measurements, corresponding to the nominal operating point of the system, are analyzed. These measurements were carried out in-situ on an on-shore demonstration wind turbine in Germany. Unlike the results of measurements of laboratory test benches widely presented in scientific publications, there is almost no publication presenting measurements carried out on a real system at scale one.

B. Arrangement #1

The first arrangement is considered the most effective state of the art, recommended for medium and large power machines [7]:

- Non-Driven End (NDE) insulated bearing,
- Driven End (DE) insulated bearing,
- Additional insulated coupling,
- Shaft grounding brush.

The shaft voltage (fig.22) and grounding brush current (fig.21) curves highlight the dynamic amplification of the ground current due to the dV/dt excitations driving the resonance of the system's {R-L-C} circuit. The current rises to 50 amps and is damped over a few periods of oscillation thanks to the resistance of the circuit. This confirms the absolute necessity of using a grounding brush for a machine supplied with a variable frequency drive.

The average rms voltage of the shaft is around 4.3 volts with peaks around twenty volts, and around 2.5 volts with peaks around ten volts for the bearing (fig.19).

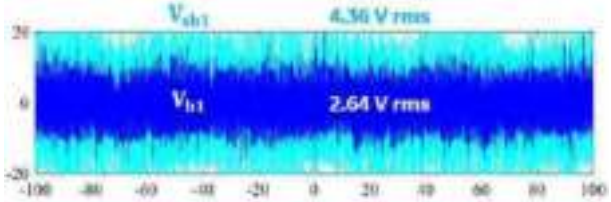

Fig.19. Shaft and Bearing Voltages vs Time @ 200 ms

The zooms of the shaft and bearings voltages highlight fluctuating excitation modes in residual dV/dt amplitudes (fig.20). A shaft voltage residual offset is observed for the dv/dt of higher amplitudes whether on positive or negative polarity. We interpret this residual bearing voltage offset because of a micro electrical discharge in the lubricant (fig.22).

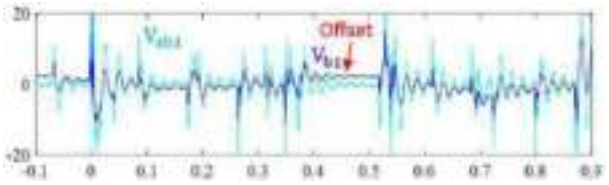

Fig.20. Shaft and Bearing Voltages vs Time @ 1ms Zoom

This transient mechanism of discharges is divided into three sequences named Step A, Step B and Sept C (fig.23 & 24).

+ Step A of plasma ignition corresponds to the voltage rise phase until the breakdown voltage of the lubricant is reached. The bearing voltage is measured of the order of a third of the shaft voltage due to the capacitive ratio between the insulation and the film of grease:

$$V_{b\,A} = \frac{C_{ins}}{C_{ins} + C_b} * V_{sh\,A} \approx \frac{1}{3} * V_{sh\,A} \quad (27)$$

$$I_{b\,A}(t) = C_{eq} * \frac{dV_{sh\,A}}{dt} \quad (28)$$

+ Step B is the discharge phase where locally the lubricant will change from a capacitive insulating state (C_b) to a resistive conductive state (R_D). The discharge threshold voltage is a function of the system conditions at that instant:

$$V_{th\,B} = f\{E_{th\,lub}, Th_{lub}, I_{b\,A}\} \quad (29)$$

The bearing and its insulation behave like an {R-C} circuit. Metallic micro debris created by the discharge impact are dispersed in the lubricant. This phase lasts until the bearing current becomes zero:

$$V_{b\,B}(t) = V_{th\,B} * e^{-t/(R_D.C_{ins})} \quad (30)$$

$$I_{b\,B}(t) = \frac{V_{th\,B}}{R_d} * e^{-t/(R_D.C_{ins})} \quad (31)$$

+ Step C corresponds to voltage offset generation. When the bearing current becomes zero, the arc is extinguished, and the lubricant recovers its capacitive insulating properties. This results in a drainage of the charges stored in the dielectric material of the insulation towards the lubricant, which explains this bearing voltage offset which is proof of discharge:

$$|V_b| = \frac{|Q_b|}{C_b} = \frac{|Q_{ins}|}{C_{ins}} = |V_{ins}| \quad (32)$$

$$I_{b\,C}(t) = C_b * \frac{dV_{b\,C}}{dt} \quad (33)$$

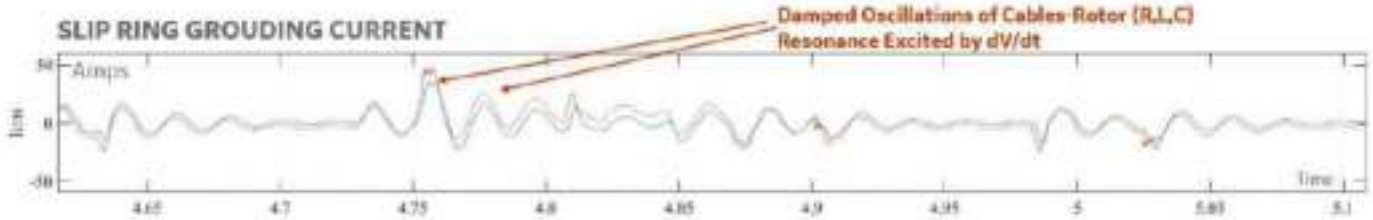

Fig.21. Grounding Brush Current vs Time

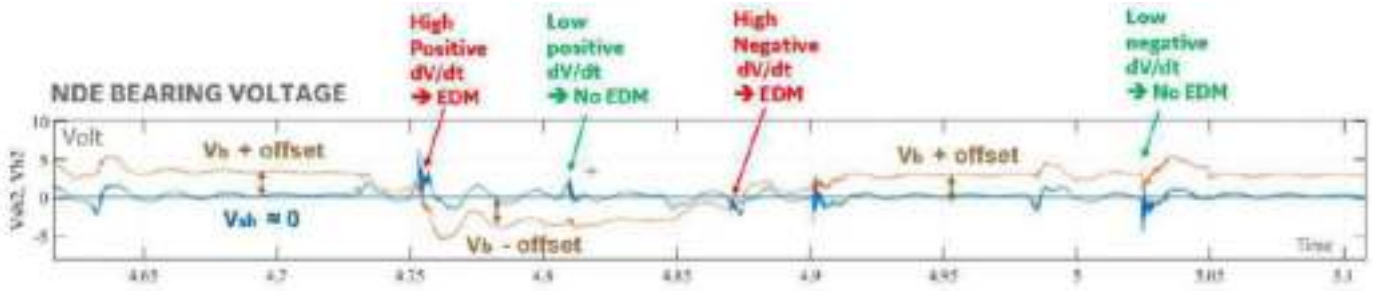

Fig.22. Shaft and Bearing Voltages vs Time

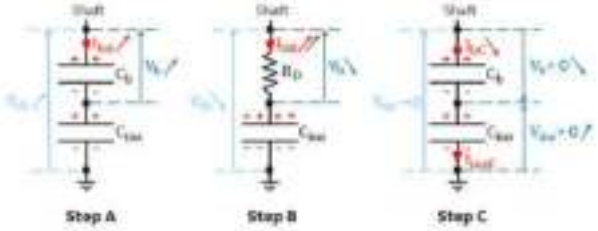

Fig.23. Equivalent Models of Discharge Steps

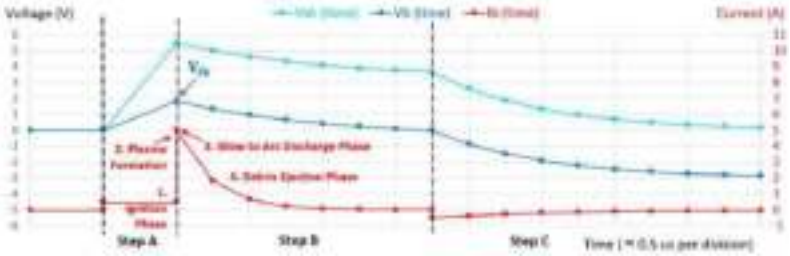

Fig.24. Discharge Voltages and Current Trends for Bearing and Shaft

C. Arrangement #2

A second arrangement, named #2, is also tested. It is patent pending and therefore not described in this publication. The average rms voltage of the bearing is divide by 10, around 0.2 volts with peaks around 2 volts (fig.25). The leakage bearing current is around 0.15 amps rms (fig.26). There is no more voltage offset so we can conclude that there are no more significant micro-discharges in the grease film of the bearings (fig.27).

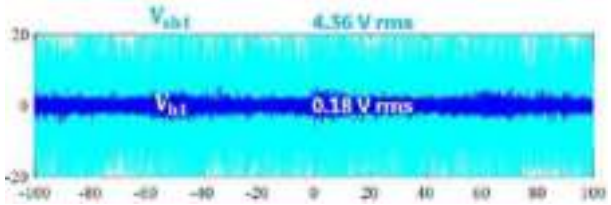

Fig.25. Shaft and Bearing Voltages vs Time @ 200 ms

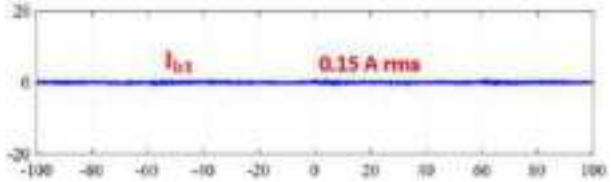

Fig.26. Bearing Leakage Current vs Time @ 200 ms

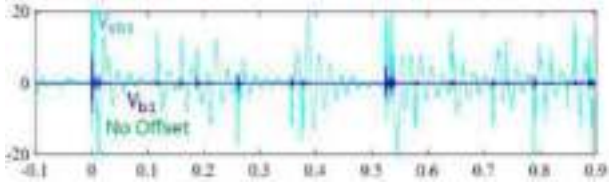

Fig.27. Shaft and Bearing Voltages vs Time @ 1ms Zoom

Table II compares the electrical life and electro-erosion indicators of this generator for the two test arrangements.

TABLE II
Electric Lifetime & Erosion Indicators

Parameter	Arrangement #1	Arrangement #2	Criteria
L_{e_fD}	13 years	13.4 years	> 10 years
W_{es}	5E+09 A/mm²	0.9E+08 A/mm²	< 1E+09 A/mm² (No Melting)
Th_{re}	50 µm	0.4 µm	< 0.4 µm (Roughness)

The electrical lifetime (L_{e_fD}) indicator for both arrangements is greater than 13 years but only differs by 0.4 years. We can suspect a lack of accuracy of this indicator built from a database of DOL-fed machines.

Therefore, it makes sense to evaluate the Electric Stress (W_{es}) and Electric Erosion (Th_{er}) indicators for this system. These two indicators show a very clear reduction in the risk of electro-erosion with arrangement #2, which makes it possible to satisfy a class of excellence in the operability of the system, with a low erosion by pitting which should not exceed 0.4 µm which is the roughness value of tracks and rolling elements.

V. CONCLUSION

This publication addressed the issue of circulating currents in the bearings of electrical machines operating in speed variation with a converter. The first goal is to understand the physics, the causality, and the orders of magnitude of these phenomena induced in the medium and high frequencies range. The second goal is to share experience feedbacks based on measurements made for a DFIG system and to zoom in the transient signals to identify mechanisms of micro-discharges induced by converter switching. The third goal is to propose three indicators, introducing a new erosion indicator, relevant to quantify the reliability of bearings and to compare two arrangements of bearings protection against arcing and electro-erosion.

VI. ACKNOWLEDGEMENTS

Thanks to Henri Baerd (GE Power Conversion), Ludger Luetkehues, Giesbert Kruger and Ivan Cuenca (GE Renewable) for their contributions to this study.

VII. REFERENCES

[1]. M. Whittle an All, “Bearing Currents in Wind Turbine Generators”, Journal of Renewable and Sustainable Energy, Vol. 5, Sept 2013.
[2]. A. Joshi, “Electrical Characterisations of Bearings”, PhD, Chalmers University of Technology, 2019.
[3]. S. Ul Haq, “A Study in Insulation Problems in Drive Fed Medium Voltage Induction Motors”, PhD Thesis, Waterloo University, Canada, 2007.
[4]. D. Busse, J. Erdman, R. Kerkman, D. Schlegel, G. Skibinski, “Bearing Currents and Their Relationship to PWM Drives”, in proc. IEEE Transactions, 1995.
[5]. A. Deshmukh, “Modelling of Anode Crater Formation in Micro-Electrical Discharge Machining”, PhD, University of Nebraska, Dec 2013.
[6]. A. Muetze, “Bearings Currents in Inverter-Fed AC-Motors”, PhD, Darmstadt University, Jan 2004.
[7]. O. Magdun, A. Binder, “Calculation of Roller and Ball Bearing capacitances and Prediction of EDM Currents”, in proc. IEEE, pp. 1051-1056, 2009.

VIII. NOMENCLATURE

a	Slope (V/s).	A, B, C	Step Indices.
A_{hz}	Hertz Contact Surface (m²).	C_b	Bearing Capacitance (F).
C_{eq}	Equivalent Capacitance (F).	C_a	Stator Ground-Rotor Ground Airgap Capacitance (F).
C_{ins}	Insulation Capacitance (F).	C_{ws}	Stator Winding to Rotor Capacitance (F).
C_{eq}	Equivalent Capacitance (F).	C_{wr}	Rotor Winding to Rotor Capacitance (F).
C	Capacitance (F).	D_T	Track Diameter (m).
En_D	Discharge Energy (J).	E_{th_lub}	Lubricant Electric Strength (V/m).
f_D	Discharges Frequency (Hz).	f_i	Frequency i=1,2 (Hz).
I_b	Bearing Current (A).	I_{cm}	Common Mode Current (A).
J	Average Current Density (A/m²).	K_{metal}	Metal Coefficient.
K_{cur}	Curvature Coefficient.	K_r	Lubrication Coefficient.
L	Inductance (H).	T	Temperature (K).
$L_{e\_60\,hz}$	Electrical Lifetime @ 60 Hz (Hours).	L_{e_fD}	Electrical Lifetime @ Discharge Frequency (Hours).
L_T	Track Length (m).	p	Pair of Poles.
Q	Electric Charge (C).	R	Resistance (Ohm).
R_D	Discharge Resistance (Ohm).	r	Rotor Indice.
SVR_s	Stator Shaft Voltage Ratio.	s	Stator Indice.
SVR_r	Rotor Shaft Voltage Ratio.	t	Time (s).
t_{op}	Operational Time (s).	t_i	Time i=1,2 (s).
Th_{lub}	Lubricant Thickness (m).	Th_{re}	Eroded Thickness (m).
$V_{u,v,w}$	Phase to ground Voltage (V).	V_{DC}	DC Bus Voltage (V).
V_{cm}	Common Mode Voltage (V).	V_{sh}	Shaft Voltage (V).
V_b	Bearing Voltage (V).	V_{th}	Threshold Voltage (V).
Vol_{cr}	Discharge Crater Volume (m^3).	Vol_{er}	Eroded Volume (m^3).
V_i	Voltage i=1,2 (V).	W_{es}	Electric Stress (A/m²).
Z_0	Impedance (Ohm).	ζ	Damping Coefficient.
ε_0	Vacuum Permittivity (F/m).	$\varepsilon_{r,lub}$	Grease Relative Permittivity (F/m).
Ω	Rotor Pulsation (Rad/s).	Ω_{rs}	Rotor Slippage (Rad/s).
ω_{grid}	Grid Pulsation (Rad/s).	ω_n	Resonance pulsation (Rad/s.)
ω_{driv}	Drive Pulsation (Rad/s).	U, V, W	Phase indices.

AFM	Atomic Force Microscope.
CM	Common Modes.
DE	Driven End.
DFIG	Double fed Induction Generator.
DFE	Diode Front End.
EDM	Electric Discharge Mechanism.
DOL	Direct-On-Line.
IEGT	Injection Enhanced Gate Transistor.
IGBT	Insulated Gate Bipolar Transistor.
NDE	Non-Driven End.
NPC	Neutral Point Clamped.
Pk	Zero to Peak.
PWM	Pulse Width Modulation.
VSD	Variable Speed Drive.
VSI	Voltage Source Inverter.
th	Threshold.

IX. VITA

Lionel DURANTAY is graduated from the ENSEM of Nancy, France (Ecole Nationale Supérieure d’Electricité et de Mécanique) with an engineering degree in 1989 then passed PhD in 1993. As R&D Leader, he has developed innovative variable speed motors & generators solutions for Oil & Gas, Renewable and Marine businesses. He has authored or coauthored 40+ technical papers. He presently holds 15+ patents. He is currently Global Product & Technology Leader in GE Power Conversion.

Kum Kang HUH is graduated from the Wisconsin-Madison University, US, with an electrical Engineering PhD in 2008. He works for 8 years as Senior Electrical Engineer for Mando Corporation in Korea. He is currently Principal Engineer, specialist in Power Systems and Electric Machines in GE Global Research Center.

Christophe GROSSELIN is graduated from the Henri Loritz Lycée in 1987 and the ENIM of Metz, France (Ecole Nationale d’Ingénieurs de Metz) in 2002 with an engineering degree. He led several positions as product manager, customer support, engineering manager in France and in China. He presently holds 4+ patents. He is currently Global Engineering Innovation & Platform Leader in GE Power Conversion.

Gaëtan MICLO is graduated from the Henri Poincaré University of Lorraine with an electromechanical master’s degree in 2008. He joined after the Converteam electric machines factory in Champigneulles where he led several positions as Manufacturing & Customer Service manager. He is currently Senior Project Manager for Renewable and Marine Programs in GE Power Conversion.

Transient Recovery Voltage Considerations when Switching a Large Captive Load with a Medium Voltage Circuit Breaker

Paper No. PCIC Europe EUR22_16

Hamad Alsharhan
Saudi Arabian Oil Company (Saudi Aramco)
Dhahran, Saudi Arabia
hamad.sharhan@aramco.com

Basel Ishwait
Saudi Arabian Oil Company (Saudi Aramco)
Dhahran, Saudi Arabia
basel.ishwait@aramco.com

Abstract **-** Circuit breakers can undergo significant stress and fail to interrupt high currents when the power system has transient recovery voltage (TRV) characteristics that exceed the rating of the circuit breaker. This paper presents a practical case of flashover incident and failure of an indoor 34.5 kV switchgear at an industrial plant substation

Index terms- Circuit Breaker, TRV, Flashover, Switchgear, Substation

I. INTRODUCTION

Transient recovery voltage (TRV) is defined as the voltage across the opening poles of a circuit breaker immediately after current interruption [1] [2] [3]. Fig. 1 is a graphical representation of this definition. The shape of TRV is defined by the connected lumped and distributed inductive and capacitive parameters of the system. For successful interruption, the breakdown voltage of the interrupting medium must always exceed the recovery voltage [4]. If the TRV peak value is above the breaker rating, the increasing TRV to the gap will re-strike the arc and break down the interrupting medium.

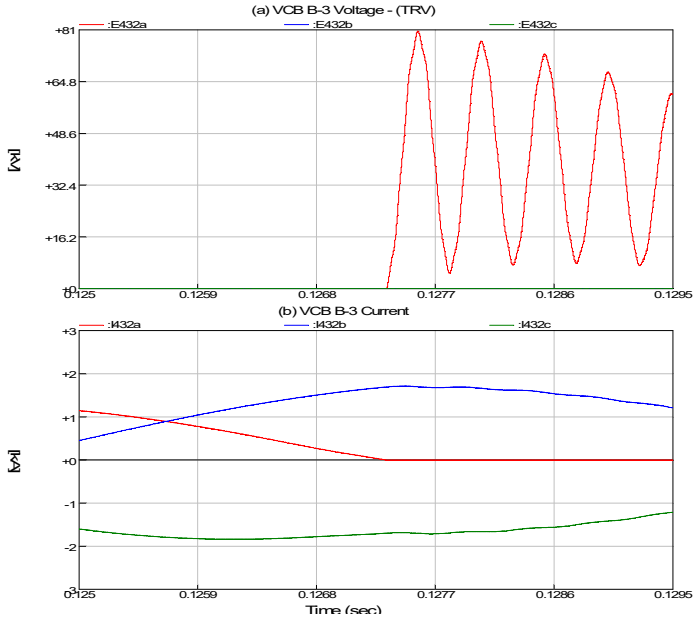

Fig. 1. Definition of TRV

II. CIRCUIT BREAKER EVALUATION AND SELECTION

The most severe TRV from an amplitude point of view follows the interruption of the first phase to clear an ungrounded three phase fault. The shift in system neutral results in a high amplitude TRV. It is a basis for rating a circuit breakers TRV capability [6]. The procedure for TRV verification and the TRV capabilities are outlined in the IEEE standard C37.011-1994. For breakers of 72.5kV and below, the TRV capability envelope is defined in (1) by a one-cosine curve as follows:

$$e_2 = \frac{E_2}{2}\left[1 - \cos\left(\pi t/T_2\right)\right] \quad (1)$$

Where E2 is the crest value and the T2 is the time reaching from zero to crest value. For different interruption currents, the breaker TRV capability envelopes have different crest values and different times to reach the crest. Voltage E2 multiplying factor K1 and time T2 multiplying factor Kt are used to calculate fraction of rated fault current interrupting capability. Both K1 and Kt are functions of the interrupting current [IEEE ANSI C37.011-1994], as shown in Fig. 2

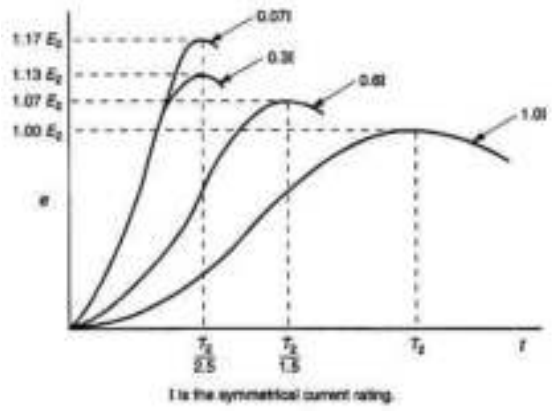

Fig. 2. TRV Capability Envelopes for Breakers Rated ≤ 72.5 kV [6]

The rate of rise of the recovery voltage (RRRV) is a method to quantify TRV and is an important factor in switchgear application [3]. It is a measure of circuit severity from a switchgear point of view. The mean RRRV is defined by (2) peak TRV over the time of reaching it [6], or

$$\mathrm{RRRV} = \frac{E_2}{T_2} \quad (2)$$

III. BACKGROUND

A flashover incident has occurred in a 34.5 kV substation switchgear, feeding 25 MVA captive transformer, which in turn feeds a 15000 HP synchronous motor driving seawater injection pump serving hydrocarbon facility. The incident occurred during the motor direct online (DOL) startup and led to 34.5 kV vacuum circuit breaker failure. The failed breaker is an ANSI C37.011

compliant general purpose, vacuum circuit breaker (VCB) with the relevant ratings as shown in Table I.

TABLE I

NAME PLATE AND ANSI CAPABILITY RATINGS OF THE FAILED CIRCUIT BREAKER [7]

Rating	Value
Rated Voltage	34.5 kV
Rated Continuous Current	1200 A
Interrupting Short Circuit Current	31.5 kA
Rated TRV Peak (E2)	71 kV
Rated Time to TRV Peak (T2)	125 µs

Fig. 3 shows a one-line diagram of the system, with the failed VCB highlighted by a red dashed box (B-3).

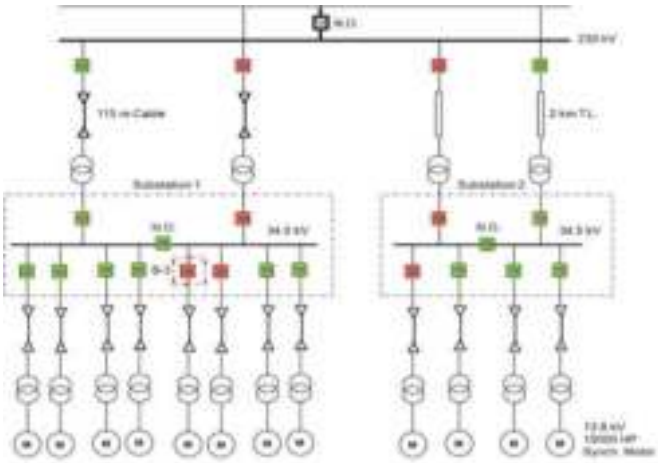

Fig. 3. Single Line Diagram (case 1a)

The sequence of events, which led to the failure of VCB were as follows:

- By an operator error the 15000 HP motor was started, by closing feeder VCB.
- The plant distributed control system (DCS) correctly issued a trip signal to VCB, after approximately 2.5 cycles (. ~ 42 ms at 60 Hz).
- The VCB responded to the DCS trip signal, and attempted to interrupt the combined inrush current drawn by the captive transformer and the motor.
- The VCB flashover and failure occurred.

These events were captured by a digital fault recorder (DFR) installed at the substation incomer breaker, and the captured voltage and current waveforms are depicted in Fig. 4. The voltage waveforms in Fig. 1 show two significant transients during the closing (1st transient) and opening (2nd transient) operations of VCB. The magnitude of the 2nd voltage transient exceeded the VCB TRV rating. The system TRV response computed by this study exceeds the ANSI/IEEE C37.011 TRV capability limits of the VCB; superimposed on the same figure (red and blue curves).

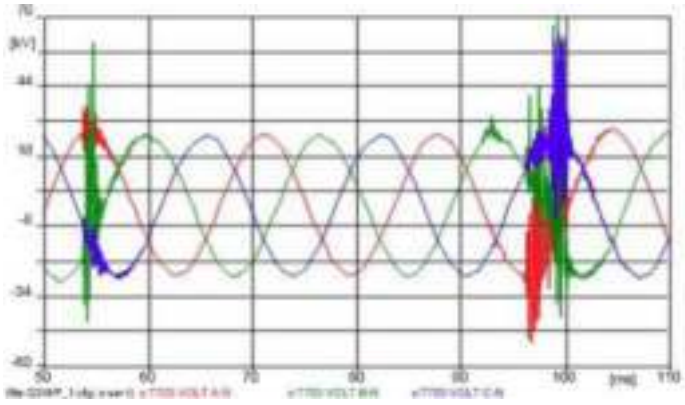

(a)

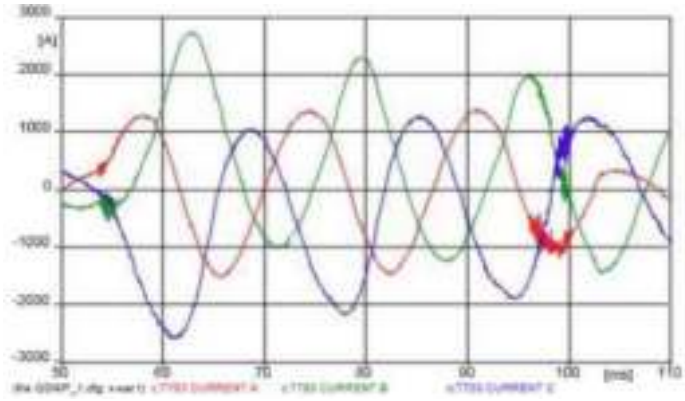

(b)

Fig. 4. Substation Incomer DFR Waveforms Capture: (a) Voltage, and (b) Current

IV. DEVELOPMENT AND IMPLEMENTATION DETAILS

A. System Reduction for TRV Worst Case Scenario

Consider the worst case scenario for system TRV computation, the studied system has been reduced to the radial system shown in Fig. 5

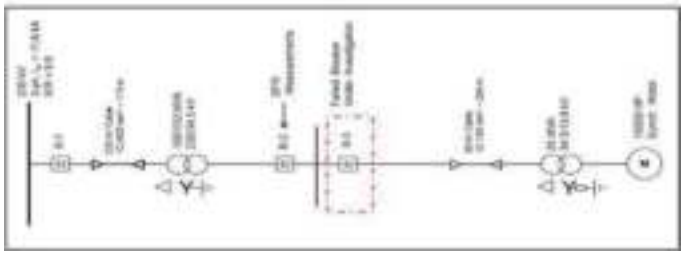

Fig. 5. Single Line Diagram (Case 1b)

This simple assumption is judged critical for the following reasons:

- The computed system TRV across the opening contacts of VCB B3; during the interruption of the inrush current of the combined captive transformer and motor loads; shall not be influenced by the damping effects of the running load in the rest of plant.
- During VCB failure incident, only 3 out of 12 plant motors were running.

B. 230 kV Utility Model

The 230 kV feeding network has been represented as a Thevenin equivalent voltage source in series with positive sequence impedance; computed from the utility 3-phase fault level and X/R ratio.

C. Cable and Transmission Line Models

The 230 kV cable, 230kV transmission line, and the 35 kV cable were modeled by a frequency dependent model (J-martie) [8].

D. Transformer Models

The incoming 100 MVA, 230/34.5 kV transformer was modeled as an ideal transformer with no saturation. This assumption is reasonable because all cases studied are overly concerned about switching maneuvers of VCB B3, and assume the lightly loaded incomer transformer to be continuously energized. A saturation transformer model has been implemented for the 25 MVA 34.5/13.8 kV captive transformers. The saturation parameters of the transformer were tuned to produce an inrush current which matches the DFR captured current waveform.

E. Synchronous Motor Model

During starting condition, a synchronous motor can be modeled by induction motor model. The model implemented in is a simple RL load estimated by the locked rotor ratings of the motor. The model was validated by comparing the model inrush current to the DFR captured current during the actual motor start-up. Surge capacitors of 0.25 µF installed at the motor terminals have been modeled.

F. Circuit Breaker Model

All circuit breakers shown in Fig. 3 and 5 were modeled by an ideal breaker/switch model, which can close at any simulation time instant, and open only upon current extinction. This model is adequate for the objective of system TRV computation. Breaker B1 and B2 shall remain closed for the entire simulation run of all cases studied, whereas B3 shall follow open-close-open sequence in all the motor starting cases; and a closed-open sequence for fault analysis cases.

G. Equipment Stray Capacitance

As reported in [1] [3], TRV analysis requires detailed modeling of system inductances and capacitances including equipment stray capacitance. Estimates for the different substation equipment were obtained from [4]. Transformers stray capacitance model was taken from [6].

V. 3-PHASE DETAILED TRV SIMULATION CASES IMPLEMENTATION

The analysis evaluation was carried out using 3-phase modeling simulation. Several scenarios were considered to decrease RRRV ($\frac{E_2}{T_2}$) to bring the TRV envelop within the CB capabilities. The simulation cases considered in this study are shown in Table II below.

TABLE II.

SIMULATION OF MOTOR STARTING (MS) CASES

Case No.	Case Description	Case Purpose
1a	Existing System TRV seen by Breaker B3 in S/S 1, while interrupting combined MS inrush current.	To simulate the system TRV behavior during the flashover incident.
1b	Reduced System TRV seen by Breaker B3 in S/S 1, while interrupting combined MS inrush current.	To validate the reduced system TRV behavior against that of case 1a.
2	System TRV seen by Breaker B3 in S/S 1, while interrupting combined Motor Starting (MS) inrush current; with RC-snubber (60 Ω, 0.5 µF), installed at load side of B3	To examine the impact of a non-typical RC snubber on the system TRV.
3	System TRV seen by Breaker B3 in S/S 1, while interrupting combined motor starting (MS) inrush current; with RC-snubber (90 Ω, 1.0 µF), installed at load side of B3.	To examine the impact of a non-typical RC snubber on the system TRV.
4	System TRV seen by Breaker B3 in S/S 1, while interrupting combined MS inrush current; with MOV arrester installed at load side of B3	To examine the impact of a typical manufacturer MOV arrester on the system TRV.

VI. SUMMARY OF RESULTS AND OBSERVATIONS

Tables III and IV below summarize the study's figures and results

TABLE III.

CROSS REFERENCE OF SIMULATION CASES AND FIGURES

Case No.	Simulation Figures
1a	Figures 6 & 7
1b	Figures 8 & 9
2	Figures 10 through 12
3	Figures 10, 13, 14
4	Figures 15 & 16

TABLE IV.

SYSTEM TRV BEHAVIOR DURING MOTOR STARTING CASES

Case No.	1a	1b	2	3	4
Computed E2 (kV)	80	81	76	68	64
Capability E2 (kV)	78	78	78	78	78
Computed T2 (µs)	241	239	646	846	170
Capability T2 (µs)	50	50	50	50	50
Computed RRRV (kV/µs)	0.35	0.34	012	0.08	0.38
Capability RRRV (kV/µs)	1.56	1.56	1.56	1.56	1.56

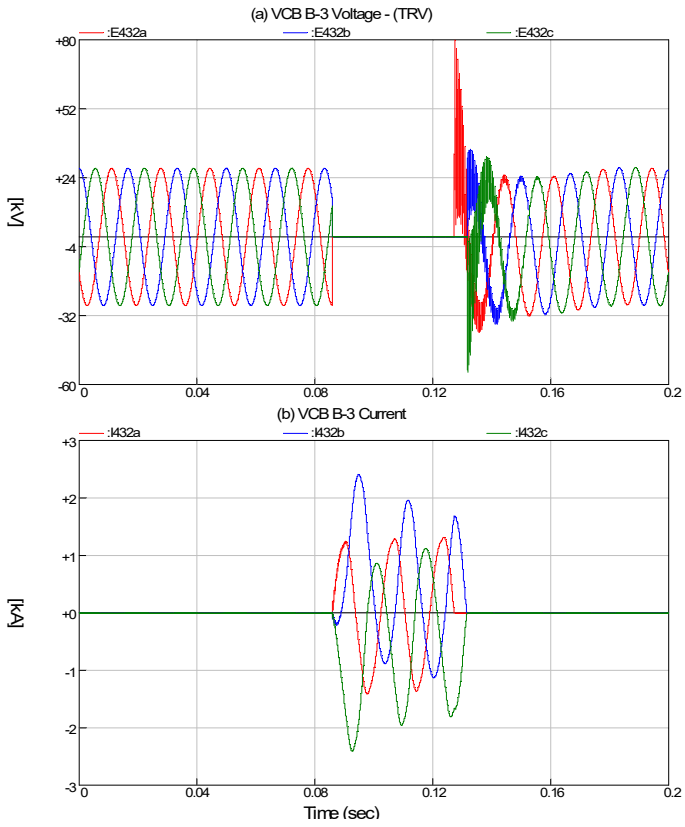

Fig. 6. Case 1a - TRV Simulation

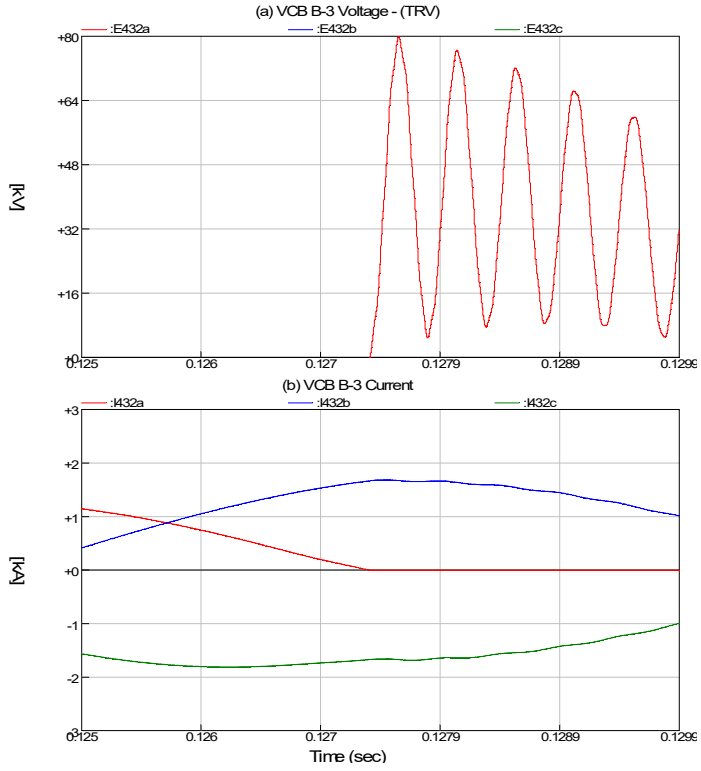

Fig. 7. Case 1a - TRV Simulation (Zoom on Figure 6)

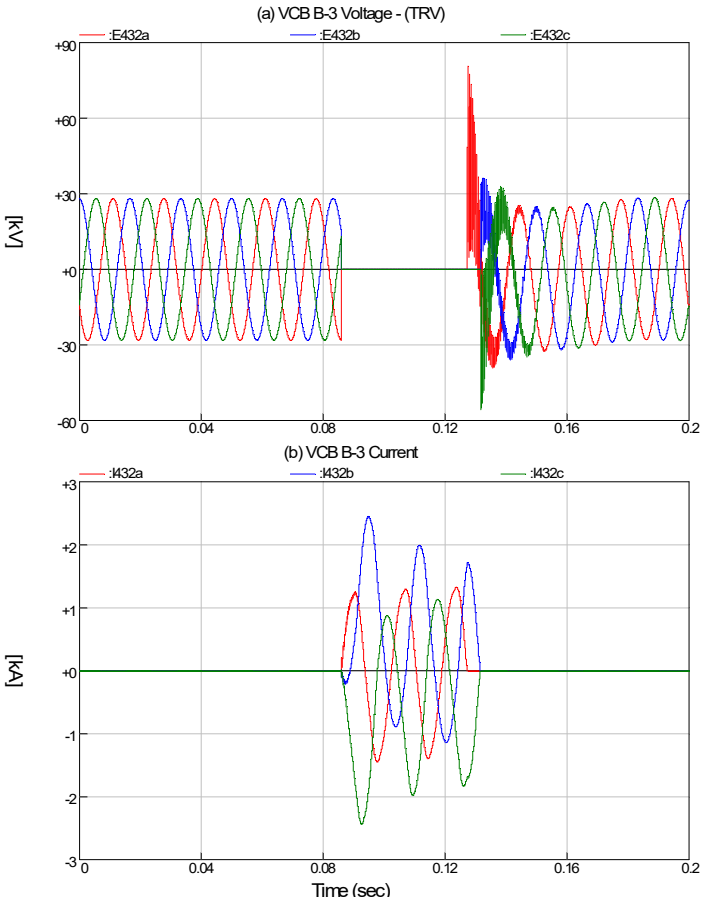

Fig. 8. Case 1b - TRV Simulation

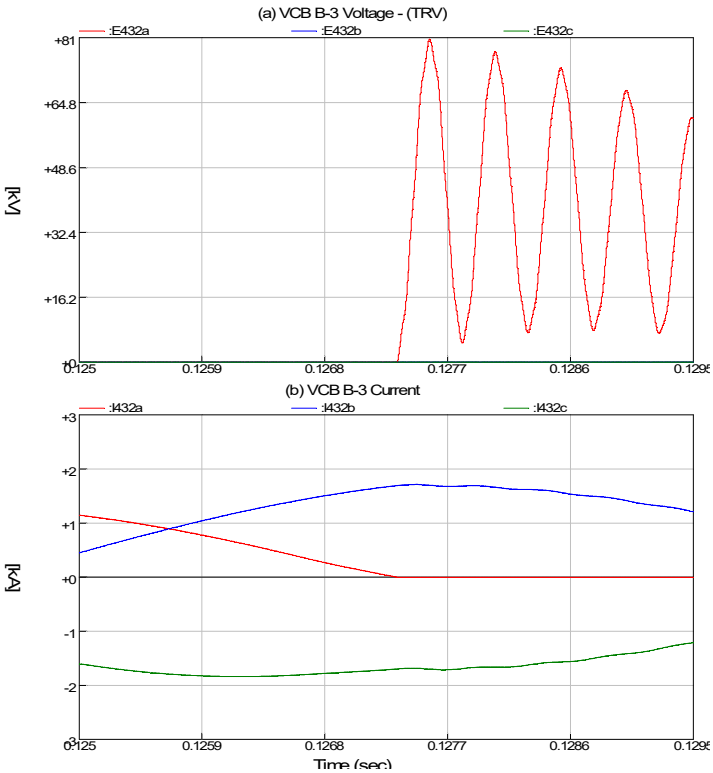

Fig. 9. Case 1b - TRV Simulation (Zoom on Figure 8)

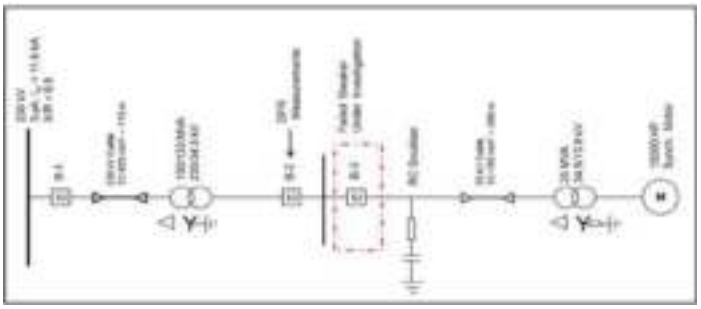

Fig. 10. Single Line Diagram of Case 2 and 3

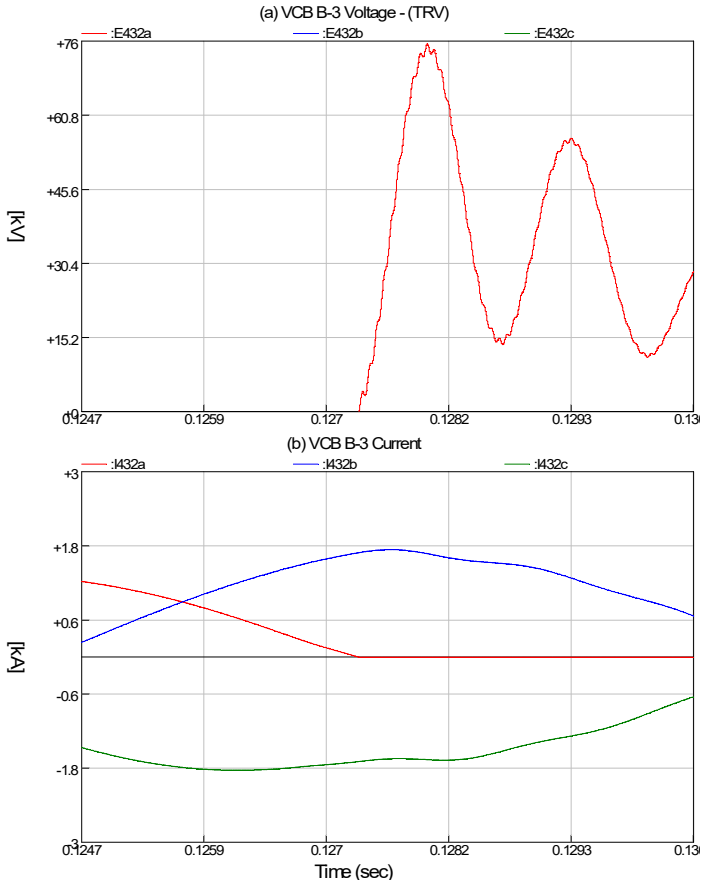

Fig. 11. Case 2 - TRV Simulation with RC-snubber (60 Ω, 0.5 μF)

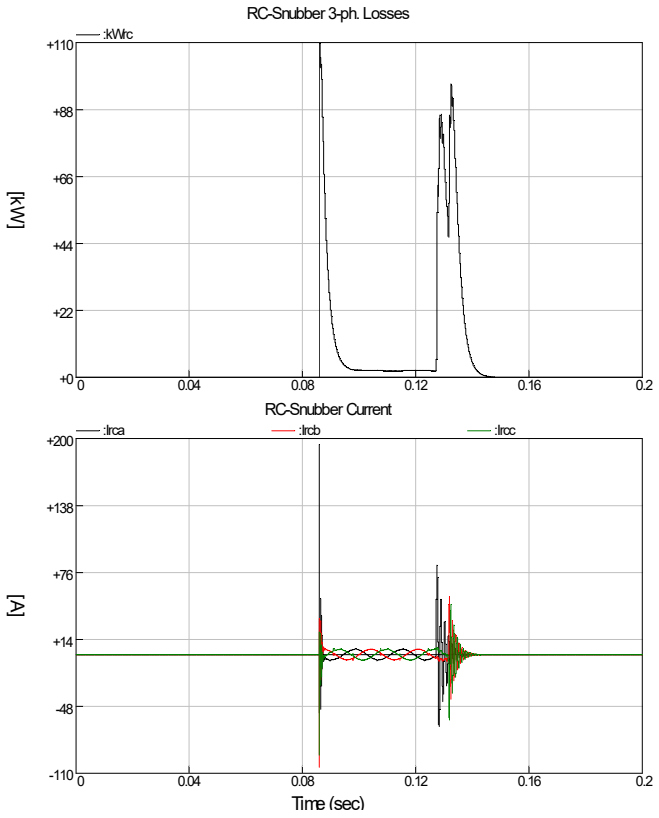

Fig. 12. Case 2 - RC-snubber (60 Ω, 0.5 μF) Losses and Current

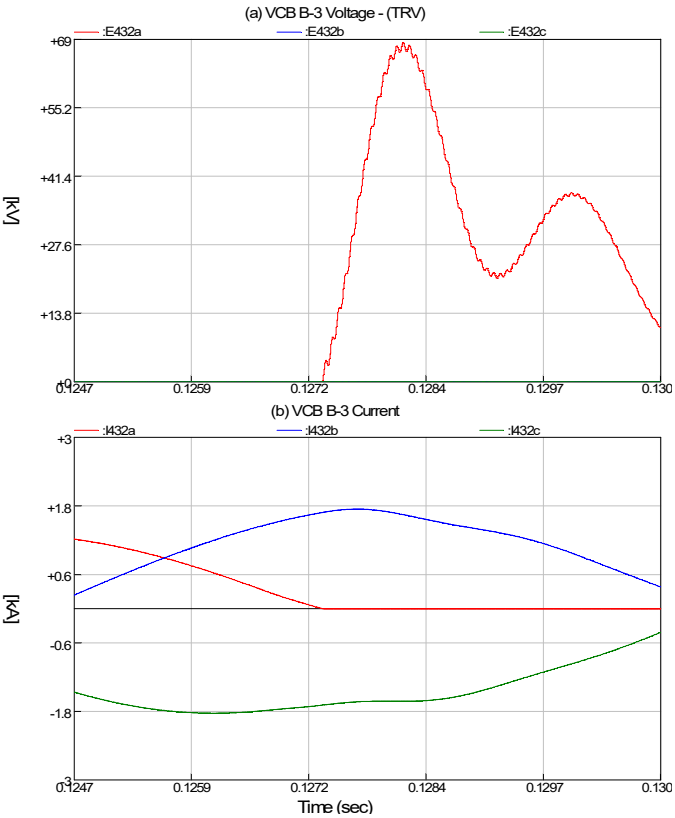

Fig. 13. Case 3 - TRV Simulation with RC-snubber (90 Ω, 1.0 μF)

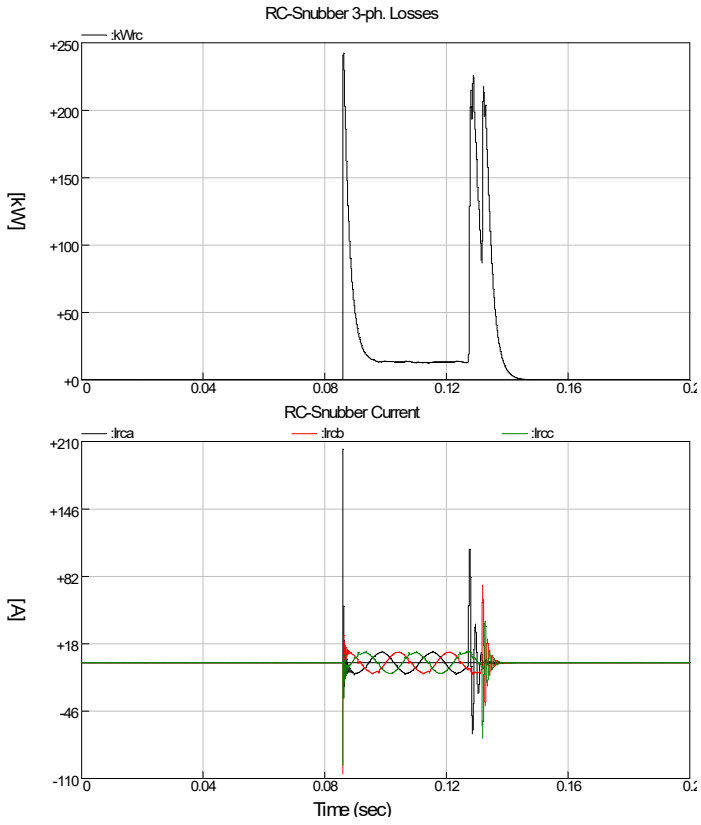

Fig. 14. Case 3 - RC-snubber (90 Ω, 1.0 μF) Losses and Current

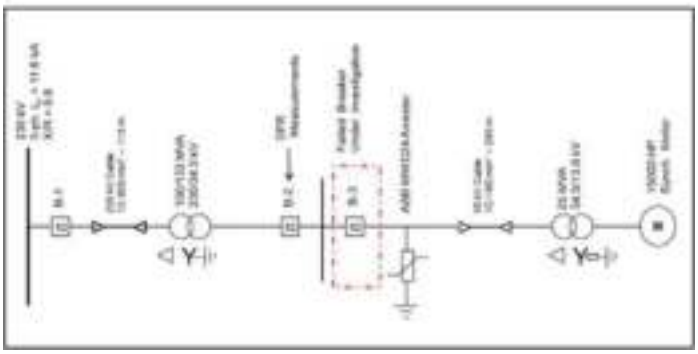

Fig. 15. Single Line Diagram of Case 4

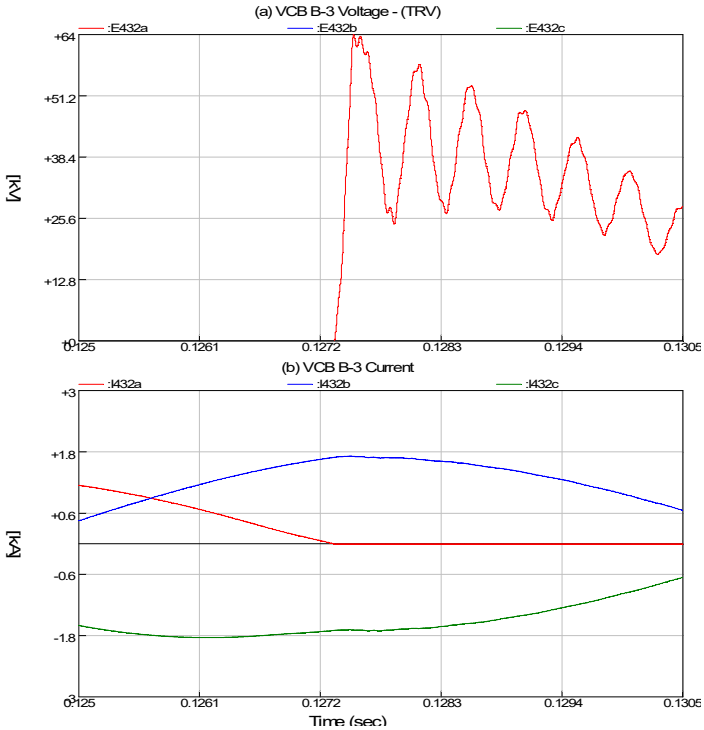

Fig. 16. Case 4- TRV Simulation with MOV Arrester

The main observations learned from the simulation cases are as follows

- The reduced model of case 1b validates the results obtained by case 1a and the assumptions made.
- The computed TRV of Cases 1a, and 1b exceed the capability of the 34.5 kV VCB feeding the captive transformer and motor [7].
- Case 2 resulted in a marginally acceptable TRV magnitude
- The TRV magnitude of Cases 3 and 4 are within VCB capability.
- All cases have acceptable RRRV.
- Although case 3 with RC snubber (90 Ω, 1.0 μF) has shown reasonable TRV behavior, this alternative has been eliminated because of the significant transient and steady state 3-phase losses of the circuit as shown in Fig. 14. Additionally, the values of RC circuit are non-typical, and would result in a physical size larger than the captive transformer. The plant available space cannot accommodate such size.
- The most viable alternative to solve the 34.5 kV VCB flashovers due to TRV concerns is the use of MOV arresters such as arrester simulated in case 4. The arrester action during voltage transients is evident from Fig. 16. Both figures indicate excellent voltage chopping behavior with no concerns on thermal run-away as the maximum computed cumulative energy (0.59 kJ) is way below the rating of the arrester (5 kJ).

VII. CONCLUSION

The interruption of high inrush currents from high power inductive loads such as captive transformer and motor combination can result in a major TRV stresses on the switching devices. This phenomena can lead to detrimental consequences for MV/HV substation operators, as demonstrated by this study as well as other publications [2][3]. The design engineers should consider the TRV phenomena and use definite type CB in leu of general-purpose CB to ensure proper protection. This study has achieved its terminal objectives by validating the analysis.

VIII. REFERENCES

[1] A. Greenwood, Electrical Transients in Power System. New York: Wiley, 1994.

[2] D.L. Swindler, P. Schwartz, P.S. Hamer, and S.R. Lambert, "Transient recovery voltage considerations in the application of medium-voltage circuit breakers," Industry Applications, IEEE Transactions on, vol. 33, no. 2, pp.383-388, Mar/Apr 1997

[3] X. Wang, et al. "Transient Recovery Voltage Investigation in the Application of 15 kV Circuit Breaker Failure," IPST-05-224, IPST05 Conference, Montreal, Canada, June 2005.

[4] IEEE Application Guide for Transient Recovery Voltage for AC High-Voltage Circuit Breakers, IEEE Std. C37.011-2005.

[5] IEEE Standard for AC High-Voltage Circuit Breakers Rated on a Symmetrical Current Basis – Preferred Ratings and Related Required Capabilities for Voltages above 1000 V, IEEE Std. C37.06-2009.

[6] IEEE Standard Rating Structure for AC High-Voltage Circuit Breakers, IEEE Std. C37.04-1999-R2006.

[7] "Instructions for the use, operation and maintenance of VCP®-WG/VCPWRG 75kA vacuum circuit breakers," I.B. 3A74792H08, Cutler-Hammer

[8] L. Marti, "Simulation of transients in underground cables with frequency-dependent modal transformation matrices." IEEE Transactions in Power Delivery, Volume 3, No. 3, July 1988, pp. 1099 -1110.

[9] J. Marti, "Accurate Modeling of Frequency Dependent Transmission Lines in Electromagnetic Transient Simulations," IEEE Trans. on Power Apparatus and Systems, vol. PAS-101, pp. 147-157, 1982.

[10] Martin Bruha, Marcel Visser, Joseph von Sebo, Esa Virtanen, Pasi Tallinen, "Protection of VSD Transformers", PCIC Europe Conference Record, 2017

IX. VITA

Hamad Al-Sharhan, FE, PE (NCEES, 2013) is an Electrical Engineer with Saudi Aramco- Consulting Services Department. Working on providing technical support and consultancy to various Saudi Aramco oil and gas plant operations. He is a licensed Professional Engineer, and received a MSEE from Michigan Technological University, Michigan, USA in 2013 and a BSEE from King Fahad University of Petroleum and Minerals, Saudi Arabia in 2008

Basel A. Ishwait, PE (IEEE M '1986) is a Senior Electrical Consultant with Saudi Aramco. In 1986, after graduating from University of Memphis, joined Engineering Design group Inc. (EDG) in Tulsa Oklahoma and for more than 15 years was responsible for the detail design of turnkey power generation plant, detail design of power distribution, and data acquisition projects serving multiple industries. In 2000, joined Saudi Aramco's Consulting Services Department as an Electrical consultant providing technical support for multiple MEGA project. He is a licensed PE and received MSc, Electrical power Engineering, Michigan Technological University (MTU), Houghton, Michigan.

CONTENTS OF INSTRUCTIONS REGARDING EX EQUIPMENT: POTENTIAL ENHANCEMENT OF INFORMATION TECHNICAL ANSWERS FROM STANDARDS

Paper No. PCIC Europe EUR22_17

Michal GÓRNY
EXKONTAKT
KATOWICE
Poland

Xavier LEFEBVRE
EXPREVENTION
CHANTILLY
France

Abstract – Recent surveys have shown a lack of consistency for the contents of instructions regarding Ex equipment. As a major contribution for safety regarding prevention and protection against explosion, the manufacturer shall provide to the user written instructions that include the necessary information for safe use, installation, repair, maintenance and/or overhaul of the equipment concerned, etc.

In addition, regarding the intended use, considerations are suggested to enhance contents through

- equipment category and/or EPL defined by the manufacturer (normal use and misuse);
- role of certification agencies regarding assessment of instructions;
- instructions as inputs regarding explosion risk assessment consideration, like hazardous area assessment (fuel dispersion, volume, hazard probability) due to the design of the considered equipment,
- inputs from specific standards available to provide general principles and detailed requirements for the design and formulation of information for use.

Index Terms - Ex equipment, instructions, standards.

INTRODUCTION

An essential safety aim of European directives and international rules is to select appropriate equipment for the intended use in view to improve the safety and health protection of workers potentially at risk from explosive atmospheres and of course at workplaces as a general requirement.

Additional requirements are detailed in ATEX 2014/34/EU directive [1] as legal regulation – instruction manual shall describe without any doubt in which workplace where an identified presence of explosive atmosphere is present (what Zone and flammable/combustible substance parameters) the equipment is intended for use.

The instruction manual is also useful for risk assessment. Some complex Ex solutions contain or create a hazardous area, then such information also should be indicated in instruction manual and can be also useful for the application of the Machinery directive 2006/42/EC [2].

Verification of the equipment level of safety only by reading the Ex marking is insufficient and requires the installer to consider all technical details as part of instruction manual.

Required documents due to certification rules have to be considered.

Equipment is defined by categories (1, 2 or 3 according ATEX directives) and/or EPL (according IEC/EN Ex standards) according to the level of protection (very high, high and normal) required for the intended hazardous area or zone. Relationships between EPL and zone are indicated into IEC/EN60079-14 [4], relationship between zone / EPL / Category is indicated in IEC EN 60079-0 [5].

Zone	Equipment protection **levels (EPLs)**	**Categories**
0	'Ga'	1G
1	'Ga' or 'Gb'	1G or 2G
2	'Ga' or 'Gb' or 'Gc'	1G or 2G or 3G
20	'Da'	1D
21	'Da' or 'Db'	1D or 2D
22	'Da' or 'Db' or 'Dc'	1D or 2D or 3D

Fig.1: Relationship between zone and EPL/category

As fixed by IECEX Scheme [3], documentation to be provided by the manufacturer of Ex equipment covers the life cycle of the product (installation and use instructions, service information, overhaul and repair data and test data for some items).

The manufacturer is responsible for providing the documentation only. The user of a product is responsible for following the manufacturer's instructions and for maintaining the product in compliance with Standards and manufacturer's instructions.

In Europe, under the ATEX Directive 2014/34/UE [1], Ex equipment is only allowed to be put into market if it is supplemented with three items:

- A copy of exhaustive and valid manufacturer's EU declaration of conformity in accordance with each applicable EU regulation,
- a legible and durable marking including suffix X or not for specific conditions for use and warning labels of any and
- a suitable instructions manual.

Electrical equipment and non-electrical equipment shall be installed and used within their ratings for power, voltage, current, frequency, duty type (electrical), temperature, pressure, flowrate (non-electrical) and some other characteristics in view to ensure the safety of the installation.

Instructions and safety information need to be provided, whether the equipment is intended for distributors, OEM partners and other end-users. This should include all the necessary information for the safe use of the product, to

enable the consumer to assemble, install, operate, store, maintain, and dispose of the equipment.

Instructions for operation should include information for restriction of use, suitable installation, need for personal protective equipment, maintenance and cleaning or repair and recycling. It is a duty for the manufacturer to determine the relevant information which should be included in the instructions and safety information for a particular equipment.

Due to EU regulations, manufacturers have to look beyond what they consider the intended use of a product and place themselves in the position of the common user of a particular product and envisage in what way they would reasonably consider using the product.

I. ACTUAL TECHNICAL REVIEW

A. Contents of Instruction manuals: preliminary overview

Instruction Manual requirements indicated in Ex standards (IEC, ISO) as technical and organizational measures able to offer compliance with EU regulations.

Ex equipment is subject to specific requirements. Manufacturers make every effort to ensure that, already at the design stage, the use of appropriate technical solutions ensuring protection against the consequences of potential ignition. A large part of safety is due to proper installation like use of fasteners, protection of flamepath, selection of cable and cable glands.

A safe installation is achieved by the equipment construction requirements defined by Ex standards and respect of installation requirements as defined by instructions and IEC/EN 60079-14 [4].

The contents of instructions for this Ex equipment are essential and are generally assessed during the certification assessment. Therefore the user is obliged to use the Ex equipment in accordance with detailed instructions issued by manufacturer in view to maintain the level of protection.

In order to facilitate the selection of the Ex equipment, to ensure proper installation, maintenance and early detection of possible irregularities, which sometimes necessitate the repair, the manufacturer provides the Ex equipment with a written instruction manual.

It seems understandable what information should be included in the instruction manual, nevertheless the standards for the Ex equipment specify what information should be included in the instruction manual.

B. Contents of Instruction manuals: Requirements in IEC and ISO standards

The General Standard for Electrical Ex Equipment EN IEC 60079-0 [5]. deals with this subject in clause 30, which specifies the minimum requirements for instructions.

The instructions prepared by the manufacturer shall include the following particulars as a minimum:

- a recapitulation of the information with which the equipment is marked, except for the serial number, together with any appropriate additional information to facilitate maintenance (for example, address of the importer, repairer, etc.); that is, the marking of the device should be clearly explained in the user manual and contact details should be provided to assist in the event of a repair.
- instructions for safety addressing the following areas:
  - on-site assembling;
    - any specialized installation information for the user, such as a specific sequence of assembling;
    - information about the mechanical assembling such as pipe connections;
  - installation and erection;
    - information, other than the general requirements given in IEC EN 60079-14 [4];
    - information about bonding, shield earthing or overvoltage protection;
    - guidance for the selection of flameproof entry devices for termination compartments […]
  - adjustment and parameter setting;
    - information about heating devices;
  - putting into service – of the equipment / of the whole installation.
    - information about verifications / tests prior to the (first) use of the equipment as required by the Type of Protection(s) – together with the sequence of conducting such verifications / tests;
    - detailed information about any special installation requirements for the Type of Protection(s) employed
  - use and setting up;
    - details which allow an informed decision to be made as to whether the equipment can be used safely in the intended area under the expected operating conditions;
    - ratings such as electrical values, ambient temperatures and pressures, maximum surface temperatures and other limit values related to a designated use;
    - information for the user, not just giving parameters, related to the need of special overload protecting devices for increased safety “e”’ motors or special requirements related to electrostatics.
  - maintenance;
    - information, other than the general requirements given in IEC EN 60079-17 [6];
    - information such as cleaning, oil level check or recalibration requirements.
    - requirements for the maintenance of the explosion protection;
    - information about troubleshooting.
  - repair;
    - information, other than the general requirements given in IEC EN 60079-19 [7];
    - information related to the fitting or removal of parts / components;
    - information about spare parts;
    - requirements for a documentation of such repairs;
    - information about needed verifications / tests for the restarting of the equipment.
  - taking out of service and dismantling;
    - information about the securing of mechanical parts to prevent a restart or about electrical disconnecting.
- where applicable, Specific Conditions of Use for equipment (from certificate or other) - this information should not be hidden in the text and should be placed within the instructions in a highlighted way, often as a special chapter;
- for Ex Components, a Schedule of Limitations is used in place of Specific Conditions (also from certificate or

other);
- where applicable, any additional information for use, including information related to possible misuse, which experience has shown might occur;
- where necessary, training instructions for a safe use;
- where necessary, the essential characteristics of tools which may be used with the equipment; such as a special screwdriver for trimming;
- a list of the standards, including the issue date, with which the equipment is declared to comply. The list of standards is not required if the certificate indicates the standards covered by the certificate and their issue dates, even if the certificate is not included as part of the instructions.

It is worth noting that the standards for inspections and repairs (IEC EN 60079-17 [6] and IEC EN 60079-19 [7]) provide detailed requirements and apply unless the manufacturer specifies otherwise. So it can be useful for the manufacturer to provide additional detailed inspection or repair requirements.

For example, if a flameproof device does not require periodic verification of the flameproof joints, the manufacturer has the option of specifying this in the instruction manual. Similarly, the manufacturer may specify a period between inspections of the device longer than 3 years. This may be advantageous for the end-user in reducing the burden of inspection.

The responsibility for such decisions is on the manufacturer side.

In the case of equipment certification (e.g. according to the IECEx certification scheme [3]), such records are verified along with the rest of the operating instructions by the ExCB certification body.

Similarly, for non-electrical equipment, the relevant requirements are given in clause 10 of standard EN ISO 80079-36 [8].

The documentation prepared shall include instructions which provide the following particulars as a minimum:
- a recapitulation of the information with which the equipment is marked, except for the serial number, together with any appropriate additional information to facilitate maintenance (for example, address of the importer, repairer, etc.);
- instructions for safety, i.e.:
  - putting into service;
  - use;
  - assembling and dismantling;
  - maintenance;
  - installation;
  - adjustment;
  - where necessary, training instructions;
- details which allow a decision to be made as to whether the equipment can be used safely in the intended area under the expected operating conditions;
- relevant parameters, maximum surface temperatures and other limit values;
- where applicable, Specific Conditions of Use including remaining hazards identified in the ignition hazard assessment report that require additional protective means by the installers or users;
- where applicable, any additional Specific Conditions of Use, including particulars of possible misuse, which experience has shown might occur;
- where necessary, the essential characteristics of tools which may be fitted to the equipment;
- a list of the standards, including the issue date, with which the equipment is declared to comply;
- a summary of the relevant ignition hazards identified, and the protective means implemented.

Unlike electrical equipment, the manufacturer and user of non-electrical equipment do not find support in standards for maintenance or repair - such standards are in the development phase, so the manufacturer should provide details of these activities.

In the case of non-electrical equipment, most of the information is derived from the ignition hazard assessment - hence the importance of this procedure.

C. Contents of Instruction manuals: Requirements in EN standards

European standards for Ex equipment under the Frankfurt and Vienna agreements are developed jointly with the IEC and ISO standards (they are the same standards). In the scope not included in ISO or IEC standards, e.g. protective systems, the requirements are included in additional standards.

A European manufacturer can find additional information in the standard EN 1127-1 [9]:

The following information, as appropriate, shall be provided:

a) specific parameters related to explosion protection; this can include:
   1) maximum surface temperatures, pressures, etc.;
   2) protection against mechanical hazards;
   3) ignition prevention;
   4) prevention and/or limitation of dust accumulation;

b) protective systems; this can include:
   1) temperature monitoring;
   2) vibration monitoring;
   3) spark detection and extinguishing systems;
   4) inerting systems;
   5) explosion venting systems;
   6) explosion suppression systems;
   7) process isolation systems;
   8) vent systems for overpressures generated from processes other than explosion;
   9) fire detection and fighting systems;
   10) explosion isolation systems;
   11) emergency shut-down systems;
   12) explosion resistant design;

c) specific requirements to ensure safe operation; this can include:
   1) appropriate accessories.(spare parts, gaskets.;)
   2) use with other equipment, protective systems and components.

Information for commissioning, maintenance and repair to prevent explosion.

Particular attention shall be paid to provide the following:
- instructions covering normal operation including start-up and shut-down;
- instructions covering systematic maintenance and repair including safe opening of equipment, protective systems and components;
- instructions with regard to required cleaning, including dust removal and safe working processes;
- instructions covering fault identification and actions

required;
- instructions covering the testing of equipment, safety systems and components, also after explosions;
- information on risks requiring action, e.g. information shall be supplied about the possible existence of explosive atmosphere identified as part of the risk assessment to avoid that the operator or other person causes an ignition source.

EN 1127-1 [9]: also draws attention to Qualifications and training: Information on required qualifications and training shall be supplied to enable the user to select qualified staff for the tasks where explosive atmospheres can occur.

D. Contents of Instruction manuals: Requirements in ATEX directive

The requirements for the instruction manual are even more precisely specified in Directive 2014/34/EU (ATEX) [1], which in the essential requirements (point 1.0.6) specifies that:

a) All equipment and protective systems must be accompanied by instructions, including at least the following particulars:
- a recapitulation of the information with which the equipment or protective system is marked, except for the batch or serial number, together with any appropriate additional information to facilitate maintenance (e.g. address of the repairer, etc.);
  - instructions for safe:
  - putting into service,
  - use,
  - assembling and dismantling,
  - maintenance (servicing and emergency repair),
  - installation,
  - adjustment.
  - where necessary, an indication of the danger areas in front of pressure-relief devices.
- where necessary, training instructions.
- details which allow a decision to be taken beyond any doubt as to whether an item of equipment in a specific category or a protective system can be used safely in the intended area under the expected operating conditions;
- electrical and pressure parameters, maximum surface temperatures and other limit values;
- where necessary, special conditions of use, including particulars of possible misuse which experience has shown might occur.
- where necessary, the essential characteristics of tools which may be fitted to the equipment or protective system.

b) The instructions must contain the drawings and diagrams necessary for the putting into service, maintenance, inspection, checking of correct operation and, where appropriate, repair of the equipment or protective system, together with all useful instructions, in particular with regard to safety.

c) Literature describing the equipment or protective system must not contradict the instructions with regard to safety aspects.

Instructions and safety information, as well as any labelling, shall be clear, understandable and intelligible

The user takes into account the instructions issued by the manufacturer to carry out repair, maintenance and/or overhaul on the basis of the requirements of the applicable EU directives (such as 2009/104/EC [10]- Use of work equipment by workers at work and directive 1999/92/EC [11] – Safety of workers potentially at risk from explosive atmospheres) and of relevant specific national legislation that regulates the repair, maintenance and overhaul of used equipment.

It is noted that since 7th ed. EN 60079-0 [5] contains a answer for the contents of Instructions with specific listed requirements.

II. POTENTIAL ENHANCEMENT OF ACTUAL CONTENTS OF INSTRUCTIONS MANUAL

A. Contents of Instruction manuals: potential enhancement of technical aspects

From the perspective of the user, a detailed instruction manual can offer some advantages, for example extended inspection intervals or a limited scope of maintenance, but on the other hand, in the case of large installations (large industrial plants) it complicates the supervision of the equipment. In the case of large plants, it is more convenient to introduce a unified system of maintenance and inspection including repair based on the standards IEC/EN 60079-17 [6] and IEC/EN 60079-19 [7] even if the costs will be higher for a single equipment.

Instruction shall include potential effects due to lack of maintenance or non-observance of instructions.

Cable glands normally do not have a temperature class or ambient operating temperature range marking. They do have a service temperature and without specific marking, the service temperature is in a range of -20°C to +80°C and their selection are essential for any type of protection used for electrical equipment.

Metallic particles inside an Ex flameproof enclosure can create an additional explosion not intended by the design of this enclosure; a potential gas air mixture can explode inside this enclosure followed by a second explosion of hybrid mixture (gas+ metallic) for which the design is not intended – then such information (restriction) should also be detailed in the Ex component (empty enclosure) instructions if any.

Cleaning of equipment (housekeeping) used in workplaces where explosive atmospheres are due to combustible dusts is a major act regarding prevention and protection against explosion. The accumulation of 1 mm or more of combustible dust on surfaces in a working area can create an explosive atmosphere; this information regarding excessive thickness is essential for safety and is a clear message to observe

Maintenance of non-electrical equipment is more complex and asks for a very exhaustive content including intervals of maintenance, key points due to influence of chemical aggression, corrosion like hydrogen embrittlement, static electricity, bonding and earthing.

The influence of radiated heat may need to be considered on the final installation through the requirements defined by IEC 60079-14 [4] or directly in case of assembly of electrical and non-electrical equipment like a gas turbine or a forklift truck.

Some standards for protective system can be offer as support of specific product like protective system like CEN/TR 16793 regarding flame arresters [12] or CEN/TR 16829 regarding bucket elevators [13]. These Technical Reports are aimed primarily at persons who are responsible for the safe design and operation of installations and equipment using flammable liquids, vapours or gases (fame arresters) and dusts (bucket elevator).

Use of gas detection may also have to be taken into consideration for suitable selection and installation; a summary of important parameters, from applicable standard IEC EN 60079-29-2 [14] and the national standard BS 60080 [15].

B. Contents of Instruction manuals: potential enhancement of general aspects

The contents and design of instruction manual is a key element of safety. The manufacturer has full information on the of explosion protection aspects and should provide it to the user in an accessible way – an IEC/IEEE 82079-1:2019 [16] or ISO 20607 [17] may be useful. Using a graphical symbols and safety signs an ISO 7010 [18] is also usable.

For some complex equipment, two types of skilled personnel are considered (see Figure 2).

Fig. 2: Maintenance by skilled persons (maintenance personnel and qualified personnel)

The availability of several training contents able to certify competence of personnel under national, international schemes are an added value for the understanding of instructions and related standards like IEC/EN 60079-14 [4], IEC/EN 60079-17[6], IEC/EN 60079-19 [7] and national rules linked to IEC 60364 series [19]. Specifically, the maintenance personnel has adequate competences, skills and knowledge to operate safely, properly, effectively and efficiently.

As tools to improve quality and design of instructions manual, some standards and guidelines are available.

IEC/IEEE 82079-1:2019 [16] as standard provides general principles and detailed requirements for the design and formulation of information for use (instructions for use) that can assist users to install, operate and maintain a product safely and appropriately. The standard states that "information for use of products applies to phases of the product life cycle such as transport, assembly, installation, commissioning, operation, monitoring, troubleshooting, maintenance, repair, decommissioning, and disposal, and the appropriate tasks performed by skilled and unskilled persons." The standard defines the purpose of the information for use and regards it as an important item for the safe and effective use of a product and necessary to fulfil legal and regulatory obligations. The standard encourages the use of competent professionals to prepare information for use.

The influence of radiated heat may need to be considered on the final installation through the requirements defined by IEC 60079-14 [4] or directly in case of assembly of electrical and non-electrical equipment like a gas turbine or a diesel powered forklift truck.

The employer shall ensure that workers have adequate information and, where appropriate The standard further refers you to use additional guidelines and standards that can be used in conjunction to ensure the information for use is of the required quality.

ISO/IEC Guide 51 [20] provides details on risk management and safety related information that can be used to prepare safety sections of product documents.

ISO/IEC Guide 37 [21] and ISO 20607 [17] establish principles and gives recommendations on the design and formulation of instructions for use of products by consumer

The principles and detailed recommendations in ISO/IEC Guide 37 [21] are intended to be applied in combination with the specific requirements on instructions for use specified in standards for particular products or groups of products. Some model formats and wordings are suggested for inclusion in standards. ISO/IEC Guide 37 [21] contains some practical recommendations and a proposed methodology for assessment, to help establish common criteria for the assessment of the quality of instructions for use.

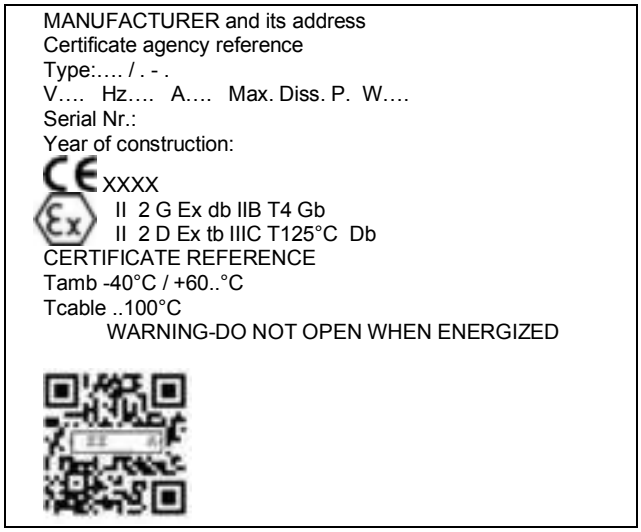

Fig.3: Example of EX equipment marking plate including QR code information

Availability of the instruction manuals on site is necessary even if more and more digital versions are available, therefore the digital version needs to take into account potential revision of the design since the first time of the put into service and any revision need to be assessed during certification. Information concerning the explosion safety of the equipment cannot be changed without approval of the Notified/Certification Body.

As well as ammonia, other candidates for alternative fuels include hydrogen, methanol, biofuels, batteries and fuel cells. For the related industrial sectors, it is mandatory and essential to inform operators regarding hazards due to these new sources of energy and instructions for safe use

of equipment designed for these new fuels and their specific hazards at work. These instructions can differ from those usually met in Oil and Gas workplaces.

C. Ex Product data sheet (ExPDS)

Information regarding to Ex aspect is placed in various chapters in instruction manual, then more useful would be to add a short table indicating the key information. ExPDS table do not replace the instruction manual. The main point of ExPDS is clearly indicating that product does not require maintenance, etc.

Example of such ExPDS is shown on Figure 4.

Ex product data sheet	
Equipment:	General purpose junction box Type: JB-001 Ex
Manufacturer	BDLER, New City 13980 P.O. Box 01-345, EU www.bdler.com
Ex marking	Ex eb IIC T5 Gb Ex tb IIIB T100°C Db
Instructions manual	DM.123-2022 dated 12.02.2022
Ambient temperature	-20 ° ... +40 °C
Certificate	IECEx 22CER0123X
Standards	EN IEC 60079-0:2018 IEC 60079-7:2015 IEC 60079-31:2013
Assembling	Not required **or** See Instruction Manual p. 3.2 Cable gland section: M24, Ex e, size according to cable used Not used entries should be blanked using Ex e blanking element
Erection	Fix the cable Mounting instruction: see Instruction Manual p. 4.1
Putting into service	No verification needed **or** See instruction p. 3.7
Explosive atmosphere	Group II: all gases and vapours group IIC, IIB, IIA all temperatures classes T1, T2, T3, T4, T5, T6 Group III: all dusts group IIIA (combustible flyings) all dusts group IIIB (non conductive dusts, non metallic dust) Maximum surface temperature: 100 °C
Ratings	250V, maximum current: see Instruction Manual, Table 5.1
Maintenance	Group II: No maintenance needed **or** use IEC 60079-17 Group III: housekeeping – no dust layer on the equipment permitted
Maintenance of explosion protection	None
Repair	Not intended for repair **or** See IEC 60079-19 Components replacement (identical) permitted Spare parts: contact with manufacturer
Specific condition for use (X-certificate)	Equipment is low energy impact protected – use additional hood.
Additional information	Warning labels in English only – using other language change the labels (supplied by manufacturer)
Special tools needed	No
Other information	None

Fig.4: Example of Ex product Data sheet

III. CONCLUSIONS

As an answer of safety at workplaces, the Occupational safety and health information and the written instructions shall contain at least information on:

- The conditions of use of work equipment.
- The foreseeable abnormal situations.
- The conclusions from experience in the use of the work equipment.

A certain barrier for the manufacturer is the need to develop the instruction manual in the user's language. Most often, this requirement does not cover the entire manual, but only the part containing the safety instructions.

Perhaps the solution would be to extract the Ex-instructions as a separate document.

Then it may then be tempted to develop a universal template for such an Ex-instruction, which could always include:

- Description of the product and definition the intended use (also containing where the product may be use)
- Marking details and explanation of all symbols used (not for product series but for a specific product), together with marking plate explanation.
- Ex safety parameters
- Type (s) of protection applied for every sub part of product with the appropriate Ex standards.

As well as the actual hazardous area classification, it should be important to consider the external influences classification for the same area. This consideration can guarantee the complete cartography for the safe use of all Ex-equipment and shall be mentioned in the maintenance plan for specific actions.

NOMENCLATURE

EPL	Explosion Protection Level
Tamb	Ambient temperature

REFERENCES

[1] ATEX Directive 2014/34/EU of the European Parliament and of the Council of 26 February 2014 *on the harmonization of the laws of the Member States relating to equipment and protective systems intended for use in potentially explosive atmosphere*

[2] Machinery Directive 2006/42/EC of the European Parliament and of the Council of 17 May 2006 *on machinery*, and amending Directive 95/16/EC

[3] IECEX scheme www.iecex.com

[4] IEC/EN 60079-14 *Explosive atmospheres - Part 14: Electrical installations design, selection and erection*

[5] IEC EN 60079-0 *Explosive atmospheres - Part 0: Equipment - General requirements.*

[6] IEC 60079-17 *Explosive atmospheres - Part 17: Inspection and maintenance of electrical installations in hazardous areas (other than mines).*

[7] IEC 60079-19 *Explosive atmospheres - Part 19: Equipment repair, overhaul and reclamation.*

[8] EN ISO 80079-36 *Explosive atmospheres – Non Electrical Equipment - General requirements*

[9] EN 1127-1:2019 *Explosive atmospheres. Explosion* prevention *and* protection *Basic concepts and methodology*

[10] Directive 2009/104/EC *Minimum safety and health requirements for the use of work equipment by workers at work* (second individual Directive within the meaning of Article 16(1) of Directive 89/391/EEC)

[11] Directive 1999/92/EC of the European Parliament and of the Council of 16 December 1999 *on minimum requirements for improving the safety and health protection of workers potentially at risk from explosive atmospheres* (15th individual Directive within the meaning of Article 16(1) of Directive 89/391/EEC)

[12] CEN/TR 16793:2016 *Guide for the selection, application and use of flame arresters*

[13] CEN/TR 16829:2016 *Fire and explosion prevention and protection for bucket* elevators

[14] IEC EN 60079-29-2 :2015 *Explosive atmospheres - Part 29-2 Gas detectors - Selection, installation, use and maintenance of detectors for flammable gases and oxygen*

[15] BS 60080:2020 *Explosive and toxic atmospheres. Hazard detection mapping. Guidance on the placement of permanently installed flame and gas detection devices*

[16] IEC/IEEE 82079-1:2019 *Preparation of information for use (instructions for use) of products -- Part 1: Principles and general requirements*

[17] ISO 20607:2019 *Safety of machinery - Instruction handbook - General drafting principles*

[18] ISO 7010:2011 *Graphical symbols. Safety colours and safety signs. Registered safety signs*

[19] IEC 60364 series *Electrical installations of buildings*

[20] ISO/IEC Guide 51:2014 *Safety aspects -- Guidelines for their inclusion in standards*

[21] ISO/IEC Guide 37:2012 *Instructions for use of products by consumers*

VITA

Xavier LEFEBVRE, PhD in Energy conversion, is qualified as IECEX Inspector since 2011 and standardization expert since 1999. He is member of IEC/CLC TC31 and CEN/TC305 committees and chairman of French Committee S66A.

Michal GÓRNY, PhD in Explosion safety, is the Managing Director of ExKontakt Poland. (Evaluation of explosion risk). He was previously the ATEX Certification Manager of GIG KD “BARBARA” Polish Notified Body; technical expert for Polish State. He is member of IEC/CLC TC31 and CEN/TC305 committees and chairman of Polish Committee EX.

IMPROVING VSD SYSTEM AVAILABILITY BY USING FULLY REDUNDANT POWER CONVERTERS

Paper No. PCIC Europe EUR22-18

Stéphane Mouty
ABB Switzerland Ltd.
CH-5300 Turgi
Switzerland

Axel Rauber
ABB Switzerland Ltd.
CH-5300 Turgi
Switzerland

Abstract - VSD Systems are thoroughly evaluated for their availability and reliability, when used in critical applications for Chemical, Oil and Gas plant operators.
The focus to avoid any unplanned process interruption with such electrical systems has increased. Having a second VSD converter used in a "hot stand-by configuration" reduces the risk of process disruption and allows easier maintenance activities, without process interruption.

Index Terms — Adjustable Speed Drive System, VSI, LCI, High Power Application, Availability, Redundancy.

I. INTRODUCTION

For industrial applications the market is moving towards solutions which are more environmentally friendly, with improved life cycle considerations. This has led to more widespread use of fully electrically driven trains see Fig1 to control loads such as compressors, pumps, fans, or other critical processes which were historically driven by gas or steam turbines.

The application of a variable frequency converter provides improved flexibility and efficiency of such solutions but remain perceived as a less reliable solution. In this article, solutions to improve that are discussed.

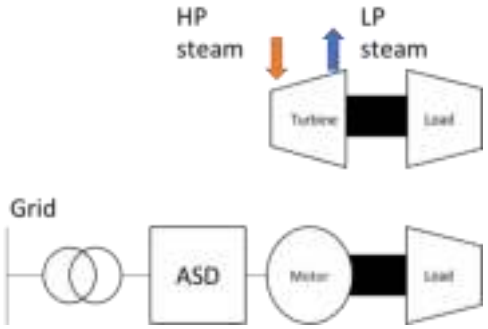

Fig. 1 Drive train with steam turbine (top) replace by electrical driver (bottom)

II. AVAILABILITY AND RELIABILITY

A. System Availability

The recent developments in ASD's have delivered improved performance in terms of availability, making the electrical drive train even more robust with regard to possible disturbances from networks, but also limiting the generation and perturbations of electromagnetic compatibility (EMC).

It is important to have a holistic system approach for the design of the hardware and the software.

For that purpose, an organization which can provide system studies and parametrization of such complete and complex electrical systems, in order to facilitate their integration is an important contribution to improve the availability.

Those studies could include failure mode analysis, torque ripple estimation, identification of network resonances, definition of filtering solutions, all with the idea to improve reliability.

For larger projects and systems, it is paramount to have a good collaboration with the OEM, EPC and Electrical Integrator to enable the cascade protections, i.e., with the aim of limiting disturbances closest to the fault locations and ensuring highest robustness where possible to internal and external events.

Of high importance is the ability to apply to the software settings using a harmonized control baseline.

An electrical system cannot be considered alone, without considering the various interactions that it will have.

1) Network Disturbances

It has always been a source of trouble for electrical systems. DOL motors create disturbances but are also affected by those network disturbances which occur especially in remote or island networks, which are normally considered as weak networks.

An advantage to use an ASD is to decouple the system via the intermediate DC bus from the network and the motor. Efforts have been made when ASD's were developed to make the electrical drive systems more robust towards network disturbances such as voltage dips, by introducing power loss ride-through functionalities.

During these abnormal conditions, it is often required to stop supplying the motors and thus the speed from the load consequently drops away. Sometimes this is not good enough for the process and the continuity might be compromised. In order to limit speed variations, a certain torque might still be required to be maintained in such conditions.

By accepting some compromise, it is possible to maintain a certain torque during the presence of voltage dips, such concepts have been described in [1]

By improving the motor control and employing an advance predictive model solution such as MPC or MPTC with LCI converter as shown in [2] it has been possible to increase the ride through time, which strengthens the system availability and reliability.

2) Torsional disturbances

Over the past years not only electrical integration of the electrical driver has been improved, but also the

mechanical aspects have been improved.

For example, in [3] and [4] special attention has been paid to the drive software, providing damping for torque oscillations, and improving the lifetime of mechanical elements such as the couplings.

Any positive contribution in special applications can help to avoid centrifugal compressor surges in O&G applications.

3) Other interfaces: LV auxiliaries

To properly operate a medium voltage ASD, some other auxiliaries are needed for items such as control and cooling systems.

Even if the power semiconductors are found to be the main reason of defects, other causes of defects can represent a non-negligeable part (50%) of failures on site as shown Fig. 2.

Failure of cooling devices can represent about 30% of failures which are recognized on site.

Maintaining the circuit boards over the lifetime of an ASD represents a major challenge. Therefore, it is important to carry out proper maintenance tasks. As a result, replacement of the control hardware might be required, which can be costly, however can also be used a chance to upgrade the hardware and software to the latest technology, ultimately leading to improved system performances.

It must also be underlined that the main issues often appear in the first month of operation, having had the system commissioned by proper trained personnel. The personnel can connect with the factory to support learnings from past field experiences and help shorten the time to problem solve and reduce site troubles.

Despite all best efforts made to make ASD's robust to the environment they are placed in, there are still possibilities to improve the robustness and availability by consideration of redundancy.

Nevertheless, bringing redundancy to the system often leads to significantly increased complexity. A good compromise and balance need to be defined.

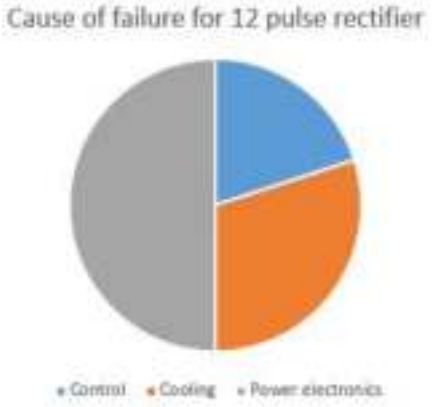

Fig. 2 Root Cause for failure of a water-cooled drive

B. Redundancy

Main effort put on what is perceived as the component with the higher complexity in the train: the variable frequency drive.

For that purpose, redundancy can be implemented at different levels. It is possible to implement redundancy to the auxiliaries.

- redundant auxiliary and uninterrupted supplies.
- redundant communication interface

Remark: redundancy of controller has shown in the past that it was bringing much more complexity than the benefits in term availability that it could generate.

When it comes to the cooling solution, there are also several leverage to improve the availability. For example, it is common to have redundant pumps or fans as well duplicate other devices includes in the cooling loops.

1) Power Semiconductors Redundancy

Regarding the power parts, solutions can also be implemented. It is possible for some ASD configuration to implement it directly at the semiconductors level.

For that a solution often called "n+1" can be met using more than one semiconductor in series.

This solution relies partly on the behavior of the switching device in case of fault.

Indeed, MV semiconductors having a "press pack" construction hardware, component as IGCT or thyristor, will be "normally closed" (short circuited) after failing. This enables a very simplistic way to have N+1 semiconductor redundancy. Very few additional components added as well as no different type of technology.

In the opposite, the "flat pack" semiconductors often used in case of IGBT modules and/or low voltage will be "normally opened" after failing. In those case, it is common to implement the redundancy at the "cell" or "power modules" level. Those have been popularized by the selection of topology using LV semiconductors, topology so called multi-cells having a lower availability due to increase of components than the topology based on MV semiconductors.

Due to the reduced availability of such topologies, in order to improve this, it is common to use power cell redundancy or cell bypass circuit to allow operation in case of a cell failure. In such case, a reconfiguration is needed before putting back the drive in operation.

A drawback is that it is not possible to rebuild redundancy in case of failure during operation and this would require the shutdown of the installation.

The topologies using MV semiconductors having a higher availability and lower part count do not necessary require redundancy at the semiconductor level to provide high reliability. Moreover, the press-pack solution such as IGCT or thyristor will be "normally closed" after failure and do not need to be bypassed.

2) Power Converters Redundancy

An alternative way to provide redundancy is to install a complete AFD in parallel of the existing one, in order to have a fully redundant VFD (i.e. 2 x 100%)

Here as well different configuration could be implemented.

"n+1" (n >1)

A solution for the increasing power requirement is to put systems in parallel. Having more than one VFD to reach the power of the motor had an impact on risk of failure. In

order to reduce this risk, the idea of increasing the available power to cover the failure of one system is frequent in systems such as 3 x 50% as per Fig3. or 4 x 33%

Remark: operation "n-1", ie when lower power available than rated, is possible but often is not bringing benefits as the power would be too low to maintain the process alive.

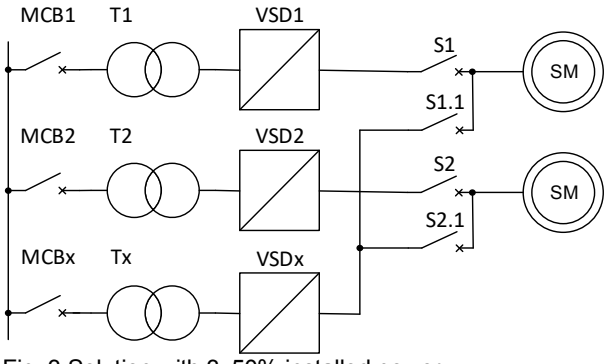

Fig. 3 Solution with 3x50% installed power

2 x 100% (or n=1)

This philosophy is based on the fact that the limitation to 2 components make it easier to duplicate the functionality as per Fig4.

Solution might be more expensive but in case where the main focus is the reliability, having 2 VFD which could be considered as independent, each would have its own supplies (main and auxiliaries which could be connected to 2 independent grids)

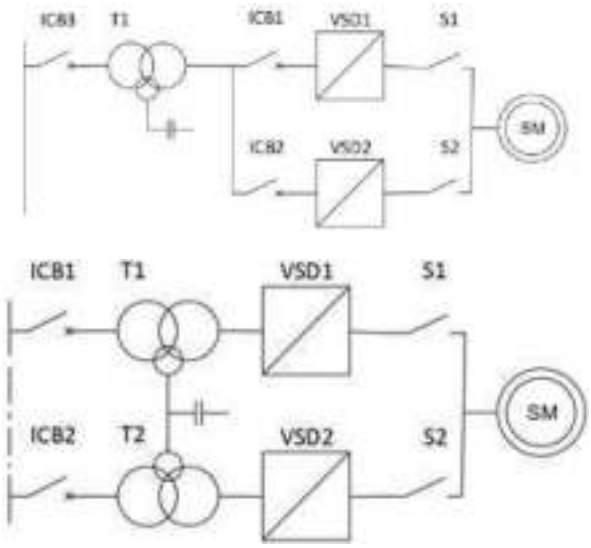

Fig. 4 Fully redundant converter (top) and variant with 2 transformers (bottom)

Benefit with the solution having transformer redundancy – complete VFD redundancy with minimum amount of single component failures that could lead to system and process trips. This is as close as we get to "True redundancy" with the possibility to rebuild the redundancy in case of failure.

Impact on reliability using the different solution has been presented in [5] and summarize in TABLE I

TABLE I
TYPE SIZES FOR PAPERS

Redundancy	**2 x 100%**	**"n+1"**
Suitability	LCI and VSI (up to 35MW)	VSI
Complexity	Lower	Higher
Protection		More difficult
Installed power	High	Lower
Control		Master / Slaves needed
Excitation	2 x 100%**	2 x 100%***

** The excitation is paired with the LCI converter, a fault of EXU as of LCI would be the reason to initiate the switch-over to the stand-by system (LCI+EXU)

*** synchronous motor only

III. POWER CONVERTERS TECHNOLOGIES

Recently requirements for applications using centrifugal compressor are looking for full electrical drive for power up to 100MW in application like MR in LNG plant.

Above 20 MW the most common motor technology used is synchronous motor due to the better efficiency.

As it was mentioned in [6], below 35MW it is common to meet VSI technology – the main reason being that a single cabinet can be used and similar efficiency than LCI system are reached but above this power it is limited to meet VSI topology due to the increase complexity link to the needs of several cabinets in parallel.

A. LCI

The topology is consisting on rectifier and inverter side by thyristors added in series to reach different voltage and power levels. The thyristor need to be fired to start conducting but they stop naturally when the current is reaching zero.

Remark: The output of 2 parallel LCI converters could be connected without the need of extra device. in case of Voltage source inverter, a damper (for example a reactor) would be required.

B. VSI

The semiconductors used are bipolar transistors which are used as "switches" able to be switched ON and OFF. As the transistor structure does not allow the current in both direction an antiparallel diode is required to be installed.

Having fuse-less protection philosophy [7] required special safety features in order to clear the arc in case of short circuit. Such solution provides not only personal safety, but also minimizes or completely eliminates hardware damages. [8]

Until the internal fault is cleared which would stand until the stop of the motor or would require an external device (Circuit breaker), the motor see a SC at its terminals, during this time, the flux is reduced tending to be cancelled.

C. Pros and Cons

The use of diode, in the different part of the converter (rectifier or reverse conducting) cannot guarantee the isolation of the drive therefore an external device is needed in order to isolate the different compartments.

Using a filter brings some flexibility concerning the harmonics cancellation. The VSI solution have often a multi-pulses rectifier in order to reduce the generated harmonics, the higher the pulse number is the more complex and the less reliable is the transformer.

Summary is provided in TABLE II

TABLE II
TYPE SIZES FOR PAPERS

Technology	**VSI**	**LCI**
"n+1" semiconductor	Complex*	Available
Fault current (SC)	Need external support to be interrupted (MCB)	Without external support current interrupted <20ms
Max Power per VFD cabinet**	36 MVA	72 MVA
IEEE519 harmonics	reach with high pulse number	with filter
Transformer	Complex	Simpler

* often possible only for complete module not on semiconductor components

** brochure values

IV. SWITCHING TO HOT STAND-BY

The challenge for lots of applications is to maintain the process running after the failure of a converter supplying the motor.

To do that a spare or stand-by converter is installed. As the idea is to react fast the term "hot stand-by" is used.

This paragraph describes the process in order to switch from a faulty to a safe converter targeting to shorter the time where the motor is not supplied and to limit the speed drop for the load to an acceptable level.

A. Switch-over Sequences

As the properties of the different converter topologies are different, the change-over from one converter to its redundant one will follow different sequences which are described in following paragraphs

1) Case of LCI

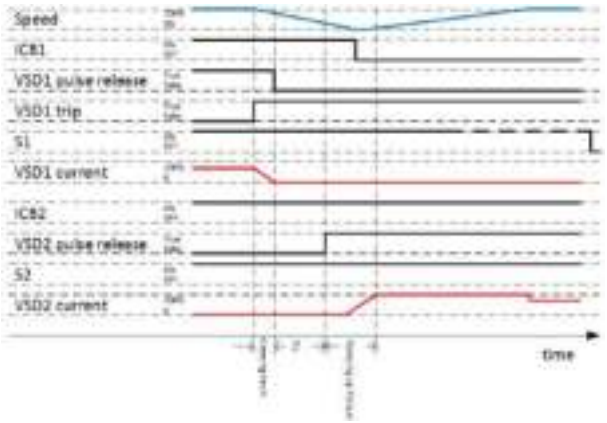

Fig.5 Switch-over Sequences LCI case

The breakers ICB1, ICB2, S1 and S2 are NC during normal operation.

In case of internal fault, the "faulty" running LCI is able to interrupt the current, the "safe" LCI is able to take over the load without the re-settings of breakers.

2) Case of VSI

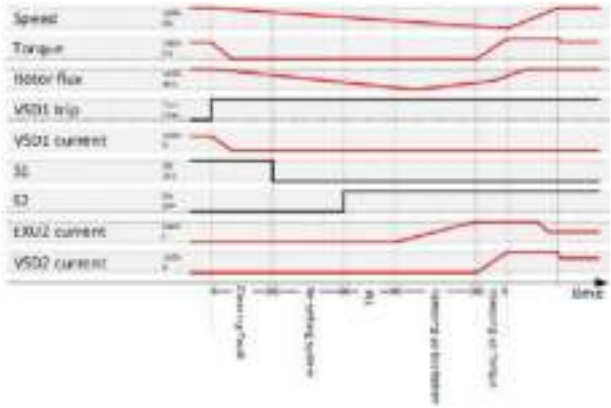

Fig.6 Switch-over Sequences VSI case

B. References

As per End User requirement, AFD system redundancy have been implemented recently for 3 different motor power as per TABLE III.

Those plants are currently under commissioning.

TABLE III
REFRENCE WITH INSTALLED REDUNDANT LCI

Plant	**Poland 1**	**Poland 2**	**Belgium**
Motor Power	20MW	35 MW	50 MW
Solution (Refence to Fig. 4)	2 x 100%	2 x 100%	2 x 100% Variant

C. HiL (Hardware in the Loop) Simulations

Using a similar solution to check the control that it had been done in presence of grid disturbances in [2],

it was possible to check the switch-over sequence and process in case of LCI failure.

The simulations also permitted the first optimization in order to improve switch-over time.

1) Test set up

The HiL simulator Fig.8 includes all control hardware and software of 2 VFDs as described Fig.7, similar as what will be used on site, with additional I/Os in order to do the interface with the HiL simulator which will simulate the main hardware (Transformer, Filter, Thyristor bridges, switchgears and Motor)

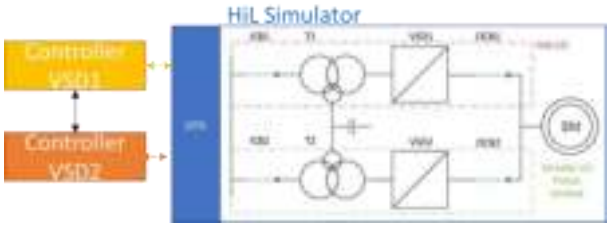

Fig.7 Concept of HiL simulations


Fig.8 HiL Simulator (top)Project control hardware (bottom)

2) Results

First try: Initial target has been to check that from the control part, all the things could put in the sequences which would allow the system to transfer the motor supply responsibility from one VFD to the second one, the results are presented Fig. 9

During this attempt the system responses: dynamic of the main parameters such as motor speed, motor excitation current were following our expectations and would not bring additional considerations which might have been overlooked.

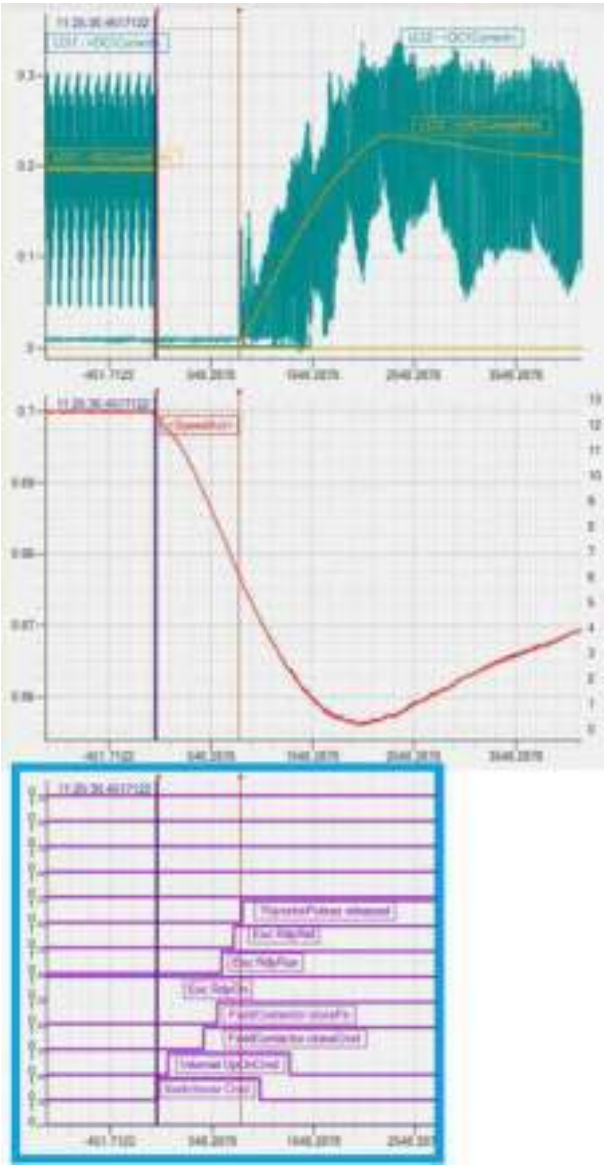
Fig.9 Results of the first try: DC bus current (top); estimated speed drop (middle); sequences (bottom)

Sequences:

- o Initiate a switchover “switchover Cmd”
- o Drive receiving “OpOn” command gets assigned Duty.
- o Duty drive performs a regular startup, with the default thyristor pulse release delay and excitation start current to flux up the machine.
- o Upon switchover, Duty drive automatically
  - closes excitation field contactor
  - generates OP on cmd
  - changes parameter ‘ThyristorPulseReleaseDelay’ dynamically to a specific delay only valid for switchover situation.
- o Tripped drive will be assigned standby drive once available again / faults are cleared.

Second attempt: having proven that the concept/sequences in order to transfer the load from one faulty LCI to the safe one was correct, the focus has been put on the research for time optimization.

One of the key elements has been the response time with the aim to reduce as much as possible the time where the load would not see torque and would ramp down the speed.

Remark: here load and motor inertia would have a big impact on what would be seen by the process itself.

After optimization the gain is visible Fig. 10 and TABLE IV.

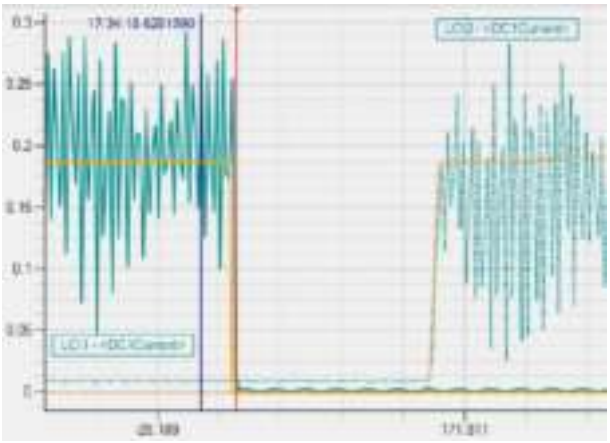

Fig. 10 DC bus current during second try

TABLE IV
PERFORMANCE OF TESTED SOLUTIONS

Case	Time to "pulse"	Time to reach full torque
1st try	800ms	2'000ms
Optimized switch-over	120ms	125ms

As it can be seen in the table, thanks to improvement the time in order, for the stand-by converter, to take over the motor control has been reduced by a factor 6 the tasks link to the control.

But where the highest benefits have been achieved is on the time to ramp up the torque.

By optimizing the excitation current it was possible to almost instantaneously re-apply the full torque to the motor.

Those encouraging results allowed us to identify possible way to optimize response time by working on the control tasks. Some additional features are planned to be checked and validated before commissioning of the first units.

II. CONCLUSIONS

Improving availability of the electrical drive train for demanding applications in order to reach level of mechanical train solutions is mainly driven by the fact that the electrical drive train improve the efficiency and limit the environment impact for players in such industry.

The use of MV semiconductors VFD, in spite of all recent improvement to make it more robust, which are still perceived as the less reliable components in such drive trains, lead customer to require the implementation solutions using redundancy.

The different way to implement such redundancy concepts have been reviewed in this article.

By having a focus on system with power high than 20MW, the possible way to have power channel redundancy were compared.

To conclude, solutions which currently are under commissioning were shown and the effort put in order to de-risk the operation were presented.

Thanks to HiL test setup the focus on the control part helped to be prepared before the on-site activities, It allows to simulate different scenarios and optimize the performances of new functionalities.

VI. REFERENCES

[1] T. Wymann, S. Van de moortel, P. Jörg, "Power Loss Ride-Through in a Variable Speed System, PCIC Europe 2014.

[2] T. Besselmann, P. Jörg, T. Knutsen, T. O0 Stava, S. Van de moortel, "Partial Torque Ride Through with Model Predictive Control", PCIC Europe 2016.

[3] S. Del Puglia, S. De Franciscis, S. Van de moortel, P. Jörg, T. Hattenbach, D. Sgrò, L. Antonelli, S. Falomi, "Torsional Interaction Optimization in a LNG Train With a Load Commutated Inverter", Proceedings of the 8th IFToMM International Conference on Rotordynamics 2010, Seoul, Korea

[4] A. Lenzi, P. Jörg, S. Falomi, D. Andreo, et al. , "Combined Torsional and Electromechanical Analysis of an LNG Compression Train with Variable Speed Drive System" Proceedings of the 38th Turbomachinery Symposium.

[5] P. Wikström, L. Terens, H. Kobi, "Reliability, Availability and Maintainability (RAM) of High Power Variable Speed Drive Systems (VSDS)", IEEE Paper No PCIC – 98-16.

[6] A. Rauber, P. d. Bakker, "Adjustable Speed Drive System Comparison - VSI and LCI for High Power Application", IEEE Paper No PCIC – 18-16.

[7] H. Ojalammi, M. Västi, W. Van der Merwe, E. Virtanen, "EFFECTS OF ARC-BACK FAULT IN VSD SYSTEMS AND HOW TO PROTECT AGAINST THEM" Copyright Material PCIC Europe. Paper No. PCIC Europe EUR19_22

[8] How to choose a medium voltage VFD: Protection concept - MB Drive Services (mb-drive-services.com)

III. VITA

Stéphane Mouty graduated from the ENSEM (Ecole Nationale Supérieure d'Electricité et de Mécanique) with an engineer degree in 2008 then from the University of Franche-Comté in 2013 with a PhD degree. In 2015 he joined ABB Medium Voltage Drives and is currently employed as a global tendering manager.
stephane.mouty@ch.abb.com

Axel Rauber graduated from the Staatliche Studienakademie Baden-Württemberg, Mannheim, Germany in 2001 with a degree in electrical engineering – Diplom-Ingenieur (BA). In 2001 he started his professional career at ABB Medium Voltage Drives and is currently employed as a global product manager. He is responsible for VSI and LCI based products for high power applications.
axel.rauber@ch.abb.com

THEORETICAL AND EXPERIMENTAL INVESTIGATIONS ON FLAMEPROOF ENCLOSURES FOR EX AREAS

Paper No. PCIC Europe EUR22_19

Nima Dalaeli, Kim Fumagalli
Technor Italsmea SpA
Via Italia, 33, 20060 Gessate
Italy

Roberto Sebastiano Faranda
Politecnico di Milano
Via La Masa, 20156 Milano
Italy

Abstract - More and more often, electrical equipment, even when they are inside enclosure, need to be often monitored and supervised by operators. This operation can introduce risk especially when they must be opened. Nowadays, most of equipment used in industries, such as Oil & Gas, chemical and pharmaceutics plant, are electrical devices that can be exposed to flammable GAS or DUST. In this kind of ambient, any ignition source like a spark could ignite the substance and leads to a fire or explosion, therefore, the opening of the enclosure is not allowed. Therefore, Flameproof enclosure (Ex d) with large window is becoming very important for hosting electrical devices in Ex area. These new products need to be designed and validate to support a so high mechanical strength (to avoid any possible deformation, failure of enclosure and flame transmission), and normally this validation is obtained only by realizing real enclosure and doing experimental tests. To reduce the number of experimental tests, cost, and time of products design to validate a Flameproof enclosure, in this paper the use of Finite Element Method for stress analysis of an enclosure Electrical Junction Box stainless steel and Aluminum with large window has been described. First, this method has been validated on enclosures realized in stainless steel. Four scenarios have been simulated to improve the yield Safety Factor from the reference model to reach 1 in the final scenario. Finally, the simulation and method have been verified by experimental tests with positive results. Secondly, the validated method has been applied on the enclosure realized in aluminum where a bigger window is installed. The simulation results and the related tests will be shared.

Index Terms — Enclosure, ATEX, IECEX, Ex area, overpressure test, FEM analysis, safety factor.

I. INTRODUCTION

When a switch is turned on or off, it can produce a brief harmless arc flash. In a normal industry, this is unimportant, but if there is a flammable atmosphere present, the arc could cause an explosion. An explosive atmosphere is characterized as a mixture of volatile substances with air, in the form of gasses, vapors, mist, or dust, under atmospheric conditions and the amount of a material required to create an explosive atmosphere varies depending on the type of the substance and flammability and the term "non-hazardous" refers to a location where an explosive atmosphere is unlikely to exist in enough concentrations to necessitate such precautions.

The “Flameproof” theory notes that if an explosion happens within the enclosure, the spreading flame will either be contained or cooled by a “Flame-path,” minimizing the possibility of igniting an explosive outside the atmosphere [1]. Electrical Junction Box (EJB) enclosures are suitable to be used in different industries and hazardous locations where there is a risk of explosion, and they are used as junction or pull box for keeping terminals, reactors, busbars, fuse carriers, relays and other electrical devices such as meters and so on.

The purpose of this study is the validation of the Finite Element Analysis (FEA) simulation method for stresses for EJB enclosures, the subsequent verification of mechanical strength by laboratory tests [2] and the use of the method for future new enclosures. Simulation of test conditions can predict the behaviors of enclosure after explosion, and it will avoid numerous practical tests and most importantly, simulations can optimize the design for avoiding product over strength and under strength limits.

FEA is a mathematical procedure that provides an analysis of how a product will react to stresses and reduces the need for numerus prototyping. The intention is not to totally eradicate prototyping, but rather to limit it by using FEA to model multiple configurations and then evaluating the most crucial ones [3]. Stress analysis in the simulation toolbox of Inventor uses FEA for the calculation of stress distribution on different spots of the geometry. A comprehensive 2D and 3D design tools with the possibility of linked stress analysis makes this software to be used for this study [4].

II. EJB 13 XL

To validate FEA simulation method for developing new EJB enclosures, it has been validated by laboratory tests and simulations of a real EJB stainless steel. EJB 13XL, reported in Fig. 1, is designed with a dimension of 870x580x385 mm made in S275JR welded steel and the cover and body were connected by using N˚28 screw ISO 4762 M12x25.

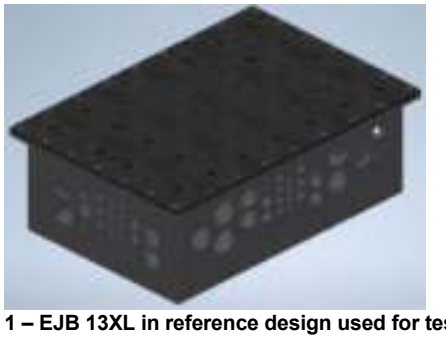

Fig. 1 – EJB 13XL in reference design used for test.

Both cover and body are designed as solid parts in the software, and they are assembled by screws, then physical properties of materials used for EJB such as yield, and ultimate strength, as reported in Fig. 2, are assigned to the parts to obtain the real sample as a 3D model.

Fig. 2 – Physical properties of S275JR Steel.

After this, to validate and calibrate the FEA method the initial investigation was the design and simulation of the EJB and compare the result with the real test.

When the FEA model gives acceptable results, further modifications will be simulated, as reported in the next paragraph, to avoid EJB over sizing and EJB under sizing (for example improving the resistance of the enclosure to meet enough safety to be sure it can pass the test).

A. Stress Analysis

The situation of the experimental test is similarly defined in the stress analysis environment of the software. The method of testing used by the laboratory was a static overpressure test for a period of 10s [5], so the simulation is defined based on static analysis to avoid impact and vibration effects and have a uniform distribution of pressure in the enclosure defined by practical tests. As reported in TABLE I, the tests have been performed according to data of Ex Test Laboratory and of the calculated explosion pressure by IEC 60079-1 [5].

TABLE I
APPLIED PRESSURE FOR TEST (BAR)

Size	Minimum Ambient Temperature			
	-20˚C	-40˚C	-50˚C	-60˚C
EJB 2 to EJB 8	13.50	17.60	17.60	17.60
EJB 9 to EJB 12	13.50	17.00	17.00	17.00
EJB 13 / EJB 13A	12.30	15.00	15.80	16.97
EJB 14	12.15	14.85	15.15	16.05

The load type that is defined for simulation is pressure, so that it is applied perpendicularly on the internal surfaces of EJB. The routine test was done with the pressure of EJB 13 / EJB 13A at minimum ambient temperature (-60˚C). So, in the simulation, P=16.97bar (P=1.697MPa) is applied to the enclosure (Fig. 3). As it is mentioned, Finite Element Method is based on subdividing a large system into smaller, simpler parts that are called finite elements by using a particular discretization known as mesh and calculations will be done on mesh and then extend to the whole model. Mesh size has a significant effect on the calculations and results, so it is crucial that the suitable size of the mesh is applied on the model to reach precise results and save calculation time.

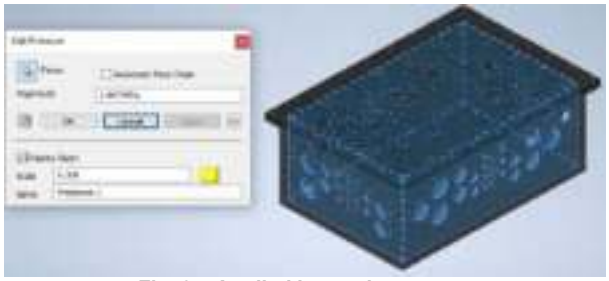

Fig. 3 – Applied internal pressure.

In the simulation, mesh size is selected somehow the solution steps converge to a unique result for the Von Mises Stress with a minor percentage of convergence rate as it is shown in Fig. 4.

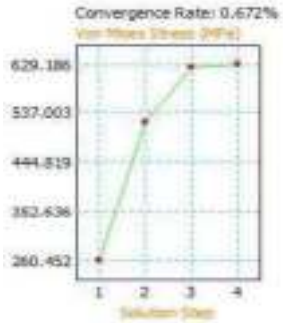

Fig. 4 – Optimized mesh curve (convergence plot).

In other words, lower amount of convergence rate shows higher independency of stress to the mesh size which means that the obtained results are more accurate. In the areas that there is possibility of failure such as center of cover, bottom of the body and flanges, smaller mesh size is applied by using the local mesh command to reach more precise result for the stress on those regions.

Definition of Safety Factor (SF) [6] is the most important point that should be considered in the simulation results based on what is indicated in the overpressure test procedure of enclosure “d” [5]. According to the standard, to pass a practical test no permanent deformation that leads to ineffective protection should be detected, for this reason, only elastic region in yellow in Fig. 5, has been considered.

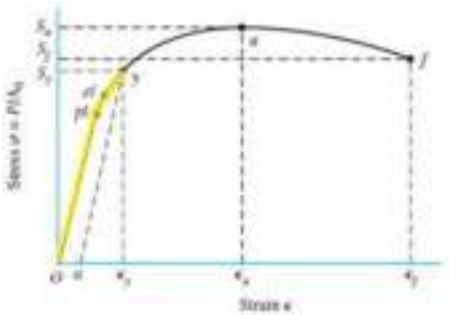

Fig. 5 – Elastic region where $\sigma<\sigma_y$ (S_y) [6].

So doing, a SF defined based on yield strength as defined as reported in Equation (1) should be always higher than 1 because the deformation in critical regions that failure happened during the experimental test will stay in elastic region.

$$\text{Yield Safety Factor}=\sigma_y/\sigma \quad (1)$$

where: σ_y is the yield stress defined as mechanical properties and σ is the allowable stress measured during the loading.

III. EJB 13 XL MODEL CALIBRATION

Comparing Fig. 6(a) that provides the result of Von Mises Stress which is a theoretical measure of stress used to estimate yield failure criteria and Fig. 6(b) that represents SF it should be easy to find similarities. So, SF can be considered a simplified method to summarize the failure recognition.

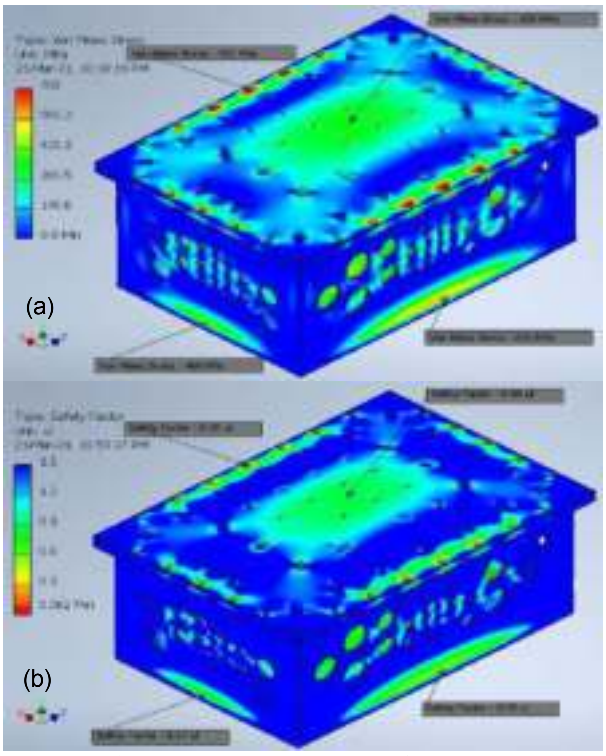

Fig. 6 – Reference model (a) Von Mises Stress and (b) Yield Safety Factor (External view).

Based on the yield definition of SF, for values of SF<1, permanent deformation will be observed in the center of the cover (SF=0.66). The red color around the flange holes shows high amount of Von Mises stress in these areas and this is due to the fact that these areas are under the effect of the pin constraint which is applied instead of screw and makes stress concentration in the software calculations. Due to effect of pin constraint on the flange holes and high value of stress effected by it, it is expected that SF is also too low. There is also SF<1 on the body walls that can create deformation on the holes edge and leakage during the test.

At the center of the bottom plate in the body, there is a high level of stress that correspond to SF=0.53 similar to the situation on the cover with even higher deformation (Fig. 7). Moreover, this failure that leads to permanent deformation. Around the welding lines there is a very low SF and it is a high possibility of failure. However, a part of the stress in this area related to the error in geometry of mesh that can make stress concentration due to very small surface of the mesh (close to zero) on sharp edges and ununiform geometry.

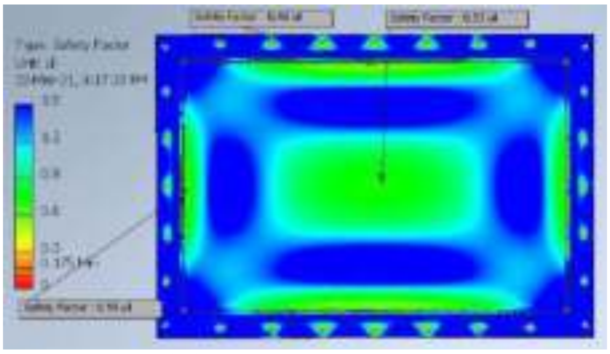

Fig. 7 – Yield Safety Factor in reference model (Internal view).

Replacing bolts with pin constraint abeles the software to measure reaction forces applied to the screws. In other words, the constraints act like a force gauge.

Results of the reaction forces are presented in the TABLE II in each pin constraint.

TABLE II
REACTION FORCE ON THE BOLTS

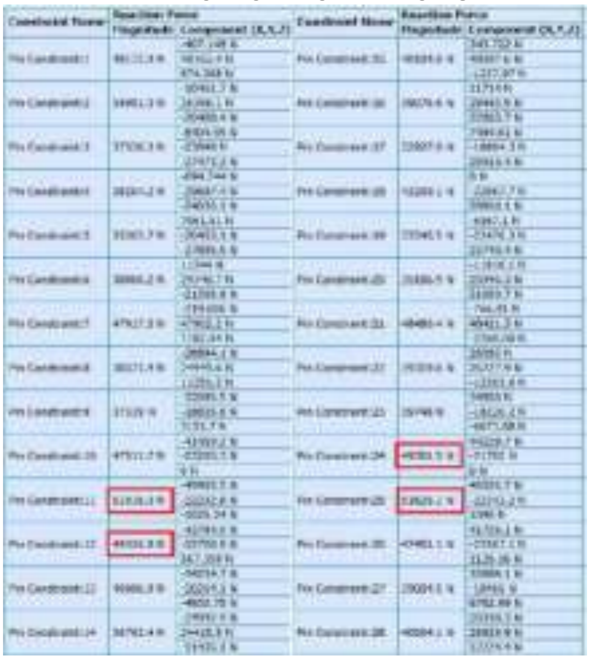

TABLE III
PROOF LOAD FOR METRIC BOLTS [7]

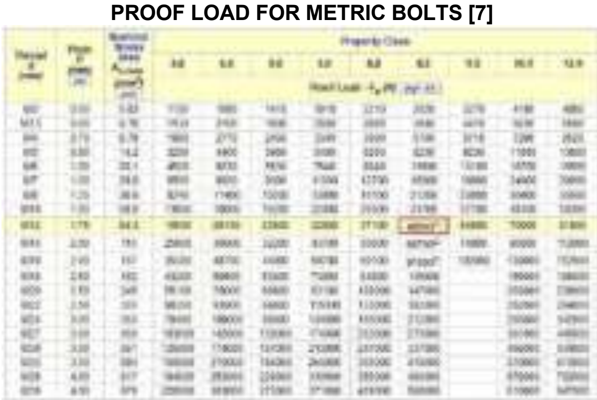

Comparing the reaction forces with the proof load of screw M12 property class 8.8 [7] which is the model used for test (TABLE III) and that can endure 48900 N, shows

that some screws carry the load higher than one that they are designed to endure.

IV. EJB 13 XL DEVELOPMENT & VERIFICATION

Improving the strength of the enclosure is done in 4 different Scenarios in an economical way to increase yield SF to an acceptable level (minimum SF>1) on the critical areas.

Scenario 1: welding line size

As it is shown in the Fig. 6(b), SF near welding line is too low in the reference design so the first idea to support bottom of the body is increasing the size of welding line because it is a minor modification, and it is also the most economical way to improve SF in this area. However, SF do not change considerably (Fig. 8) because amount of stress is too high, but this change provides a positive improvement in overall and specially in case of stress distribution near the flange holes.

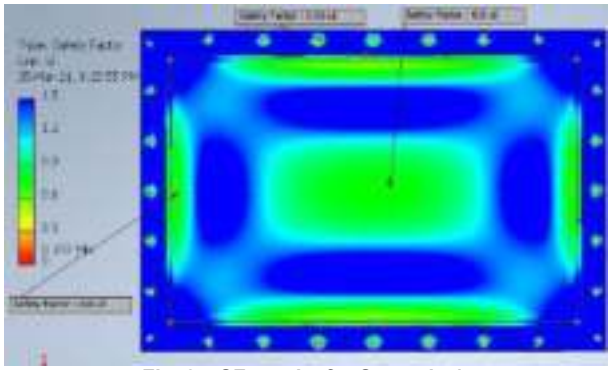

Fig. 8 – SF results for Scenario 1.

Scenario 2: Number and size of flange screws

In this step, the main goal is finding the suitable screw to carry out all the reaction force without any damage to the thread and can reduce the gaps between flanges to keep the flame inside the enclosure during the non-transmission test.

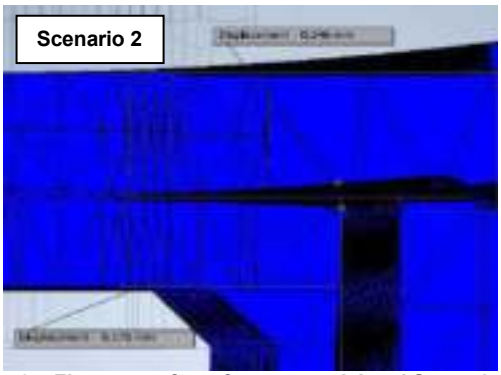

Fig. 9 – Flange gap for reference model and Scenario 2.

The possible operational conditions are considered in the VDI guideline 2230 [8] and according to the measured forces, the suitable size of screw with property class 8.8 is M16. As it can be seen in the reference model, stress distribution along the length of the enclosure is more than the width, and the intensity is higher in the middle. For this reason, 34 screws are used in total with new arrange (Fig. 9).

Scenario 3: Thickness

Increasing the thickness is the fundamental and the most expensive solution for rising the SF, so it is important to change only the thickness in critical areas where SF is low, and deformation is high because these situations can endanger the level of protection of the enclosure. According to the obtained results from previous steps, thickness increase of the bottom plate of the body and cover, respectively, are in priority than other areas, so the bottom thickness is raised by 5 mm and the cover is increased by 2 mm. It can be seen from Fig. 10 that SF>1 on the center of the cover which means that the cover experiences a temporary deformation and then it will back to initial condition because it stays in elastic region. On the other hand, SF at the bottom of the body increases from 0.6 to 0.87 but it is still not enough and further changes are required in this area.

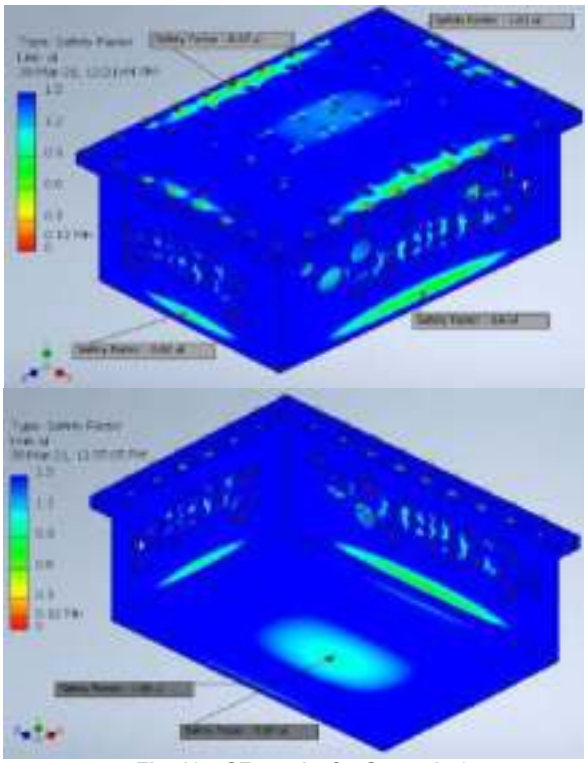

Fig. 10 – SF results for Scenario 3.

Scenario 4: Angle support L on the body

Thickness of the bottom is 20mm and according to standard size of the stainless-steel plate in the market, the thicker size that can be used is 25mm which rises the enclosure mass by 20kg and considerable effect on the final cost. The solution is using angle support L so that it strengths the weak points without significant change on the total mass and additional cost of L supports and welding is lower than using a 25mm thickness plate. Results of simulation shows that angle support L can increase SF considerably by only 5kg extra mass. The supports act directly on critical areas and as it can be seen form Fig. 11 that SF finally reaches to higher than one at the bottom.

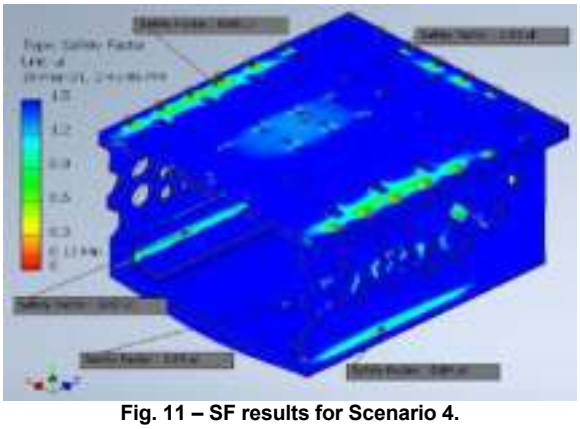

Fig. 11 – SF results for Scenario 4.

Different scenarios are defined to improve SF in the area where there is high possibility of failure. All these scenarios would have been tested step-by-step with a huge waste of time and money, which could be avoided by using FEA.

Verification by experimental test

The overpressure test was done at 4 steps in 12.2 bar, 14.9 bar, 15.2 bar and 16.1 bar by considering the internal volume of enclosure and according to the ambient temperature -20°C, -40°C, -50°C and -60°C. The duration of test was 15 s for each pressure based on the required time for static overpressure test [5]. The screws were checked after the test and any damage on the thread part of screws and flange holes were not detected as reported in TABLE IV.

TABLE IV
OVER-PRESSURE TEST STEPS OF EJB 13XL AT INERIS LABORATORY [9]

Reference Material	Reference Pressure	Correspondence	Theoretical Pressure	Real Pressure	Hold Time	Deformation or leakage seal observed	Result
20-AA-337	NC	NC	12.2 bars	12.2 bars	15 s	No deformation observed	Positive
20-AA-337	NC	NC	14.9 bars	14.9 bars	15 s	No deformation observed	Positive
20-AA-337	NC	NC	15.2 bars	15.2 bars	15 s	No deformation observed	Positive
20-AA-337	NC	NC	16.1 bars	16.1 bars	15 s	No deformation observed	Positive

Non-transmission test was also done with injecting 37% H2 gas in volumetric ratio with air for Group IIB+H2 (EJB enclosures are a part of them) [5] inside the enclosure and any flame was not detected after ignition and the test was positive (Fig. 12).

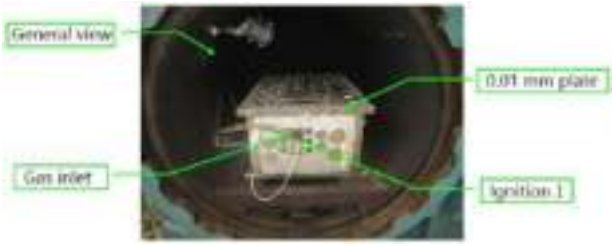

Fig. 12 – Non-transmission test of EJB 13XL at INERIS laboratory [10].

As desired, the results of these simulations are validated by experimental tests and according to the positive result of these tests, it can be sure that simulations considerably show the real behavior of the enclosure during the tests so, the method and criteria of the simulations used for EJB 13XL can be considered as a reference point for validation and comparison of the results other similar applications as EJB Aluminum with large glass window.

V. EJB ALUMINUM WITH LARGE WINDOW

The goal of this chapter is evaluating the possibility of a large window design on the cover of enclosures without any change in the cover mold in different sizes (TABLE V) from EJB 2 to EJB 14 [11] according to the validated simulation method from previous chapter. It means that the only variable factor is the window size, glass thickness and its location on the cover. EJB Aluminum enclosures are made by Aluminum EN AC-43100 material and the glass is tempered glass with high resistance.

TABLE V
EJB ENCLOSURES IN ALUMINIUM WITH WINDOW [11]

ENCLOSURE MODEL	OVERALL DIMENSION *Length x Width x Height* [mm]	WINDOW SIZE [mm]
EJB-2	298x238x163	110x75
EJB-3	410x236x167	110x75
EJB-3A	410x236x191	150x75
EJB-4	415x300x165	150x75
EJB-5	477x297x221	150x150
EJB-6	478x404x226	150x150
EJB-8	630x361x246	150x150
EJB-9	532x465x252	150x150
EJB-10	754x366x294	150x150
EJB-11	592x501x257	150x150
EJB-12	801x450x300	150x150
EJB-13	830x604x298	300x75
EJB-13A	830x604x404	300x75
EJB-14	970x770x478	300x75

Glass thickness is calculated according to the TIMOSHENKO formula from equations (2) and (3) [12] by considering SF=3 theoretically for the largest size of window. A so high SF value is related to the impact test that will be done before overpressure test on the glass and makes it more vulnerable.

$$s = \sqrt{6 \cdot \beta \cdot q \cdot \frac{a^2}{\sigma}} \quad (2)$$

$$f = \frac{\alpha \cdot q \cdot a^4}{0.073 \cdot s^3} \quad (3)$$

where: s is the glass thickness (monolithic float sheets) in mm; f is the deflection under the load in mm; q is the applied pressure on the surface of the glass (plus self-weight when placed horizontally) in Pa=N/m^2; a is the Shorter side of the plate expressed in m (in the case of support only on two opposite sides, the length is that of the free sides); σ is the breaking stress for glass (Tempered glass in this case) in MPa=N/mm^2; α and β are dimensionless coefficients function of b/a, that is larger side b on smaller side a [12] so a has to be always less or equal to b. In the case of support on two sides, consider $b/a=\infty$.

The glass is glued to cover by a layer of silicon and internal installation of the glass provides larger glued area to avoid leakage and stop possible sliding of the glass on the cover surface (Fig. 13).

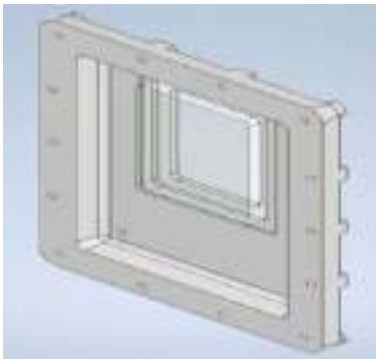

Fig. 13 – Internal view of the cover.

The goal of this investigation is the evaluation of permanent deformation and failure (breaking point) of the cover. So, two safety factors are defined based on yield and ultimate strength to check both possibilities. It should be mentioned that yield SF is not defined for glass because it is a brittle material, and it does not have plastic region and stress will rise till breaking point so ultimate SF is chosen for glass on the software. EJB aluminum with window should be designed so that they can resist in equivalent pressure at T= -50 ˚C according to TABLE I.

The results of simulation are provided for all models reported in TABLE V of EJB enclosure and among the results data, it is mainly focused on the SF and displacement in different spots of the cover.

EJB 2 is the smallest size of EJB series and cover without window passed the overpressure test in 4 times of the refence pressure (36 bars) so as it was expected, simulation results are satisfying for applying the window. As already discussed, the weakest point is at the center, so it is not surprising that SF is the lowest there. Yield SF is equal to 1.2 on the cover (Fig. 14) and it means that the cover will return to initial condition after 0.35 mm displacement (TABLE VI). High level of SF on the glass is related to its location where window applied so it has lower deformation and because of the SF amount that is considered for glass thickness calculation.

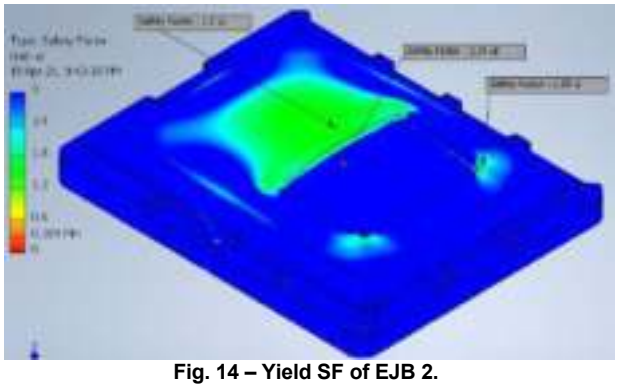

Fig. 14 – Yield SF of EJB 2.

EJB 14 is the largest enclosure, and it is expected that it has high displacement at the center, so the window with dimension 300x75mm is located somehow glass suffers the lowest bending. Yield SF=0.66 on the sides is lower than the one in the center which is 0.78 (Fig. 15) but that area is affected by the pin constraints applied on the flange holes. SF on the glass near the window edge is 1.18 that is the lowest amount calculated for glass in all series of enclosures.

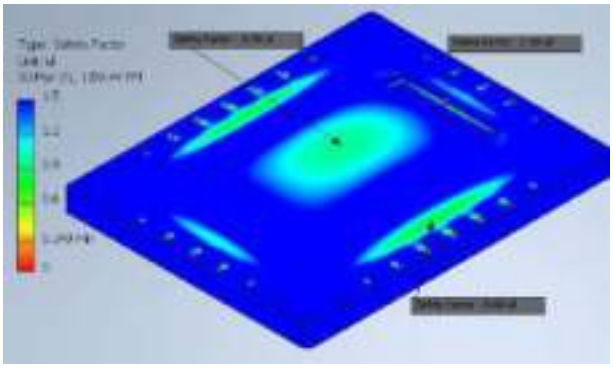

Fig. 15 – Yield SF of EJB 14.

TABLE VI provides an overview of the simulation results for all series of EJB aluminum enclosures with window to check the possibility of designing window on the cover. Having yield and ultimate SF on the cover provides more precise analysis about situation of the cover after tests. As it can be seen, there is no risk of deformation and breaking from EJB 2 to 3A because both Yield and Ultimate SF are higher than 1 and from EJB 4 to EJB 6 is possible to apply the window with very low risk of deformation (Yield SF=0.8) because ultimate SF and low deformation make it sure that cover will not break.

From EJB 8 to 14 there is a higher risk of permanent deformation that leads to leakage during the experimental test due to their larger dimensions and in some cases such as EJB 9 and 11 there is a high breaking possibility in 17 bars.

In overall, EJB 9,11 and 13 can be suitable cases for overpressure test as they are more possible to have leakage or break during the test and they are in different range of dimensions so if they pass the test positively, others can be safe due to higher SF otherwise, the thickness of the covers should increase.

TABLE VI
SIMULATION RESULTS OF EJB ALUMINIUM WITH WINDOW

ENCLOSURE	WINDOW SIZE (mm)				DEFORMATION (mm)	SAFETY FACTOR		
						COVER		GLASS
	110*75	150*75	150*150	300*75		YIELD	ULTIMATE	ULTIMATE
EJB-2	*				0.35	1.2	2.01	2.29
EJB-3	*				0.41	1.08	1.74	2.44
EJB-3A		*			0.28	1.59	2.68	3.24
EJB-4		*			0.6	0.83	1.4	1.87
EJB-5			*		0.69	0.79	1.36	2.26
EJB-6			*		1.04	0.8	1.33	1.47
EJB-8			*		1.28	0.65	1.1	1.33
EJB-9			*		2.37	0.46	0.76	1.26
EJB-10			*		1.2	0.7	1.26	1.46
EJB-11			*		1.93	0.64	1.06	1.9
EJB-12			*		1.3	0.75	1.26	3
EJB-13/13A				*	2.27	0.71	1.12	2.29
EJB-14				*	2.86	0.78	1.24	1.18

Tests carried out on all these enclosures with large windows were successful with only the addition of a rear cover reinforcement for the highest pressures only and therefore for temperatures of -50°C.

VI. CONCLUSION

There are a lot of limitations in design of Ex enclosure because of the environment that usually this equipment will be used, so a high level of safety is required and consequently, the price is higher than normal enclosure. Simulation is a method that gives the designer a chance to design precisely and effectively, but the results need to be validated in reality. In this study, simulation results are verified with experimental test for EJB 13XL and then the verified simulations are considered as a reference point to simulate EJB Aluminum with large window and it is also possible to use them for other similar products.

The key factors in design of an equipment are geometries and materials. There are limitations for increasing the thickness in enclosures and it cannot always solve problems. Increasing the thickness means increasing weight and it can be a problem for transport and installation on the structure. Changing material is the solution that can deal with thickness limitation and extra weight but to guarantee the same level of safety, the replaced material must have higher yield and ultimate strength than the previous one.

Nowadays, there are some materials such as metal based composite that can be stronger than stainless steel and lighter than aluminum but because of the higher cost of the production, they cannot compete with current metals in the market. In near future, the cost of aluminum and steel will increase due to scarcity of the resources meanwhile the technology of composite material will develop to reduce the production cost. So, it will be a big step to produce composite enclosures as a pioneer in Ex market with larger dimensions and ability to keep higher pressure.

VII. NOMENCLATURE

FEA Finite Element Analysis

VIII. REFERENCES

[1] EN/IEC 60079-1; Ch.5.2.

[2] https://marechal.com/technor/en/gamme/enclosures/

[3] https://www.linkedin.com/pulse/how-finite-element-analysis-can-help-you-why-useful-your-madier/

[4] https://www.autodesk.com/products/inventor/overview?term=1-YEAR

[5] EN/IEC 60079-1, Ch.15.2.1.

[6] Beer Johnson Mechanics of Materials 6th Edition, Safety Factor.

[7] https://www.engineeringtoolbox.com/metric-bolts-minimum-ultimate-tensile-proof-loads-d_2026.html

[8] Design Guideline VDI 2230 - Bolted Joint Design to VDI 2230.

[9] Overpressure test "d", TEST MO0690 - EVES 20/0431, INERIS laboratory.

[10] Non-transmission test, TEST – MO0054 – EVES 20 / 0407, INERIS laboratory.

[11] https://marechal.com/technor/en/gamme/enclosures/gas-group-iib--h2/ejb-aluminium-122

[12] Saint Gobain “Glass Manual”-1997 edition-pages 32-33.

IX. VITA

Nima Dalaeli graduated from Politecnico di Milano University in 2021 with a MSc degree in Energy Engineering. He was an R&D Mechanical Engineer at Technor Italsmea Company from 2020.

nimadalaeli@gmail.com

Kim Fumagalli graduated in Electrical Engineering from the University of Politecnico di Milano in 2005. He has obtained the Ph.D. degree in Electrical Engineering at Politecnico di Milano, Milan, Italy, in 2009. His research areas include LED Source and LED Lighting System, Electrical and Lighting systems for Ex environment, Batteries and Cells, PV panels, Industrial Trucks and Internal Combustion Engines for Explosive Atmosphere, Ex Products Certification and Testing. He is a R&D Director and Ex Authorized person of Technor Italsmea. He is a member of the IEC Work Group WG40, WG37, MT60079-1, MT60079-2, MT60079-7, MT60079-14, MT60079-18 and MT60079-28. He is a member of Standards Committee of CEI (Italy) CT31 and SC34D. He has received IECEx Certificate Personnel Competence. He is a member of the PCIC Europe committee and holds the position as Assistant Technical Secretary. He has authored several papers.

k.fumagalli@italsmea.com

Roberto Sebastiano Faranda received the Ph.D. degree in electrical engineering from the Politecnico di Milano, Milano, Italy, in 1998. He is currently Full Professor with the Department of Energy, Politecnico di Milano. His research areas include power electronics, power system harmonics, power quality, power system analysis, smart grids, Ex environment and distributed generation. Dr. Faranda is a member of the Italian Standard Authority; the Italian Electrical, Electronic, Automation, Information, and Telecommunications Federation; and the Italian National Research Council group of Electrical Power Systems. He has authored more than 150 papers.

roberto.faranda@polimi.it

Life Extension of Power Transformers with Proper Moisture Management

Paper No. EUR22_20

Drew Welton
Intellirent
Roanoke, TX
USA

Charles Sweetser
OMICRON
Waltham, MA
USA

Abstract - Excessive moisture within the oil and insulating materials of a transformer has a significant effect on the life cycle of these critical and expensive assets. Moisture is one of the most influential elements that can accelerate ageing in oil, paper, and pressboard insulation, possibly resulting in severe damage and premature failure. In this session we will discuss how moisture accumulates, how it effects the aging process, and how significant damage or failure from excessive moisture can occur. We will look at ways to determine the amount of moisture that is present, including the challenges associated with using traditional dissolved gas analysis, (DGA), or oils screens for moisture determination. We will explore more modern techniques such a dielectric frequency response, (DFR).

Index Terms — Insulation properties, polarization losses, conductive losses, degree of polymerization, dielectric frequency response.

I. Damaging Effects of Excessive Moisture

It is worthy to mention the dangerous effects of moisture and high temperatures in insulation systems. Together they negatively affect the performance and life expectancy of insulation systems. Moisture and/or high temperatures contribute to the following:

- Decrease in dielectric withstand
- Accelerated cellulose aging
- Bubble evolution

Moisture enables acids to serve as a catalyst to assist the breakdown process of the insulation. As the polymer chains of the cellulose are broken down into smaller chains, the cellulose over time becomes brittle. This brittleness can be measured by the Degree of Polymerization (DP), where new cellulose has a DP of 1200 and a DP of 200 indicates "end-of-life."

Moisture lowers the bubbling point in the transformer. This creates voids in the insulation and can result in partial discharge (PD). PD can lead to excessive deterioration of the insulating paper which can become irreversible. (fig.1)

Figure 1 -Severe breakdown of paper insulation

In Fig.2 we compare operating temperature, along with moisture content, and how it corresponds to life expectancy. Overheating can be the results of overloading, poor cooling systems, or abnormal operating conditions such as excessive volts per hertz.

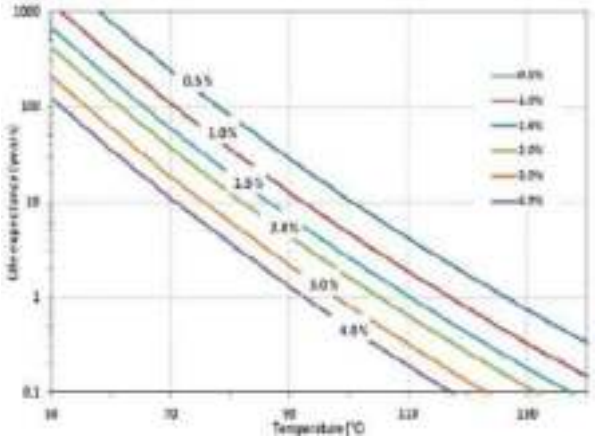

Figure 2 – Life expectancy proportional to temp and % moisture

II. Causes of Excessive Moisture

Excessive moisture in a transformer's insulting system can be summarized as follows:

A. *External Moisture Ingress*

Moisture intrusion from outside humid air makes its way into the transformer by:

- Leaking seals or gaskets surrounding the bushings or radiator
- Free breathing conservator without a descant, or improper descant
- During bushing changes or installations
- During the manufacturing process

B. *Natural Aging of the Insulating Materials*

- Degeneration of the cellulose material and paper within a transformer ultimately determines its service life
- The measure of cellulose health is referred to as "Degree of Polymerization. (DP)
- As the cellulose ages, resin bonds break down into smaller lengths, and the DP values fall
- The breakdown of the resin bonds produces CO, CO_2, and H_20
- The water molecules greatly reduce the mechanical forces the insulating system can withstand.

C. *Moisture Assessment Samples*

As an industry standard, IEEE C57.106-2002 states that for new transformers moisture content should not exceed:

- 500 kV- Less than .05% by weight
- 69-240 KV- Less than 0.8% by weight
- 230 kV and below- 1.25% by weight

as an example:

- New 450 MVA, 245-20 kV two-winding transformer weighs ~ 250T
- •Core & coils 125T of which 25T is cellulose
- At 2% water, there is 500 kg (132 US Gallons!) of water in the insulation.
- To achieve recommended 0.5% moisture content, 375 kg (99 US Gallons!) of water must be removed prior to installation.

Typical increase of moisture in a transformer can be in the order of 0.05 to 0.2%/year depending on the design. Figure 3 classifies the degree of moisture content and the scale of criticality based on various industry recommendations.

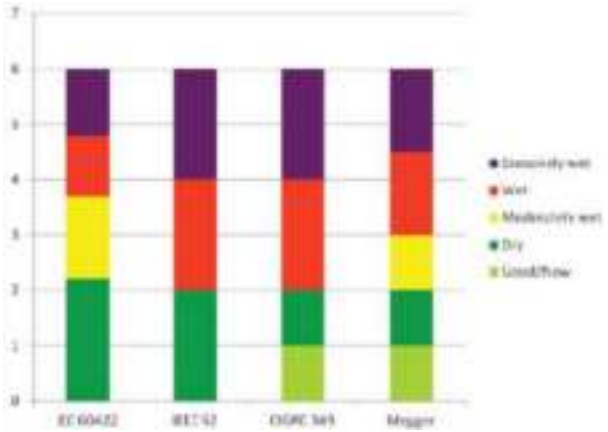

Fig. 3- Moisture assessment examples.

III. Moisture Measurement Methods

There are several methods available to measure the moisture content in the solid insulation of the transformer.

A. *Direct Method; Karl Fischer Titration*

Taking a paper sample from the transformer's insulation for laboratory analysis. However, several factors may affect the results of KFT analyses:

- There can be an ingress of moisture from the atmosphere during sampling, transportation, and sample preparation. This happens particularly during paper sampling from open transformers.
- Cellulose binds water with chemical bonds of different strengths. It is uncertain whether the thermal energy supplied releases all the water.
- Heating temperature and time changes the released water.
- Another issue for direct measurements of moisture in cellulose is the uneven distribution of moisture within the transformer.
- KFT results also suffer from a poor comparability between different laboratories

B. *Indirect Methods; Moisture-in-Oil*

Measuring moisture levels in oil is probably the most common method for moisture assessment. Many operators of power transformers apply equilibrium diagrams to derive the moisture by weight (%) in cellulose from the moisture by weight in oil (ppm).

This approach consists of three steps:

- Sampling of oil under service conditions
- Measurement of water content by Karl Fischer titration

- Deriving moisture content in paper via equilibrium charts

The procedure is affected by substantial errors, e.g.:

- Sampling, transportation to laboratory and moisture measurement via KFT causes unpredictable errors.
- Equilibrium diagrams are only valid under equilibrium conditions (depending on temperature established after days/months).
- A steep gradient in the low moisture region (dry insulations or low temperatures) complicates the reading.
- The user obtains scattered results using different equilibrium charts.
- Equilibrium depends on moisture adsorption capacity of solid insulation and oil.

C. *Relative Humidity*

Measures moisture saturation using a capacitance probe.

D. *Polarization/Depolarization Current (PDC)*

A time domain current measurement records the charging and discharging currents of the insulation. They are usually called Polarization and Depolarization Currents PDC. Figure 4 illustrates the test current response of a PDC measurement.

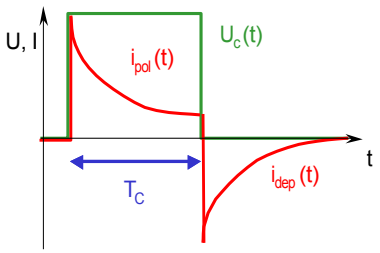

Figure 4 - PDC Wave Shapes

E. *Power Factor Frequency / Tan Delta Measurements*

Tradition 50/60Hz Tan Delta, or Power Factor measurements indicate the overall health of the transformer's insulation system. Insulation systems consisting of cellulose and oil exhibit both polarization and conductivity phenomena.

These two phenomena occur simultaneously, and superposition must be applied to separate the effects of both cellulose and oil

.

Moisture, temperature, and aging by-products influence both polarization and conductivity domains, where moisture has the greatest influence. Both polarization and conductivity effects can be represented by the losses they create. Plotting dissipation factor as a function frequency provides insight regarding the characteristics of moisture, aging, temperature, contamination, oil conductivity, and the influence of external environmental conditions.

- *Polarization Losses*

In the frequency range in the neighborhood of DC(0 Hz) to 10 kHz, two types of polarization losses exist, interfacial polarization (0.3 - 0.5 mHz) and molecular polarization (10 kHz).

When combining insulating materials within an insulation system, such as cellulose paper and mineral oil are combined, an interfacial polarization zone can be defined. Interfacial polarization is typical for non-homogeneous dielectrics with different permittivity or conductivity. The result will be the accumulation space charge carriers at the oil/paper interface. The interfacial polarization is the resonance that occurs between the propagation speed and distance traveled of the space charge carriers as a function of the insulation geometry (ratio between oil, barriers, and spacers). Depending on the moisture content and conductivity of the cellulose and oil, respectively, interfacial charge resonance occurs at different frequencies, e.g. 1 mHz for dry and cool insulation systems, and >1 Hz for wet and hot insulation systems.

In cellulose and oil insulation systems the individual molecular structures produce polarization losses. These losses can peak around 10 kHz. At or near 60 Hz, these losses cause the power factor values to slightly increase and decrease proportionally with frequency for healthy insulation systems. Figure 5 illustrates this behavior in the 10 Hz to 1 kHz range.

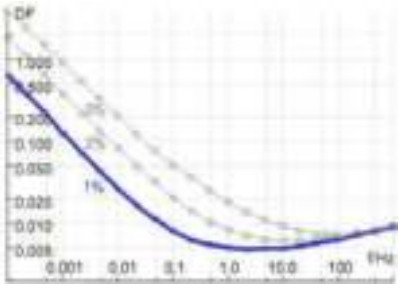

Figure 5 – Polarization Losses in Cellulose

- *Conductive Losses*

Both cellulose and oil exhibit conductive losses, however oil is unique in the fact that by itself it solely produces conductive losses. Figure 6 illustrates contact conductive losses in oil. While conductive losses are seen in both cellulose and oil, the losses in the oil dominate. At very low frequencies occurring below the interfacial polarization range, the opposite is true, the conductive properties of oil are minimized as compared to cellulose.

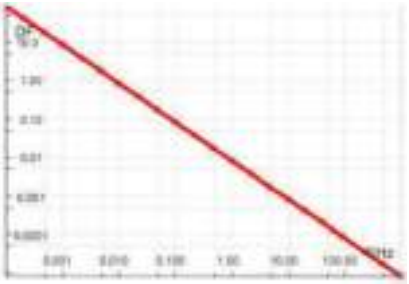

Figure 6 – Conductivity Losses in Oil

F. Dielectric Frequency Response (DFR)

The Dielectric Frequency Response test measures and models the properties of insulation systems across a wide frequency range, e.g., 0.1 mHz. to 1000 Hz. This frequency range spans over 7 decades enabling separation between the effects of polarization losses, conductive losses, and aging by-products within the overall insulation system. Modeling algorithms are applied to estimate moisture, conductivity, and insulation geometry.

Figure 7 displays the dielectric behavior of solid insulation and oil having 1.0 % moisture content at 20 □C. The frequency range of 10 Hz - 1 kHz is dominated by the cellulose insulation, however the measurement cables and the connection technique also influence this region. Oil conductivity causes the steep slope at 0.01 Hz – 1 Hz. Conductive aging by-products increase the oil conductivity and thus influence this area. The interfacial polarization (insulation geometry, duct space characteristics, ratio between oil, barriers, and spacers) determines the "hump" in the very low frequency range. The higher the ratio of oil to pressboard in the duct space, the more dominating is this effect. Finally, the moisture effects within the cellulose appear again at the frequencies below 0.5 mHz.

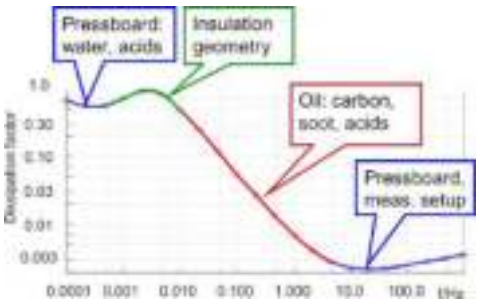

Figure 7 - DF vs. Frequency

IV. Drying Methods

The different methods for drying can be summarized as follows:

Two major techniques are used:

- *Drying the insultation by drying the oil*

This method can be performed with molecular sieves, cellulose filters, cold traps, combined oil regeneration and degassing. Considerations for these methods should include keeping the transformer in service during the drying process, cost of the drying process, and size of the transformer. Newer technologies in high volume filtration systems offer a cost-effective solution, along with the ability to remove combustible gasses during the filtration process.

Modern on-line drying systems utilize large capacity absorbent filters that store the water during the filtering. At regular intervals the filters are automatically regenerated (re-dried). Regeneration of the filters at regular intervals considerably increases water removal efficiency and accelerates the water removal process from the transformer. One benefit of using this method over alternative continuous high vacuum systems is that it does not remove the nitrogen blanket from the transformer, disturb the oil dissolved gas analysis, or alter the oils chemical qualities. These systems also allow for remote monitoring via cellular modem.

- Case study using a modern, high capacity online drying system:

A portable online drying system (fig.8) was used on a group of near identical, 3 ph - 66/22 Kv, 10 Mva transmission transformers over 40 years old with 12,000 liters of oil and free breathing.

The pre-filtering water in cellulose was calculated at 4.44% at midday, and as the transformer increased in load/temperature, the 5pm calculation was 4.32%. This is a normal event.

When the transformer was re-analyzed after 72 days of drying, the 12:00pm water in cellulose calculation was 2.91% and the 5pm 2.64%. Most importantly, the oil relative saturation has reduced by 13% at the same load point, and the dielectric is markedly improved. This process was conducted without the need of taking the transformer off-line.

An additional drying cycle of 2 weeks eventually reduced the moisture content down to just under 2%.

Figure 8 – Portable online Drying System

- *Drying the insulation with heat and vacuum*

A popular method for drying the insulation of a new transformer is through vapor phase drying, performed in a manufacturing setting. This process does not lend itself well to transformer drying in the field for a variety of reasons, including the difficulty of removing residual kerosene which can cause a potential change in in transformer oil flash point. Vapor phase drying methods can also create further breakdown of the cellulose within an aged asset.

V. Conclusion

Moisture is one of the worst enemies of a power transformer. It limits its loading capability, accelerates its ageing process, and decreases its dielectric strength. The water/moisture in a transformer resides in the solid insulation, not in the oil. Dielectric frequency response measurement is a good technique for moisture assessment as it can measure moisture content in the cellulose insulation, the conductivity/dissipation factor of the insulating oil accurately (corrected to 25°C reference temperature), and the power frequency tan delta/power factor, accurately (temperature corrected to 20°C reference temperature). Drying a power transformer can effectively be performed with modern filtration techniques without taking the transformer offline.

VI. References

[1] IEEE C57.161-2018, " IEEE Guide for Dielectric Frequency Response Test".

[2] M. Koch, M. Krüger: “Moisture Determination by Improved On-Site Diagnostics”, TechCon Asia Pacific, Sydney 2008

[3] S.M. Gubanski, P. Boss, G. Csepes, V. Der Houhanessian, J. Filippini, P. Guuinic, U. Gafvert, V. Karius, J. Lapworth, G. Urbani, P. Werelius, W. Zaengl. "Dielectric Response Methods for Diagnostic of Power Transformers” Preport *of the TF D1.01.09* , CIGRE 2002

VII. Vita

Drew Welton (IEEE Senior) is Vice President of Sales for Intellirent, division of Electrorent, providing strategic leadership to the sales team and creating new business development for the industrial testing, power producing industries. Welton was previously the North American Regional Manager for OMICRON, starting in 1997. Prior to his career with OMICRON, Welton was a Regional Sales Manager with Beckwith Electric. He also served as National Sales Director for Substation Automation with AREVA T&D. Welton has written numerous articles on substation maintenance testing and has conducted training sessions for substation technicians and engineers at utilities and universities across North America. He is a 20-year Senior Member of IEEE-PES, IAS, and an active member of the Transformers Committee. He has been a contributor on several PSRC working groups and presented at many industry conferences specific to power system protection and control. He has a bachelor's degree in Business Administration from Fort Lewis College, Durango, Colorado. dwelton@intellirentco.com

Charles Sweetser received a B.S. Electrical Engineering in 1992 and a M.S. Electrical Engineering in 1996 from the University of Maine. He joined OMICRON electronics Corp USA, in 2009, where he presently holds the position of PRIM Engineering Services Manager for North America. Prior to joining OMICRON, he worked 13 years in the electrical apparatus diagnostic and consulting business. He has published several technical papers for IEEE and other industry forums. As a member of IEEE Power & Energy Society (PES) for 17 years, he actively participates in the IEEE Transformers Committee, where he held the position of Chair of the FRA Working Group PC57.149 until publication in March 2013. He is also a member of several other working groups and subcommittees.
charles.sweetser@omicronenergy.com

Digitally Enabled Predictive Maintenance Solution for Electric Motors

Paper No. PCIC Europe 22_21

Dr Ankush Gulati
ABB
Singapore

Veronica Chew
ABB
Singapore

Cajetan T Pinto
ABB
Spain

Hock Cheong Ng
Denka
Singapore

Abstract - Advances in connectivity solutions, low-cost wireless sensors and cloud storage have made wider adoption of predictive maintenance for low voltage motor driven systems, more viable. A monitoring device with multi-parameter sensing functionality can help monitor and trend the wear of rotating machine components and identify factors that contribute to such degradation. When compared to just monitoring overall vibration and temperature, capturing leakage flux and acoustic signals, and using advanced analytical methods, add more to the detectability of likely faults. However present-day technology and solutions are not without challenges. This paper brings out the deployment of a wireless smart sensor-based solution as an integrated predictive maintenance system with remote monitoring for electrical motors at a Chemical plant. Application of maintenance support tools that use information from monitored assets to address maintenance needs in the short to medium term are also discussed. Successes of this approach have resulted to a 100% reduction in motor downtime and have also helped with the identification of process related issues, resulting in increased reliability and OEE.

I. INTRODUCTION

Moving to a predictive maintenance approach has been shown to reduce unscheduled maintenance, catastrophic failures, mean-time-to-repair and maintenance costs, whilst increasing asset and process availability and reliability. In a survey of 500 companies that implemented predictive maintenance methods, it was seen that such adoption resulted in a 55% reduction in catastrophic failures, a 60% reduction in mean-time-to-repair and a 30% increase in availability [1].

Though the benefits of implementing condition-based approaches for maintenance are clear, the wider adoption of predictive maintenance has been rather slow mainly due to the high cost of its implementation – and even more so when considering lower cost assets such as low voltage motor driven systems.

Industry 4.0 has now brought about a paradigm shift in the ability to look at plant wide predictive maintenance afresh. Advances in connectivity solutions with the development of low-cost wireless sensors and cloud storage options, have made collecting and analyzing large amounts of data viable. Insights are available that not only support maintenance decisions, but also help to throw light on process issues, and even validate if the right asset was selected for the application.

Integrated monitoring devices with multi-parameter sensing functionality are deployed to monitor and trend wear of rotating machine components, and to identify factors that contribute to such degradation. When compared to just monitoring of overall vibration and temperature, capturing additional data from leakage flux and acoustic signals, and using advanced analytical methods add a lot more to the detectability of likely faults and the discernability of underlying causes.

However, technology and solutions available presently are not without challenges. In plants where planned maintenance outage intervals could be over a year, early detection is critical - and limitations of the sensitivity of measurement devices to pick up faults could result in delayed actions and even precipitate secondary damage. Additionally, it could be difficult to identify the exact cause of a problem when more than one fault is simultaneously present, or when measurements can be affected by coupled equipment that is not monitored.

This paper brings out the deployment of a wireless smart sensor-based solution as an integrated predictive maintenance system with remote monitoring for electrical motors installed in a chemical plant. While addressing the challenges involved in maintenance planning, the paper also discusses the application of maintenance decision support tools that use information from monitored assets to address maintenance needs in the short to medium term.

Successes of this approach have contributed not only to “zero failure” objectives but have helped with identification of process related issues and their timely resolution, resulting in increased motor reliability, availability as well as process Overall Equipment Effectiveness (OEE).

II. TRADITIONAL APPROACH TO CONDITION MONITORING/PREDICTIVE MAINTENANCE

In the simplest terms, predictive maintenance could be defined as a maintenance philosophy associated with monitoring the health of an asset and then based on the gathered data, carrying out analysis to predict the when, what, and why – when would the asset require maintenance, what is required to be done, and why is it required. Engineers and technicians usually use specific tools to collect asset data manually at regular time intervals. Traditional approaches have used portable instruments for vibration, thermography, lubricant analysis, and even electrical signature analysis when monitoring motors. Upon periodically collecting data, engineers consolidate the information manually for record purposes and more detailed analysis. The strategy for collection of data at this plant site was based on measurement of overall vibration levels along with spot surface temperatures on a quarterly basis and recorded manually (See Fig 1)

MAINTENANCE CHECK LIST (YEARLY)				
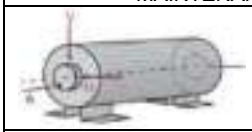	JAN	APR	JUL	OCT
DE-H (mm/s)				
DE-V (mm/s)				
DE-A (mm/s)				
NDE-H (mm/s)				
NDE-V (mm/s)				
NDE-A (mm/s)				
TEMP (°C)				

Fig. 1 Sample check list used by the plant

To perform such predictive maintenance is not only time consuming and labor intensive, but it also brings along several limitations and risks such as:

A. Faults and failures between data collection occasions

For data collected manually every 90 days, there is always a possibility of a defect developing between data collection periods, which would remain undetected until the next instance of data collection. This leaves the asset unmonitored for the duration between data collection instants, and faults that develop during these unsupervised periods could increase the risk of an unexpected failure.

B. Non-repeatability of data

With manual data collection, data could vary on each instance of measurement due to differences in sensor placement or instrument settings. The resulting measurement differences could hinder analysis when comparing trends.

C. Changes in operating condition

It is possible that changes in load or other process parameters affect measured data. When data is measured on a one-off basis, it is not possible to ensure that operating conditions are identical when comparing data trends.

D. Inaccessible machinery

At times, it becomes extremely difficult to access machinery due to physical impediments or even its location. Examples are motors located in confined spaces, at high levels where scaffolding access is required or applications that have motors housed within an enclosure, with no possibility of access during operation. In such cases equipment monitoring is not only difficult, but when attempted could be unsafe.

E. Manual analysis

Manual aggregation and analysis of the collected data is time consuming, cumbersome, prone to error, and makes maintenance prioritization a challenge, particularly when many motors are monitored. Delays in timely actions due to a time-consuming manual could end in costly lapses.

III. MAINTENANCE STRATEGY AT SITE

The maintenance strategy that has been in use in the plant is hybrid in nature, relying on a combined approach of time-based and condition-based maintenance.

Outages of around two days for such maintenance typically happen twice every year. In the time-based approach, motors are subjected to a full maintenance process once in three years that involves change of bearings and an overhaul of the stator windings. These time-based service actions were supplemented with outcomes from periodic route-based vibration measurements. With this approach the plant experienced an average of six motor failures per year.

One major challenge was to attend to all identified motors with full scope maintenance during the planned outages and as a result, it became important to prioritize maintenance and to pinpoint necessary activities to be performed during maintenance.

As the approach did not help in reducing the number of failures, it was decided to adopt methods that included a closer surveillance or tracking of the motor condition along with better and earlier discovery of defects, as well as identification of underlying causes. This approach could help in adding focus to the service actions during regular maintenance, which would mean identifying and addressing of root causes, prioritizing the motors that would need more intensive service actions and, in some instances, also adjusting the outage plan for a motor.

IV. REDUCING FAILURES

A target was set to bring down the average number of unexpected failures from around six per year down to around three failures per year within a two-year period. To reduce the risk of unexpected failures, it was decided to adopt a monitoring approach that kept a close track of the motor condition while addressing the following:

1. Increase the detectability of problems: Picking out faults and anomalies at an early stage and minimizing false positives and negatives
2. Increase discernability of fault detection: Determine and isolate faults when simultaneously present, including fault contributors and root causes
3. Improve failure prevention: Determine preventive actions in a timely manner

The method for monitoring would need to cover the major failure modes of the motor as well as address the underlying causes of the failures.

An integrated monitoring device with multi-parameter sensing functionality developed, was selected to monitor, trend the wear of rotating machine components, and identify factors contributing to such degradation.

The integrated sensing device, a smart sensor, focused on tracking the bearing condition, monitoring the temperature of the motor body and has the capability to pick up stray flux and acoustic signals. This approach covered close to 70% of the failure modes that have been described in literature [2] - considering their linkages with underlying causes and contributors (see Fig. 2).

A combination of signals that are made available at the same occasion with an integrated sensing device on the motor, increases the possibility to combine data and

confirm defects with a greater confidence level.

Most of the failures of low voltage motors (over 50%) occur due to bearing failures. [2]

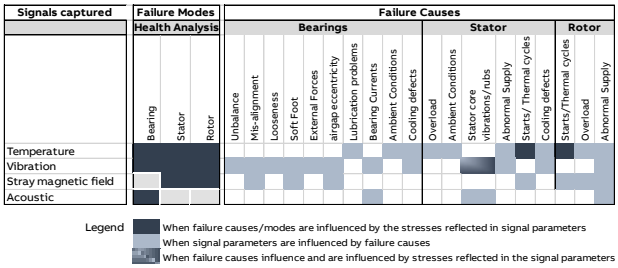

Fig. 2 Identifying motor failure modes

If bearing damage goes undetected it could lead to significant secondary damage spreading to other bearing assembly components, the shaft, and ultimately to a stator-rotor rub, resulting in a stator winding failure. This kind of failure often causes severe hot spots in the stator and rotor core and the extent of repair required is so extensive that it could often end with the replacement of the motor. The recovery time is significant both with repair or new replacement motor options - and even in cases when the hot standby is available, the risks of plant downtime could be considerable.

The area of insulation condition monitoring of the stator winding (accounting for around 15% of failures) could not be justified by direct on-line monitoring methods. With the stray flux being monitored, it was possible to address the problem of inter-turn fault detection. But this was seen to be more of a “protection” approach that left very little time to act. More advanced techniques would require monitoring of leakage currents or even partial discharges in variable frequency drive connected motors and would not be cost effective. And so, an indirect approach using temperature, overloading (that could contribute to over 50% of stator winding failures [2]) along with stator body vibration, was used. This was supplemented with periodic winding insulation measurements when the motor was stopped. Stray flux signals were used for slip estimation, detection of rotor winding defects [3], and air gap eccentricity

To select the motors to be fitted with the smart sensor device, an overall criticality analysis was performed for motors in the plant using a hierarchical approach where downtime costs were the largest determinant of the assessment. Around 60% of the motors identified in critical applications were rated under 30 kW.

V. SOLUTION DEPLOYMENT

The system deployed at the site consists of a smart sensor specified in Table 1, with multi sensing capabilities earlier described, typically mounted on motor body [4]. One sensor is used for each motor. These are battery-powered wireless sensors and communicate to a gateway via Bluetooth. Default measurement frequency is once per hour with the sensor having capability to store upto one month of data. The gateway specified in Table 2, sends data to a cloud using plant Wi-Fi or 4G dongle with SIM cards.

The smart sensors deployed were suitable for hazardous area use and intended for motors with following specifications, irrespective of the manufacturer:

1. Industrial AC induction motors
2. Continuous or intermittent duty
3. Frame sizes – IEC: 56 – 500. NEMA: 42 - 449, above NEMA: 5000 - 6800
4. Fixed speed or variable speed

Lifetime	Up to 15 years of operation under standard conditions (Standard conditions of operation: sensor measurement interval of 1 hour; raw data collection once per day; non-condensing environment; measured asset skin temperature: +15 °C to +50 °C)
Vibration Measurement	
Acceleration low frequency (x, y, z direction)	
Amplitude range	0.03 – 157 m/s^2
Frequency bandwidth	0.4 Hz – 3.3 kHz
Acceleration high frequency (z direction)	
Amplitude range	0.1 – 490 m/s^2
Frequency bandwidth	2.4 Hz – 10 kHz
Magnetic Field Measurement (x, y, z direction)	
Amplitude range	01 – 1600 µT
Frequency bandwidth	0.1 – 280 Hz
Ultrasonic Sound Measurement (microphone)	
Amplitude range	0.6 N/m2 – 20 N/m^2
Frequency bandwidth	100 Hz – 80 kHz
Temperature measurement (asset skin temperature)	
Measurement range	-40 °C to +85 °C
Resolution	0.1 °C
Wireless Communication	
Bluetooth® 5.0, Bluetooth® Low Energy	

Table 1 Sensor specifications

Range	Approx. 50 m (can vary in an industrial environment depending on facility layout)
Power Supply	PoE (Power over Ethernet)
Radio frequency	ISM band, 2.402 GHz – 2.480 GHz
Data transfer	Wi-Fi, LAN 4G/LTE USB dongle

Table 2 Gateway specifications

The site at first deployed the monitoring solution for 23 motors and then extended the same to 176 motors. As seen in the layout in Fig 3, sensors communicate via gateways to the cloud. Insights from cloud are available to the plant personnel on a smart phone app and cloud

portal. The arrangement facilitates remote monitoring and failure risk management.

From the experience in this installation, we saw the benefit of starting with a small sensor cluster that connected to a dedicated gateway having direct cloud communication. More clusters were built as we gained experience and confidence in the solution. On an average each gateway was positioned to support up to twenty-five sensors depending on their distance from sensors and other obstacles.

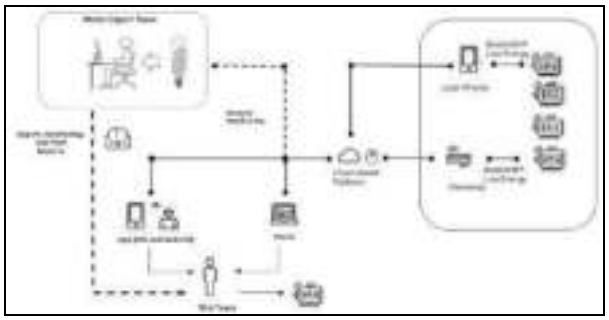

Fig. 3 Layout of site deployment

VI. PARAMETERS MONITORED AND TRENDS VISUALIZED

Health and operational parameters monitored as obtained from the processed signals and trended in a cloud-hosted portal, include:

1. Health parameters
    a. Radial/ Tangential/ Axial vibration (Velocity and acceleration rms) and Overall vibration (velocity rms)
    b. Bearing condition index
    c. Skin temperature (ºC)
2. Operating parameters
    a. Speed (rpm)
    b. Operating hours
    c. Number of starts and starts per hour
    d. Supply frequency (Hz)
    e. Power (hp/kW)
3. Other parameters
    a. Regreasing countdown
    b. Overall condition

Stress factors that are monitored and trended include body vibration and body or skin temperature. Vibration levels in three orthogonal directions (radial, tangential, and axial) are displayed in the portal as rms values of velocity and acceleration.

A bearing condition index is constituted from the on-sensor processing predominantly of vibration signals which includes the time domain analysis of the raw signal, particularly of the shock pulses and the high frequency vibration content. More advanced approaches that use similar sensing have been described in [5]. The bearing condition index is trended in the portal and provides information of the development and evolution of bearing defects, essentially reflecting progressive degradation of the bearing. Bearing defects that could be detected included spalls in the bearings that resulted from the stresses generated by underlying causes such as unbalance or misalignment or even vibration stresses that originate from the driven equipment. Re-greasing intervals are recalibrated using information from the trends of operating parameters.

Visualization of the information included trends of individual parameters, as well as indices that reflected the overall stresses on the motor. When used in combination with measured degradation (e.g., the bearing condition index) and estimated degradation from operating parameters (e.g., re-greasing requirements), a motor condition index is derived and displayed.

Operating and condition-based or health parameters are cross-correlated to analyze likely causes of increasing severity of stress and degradation quantities. This helps in discriminating faults e.g., in VFD connected motors where speed and vibration levels are co-related to identify resonance conditions, or mechanical unbalance.

Other fault discrimination is also done by triggering the collection of raw data when severity exceeds the alarm level. Raw data is processed in the time and frequency domains to help identify and trend specific problems. While the approach used has a wide coverage of defects, it is not always possible to get to the underlying causes and identify the levels of contribution by these causes when more than one defect is simultaneously present.

VII. SELECTED DEMONSTRATIVE CASES

A few examples from the monitored motors in the plant are presented below to illustrate the possibilities of exploiting the deployed technology to derive insights that could aid maintenance decisions.

A. Understanding Process Insights

Vibration levels related to process changes are commonly seen in operation. However, they are usually not clearly identified due to lack of data when engineers collect vibration levels on a three-monthly basis. As seen in Fig. 5 where vibration data is collected on an hourly basis, it is observed that processing of product B causes the vibration level to increase 3 times more than that of product A. On further analysis of the vibration trends, the difference in vibration level was due to a difference in the grade and content of lubricant present in both products. A different grade lubricant with lower content in product B resulted in higher reflected vibration stresses in the motor. If there is an increased demand for product B, it would mean prolonged operation at higher vibration levels, quicker motor degradation and greater failure likelihood. This phenomenon was not recognized in the plant prior to monitoring the motor with the smart sensor.

Fig. 5 Vibration trend of different products

Similarly, in Fig 6, we can see the change in vibration level while motor speed is rather constant. On further investigations, it was noted that the change in vibration coincided with valve throttling.

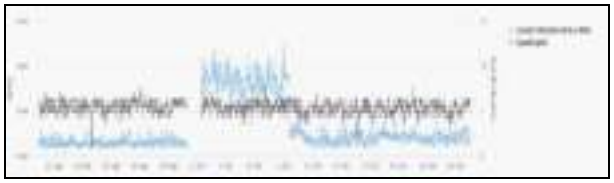

Fig. 6 Overlay of vibration and speed trend

B. Remote monitoring: Being prepared before inspections

With 24/7 data collection and surveillance of motor condition, it is important to optimize threshold settings to receive alerts on the onset of developing abnormalities. In Fig.7 we observe a sudden increase in the body temperature of a fixed speed motor, when operating load did not change. An on-site verification revealed that an absorbent pad was stuck on the fan cover, thereby affecting the motor cooling. Continued operation with reduced cooling would subject the motor to increased thermal stresses and result in reduced life. Timely alerts can provide inputs for more meaningful daily plant walk downs.

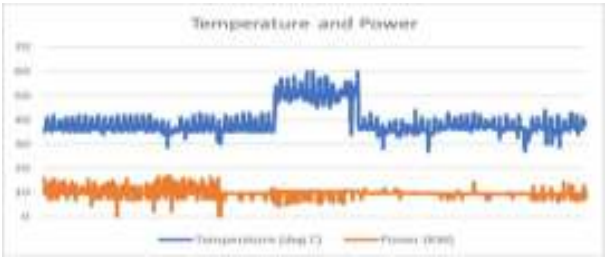

Fig. 7 Temperature Trend

In Fig. 8, a significant increase in the vibration level was observed due to a heavy build-up of sticky polymer on the feed roller. Residual build up on the roller was a known issue, but only after monitoring the motor it was discivered that it led to a 5-8 times increase in the motor vibrations. The motor would have typically operated till the end of production cycle. However with monitored information, plant personnel could plan for regular checks on the feed roller and clean up the polymer build-up to avoid exposing the motor to high stresses for prolonged periods.

Fig. 8 Vibration increased when polymer stuck on feed roller

With a simplified bearing condition index, the user is kept informed on developing bearing defects when they cross pre-determined threshold levels. In fig 9, when the bearing condition index started to increase above the set threshold January 2020, the bearings were regreased and the values temporarily improved. In the following two months, the bearing condition index crossed the alarm levels and stayed in the alarm zone with no improvement after regreasing. Remote raw data collection from the sensor, provided the time domain, frequency spectrum and bearing envelope (Fig. 10), which helped confirm a developing bearing fault. With the early identification of developing bearing problems, plant personnel could plan for a shutdown to change bearings and pre-empt failure. Upon re-installation of motor, the bearing condition index is seen to return to normal values.

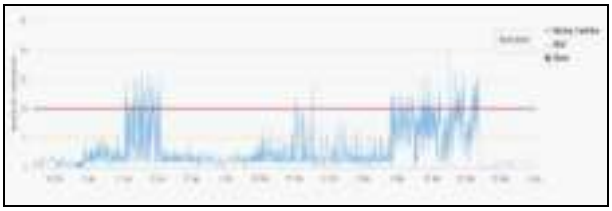

Fig. 9 Bearing damage

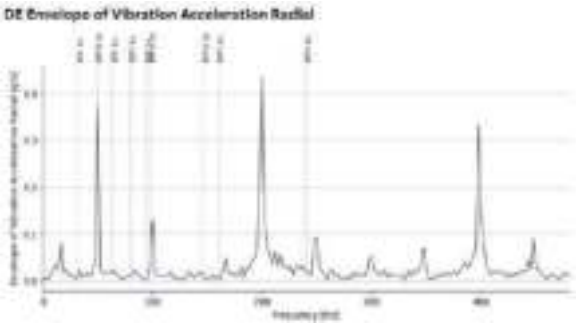

Fig. 10 Bearing damage as indicated in the envelope spectrum of vibration acceleration

VIII. FROM MONITORING TO MAINTENANCE

Regular monitoring and analysis by experts are made possible through automated notifications that are triggered from the cloud-based portal. The monitoring scheme also allows for the use of advanced analytics to identify developing anomalies.

Trending, baseline development and asset-specific smart alert and alarm configurations, were implemented while monitoring the motors. Information derived from such monitoring was combined with an “urgency matrix” to derive a schedule for maintenance actions.

A key feature of the solution is the ability to trigger remote raw data measurements that allow for a spectrum analysis.

A. Urgency matrix

The urgency matrix combines information from degradation, and stress levels to decide the urgency of maintenance or repair (see Fig.11)

A degradation index is computed from information that describes condition of the bearings, their lubrication, and the condition of the rotor and stator windings, using a combination of measured and estimated damage factors.

A stress index is calculated from measured vibration, temperature data, and from estimated stresses that originate from electromagnetic reasons (for example air gap eccentricity or supply conditions).

A combined representation of the state of degradation and the stresses acting on a motor provides the possibility to determine how quickly maintenance should be done, solely from the perspective of degradation. This approach can always be supplemented with information on the criticality of the application to prioritize maintenance.

When degradation levels are high it could call for replacement or renewal of the part (e.g. the bearing) or material (e.g. grease). If stress levels are high, it would mean investigating root causes and taking steps to reduce the stress (e.g., improve alignment to reduce high vibration levels or correcting soft foot)

In a newly replaced bearing, the levels of degradation measured and recorded in the portal would be low. The stress level however is dependent on whether corrective maintenance was done to reduce abnormal forces on the bearing. If we replace a part e.g., the bearing, but do not address the stresses that could have resulted in a bearing failure - then we run the risk of future repeated failures with perhaps lower Mean-time-between-failure (MTBF).

The status in the urgency matrix would depict actions that would be needed to reduce the stress levels (e.g., by improving alignment). If degradation levels were high and the stresses low, we would keep a close watch on defect growth and change the bearing when the status in the urgency matrix was indicative. The urgency matrix could be used for an entire fleet of motors in the plant or even to trace the trajectory of a motor during the evolution of defects. Maintenance plans can be drawn up on a 6 monthly basis using the urgency matrix and helps translate monitoring into maintenance actions – what and when.

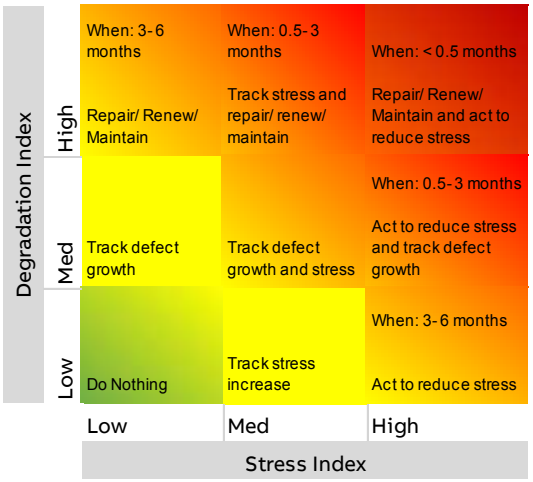

Fig. 11 Urgency Matrix – example of service actions and their timing

IX. OUTCOME AND NEXT STEPS

In the preceeding sections, the implementation of an approach that combines preventive and predictive maintenance to maximize the reliability of motors in a chemical plant has been discussed. Examples given demonstrate the possibility of effectively planning maintenance for motors, increasing the time between maintenance and avoiding unexpected failures.

Soon after the installation of the digital monitoring system in 2018, the plant saw quick gains by getting new insights into what could potentially cause failures in the motors and performing timely service. Walkdown inspections became more effective. No unexpected motor failures were recorded and this subsequently brought about a 100% reduction in downtime of the motors monitored.

Next steps include the integration of data from equipment health monitoring with that of process data. By having an overview of the entire operating process, this would not only streamline analysis to identify causes of stress within the production line, but also improve the diagnosis of motors.

X. REFERENCES

[1] R. Keith Mobley, 2002, An Introduction to Predictive Maintenance.

[2] O. V. Thorsen and M. Dalva, “A survey of faults on induction motors in offshore oil industry, petrochemical industry, gas terminals, and oil refineries,” IEEE Trans. Ind. Appl., vol. 31, no. 5, pp. 1186–1196, Sep./Oct. 1995.

[3] Stephan Wildermuth, Ulf Ahrend, Christoph Byner, Pawel Rzeszucinski, Daniel Lewandowski, Maciej Orman, “Condition monitoring of electric motors based on magnetometer measurements”, Proc. 2015 IEEE 20th Conference on Emerging Technologies & Factory Automation (ETFA)

[4] Manuel Oriol, Der-Yeuan Yu, Maciej Orman, Neethu TP, Geir Svoen, Philipp Sommer, Gerd Schlottig, Alexey Sokolov, Ștefan Stănciulescu, Felix Sutton, “Smart Sensor for hazardous areas”, ABB Review, 02/2020, pp (23-27)

[5] Pawel Rzeszucinski, Maciej Orman, Cajetan T. Pinto, Agnieszka Tkaczyk, Maciej Sulowicz, “A signal processing approach to bearing fault detection with the use of a mobile phone”, Proc. 2015 IEEE 10th Int. Symposium on Diagnostics for Elec trical Machines, Power Electronics and Drives (SDEMPED), pp. 310–315.

XI. VITA

Dr Ankush Gulati a PhD from Cranfield University, in the field of diagnostics for gas turbines also did his master’s from the same university specializing in Gas Turbine Technology. He has authored several papers in the field of diagnostics for gas turbines and awarded two joint patents in this field. He has a wide and varied engineering and service management experience as Marine Engineer officer in Indian Navy and then ABB, a large part of this dedicated to condition monitoring and diagnostics. He is presently responsible for Sales Management of Services in Motion business area of ABB for Asia, wherein he has also been instrumental in developing bespoke solutions around connected assets.

Veronica Chew graduated from the University of Western Australia with a Bachelor of Electrical and Electronic Engineering. Since 2013, she has been involved in the field of condition monitoring and predictive maintenance for electrical motors and generators. She is currently leading the smart solutions for asset management at ABB Singapore.

Cajetan Pinto graduated from the Mumbai University in 1982 with a BE degree, and from the University of California Irvine in 1985 with an MSEE degree specializing in electromagnetic energy conversion systems. He has been working with ABB for over 24 years and for over half that period has been the Head of R&D for ABB Motors and Generators Service. Cajetan is currently Innovation Champion ABB Motion Services and is based in Madrid. His focus areas of research include diagnostics, condition monitoring & reliability, motor and generator re-engineering, maintenance technologies, new service processes and materials for service. He has authored and co-authored over 40 conference papers in the field of condition monitoring and diagnostics

Hock Cheong Ng graduated from the Singapore Polytechnic. He has been with Denka Chemicals since 1984 and held various positions involved in the production and maintenance team. Focusing more on asset health performance management in the recent years, he spearheaded the digital transformation and IoT initiatives in achieving significant savings for the plant. He is currently holding position of advisor to maintenance team and head of project investments.

Commissioning Tests to Assure MV Power Cable Systems meet IEC/IEEE standards

Paper No. PCIC Europe EUR22_22

Rene Hummel
IMCORP Europe
Rene.Hummel@imcorp.com
Germany

Ben Lanz
IMCORP
Ben.Lanz@imcorp.com
USA

Michael Joseph
IMCORP
Michael.Joseph@imcorp.com
USA

Abstract - Many common solid-dielectric Medium Voltage cable system commissioning tests are not comparable with factory tests and provide little or no certainty of future performance. One of the most effective dielectric tests performed in the factory and the field on solid-dielectric cable system components is the off-line 50/60Hz Partial Discharge (PD) test. Data collected over the last two decades supported by test experience on over 200,000 cable system tests will demonstrate the significant improvement in cable system reliability performance that can be achieved using this approach in the field.

Index Terms — MV cable, commissioning testing, Partial Discharge, withstand

I. INTRODUCTION

Petrochemical facilities need a safe and reliable cable system infrastructure. Unplanned outages and failing cables involving a flashover can lead to a huge loss of revenue or even catastrophic incidences, depending on the location of such an event in a plant. To assure cable system reliability, commissioning tests are typically conducted after the installation of new components. The industry offers a wide range of tests that can be performed. Field testing guides give some direction on how to use these test systems. However, neither the manufacturer of test equipment nor the authors of field guides provide proper certainty on future system performance. Often it is described how to handle the equipment and how to interpret some of the results. Proper guidance on counter-measures, in cases where results are flawed, are not given and future risks for the cable systems are not discussed.

The “gold standard” on insulation integrity testing for Medium Voltage (MV) power cables and accessories is the off-line 50/60Hz Partial Discharge (PD) test. IEC and IEEE standards demand to perform these off-line 50/60Hz PD tests as factory tests on each cable. Usually, these tests are performed under advantageous laboratory conditions such as shielded rooms / Faraday cages and special power sources with low noise..

Ideally, this quality control test should be performed in the field as well. An off-line 50/60Hz PD test reveals not only issues of the cable insulation and accessories, but also shows possible workmanship issues during installation. Specific test parameters must be met in order to assure that the field test results are comparable to manufacturers’ acceptance standards. Meeting these parameters in the field was difficult to impossible for a long time. Evolving computer science, artificial intelligence and advanced adaptable software algorithms allow the industry to meet these parameters in field now.

This paper will provide examples of applying factory comparable 50/60Hz PD standardized tests the field. Case studies will provide examples of the types of defects which a 50/60Hz PD test, according to manufacturers IEC/IEEE standards, pinpoints in the field. Many of which would be, or were missed by, other types of commissioning tests.

II. GENERAL INFORMATION

The vast majority of power cable systems installed today are insulated with extruded materials that belong to 2 main classes: (a) polyolefins – encompassing polyethylene (PE), cross-linked polyethylene (XLPE), and tree-retardant cross-linked polyethylene (TR-XLPE), and (b) ethylene-propylene rubber (EPR).

In the petrochemical industry, most cable systems are installed underground or in above ground cable trays. Experience of over 200,000 cable tests indicates that cable system deterioration, caused either by operational stresses, manufacturing defects, or workmanship issues during installation, manifests itself through discrete defects. Defects in installed solid dielectric cable systems initiate a deterioration process associated with PD. This failure mechanism causes the process of insulation erosion, beginning with a small part of the insulation only. Over time the heat of PD, 5000°C-7000°C, erodes the insulation further and further, often resulting in a full flashover and/or destruction of the full insulation.

Cable defects uncovered during commissioning tests include voids, protrusions, delaminations, and physical damage. Some examples of workmanship issues with accessories are poor cable preparation involving nicks, cuts, dimensional and alignment errors, poor void filler application, and contamination. 50/60 Hz PD commissioning testing to assure MV power cable systems meet IEC/IEEE standards and its importance to assuring the reliability of critical power cable systems will be thoroughly discussed in the following sections of this paper.

III. CABLE TESTING IN THE PAST

In the beginning and middle of the last century, most cables were paper insulated lead covered (PILC) cables. Most of these cables failed due to localized increase of insulation conductivity, either caused by a lack of oil fill with the presence of air, yielding carbonized paper tapes or the presence of water leading to ionic conduction. For such cables, a direct current (DC) high potential withstand test (DC HIPOT) for a defined duration, was a great tool

because it is highly sensitive to conductivity. A DC HIPOT test was required and performed in the factory on new PILC cables. This led to the motivation to repeat the same test in the field as well.

In the 1960s the first solid dielectric cables were introduced. Cable manufactures learned that the primary failure mechanism of this type of insulated cable was associated with PD and not conduction. The factory PD test (back in the 1960s called “corona test”), was able to detect PD activity in cables and accessories. It involved expensive equipment such as oscilloscopes and required laboratories with an electromagnetically shielded room. Over the years, cable manufacturers realized, that the DC HIPOT is an ineffective test for solid dielectric system components. The electric field grading capabilities of most accessories rely on a capacitive field grading under alternating current (AC) loads which behaves very differently under DC conditions. Thus, DC HIPOT testing has been removed as a requirement from some of the factory standards for over 20 years now.

The complexities of the PD test in the field led the industry to continue to use the most widely available and recognized commissioning test (the DC HIPOT). As DC voltage does not cause PD that leads to failures in defective extruded insulation during the commissioning withstand test , very low frequency (VLF) or 0.1Hz AC test was introduced in the mid-1980s. Unlike DC voltage, VLF voltage is able to produce sustained PD activity while injecting significantly lower amounts of space charge when compared to DC. Many standards suggest a testing time at an elevated voltage for 30 minutes or longer. The intention of this overvoltage test is push existing and significant cable issues and defects to failure. The downside of this approach is that without the proper sensitive diagnostic measurement equipment accompanying such tests, VLF can trigger failure mechanisms that will erode the insulation without resulting in an immediate full dielectric failure, potentially leading to subsequent failures in service.

In the mid-1990s, the first generation of digital signal processing equipment was introduced to field testing. Most of these tried to solve the background noise dilemma, in absence of a shielded room, associated with PD testing in the field. Different companies developed different solutions to reduce background noise to offer sufficient sensitivities to on-site tests. The struggle with on-site background noise and the disadvantages of VLF led to the development of a PD test technology that can provide field test results that are comparable with the cable manufacturers’ standardized factory quality control tests. To achieve this, an off-line 50/60 Hz voltage source is used, together with PD diagnostics equipment, which has been used over the past 25 years. This has evolved into a robust condition assessment equipment for commissioning tests and predictive diagnostics solution for power cable systems.

IV. OFFLINE 50/60Hz TESTING

Off-line 50/60 Hz partial discharge [1] diagnostic tests offer a major advantage over traditional withstand tests. It enables the user to perform non-destructive cable assessments while detecting partial discharge, pinpointing the defect location, and providing the details necessary to take precise repair action without destroying the cable.

Cables are subjected to overvoltages caused by switching, lightning and other transient events. Cable systems need to endure thousands of such events over their lifetime. Thus, it is important such transients do not trigger PD. PD triggered by transients will erode the insulation during each event, until the so called partial discharge inception voltage (PDIV, turn-on voltage) is lower than the operating voltage. Once PDs are occurring at the nominal operating voltage of a cable, it is only a matter of time until the cables fail in service.

Therefore, the IEC and IEEE standards demand to test the cable systems with an elevated voltage, well above the operating voltage to ensure there is conservative margin. Different standards from around the world request precise voltage levels for cables and the used accessories, such as end-terminations and joints. The table below gives an overview of the test requirements for IEC and IEEE.

TABLE I

Standard	Test Frequency	Test Sensitivity	Voltage Level
Terminations			
IEC 60502-4	50/60Hz	≤ 10pC	≤ 1.73U_o
IEEE 48	50/60Hz	≤ 5pC	≤ 1.5U_o
Joints			
IEC 60502-4	50/60Hz	≤ 10pC	≤ 1.73U_o
IEEE 404	50/60Hz	≤ 5pC	≤ 1.5U_o
Separable Connectors			
IEC 60502-4	50/60Hz	≤ 10pC	≤ 1.73U_o
IEEE 386	50/60Hz	≤ 5pC	≤ 1.3U_o
Medium Voltage Cables (≤ 36kV)			
IEC 60502-2	50/60Hz	≤ 10pC	≤ 1.73U_o
ANSIICEA S97/94-682/649	50/60Hz	≤ 5pC	≤ 4.0U_o

V. STANDARDIZED PD TEST REQUIREMENTS

Standards writing organizations such as IEC, IEEE, ICEA and others have developed requirements for factory PD tests and pass/fail criteria on the basis of the following four generalized parameters:

1. sensitivity assessment / background noise reduction of the test equipment
2. apparent charge magnitude calibration
3. voltage source frequency
4. PD test voltage level.

Sensitivity Assessment / Background Noise Reduction

PD tests, according to the standards, must demonstrate effective background noise reduction through the process of a sensitivity assessment. To ensure all possible PD pulses can be detected in a cable system, a calibrated pulse must be injected anywhere in the cable and must be detectable with the testing equipment. Due to the lowpass characteristic of the cable and the signal dampening process, the injection point usually is chosen to be the far end of the cable. By doing so, it can be assured, that even pulses from the far end can be detected properly.

IEC 60502 demands that the calibration pulse must be equal to the maximum allowable charge of 10pC. Furthermore, the signal to noise ratio SNR (calibration pulse to background noise) shall be 2 or greater. This concludes that the background noise shall not be bigger

than 5pC.

This sensitivity assessment process allows the specifying engineer to assure that there is no PD activity above the allowable charge (IEC 60502: ≤10pC). In order to localize a possible PD in the cable, the process of reflectometry is used. In such a process, the original pulse from anywhere in the cable and its reflection from the far end of the cable must be detectable. To make certain all PD above the allowed value can be localized, a 10pC calibration pulse must be able to do a full round trip, travel from the near end of the cable to the far end of the cable and back again. Still, the SNR should be equal or greater than 2.

Such sensitivity assessment is a crucial step in the test process. If a PD test cannot detect a signal of 50pC in magnitude, the test could be missing 60% of PD activity in the cable when compared to a test with 5pC sensitivity [2].

Apparent Charge Magnitude Calibration

All calibration and PD signals must be presented in a unit of charge, as required in the standards listed in Table 1. Due to losses, attenuation and dispersion in the cable system, the real charge of a PD pulse cannot be determined. Therefore, the term "apparent charge" was introduced. It describes the measurable charge at the terminals of the measurement system. Injecting a known calibration pulse anywhere in the cable and recording it at the intended test measurement point, allows the PD testing system to display all results in reasonable pC values. This is crucial to obtain test results that are comparable with manufactures' standards.

Frequency of Voltage Source

To perform a PD test, the cable under test must be excited with an overvoltage at 50/60Hz, as required in the IEC and IEEE standards. If a voltage waveform other than 50/60Hz is used, e.g. 0.1Hz or a system that charges the cable with DC voltage to create a decaying oscillation, the PD inception voltage (turn-on voltage for PD) can vary over 100% [3]. This could lead to damaging a cable with PD activity which would normally not occur at 50/60Hz, or result in missing PD activity that will happen while in service at normal power frequency. More and more cable and accessory manufacturers deny claims from clients that test with different voltage waveforms than 50/60Hz. Some even deny any warranty, if the accessories have been tested with some form of DC or 0.1Hz (VLF), as the capacitive field grading are designed for 50/60 Hz and not DC or VLF.

PD Test Voltage Level

An elevated voltage is required by all international standards (Table 1). IEC 60502 requires the cable system to be energized at 50/60Hz to the test voltage of 2.0Uo for 10 seconds, and then lowered to 1.73Uo before measuring PD. Without an external elevated 50/60Hz voltage, a PD test can provide completely inaccurate measurements of PD inception (PDIV, turn-on) voltage or PD extinction (PDEV, turn-off) voltage [3]. Standardized PD test pass/fail criteria are based on accurate PDIV and PDEV measurements and the use of a standardized 50/60Hz voltage source to produce a continuous overvoltage, to assure comparability to industry standards.

On-site PD tests do not always achieve the factory test criteria, but in over 200,000 performed tests in the field on medium, high and extra high voltage cable systems, more than 95% of tests achieved better than 5pC sensitivity and were able to achieve voltage levels as required in the IEC/IEEE standards. According to the standards, the sensitivity which is actually achieved must be documented and should be part of the report, in order to allow for a reasonable assessment of the PD test reliability. The application of Medium Voltage factory PD test standards in the field can be summarized as the "application of a continuous 50/60Hz overvoltage while measuring the cable system's PD response with better than a calibrated 10pC sensitivity per IEC 60502 (5pC for IEEE & ICEA standards)."

VI. CASE STUDIES

Case Study 1

During a planned outage, a petrochemical facility installed twelve MV cable systems linking a critical plant process to a substation. The plant owner was especially concerned about this installation as a failure in one of these cables could potentially cost over €1million. The cable systems were installed by a reputable contractor who had been installing cable systems at the plant for over 25 years. The plant owner requested that the installation contractor perform a DC HIPOT test. Each cable passed the DC HIPOT test without a problem, indicating that all the cable systems were fit for energization. Following the DC test, the cable owner requested an off-line 50/60Hz PD test according to the standards indicated in Table 1. The off-line 50/60Hz PD test located a termination that showed severe PD well below the IEC 60502 requirements on a 791m long cable span. Further investigation revealed that the contractor had difficulty installing a cold shrink termination and had accidentally displaced the stress control mastic, which created an electric stress enhancement at the end of the outer semi-conducting layer cutback. (See Figure 4). According to the manufacturer of this termination, this error is very serious and the termination would likely have failed in service after a short time. The termination was replaced and a retest demonstrated that the repair passed the manufacturer's PD test criteria (IEC 60502).

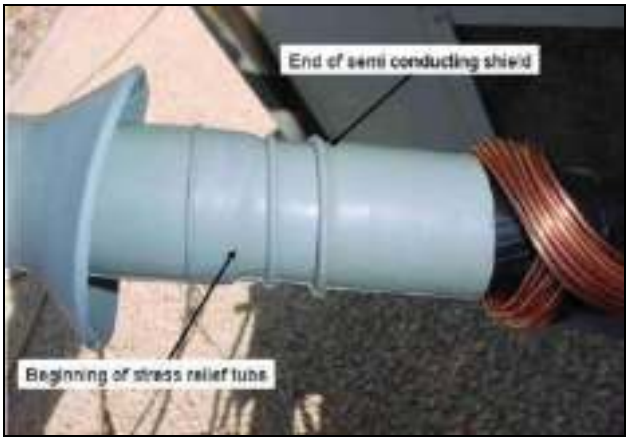

Fig. 1 Semi conductive shield and stress relief tube are not aligned in an open air termination

Case Study 2

In a power generation plant, critical cables to a substation were commissioned using an off-line 50/60Hz PD diagnostic test. All the terminations of four cables (3-phase) were found to be performing well below the IEC 60502 requirements. Despite the results, the contractor insisted that the terminations were installed correctly. Being unfamiliar with the latest diagnostic technology and industry standards, the contractor performed a 0.1Hz VLF withstand test on all of the cable systems in question. None of the cables failed during the VLF withstand test. Under the assumption such a test is sufficient, the cables were put into service. Within one month, one of the terminations recommended for repair by the off-line 50/60Hz PD test failed (see Figure 2). This led to a downtime of the power generation plant, as all substandard terminations had to be repaired. This is only one instance, but it is typical of many others which have been documented by the authors.

Fig. 2 Cable Termination with Substandard Installation (left); Same Cable Termination with Failure Less Than 1 Month Later (right)

Case Study 3

A petrochemical plant was experiencing an average of one failure every three years for a total of three failures over a 10-year period. On a regular basis, all 44 of the plant's 3-phase EPR-insulated cables were subjected to a traditional DC HIPOT maintenance test. The cables routinely passed the DC test but continued to fail in service. Fault records and subsequent off-line 50/60Hz PD diagnostic tests confirmed that the terminations were the weakest points on the system and causing most of the failures. After performing the off-line 50/60Hz PD diagnostic test, the results were used to make specific repairs to approximately 10% of the terminations, 5% of the splices and 2% of the cable segments. Since the PD test and repairs, the site has not experienced a single failure. If the failure rate prior to the PD test and repair activities had continued, this plant would have experienced three more costly unplanned outages during the subsequent 10-years.

Case Study 4

Critical power plant cables consisting of over 20 km of MV cable systems were tested using a DC HIPOT test. All cable systems passed the test and were put in service. Within the first 3 years, the cable system experienced 9 failures. Each failure cost the owner of the plant approximately €15k to €35k. After a loss of over €200k caused by failures, the operator performed an online PD test with the hope of exposing the remaining issues. The online PD test did not detect any PD in the cable system. Thus the cable owner believed, the cable system was in good condition and no action was needed. In the following year 3 more failures happened. With total outage costs of about €300k, the operator decided to perform an off-line 50/60Hz PD tests.

The off-line 50/60Hz PD test pinpointed 15 defects and recommended the necessary actions to correct each issue. The cable owner used the meter-by-meter profile produced by the test to identify 6 cable insulation, 4 joint, and 5 termination issues that did not meet the IEC/IEEE standards and were likely to fail significantly short of the system's design life. This proactive approach prevented as many as 15 failures. This site did not report any failures for 15 years after implementing the recommended actions and commission testing the repair work.

Fig. 3 Cable failure after DC HIPOT and prior to off-line 50/60Hz PD test

Case Study 5

A 150MW wind farm commissioned the newly installed Medium Voltage cables using a VLF AC withstand test. All cables passed. Within the first few years of operation, several MV cables failed. On one such occasion, the wind farm experienced a failure on a circuit supporting 16 turbines, 1.5MW each. The average wind speed during the failure was 8.4 m/s. According to an internal report, the nine-day production loss cumulated to €109k. Additional costs of €31k for the emergency fault location and €9k for the emergency repair cost, added up to around €149k. The wind farm owner requested the system be tested using an off-line 50/60Hz PD test. The PD test located 5 terminations, 3 joints, and 12 sites in the cable insulation which did not meet international standards.

Case Study 6

Two cable systems supporting a critical plant were installed under the ground in a fluidized backfill for the purpose of enhancing ampacity. After installation, the cables passed a VLF withstand test. An off-line 50/60Hz

PD test was performed and 7 PD sites not meeting the international standards were located in the cable system (see example in Figure 3). The damaged is believed to have been caused by the aggregate of the backfill getting in between a mechanical guide and the cable jacket during the installation process. The pressure from the guide caused the aggregate to puncture the jacket and outer insulation screen.

Fig. 4 Cable Damage passing VLF test but pinpointed within 10cm by 50/60Hz PD test

Case Study 7

A power plant owner specified an off-line 50/60Hz PD test with 5pC sensitivity as part of its newly-built site commissioning process. After several cable defects were identified, the site contractor questioned the validity of the 50/60Hz PD assessment and retested the substandard cable segments using a VLF PD test. A formal investigation at an independent laboratory through a dissection and root cause analysis confirmed that all identified defects were manufacturing defects that did not meet the international standards. In contrast, the VLF PD method failed to locate any of the defects in the same analyzed segments.

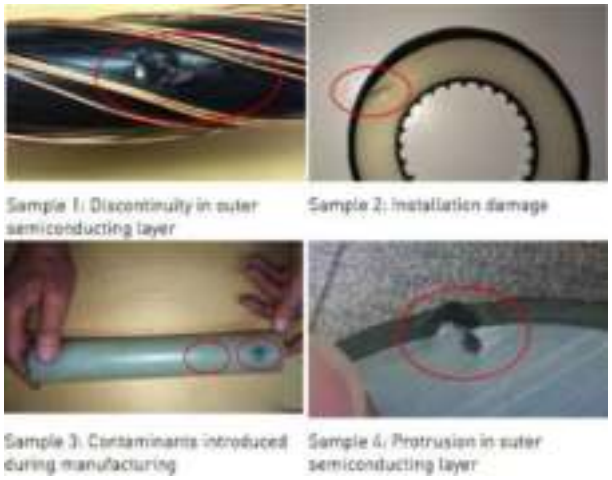

Fig. 5 Samples of found issues in cables

VII. DISCUSSION

Above case studies provide a small glimpse into the 100s of documented cases which demonstrate that many widely used cable system commissioning tests, that are not meeting the international standards concerning voltage waveform and PD sensitivity, cannot be used to ensure reliable MV cable systems.

Some readers who are familiar with DC and AC withstand tests for commissioning may notice that this paper did not discuss withstand test maximum durations or voltages. This subject has been a continuous source of discussion in the industry for over two decades. Based on the authors' experience, this discussion may be somewhat misleading. Estimating the time to failure for most defects under specific voltage withstand conditions is a fundamentally flawed approach.

The time-to-failure in solid dielectric defects under withstand conditions depends on many parameters which are unknown variables. These include the defect geometry, the materials involved, the local stress distribution, and space charge effects. Since these parameters are unknown, it is nearly impossible to determine how much of the insulation has been eroded during the withstand test.

In a 3-year study [4], the Electric Power Research Institute created typical cable workmanship errors including misplaced stress elements, knife cuts to 30% of the extruded insulation, and conducting residue left along the cable insulation shield cutback. All of the samples included in the study did not meet IEC 60502 PD performance requirements Although it is highly likely that these errors would have caused a service failure, all of the workmanship defects survived a 4-month AC withstand at 2 times the operating voltage ($2U_0$), while showing continuous PD activity. One of the conclusions of this study is that while AC withstand tests are intentionally designed to be destructive, one cannot rely on these tests to break down many serious insulation defects during the short withstand period.

Since the off-line 50/60 Hz PD test is non-destructive and predictive, it represents a significant breakthrough for critical facility engineers who are required to assure safe and reliable MV cable systems. The technology enables engineers to specify and quantify cable system installation quality levels on a component-by-component and meter-by-meter basis. With this system profile information, owners can now hold contractors accountable for substandard workmanship prior to the end of the warranty period. Once performance of each component of an installed cable system meets or exceeds IEC/IEEE standards, the baseline profile can be compared to future diagnostic tests for trending purposes. This information can be used as a factual condition basis to optimize and extend the period between future maintenance cycles.

This paper is based on experience gained during over 200.000 off-line 50/60Hz PD tests performed on MV cable systems in Europe, Middle East, North America and Asia. Some readers may believe above case studies are statistical anomalies, the authors' experience indicates that the majority of MV cable systems are likely to have a few percent of components which are not built to manufacturers' expectations. In a recent survey of over 100,000 off-line 50/60Hz PD commissioning tests on critical MV cable systems 3.0% of terminations, 4.4% of joints, and 1.6% of cable segments did not meet IEC/IEEE standards.

Another useful statistical comparison can be derived by comparing off-line 50/60Hz results to other types of commissioning tests. This analysis provides a test-by-test comparison estimating the percentage of substandard components that would likely be detected. The comparison case on MV cable defects show that VLF AC withstand detects (fails) less than 2%, a DC withstand detects (fails) less than 1% and an online PD test detects less than 2% of defects which do not meet IEC/IEEE standards and are considered to shorten cable life. General condition assessment tests such as dissipation factor (or tangent delta) at a single frequency or a spectrum of frequencies (dielectric spectroscopy), polarization voltage (or return voltage), relaxation current, and others have not been included in this paper. While these tests can provide an overall assessment of the deterioration of certain dielectric properties, they cannot pinpoint the location of defects responsible for this deterioration, and are generally not recommended for commissioning new MV cable systems since their dielectric properties are still intact.

VIII. CONCLUSIONS

This paper shows that only few commissioning tests systems are useful to assure MV power cable systems meet the IEC/IEEE standards. As demanded in the standards, only off-line 50/60Hz PD test meeting the strict IEC/IEEE specification can provide an after-installation commissioning test which can ensure MV power cable systems meet manufactures' performance standards.

In general, to assure reliability, cable owners should consider testing cables and accessories, that are designed for 50/60Hz usage, with continuous 50/60Hz overvoltage while measuring PD with better than 10pC sensitivity per IEC 60502 (5pC for IEEE & ICEA standards).

In summary:

- Failures on critical power cable system are very costly and thus an effective commissioning test method is needed
- One of the most effective dielectric tests performed in the factory on solid-dielectric MV cable system components is the off-line 50/60Hz partial discharge (PD) test.
- Nowadays, it is possible to obtain the same quality of results in the field as well.
- The vast majority of failures in newly installed solid dielectric MV systems are initiated by a discrete deterioration process associated with partial discharge (PD) and not conduction.
- Traditional DC or VLF AC withstand tests are not likely to detect (fail) the majority of significant defects
- Momentary PD tests performed at the operating voltage (online PD tests) are not comparable to factory standards and are not likely to detect the majority of significant defects shorting the cables' life
- A continuous 50 or 60Hz voltage source is necessary in order for a test to be comparable to international standards (IEC/IEEE).
- An overvoltage of at least $1.7U_0$ is necessary in order for PD test results to be comparable with a factory test.
- A sensitivity assessment is critical to assure the test equipment is working properly and that results can be compared to factory test requirements.
- A pC magnitude calibration is necessary to assure that the apparent magnitude of any PD activity can be displayed in reasonable pC values and the test results are comparable to those obtained according to IEC/IEEE standards

VI. REFERENCES

[1] M. Mashikian, A. Szatkowski, " Medium Voltage Cable Defects Revealed by Off-Line Partial Discharge Testing at Power Frequency ", IEEE Electrical Insulation Magazine, July/August 2006, Vol. 22, No. 4, p. 24-32.

[2] S. Ziegler, B. Lanz, "Demystifying Sensitivity Assessment & Magnitude Calibration of Locating PD in Cable System", IEEE PES ICC Subcommittee F, Fall 2009

[3] D. Kalkner, R. Bach, "Electrical Tree Growth" Research and Development, Annual Report 1992, TU Berlin High Voltage

[4] Estimation of the Future Performance of Solid Dielectric Cable Accessories, Electric Power Research Institute (EPRI), Palo Alto, CA: 2003. 1001725.

IX. VITA

This section provides a short biographical or autobiographical account of the author(s). Please add also a photo of the author(s). Examples:

Rene Hummel graduated from the University of Technology in Berlin, Germany, with a Diplom Engineer degree in High Voltage. He tested for Partial Discharge, giving consultancy and technical trainings in 40+ countries on 5 continents. He is a member of several IEEE ICC standard committees and has authored 25+ previous papers.
Rene.Hummel@imcorp.com

Ben Lanz graduated from the University of Connecticut, with an Electrical Engineering degree. He has provided technical oversite 200k+ cable system tests and 1k+ dissection and root cause analyses on defective components over the last 25 years. He is a Senior member of IEEE PES and ICC and an active member of IEEE DEIS and IAS, and APC, CIGRE, NETA, EPRA and has published dozens of contributions on the subject of power system reliability.
Ben.Lanz@imcorp.com

Michael Joseph graduated from Rensselaer Polytechnic Institute in Troy, NY, USA with a B.S./M.Eng. in Materials Science and Engineering. He has over 13 years of experience in PD testing, including 10 years of managing qualification and factory production testing for MV/HV solid dielectric cable. He is an active participant in several working groups as a Senior Member of the IEEE PES-ICC.
Michael.Joseph@imcorp.com

PCIC EUROPE 2022 :
How to digitalize an equipment for operational excellence and eco-conception

Paper No. PCIC Europe EUR22_24

Guilhem Jean
2B1st Consulting
943 route des Pecles,
74400 Chamonix
France

Philippe Eyraud
Mixel
1 place du Paisy,
69750 Dardilly
France

Abstract – There are two possible approaches to the digitalization: one top-down, the other bottom-up. While the top-down approach seems reserved to operators because requiring a global overview of the digitalization, the Original Equipment Manufacturers (OEMs) and Manufacturers can bring part of the digitalization solution with a bottom-up approach. By digitalizing their equipment, OEMs and Manufacturers can not only reach higher operational excellence but also reduce the carbon footprint of project and operations.
The purpose of this article is to present a method and an example on how to digitalize your equipment.
The first part will explain the logic and the pitfalls of the digitalization. The second part will be dedicated to detail the process for a successful digitalization. The last part will high light the theory with a practical case : the connected agitator, benefits and specifications.

Index Terms — PCIC Europe Paper Format, Writing instructions, Style requirements.

I. INTRODUCTION

More half of all the spendings of Operators of the Oil & Gas industry dedicated to innovation, are focusing on digital technologies. For an industry known for its risk averse approach to innovation, the Operators are now looking to embrace the use of new technologies with quite some logic.

By nature, the complexity of projects in Oil & Gas industry may be the highest one amount all the sectors of the global economy. From filed EOR, to deep offshore drilling, or north pole production, the petroleum industry has been prompted to succeed against the harshest challenges. And this is no surprise if Oil & Gas projects all require a huge engineering effort to be executed, hiring the largest EPC companies worldwide. It is all because of the complexity of this industry.

And this the perfect playground to use the digital technologies. New technologies can go beyond oneself understanding and solve problematics larger than the human mind could do. Not to replace the knowledge of people but to become the tool solving problematic too complex for human capacities.

In this white paper we will try to explain the idea, the process, the execution of a digitalization we made of an equipment to solve two problematics : better operations for the Operators; and a better design to save time/cost/energy.

II. LOGIC AND PITFALL OF THE DIGITALIZATION

The first need when talking about digitalization is to clearly set the boundaries of the concept, and even more not to create a confusion between digitization and digitalization.

Digitization is the conversion of any type of information from an analog format (text, sound, picture, video, etc.) to a digital format. Once digitized, the information is available to be proceeded or stored by electronic devices. For example, a scanner digitizes documents.
Digitalization is for an entity the use of digital technology to proceed tasks. Organizations digitalize their activities to develop new services and become more productive. For example, emailing is the digitalization of the mail service.

In this paper, we will only treat of the subject of Digitalization, considering the Digitization already made in preliminary steps.

A. Logic of the Digitalization

Digitalization concept is to use the service of new technologies for innovation. Among the new technologies we can quote the most interesting one such as Big Data, Artificial Intelligence, Augmented Reality, Cloud hosting. Being innovation by themselves, these technologies are not innovation in the Oil & Gas, but their applications and good use is. Thus is the idea of the concept Industrie 4.0 : applying new technologies to revolution the industry .

In fact, the goal and main logic of the digitalization is to use the new technologies to carry on the Oil & Gas industry activities in a more efficient way. The final aim is to use digital technologies as a driver of innovation in the petroleum industry to, for example, save energy, reduce costs, design faster, etc. Not to carry on different activities but to do these activities differently for the best.

Digitalization is broad concept with many possibilities to impact our industry, but we can define 3 large scopes of application, in link to Industry 4.0 :

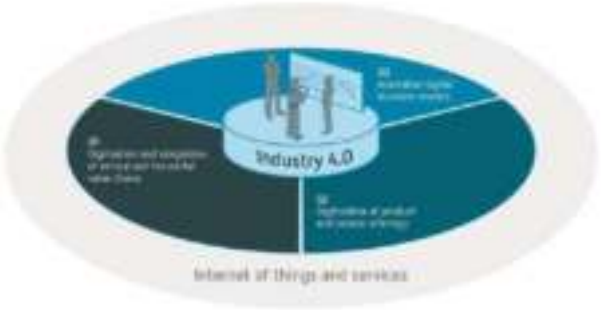

1. Digitalization and Integration of vertical and horizontal value Chain

   The first use of the digitalization is often to improve internal processes in a company, but once this is made, the next step is to integrate the processes of its value chain. By integrating part of its supply chain or value chain, companies have more control on their activities because it is a way to consider the company environment into the optimization process of its internal activities.

   This integration of our supply chain can appear as far fetch but it is in reality a daily practice for most of the actors of the oil & gas. For example, integrating the delivery time of your suppliers into your production system, merging the specification papers of a part to your equipment spec, All the projects, all the production system in Oil & Gas is the result of an integration of skills and expertise from many companies. Now the digitalization comes a mean to smooth these interfaces and deepen the relationship between entities.

   If we reuse the digital technologies on the examples above. We can easily create through the cloud an interface between the ERP of different suppliers and your company. So, when making a production plan, your internal software can go check the capacities from all the different suppliers and thus propose different scenarios based on the price, the quality, the delivery. Letting you decide about the best configuration to put in place. This example is already live with a german electrical cabinet manufacturer able to probe all the distributor parts available in order to design the cabinet with the minimum time of procurement

   Same goes for merging the specifications of your suppliers' components with the ones of your equipment. It has been a paperwork for decade, but thanks to digitalization and 3D Digital Twin, it is now feasible to transfer and aggregate all these data digitally and pass them more efficiently to engineering and operators.

   Once again, the relationships between all the layers of a supply chain and value chain are no news, but the digitalization is really deepening the possibilities of these partnerships. To the extend, where the concept of Extended Enterprise has been created to specify this new kind of relationship where companies do not work as a "chain" anymore but as a "network".

2. Digitalization of product and services offering

   The digitalization of a product or a service is usually the most natural application of the new technologies in our field, or it is a least the simplest to represent. In this case the digitalization main objective can be to add a digital layer on top of a product or a service, and can be to create a fully digital product or service.

   To illustrate these two possibilities, we can refer for the first one to the example later explain in this paper of the agitator digitalization. The aim of this project of agitator Digital Ready is its internal capacity to capture data about its operations and about its environment in order to participate actively in the Digital Twin of the Operator. By acquiring these, data from the agitator, the Operator is able to optimize operations, decrease downtimes and failure, simulate production, trace the quality of the actions, etc. In this case the digitalization is overpowering the functionality of the product in order to create more value for the users in operations thanks to this digital layer.

   A common example for a fully digital service created by the digitalization is the service of maintenance predictive proposed by many solution providers. Most f the time, these applications are proposed to operator as an add-on to plug on their scada system to detect deviation in assets running data to alert upfront the Operator on risk of failure. Over the last years, these solutions have proved their efficiency and have become a must have for smooth operations. This type of offering and service was enabled by the use of Artificial Intelligence for the digitalization f the industry.

3. Innovative Digital business models

   Last in the order of this paper because the last of the Digital Transition step, is the emergency of new innovative Digital Business model. Linked to the establishment of the first two categories innovation which will generate new value, part of this value will of course need to be monetize. The monetization and the capture of this new stream of value will be done via the existing business relations between actors of the oil & gas industry, but part of this emerging innovation will require the creation of new business models.

   There not so many examples we can quote from the oil & gas itself, but this is the case on other industries. Just on the example of the airline industry where motors OEM sells their assets by a subscription to the number of running hours, and not at a fix rate. This business model integrates a sort of lending of the asset but also the maintenance of it. For the manufacturer it enables a long-term business model and give them the maintenance responsibility. For the airline, it ensures the motivation of the maintenance to make the airplane as ready to fly as possible and thus limit the number of flight delays.

   In more theoretical point of view, the digital transition is enabling companies to pass from reactive business model to pro-active ones. In our industry the reactive business model would be : the production line is down, operator call its service company, the service company pays a visit, the disruption is solved. In a pro-active business model where data are connected: auto-detection of an anomaly, service company pays an early visit, problem is solved before shutdown.

Digitalization has been tagged as the fourth industrial revolution not only because of the technical possibilities enabled by the new technologies, but also for the evolution of revolution it will generate in terms of people, business and legal organization between companies.

B. Pitfall of the Digitalization

Digitalization is an ocean full of opportunities as much as it is of pitfalls and traps.
We all know many examples of large failure when it comes to digital transformation where the results never matched the investments and efforts. Like any other innovation, the success of digitalization is never guarantee.

Digitalization needs to avoid 3 common mistakes which are preventing organizations, especially large, to create value. All of these mistakes are usually made at the beginning of projects, and when found later are impossible to turn around. These 3 common pitfalls are:

1. Approach Digitalization for its technology purpose

   As we explain on the previous party, the aim of digitalization is to use new technologies as an enabler of innovation. But unfortunately, we too often see popping up initiatives where the technology is put at the center of the work. From day 1, the digitalization is in peril because teams are sometime trying to push technology for its own sake and not to create value. With the wrong aim, these initiatives have the highest chance of failure

   Those situations are often created by top management answering to the shareholder of trendy topics. Lately, the last topic in all the focus of C-level is the blockchain. Even if blockchain is a great technology, no real profitable use case has been proven. Yet many companies have launched programs to create their own blockchain for the sake of communicating about this technology inside their company.

   This pattern of failure is today on Blockchain, was yesterday with Virtual Reality, and will emerge with a new technology tomorrow. Even if those technologies created value in few cases, it clearly never matched with the money and time invested. The main reason behind those failure was the wrong aim from the beginning to push a technology for the only sake of its own innovation, and not to create value. New technologies need to remain tools in the toolbox and go beyond the hype they create, to be used only when they are required. If not, digitalization will remain unproductive and ineffective, missing on the long term is opportunities.

   To be successful, the digitalization has to be approach like any innovation and aim to create value by solving pain points, increasing efficiency, or creating new services.

2. Approach Digitalization only globally

   In the first paragraph we explained how the digitalization was connecting the value chain and how its impact was global. Yet its implementation may not follow the same path. Many large companies have created large programs for digitalization with new business units in charge of pushing the digital in the entire company. Even if it is mandatory to gives a corporate framework to the digitalization, to make sure the work done does not deviate from the global aim, it is important not to push the digitalization only from the top of the corporate ladder. Digitalization, like any other innovation have to emerge from the pain point and in our industry from the operations or projects.

   Too often companies commit this pitfall to push the digitalization from the top with its global vision and global objective. Because, later on this vison is pushed to the operations who are asked to adapt based on this new dynamic. But the operations hardly adapt to innovator wish if the added value is not tangible for their daily emergencies or daily delivery. This is the reason why, most of the “Top-Down” digitalizations ended badly: the concept and idea were good, but the execution failed because of low support. The same schematic happens in the 90’ when companies were trying to push “quality” policies through the top management by creating “quality control” positions. It only really created value when organizations stated quality was part of everyone job.

   In our case of Digitalization, the pattern is sensibly the same. The digital transition will impact everything and every position of a company. It is thus important to take the matter from the birth of the company reason. Meaning the digitalization has to begin in the core operations. In this case, any paint point can become a Use Case of Digitalization with a clear added value. This approach often referred as “Bottom-Up” offers a good way to create value from your Digitlaization and achieve step by step a larger scope of digital transition. These small or medium initiatives are also productive on the global scope because thanks to the global framework initially put in place, you can be sure, the developments can be repeated or scaled up.

   Thus, the digitalization to be successful has to start small and grow inside a company from its core operations to create value and create momentum.

3. Approach only the technology of Digitalization

   The use of new technologies is at the heart of the Digitalization, as an enabler to create value. The new technologies are far beyond in advance of the problematics of our industries. Yet many projects of digitalization fails even if the technology seems ready. In this case the pitfall organizations

commit is to think only the technology will matter in the success of their digital transition. In fact, for few years now, new technologies are more than ready and mature to be applicated on our use cases. Unfortunately, in most of the case the failure is not technological. Failure comes from the environment of the company or of its partners.

An easy example of this type of pitfall is link to big data initiatives, especially those where companies try to have predictive maintenance. The algorithms in charge of the machine learning are all available and easy to implement. What is not easy at the opposite is the access to the rough data the algorithms will crunch. Accessing databases, or joining databases is not so much a technical challenge, yet many entities are struggling to do it because of legal and governance questions. It is important to realize in a context of oil & gas project, the operator is not the owner of all the data generated by the assets. In the same way, you can buy a car, but you are not the owner of the data generated by the vehicular. Operators are not the sole owner of the data generated in their projects, so when it comes to using these data for a predictive maintenance use case, Operators have to agree with partners on the data governance and the business model to create value for each one of them. In this case, the technicality of the digitalization is not a problem, the challenge comes from the partners organization and agreement.

In too many cases, the legal and business aspects of digitalization are forgotten or underestimated to focus on the technology itself. At the opposite, the digitalization to be successful has to start by setting the legal and business boarders to insure the compliance and the value creation of their later technology solution.

III. PROVEN PROCESS OF DIGITALIZATION

As explained through the beginning of this paper, Digitalization is a broad concept able to take different pathways to achieve its goal. In this part of the paper, we will present a path among others which has been proven in several occasions to be successful.

A. Value creation

Before jumping on the road to digitalization, it is quite important to set the goals of it, and as such define what is a successful digitalization.
Once again, many expectations can flow form a digitalization project impacting all the step of a project lifecycle. Yet from a general point of view, a successful digitalization projects is a project which has created value for its actors. If a project has failed to create and show it has created value for its stakeholders, then the digitalization cannot be considered as successful.

In a project, value can be created by different means :

1. Saving time
   Of course time is money, but digitalization may have to benefit from being more tangible than this maxim. To give some context, digitalization can in some cases accelerate a project or operations. A clear example of such acceleration is the use of the 3D Digital Twin of plant during its construction to assemble the different design and find the layout. By using such a Digital Twin, engineerings and contractors are able to scenarize the global design of the plant and chose the quickest one to build.
   In this particular case, using the same resources at the construction stage, contractors will build the plant faster. Thus saving time, and pushing the project for an earlier first day of operation.
   The value created by saving time can be easily calculated via the Return Of Interest (ROI).

2. Saving money
   On this aspect, the gain is quite clear on how saving money is a value creation. A penny not spent is the best source of value.
   An easy example of it comes with the more and more common usage of predictive maintenance tools. Imagine using such a digital solution on a MV motors running on a compressor. The predictive maintenance tool is able to detect early sign of rupture in the bearing of the motors and such send a warning.
   Without such a solution, the motor will have most likely turned until bearing explosion, causing damage to the motor rotor. Avoiding some expensive damages, this predictive warning transformed a rotor maintenance and reparation into a bearing replacement.
   The savings in this kind of operations are direct and happens quite often, representing a large pool of value to be created.

3. Increase performances
   In a sector like ours of process and operations running 24/7, the performances have a direct impact on the profitability.
   More and more, Operators use digital technologies to optimize their performances, as the process digital twin is trying. It is the use of running data to analyze and optimize the operations of a real-world process over time. The model represents the key characteristics of the selected physical process, to find the best suitable configuration of production. Thus, production configuration can be adapted in real time to reduce the cost, maximize production, or increase margin.
   All those means to of course generate more value from the same operations.

4. Reduce downtimes
   Downtimes are for sure the nightmare of every operators and a large source of extra cost. Extra costs occur by the cost to repair the cause of downtime, as well as costs appears by the losses of non-production.
   A daily use case is the installation of a new equipment. In same case, this installation will require a stop in the production to switch equipment. Thanks to the 3D digital twin, operators are able to perform a spatial analysis on the plant. Considering the perceivable architectural elements with their boundary, the solution is able to stress the feasibility of an

installation and run its simulation. So later in action, operators are more efficient in their manipulations.
The value created by restarting production earlier is easy to calculate and value for operating companies.

Once this value created, it is of course mandatory to measure it. Without the measure of the value created, it will be impossible to prove or estimate the value of a project and thus impossible to motivate the investment to initiate the process.
A successful digitalization is a transformation enabling to create value and able to measure the value created.

B. Team and Business Model

Once the value creation and its measurement identified, it is important for the leader of a digitalization process to build a robust team and draw a first business model.

It is quite clear today that one single actor is not able to have all the solutions and all the opportunities of digitalization. As such, the digital transformation will happen across all the supply chain of our industry.
For a leader, it is important to build up a strong team to approach the complexity of digital topics. A strong partner in a project will be a company with a strong technological background ready to innovate, and also a company you can trust to share knowledge with. Digital projects will always require the exchange of data and information, which will require a commitment stronger than legal NDAs.
Finding the right partners is not enough, it also important to pay attention to the way the puzzle will be assembled.

The best way to organize the collaborative team is to put in place the correct business model.
A good business model is able to measure the value created by digitalization and transfer part of the value created to the digitalization team. In this sense, Digitalization may require the use of new business models not so common in the energy industry, but which are at use in others.
A good business model will help bring the different partners around the table to start the project, but a correct one will also be able to retain the partners around it.
As such the correct business model is thus the one able to capture part of the value created at the client, but also model the relationships between partners.

New business models could be explored in the future years, such as leasing of equipment, contract per running hours, etc.
But one thing is sure, once the value identified, the team settled and the business model in place, the technical aspects of the digitalization can start.

C. Top-Down of Bottom-Up

Depending on where you stand in the value chain of the process industry, you may choose between two different approaches of the digitalization, the Top-Down or the Bottom-up to tackle the technological aspect of the digitalization.

Both approaches present their pros and cons, but it is important for any of them to keep an agile method and scenarize the different technological resolutions of the initiatives.
Some solutions may be more complete but too expensive, some can be lighter but good enough, etc.

In that respect, the Top-Down approach is dedicated to the End Users and requires investments at the scale of these facilities. This Top-Down approach fits perfectly on new projects, especially in offshore or harsh environment. In these cases, Industrie 4.0 digital technologies can provide End Users with step change in Capex and Opex.

In opposite way, the Bottom-up approach may please all the players of the value chain from the bolt manufacturers to the End User.
It begins with the digitalization of components or small equipment. Then, it escalates to machines, to the process and on last stage at the whole plant. This approach is easy to implement especially on existing facilities. There, it brings quick wins at small risks with great pedagogical value in organizations.

At the end, the purpose of the Top-Down and Bottom-up approaches is to build the digital process loop by one way or another.

D. The Digital Process Loop

As previously said, the digitalization is not the target by itself, it is a mean to create value. The best way to ensure you digitalization process will generate value for the example of operations is to integrate the operator vision of a Digital Process Loop.
In the picture below, we illustrate how to build the digital process loop in parallel to the usual process control system loop.

Compared with the existing conventional process control loop, the digital process loop provides End Users with three key major benefits.
First, it offers far shorter response time, then it guides the operator straight to the root cause, finally it allows to model scenarios for resolution. These capabilities change the game in running large and complex operations.

In the picture above, the idea is to capture most relevant data from the installed base. Then, after a first treatment the purpose is to produce passive data and active data.
The passive data are related to the components and the equipment while the active data translate the process status. The passive data helps to build the Digital Twin of the components and the equipment, then the combination of passive data and active data contributes to build the Digital Twin of the process and the whole plant.

Anyway, collecting these data and treating them to build up the digital loop require multiple competences. Some of them belong to the End User, but most of them standing in its supply chain.
Therefore, creating value from the digital process loop is the results of collaborative process involving key players, in the right business model with the right approach.

IV. ECO-CONCEPTION & DIGITAL READY

This part of the white paper is now going to present a practical example of digitalization. Under the example of an agitator, we will present how Mixel digitalized their equipment.

A. Context and scope of the digitalization

Agitation is a complex step in any process because it requires to master all the different disciplines of mechanic, hydraulic, viscosity, electricity, and automation; to realize the expected agitation and produce the right quality of output product.

In this sense agitation is quite a paradox because it is present in almost all the processes such as water treatment, chemical, food; and it is an operation quite crucial for the process; but yet so little do we know about this knowhow.
In fact, the knowledge about agitation is very much concentrated in few OEMs concentrating the vast majority of the market. And those companies acquired their expertise from decades of experience in design and in operations of their assets. The theoretical models and comprehension of agitation processes is not quite there yet. Or at least not precise enough to match with the current expertise of those OEMs.
Agitators being complex by nature, at the heart of the process, with an high criticality and a lack of theoretical understanding; made it the perfect candidate for a digitalization.

In our example, the digitalization was balanced into two projects running one after the other to serve two different purposes.
The first project named “Eco-Conception” is an R&D approach to optimize the design of agitators and reduce the need for resources by avoiding over quality.
The second project named “Digital Ready” targets to connect the agitator and capture more data from this critical operation to be used by the operator.

In term of team, Mixel partnered with 2B1st Consulting and Vibratec for the execution of the project. One expert of the digitalization, the other expert of instrumentation and signal analysis.
Concerning the Business model to be adopted by the collaborative team, 2B1st and Vibratec were hired to execute a prestation and would not claim any Intellectual Property from the innovation created by the project.
As such, Mixel is consequently the sole owner of the Intellectual Property generated by the Eco-conception project and will also be the sole partner involved in the commercialization on Digital Ready agitators.

In this example, the digitalization project was aiming to learn more about the agitation equipment for one part. And for the other to create a digital twin shell to be proposed as a service to the agitator customers.
As our project was centralized around the equipment, we were by nature in a bottom-up approach. Coming from the below layers of the supply chain to propose a digital solution to operators and engineerings.

The aim was double. First learn more about the operational characteristics of agitators and their dynamic mechanical behaviors to later optimize their design. Second, proposing a digital twin solution to operators to integrate the Digital Process Loop at its roots by capturing more Passive and Active Data.

B. Eco-conception

This project took its essence from field feedbacks.
An agitator is composed of different parts: Electrical motor, gear box, shaft, and propeller. Along the years most of the maintenance requirements were on the gears box and the electrical motor. In fact, the shaft and the propeller never break despite operators using the agitator in conditions way beyond their window of design with viscosity double the supposed one.
This early deterioration of the gear box could be avoided if the shaft was more flexible and thus transmitting less efforts to the gear box and motor.
In term of maintenance cost, it would be better for the shaft to be more flexible and preserve the bearings. Even if the shaft would come to a rupture, it would be better to break the shaft than the gear box.

In order to acquire more flexibility, the goal of the project was to measure the real flexibility and efforts applicated to

the agitator during a process test and compare those numbers with the theoretical numbers estimated by the design.
By comparing both, it would later be used to optimize the models of design in order to reduce the stiffness and increase the flexibility, and consequently durability.

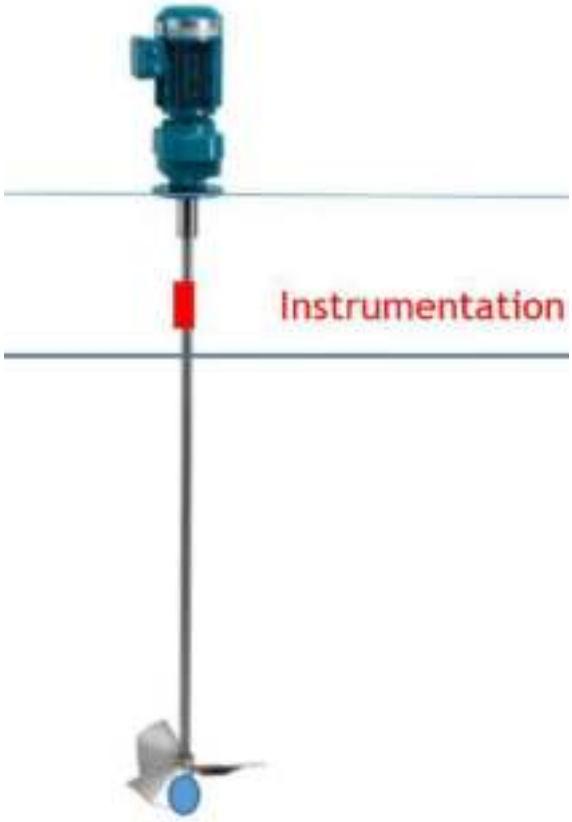

Fig. 1 Instrumentation of the agitator

It was decided to equip the agitator with different types of instrumentations:
-In red above the water, 3 strain gauges in order to capture all the efforts applied to the shaft. Those efforts are the flexion, traction, compression, torsion.
-In the red above the water, a rev counter to measure the rotation speed, and torque
-In blue below the water, 2 accelerometers to capture the turning position of the propeller and by calculation obtain the shaft deformation
-On the motor, 2 vibration captors in 3 axes.
-On the electrical drives, tension and intensity were monitored

A serie of tests was programmed to vary the propeller, shaft diameter, rotation speed, and analyze their impacts on efforts and deformation. In the table following and the picture, you will be able to see the different type of test conducted.

Fig. 2 Different set of propellers to be used

TABLE I
Agitator test configuration

Test Id	Parameters		
	Propeller diameter (mm) Propeller type	Shaft (mm) Shaft height	Rotation speed (rpm)
1	1200 TTA	73 3 m	30 / 45 / 55
2	1200 TTA	73 4 m	30 / 45 / 55
3	1200 TTPA	73 3 m	50 / 65 / 80
4	1200 TTPA	73 4 m	50 / 65 / 80
5	1200 T3P45	73 3 m	40 / 50 / 60
6	1200 T3P45	73 4 m	40 / 50 / 60
7	1700 TTA	73 3 m	20 / 30 / 40
8	1700 TTPA	73 3 m	25 / 40 / 55
9	1700 T3P45	73 3 m	25 / 35 / 40
10	900 TTA	60 3 m	40 / 60 / 80
11	900 TTA	60 4 m	40 / 60 / 80
12	900 T3P45	60 3 m	60 / 80 / 95
13	900 T3P45	60 4 m	60 / 80 / 95
14	900 TTPA	60 3 m	80 / 100 / 120
15	900 TTPA	60 4 m	80 / 100 / 120

To push the tests to the limit, it was also decided to add 2 stress tests aiming to go to the rupture of the shaft in

order to find the elastic limit of the agitators. These tests were performed by increasing the speed rotation of the agitator way beyond their operational limits and ended up by the rupture of the steel shaft.

All tests carried on, have been successful in showing a margin between the estimations given by the design simulations and the field values measured during tests. The difference between both family of figures had little variation in ratio. Meaning modelization figures of effort were quite aligned with their tests results. In general, the ratio between simulated value and measured were about a third.
This ratio being quite constant between the different tests, tend to show the quality of the models used for design. In fact the models only needed to a calibration to fit perfectly on the reality of agitator operations.

Beyond the learnings done on the mechanical aspects of the agitator through efforts and deformations, it was also the occasion to link those variables to the electrical/vibration ones.
In fact, the second goal of this eco conception was to detect and evaluate the patterns of deformation/efforts through the other type of data collected. The aim of this pattern recognition was not directly done for the eco conception project, but for the following one Digital Ready.

C. Digital Ready

The essence of the Digital Ready project is to enable operators to use the digital twin of their agitators to better operations and maintenance. To do so Operators needs to be able to detect early signs of maintenance needs as well as acquire warnings of failure which today is not possible for agitators.
In term of functionalities, those needs translated into the aim to enable the agitator to capture data and share those with operators, in addition to a brick of knowledge. The knowledge brick being the expertise for operators to translate data into information. In our case the information could be deviation due to maintenance need or warning about product quality in the process of agitation.

Of course, with all the instrumentation used during the Eco Conception tests, any type of deviations could have been easily detected, but in the field it was not realistic to propose such a complex and expensive solution for operators.
Usually, agitators on the field are not equipped with any instrumentation, we thus needed to propose a solution affordable for capturing the data and transmitting them to the operator. The effort was to limit the instrumentation as well as bringing a simple connectivity solution.

In plants, variations in electrical intensity or vibrations are easy to measure and a specific analysis of those signals must make it possible to detect malfunctions. During the Eco-Conception tests, we aggregated several physical quantities measured in a synchronized way to be able to determine during the development of the Digital Ready project the pattern through each variables measured.

Given good results of malfunction identification through each type of variable we decided to concentrated our efforts on the vibrations and electrical intensity, to be captured and transmitted to operators.

Using only two pieces of instrumentation, we could transfer to operators the vibration and the intensity. These two variables are enabling operators and software to analyze two direct values but also its combination. Using those 3 channels of information, we were able to identify all the malfunction of the equipment and problem in the process.

At this point, the challenge was to propose an integrated solution available to be sold in a package with the agitator and which could be added to any operator digital environment.
The decision was thus to integrate the intensity and vibration captors directly in the motor and gear box group. Those captors will be standardized to fit all the portfolio of agitator. The captors will be linked to a gateway attached on the equipment as well. The gateway being adapted to the client in order to fit to its communication infrastructure (Bluetooth, LoRa, wifi).

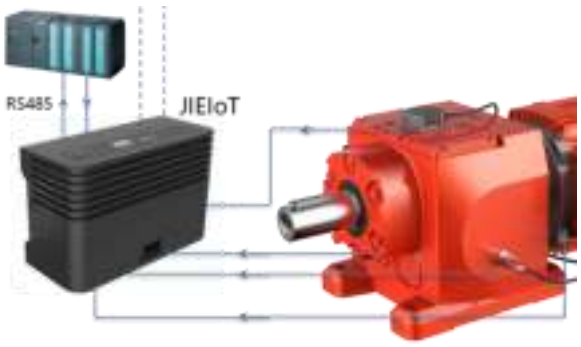

Fig. 3 Captors and gateway installed on Agitator

The arbitrage was decided to adopt a simple solution to put in place and use for operators to service 99% of their needs regarding agitators.

The solution created for the Digital Ready project was of course perfectly suited for brand new agitators sold to customer but could also be installed in retrofit for existing plants. To go beyond, the solution was neither brand specific and could service all the type of agitators, given the knowledge acquired by the Digital Ready project into identifying patterns of deviation.

The first feedback from field is positive in term of installation and integration for operator into their digital environment. Now gaining some experience, the set-up has already caught its first deviations and served its purpose to alert operators to optimize the plant process.

II. CONCLUSIONS

In this article we have tried to present the theoretical as well as the practical aspects of the digitalization of an equipment for the Energy industry.

Looking back at 2014 when new technologies were trying to find their usages in the industry, we now have a more practical vision of the impacts and benefits for our operations. The intention of this white paper was also to

go beyond the hype of some technologies and to share some good practices. From years of digitalization projects and their challenge, our goal is also to enable other actors to follow the path and bring more digital technologies to the service of our sector.

The example of the agitator Eco Conception and Digital Ready are of course transposable to any type of equipment and should be used as such.

The capture of more data being at the core of the digitalization need, equipments, because of their proximity with the process, are of course the first brick to be implemented on the path to Industrie 4.0 plants. But the digitalization of agitators even if creating a lot of value by itself, is not enough. We need to replicate this example to all the types of equipment, being mechanical, electrical or automation to optimize our operations globally and carrying on doing better at delivering energy.

III. ACKNOWLEDGEMENTS

Being the work of the two authors of this paper, it is of course the role played by the commitment of several of a competent and passionate team that proved its value in the success of this project.

To do so, it is for us mandatory to recognize the work of Mixel Team, lead by Victor Ruys (head of R&D). The expertise of Vibratec's people into the instrumentation and treatment of the data captured during the Eco Conception tests was also crucial for the good execution of the project, especially Hug Siwak (Expert in Instrumentation, Analysis, and Simulation), Arnaud Chillet (Expert in Instrumentation and Analysis).

IV. VITA

Jean Guilhem graduated from the engineering school Supélec Paris with a specialization in Electro-communication. After several experiences in Siemens Oil&Gas and Air Liquide Large Industry working on digital topics, he received a MBA degree from the SDA Bocconi in Milan. Joining 2b1st Consulting in 2018, he is now Operations Director.
guilhemjean@2b1stconsulting.com

Philippe Eyraud graduated from the engineering school INSA Lyon in 1986 and of an MBA EM Lyon the following year. Philippe has been for 32 years the Owner and President of Mixel SAS, the specialist of industrial agitator, based in France and in China. Philippe also has the title of Adviser to the French Ministry of Commerce on international business.
p.eyraud@mixel.fr

DIGITAL SUPPLIER INTEGRATION A KEY TO LOW & UNMANNED INSTALLATION

Svein Edvin Håvåg
ABB AS
Kokstadvegen 23B
5257 Kokstad
Norway

Ine Fossen
ABB AS
Snarøyveien 30
1360Fornebu
Norway

Tor-Ole Bang Steinsvik
ABB AS
Snarøyveien 30
1360Fornebu
Norway

Abstract - If you are to achieve low and unmanned installations, reactive maintenance activities must be eliminated as far as possible and significant reduction in planned maintenance activities must be accomplished.
Prediction and planning of the maintenance task several years upfront is also an important aspect in a 2–4-year maintenance campaign strategy.
Reducing the need for traveling to site for fault tracing for operator or supplier service maintenance crews is also an important aspect, especially on un-manned installation.
The key to achieve this goal is to establish a fully-fledged condition-based monitoring solution where the equipment suppliers are integrated in the concept in close to real time. Giving the supplier access to all relevant equipment and process data in a user-friendly web-based format makes it possible to leverage the equipment supplier's competence for day-to-day maintenance decision making. This can close the gap to replace the traditional site-based senior engineer that could listen, see, smell and or use the inner "feeling" to identify if something was likely to fail.

I. INTRODUCTION

Do to need of reducing CO2 footprint, reducing risk (HSE) and optimizing the operation cost specially at offshore asset low manned operation is a highly important target. There is also a need to go towards unmanned facilities or just having a marine crew onboard to maneuver the asset if needed, (big storms, Iceberg)
In this Paper we will elaborate around the technical aspect of the abstract, we will also look in the project: Digital supplier integration Gina Krog – Integrated operation center.

II.CONNECTIVITY

For low and unmanned installation, connectivity plays an important role. In the case of condition monitoring, connectivity means to collect data and make it available for humans and/or machines to interpret data in an intuitive way. Over the last few years, "Internet of things" (IoT) has developed at an incredible pace. IoT incorporates several protocols for connecting to devices and moving data, whether being networked or wireless protocols. Along with trends in SW development, such as microservices and platform independence of applications, a combination of these trends paves the way for solutions in the low and unmanned installation domain.
To ensure solid solutions for connectivity, there is a need to collect data directly from field devices and gateways and efficiently distribute data with minimized risk of losing data. Also, the complexity of the different protocols and systems is removed and transform it to a unified way of treating data and what it represents.
As a result, the demand for a connectivity solution that connects to the device, gathers data, and exposes it on a common interface where the complexity of the field protocol is extracted is clear for low & unmanned installations. The application should also have short term storage to not lose data and ensure that the client cannot access the field devices directly ("read only"). By utilizing microservices one can create a flexible application for collecting and exposing field device data by making an application where the "core" should contain short term storage and a common interface to other applications. The connection to field devices will vary based on protocol, but these can be uncoupled from the "core" by utilizing microservices architecture.
By doing this transformation, the development and deployment of applications based on this data is much easier to accomplish, because the developers/system integrators only need to consider one interface, meaning that everything from machine learning to simple visualization avoids the complexity of field devices and systems.

III. DEVOPS WEEL

The data can then be used in cloud-based digital tools which enable the integration of the OEM`s (Original Equipment Manufacturer) in a faster and leaner way. New principles in software development with platform independence cloud solutions enable the provider to update and improve the solution without interrupting the user. By combining data connectivity, cloud applications and unique product and service competence anywhere on the globe, OEMs can support the operation and maintenance personnel in a faster and cheaper way by implementing modern methodologies for software development

and operations, like DevOps. In this way, suppliers can deliver and maintain solution of relevance to users on low & unmanned installations.

IV.DIGITAL SUPPLIER INTEGRATION GINA KROG – INTEGRATED OPERATION CENTER.

In this section we will look closer to the technical solution and collaboration for Digital supplier integration Gina Krog Pilot and how we sees this is one of the keys for low & unmanned installation.

The OEM and The operating company for Gina Krog have launched a pilot project called Digital Supplier Integration, where the OEM collaborates with The operator on digital integration. The aim is to improve operations at offshore assets.

The project enables a digital transformation of monitoring of critical electrical systems on the platform, accelerating Operator's condition monitoring capabilities with a focus on improving safety, reducing operational costs, and increasing production efficiency.
Adopting a collaborative maintenance model enables Operator to start the journey from today's calendar-based maintenance program towards prescriptive maintenance.

A. Technical Solution:

Data will be transferred from the platform's power management system and electrical condition monitoring system to Operator's OMNIA cloud platform, using an onsite data pump.
Live data will be securely streamed to OEM own cloud, where a dedicated team will utilize the data to continuously improve condition monitoring technology and tools to be used by the OEM`s Reliability Service team.
By streaming data directly to cloud, end user is securely transporting high-level information from assets that will deliver transparency on performance, better predictability, and process optimization.

Gina Krog had a Condition Monitoring System for the electrical equipment in place from production start, the Asset Optimizer - Maintenance Workplace condition monitoring framework

Fig.1 Topology

The Asset Optimizer - Maintenance Workplace covers the following equipment:

- Base System
- 800xA PMS
- Power Transformer Monitoring
- 110 kV GIS Switchgear Monitoring
- 11 kV Switchgear Monitoring
- Dry Transformer Monitoring
- Low Voltage Switchgear Monitoring
- System 800xA Historian Database
- COM600 Disturbance File Recording

The Maintenance Workplace provides a work process for making decisions about maintenance actions. The aim was to give the following benefits:

- The condition monitoring will allow for a higher degree of predictive maintenance. Typically, the maintenance programs for the equipment are based on service inspections at regular intervals (yearly in most cases) unless the rate of wear or operational time is monitored. The Maintenance Workplace provides this monitoring of wear and operational time which makes more efficient planning of service possible.
- The trending of parameters and statistical functions that come with the System 800xA Historian database provides a basis for longer term evaluations of the equipment performance. This is a valuable tool when planning upgrades and modifications.
- The introduction of the Maintenance Workplace with the Asset Reporter function ensures that all maintenance relevant events and alarms are accompanied by a written report on severity, possible causes and suggested actions. This makes the decision process w.r.t maintenance quicker and helps fault finding and problem solving in general.

The overall economic benefit from this system primarily lies in improved plant integrity, i.e., that down-time due to equipment failure can be avoided to a greater degree. The secondary economic benefit is that it allows for a more efficient use of external maintenance services.
However, as the Asset Optimizer - Maintenance Workplace was an extension of the PMS (Power Management System), access for users was based on access rights regulated by the work permit process. The problem with this was that access to the user interfaces is very limited and that ad-hoc usage is impossible. Also, the user interface is set up in a standardized way and adjustments and improvements are not easily implemented. It was clear that this was a bottleneck for remote users and especially for supplier integration.
This limitation was the key driver for exploring the capabilities of the new edge and cloud technologies that have recently become available. This was the basis for a co-operation project between OEM (Original Equipment Manufacturer) and Operator named IOC (Integrated Operations Center) Digital supplier integration Gina Krog Pilot.

B. Streaming Technology

The datapump is designed as an Operational Technology (OT) component with limited Internet connectivity and will be deployed in the industrial domain to pull data from field devices and systems.
From southbound to field equipment, the port and communication interface used is dependent on the protocol type. From the field plug to The datapump AMQP is used. Northbound to the IT (Information Technology) side, the AMQPS protocol is used for communication with other systems and networks, supporting both TLS (Transport Layer Security) and authentication. It also offers one-way communication (push), only allowing for out-bound traffic. A buffering mecha-

nism is used to avoid data loss and efficient data transferring, ensuring optimized performance in all deployment scenarios.
The datapump architecture is based on microservices. Microservices enables flexible deployment and compatible upgrades without disturbing ongoing processes. SW can also be installed on customer sites without installing more than needed, increasing security and performance. Direct access to the field devices and field network is restricted by design, all data are accessed via proxy. The datapump is designed to run in docker, and the recommended OS (Operating System) for production deployment is Ubuntu LTS Versions However, The datapump can run on any Linux/Windows OS.
The datapump package is based on the latest trend in SW development, being micro-services and platform independency. The datapump extracts different protocols and systems and transforms it to a unified way of treating the data as what it represents. The ability to collect data directly from field devices and gateways in addition to process values from the existing control systems is essential to get the necessary improved surveillance and monitoring.

Fig. Datapump dataflow diagram

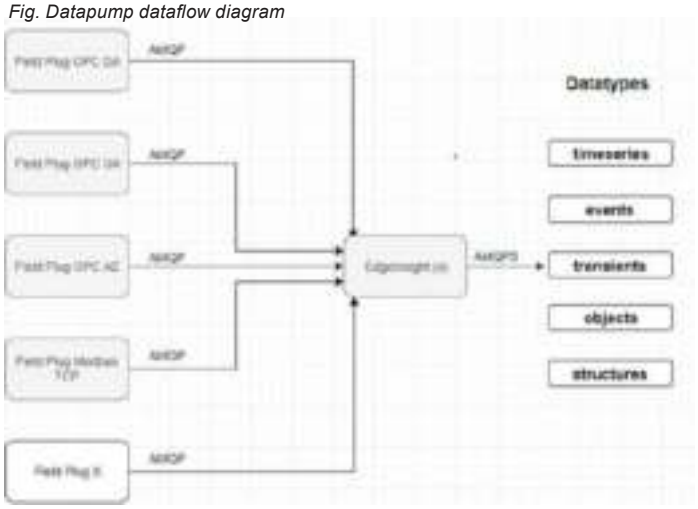

Fig.2 Datapump dataflow diagram

The datapump connects to the device, gathers the data, and exposes it on a common interface where the complexity of the field protocol is extracted. The datapump has a built-in short-term storage to buffer data and a proxy function to ensure that the client cannot access the field devices directly. The connection to field devices will vary based on protocol, but these can be uncoupled from the “core” by utilizing micro-services architecture.The datapump utilizes AMQP as a standard interface, and uncoupled plug-ins as connections to field devices. This design allows for traversing network layers, thus integrating with anything from control systems and field devices to databases and cloud technology.
Northbound to the IT side the AMQP protocol is used for communication to other systems and networks. The datapump supports TLS and authentication and one-way communication (push), meaning only outbound traffic allowed. The OPC UA protocol is an alternative and supports TLS, however, currently, the OPC UA protocol depends on a client/server approach, meaning only two-way communication is properly supported.
Southbound to field equipment the port and communication interface used is dependent on the protocol type of the field plug. AMQP is used between the different field plugs and the The datapump core
Data availability and potential data loss due to network issues or failing HW/SW components are handled through a queue centric design. Each field plug has an internal buffering mechanism, that will buffer data internally in the field plug if The datapump is not reachable. When the connection is recovered, all buffered data will be sent. Buffering is supported between all components to avoid data loss.
The data from field plugs is transformed to keep all context from the underlying system for the following data types:

- Objects - contains metadata on the objects found in the different field plugs
- Structures - contains metadata on the structure found in different field plugs (hierarchy relation between the objects)
- Time series - contains the time series data being produced by different field plugs
- Events - contains alarm & event type of data from different field plugs
- Transients - contains high frequency data (typically from 1000 to hundreds of thousands of samples within a short time) from different field plugs

C. Dashboard Tool:

The Dashboards is a modern cloud-based web application, which makes it possible to easily visualize real-time data from the production plant to be accessed on any Internet-connected device. It can be used to highlight certain areas of the plant by developing different views and dashboards, and it also enables decision-makers to make effective use of this information, by giving them the opportunity to:

1. Get a quick overview of the equipment health and operational status
2. Combine and compare condition data, alarm and events and process data all in a single view
3. Quickly set up personal views to troubleshoot potential issues.
4. Comment on problems or opportunities detected and share this information with others.

The Dashboards user interface is HTML5, which makes all functionality in the application accessible from web browsers.

Fig.3 Example of Electrical Single line Dashboard

D. Trending Tool:

Fig.4 Tendering Tool

The cloud-based version of Event Log Viewer runs directly on top of The datapump and gives easy access to all historic alarms and events to any user in an easy-to-use interface. During operation, op-

erators and maintenance personnel frequently examine event and alarm sequences to retrieve information about the control system. This may be to investigate what occurred during a shutdown, confirm that everything progressed as expected during startup or to ascertain that new logic is working as expected.

The trending tool is the preferred tool of our process performance specialists, which has evolved over the last few years to support them in their hands-on work in improving customer operations. It is a cloud-based tool for analyzing and viewing historical process data, alarms, and events. The trending tool is typically used for ad hoc trending where the user quickly can select a set of tags and trend them at preferred time range.

Key benefits of the Web trend are:

- Simple and easy to understand user interface
- Web-enabled trending which can be accessed directly from your browser
- Advanced visualization Of data
- Easy to share and bookmark trends
- Collaboration support through the comment feature
- Enables process values and alarm and events from the control system in the same trend for advanced analysis scenarios
- Simple and easy to understand virtual tag creation

The functionality of the The trending tool application holds three main parts. First is a set of tools useful for configuring trends, further is the selection and configuration of tags and options to manipulate timeframe and zoom factors. Lastly, a chart area illustrating trends, comments, and annotations.

However, The trending tool is more than just a trending tool. It also holds features enriching trends with drawings, making it easy to add custom information and share this with other users. If users want to share data with someone not having access to the application or use other tools to work with the data, trends can easily be exported, as files with comma-separated values can be downloaded to the user's computer.

E. Event Explorer Tool:

Fig.5 Event Explorer tool

The cloud-based version of Event Log Viewer runs directly on top of Ability The datapump and gives easy access to all historic alarms and events to any user in an easy-to-use interface. During operation, operators and maintenance personnel frequently examine event and alarm sequences to retrieve information about the control system. This may be to investigate what occurred during a shutdown, confirm that everything progressed as expected during startup or to ascertain that new logic is working as expected.

F. Operation Model:

As the pilot progresses, OEM will take over day-to-day condition monitoring operations for the critical electrical equipment, to be managed offsite by OEM Reliability Service team. This will be done in close co-operation with Gina Krog personnel and operator Integrated Operations Center (IOC). Operator engineers will work inside Operator Enterprise Resource Planning (ERP) system, helping with generation of notifications.

1) Other benefits of using an Edge Device:

- HSE, it is impossible to affect the system at site because you are only working in the Microsoft cloud environment. You do not need to be afraid that you can cause some failure at site.
- No use of work permits
- Better signal quality, you avoid several steps that can potentially reduce the quality /resolution and time loss

2) Further development and value (from OEM perspective):

- Further value by onboarding other assets, utilize Fleet monitoring benefits.
- Development of new tools/ use cases/ use of AI/ML (Artificial Intelligence/Machine Learning) to earlier detest faults and predict several years upfront when maintenance is needed.
- Elaborate combination of other tools like simulators to predict consequence if components or systems are failing.
- Implementing ERP systems: project specific documents and manuals will reduce maintenance administration time and time spent in a critical troubleshooting situation.
- Automated Notifications in the ERP System
- Onboarding other systems at the Asset like Motors/Drives etc
- Better prediction with use of high-speed data

V. CONCLUSION

To meet the goal for achieving low and unmanned installations, integrate the OEM a digital partner along with other companies that can supply more value in the operation phase but also in the engineering phase is one of the keys to success. Utilizing the OEM`s fleet perspective and equipment knowledge will hopefully lead to better KPI`s of reducing CO2 footprint, reducing risk (HSE) and optimizing the operation cost.

VI. REFERENCES

Press release : ABB collaborates with Equinor on digital integration to improve operations at offshore assets.

VII. VITA

Svein Edvin Håvåg has been in ABB since 2006, working with control systems, Electrical systems/instrumentation and Digitalization. He now held the position as Sales responsible for Asset Management & Energy Management in IA Energy Industries.
svein-edvin.havag@no.abb.com>;

Tor -Ole Bang Steinsvik has been in ABB for over 25 years. Working with control systems and have had several managing positions the last decades. He now held the position as Condition Monitoring Solutions and Services Lead in IA Energy Industries – Digital Services
tor-ole.bang-steinsvik@no.abb.com

Ine Fosen is working as Business Developer in in IA Energy Industries, Digital Services.
ine.fossen@no.abb.com

CREATING AN ALGORITHM TO IDENTIFY PATTERNS FROM POWER GENERATION ASSET & IIOT SOLUTIONS

Paper No. PCIC Europe EUR22_31

Mateus Nicoladelli de Oliveira
WEG Equipamentos Elétricos
Jaraguá do Sul, SC, Brazil
nicoladelli@weg.net

Ademir Nied
UDESC Electrical Engineering Department
Joinville, SC, Brazil
ademir.nied@udesc.br

Abstract - Understanding the real operational status of a fleet's assets is challenging and highly desirable, it can maximize the time between unexpected shutdowns and improve the fleet performance. Digitalized signals from industrial electrical and mechanical equipment are becoming more and more available at the automation level. Currently, most high value-added assets, such as compressors, pumps and generators, they are equipped with monitoring devices which can remove the asset from service in case of severe problems, as high temperature and excessive vibration. In general, these devices are unable to identify an incipient operational deviation, which in the medium to long term may cause a sudden shutdown or unavailability period.

In this paper, a workflow is proposed to guide the algorithm creation process, focusing on the operational pattern detection, based on data from SCADA (supervisory control and data acquisition) or dedicated acquisition system. Additionally, the areas of competence and the interface between them are discussed observing the proposed workflow.

To evaluate the proposed workflow, a classification model and a regression model are built. The first applies a Random Forest model and the second an artificial neural network (ANN), a Time Lagged Feedforward Network (TLFN) focused model, configured as a regressor. The classifier identifies a specific operation pattern and the ANN emulates a component temperature under normal condition. The results noted at this conceptual study shows that the proposed workflow can be a good methodology for advanced algorithm construction.

Index Terms - Neural networks, industrial internet of things, machine learning and operational pattern detection.

I. INTRODUCTION

Almost every industrial asset troubleshooting technique uses time series analysis as well as correlation analysis. The effectiveness of the troubleshooting process depends on three important aspects: team experience, team expertise and the data quality. Those elements are also critical and important for a high-level Industrial Internet of Things (IIoT) Solution creation.

Fig. 1 – Basic levels of IIoT Solutions

Fig. 1 shows the basic three levels of IIoT Solutions, the base is the data acquisition and storage. The IIoT projects must focus first on existing sensors (green) and digitalized data, which accelerates the project start-up. The second level is the Data-Informed Solutions, exploring the data visualization to describe the asset operation, supporting the troubleshooting tasks. The Data-Driven Solutions is the higher level, here the previous asset knowledge, the expertise and operational domain are used to create value and important insights, via customized report/dashboards, advanced algorithms and others.

For this case, the expected result from an algorithm are the creation of insights to support the O&M team to prevent unexpected asset downtime, especially such ones that are long-terms or expensive.

This paper covers four main topics: First, the application background, some aspects of IIoT Solutions and the basics between the asset data acquisition and value creation.

Second, the exploratory analysis of time series data and the creation of Data-Informed reports are presented.

Third, are the basics to start the algorithm construction, it supports the creation of insights and value for IIoT Solutions. Fourth, is the production level, presenting a suggested Data-Informed dashboard, and the pattern detection from univariate and multivariate dataset.

II. APPLICATION BACKGROUND

Fig. 2 shows a simplified architecture of power generation asset. The edge devices are designed to act during the asset operation, controlling its power generation and protecting the components against faults.

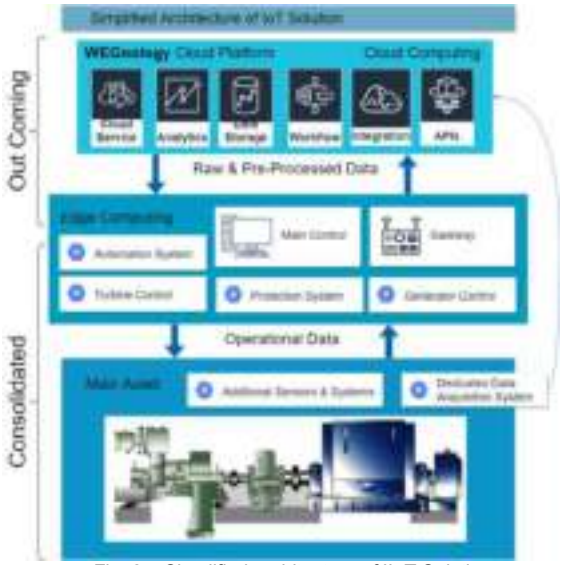

Fig. 2 – Simplified architecture of IIoT Solution

Such edge devices have been designed in this manner up until recent date, they can measure, control and protect the assets using the instantaneous measurements. In general, they were able to store few data in memory and have limitations to be integrate with other systems.

a. Data Acquisition

Details of data acquisition such as format, sample rate, sensors and parameters selection, data pre-processing methods, and compression at edge level are key factors. The setup of those details must consider the IIoT Solution level, which is guided by the problem-solving approach and expected advanced analysis.

The Table I shows three basic levels of data acquisition for asset operational parameters. The low frequency data acquisition is easily obtained from the SCADA. This kind of data is useful for medium and long period analysis, i.e., hours, days, and longer.

Usually, the medium and high frequency signals are associated with protection and control devices. This level of sample rate unlocks the transient and spectral analysis.

Table I – Data acquisition levels for operational parameters

Acquisition Sample Rate	Application	Expected Cost
Low Frequency [< 10Hz]	RMS Values for Steady State Analysis	$
Medium Frequency [10Hz < 1kHz]	RMS Values for Transient Analysis	$$$
High Frequency [> 1kHz]	Waveform Values for Transient & Spectral Analysis	$$$$$

Depending on the desired level of monitoring and data analysis, the data acquisition quality must take into account the accuracy and sample rate. In general, the sample rate and the data integration represent a bigger problem than the accuracy. The asset nature and the desired troubleshooting level determines the sample rate.

There are other challenges for data acquisitions too, the major ones are the timestamping, that must keep the time synchronism between the acquisition devices and the communication protocols. The real case used in this paper use low frequency data acquisition, with pre-processing at gateway level. The parameters under study are voltage and current from main stator (RMS), current and voltage from exciter, active and reactive power, bearing and stator temperatures and bearing vibration (RMS).

b. Asset Events Evaluation for Data Acquisitions

As noted during this case study, the machine learning algorithms can operate with a varied combination of model setting, which will depend on the available data, the nature of the problem and data science team background.

Welte et al. [11] addresses some relevant aspects of maintenance in large assets. He comments on the complexity in the physics-based and data-based analysis approach, as shown in Fig. 3. For example, electric rotor isolation failure detection (case 1) must be treated with a physical approach, that is, it depends on specific measurement on this rotating component. For noise analysis (case 4), the approach with advanced data analysis may be more advantageous.

Fig. 3 – Relation between asset event, complexity and approach

c. Sensors, Gateway & Edge Computing

The sensors and gateway play an important role inside an IIoT Solutions, they are responsible for getting the data from the asset, creating the payload, storing the data during offline periods and uploading it to the cloud when connected. Besides those tasks, the gateway must be able to keep the solution safe, considering all aspects of cyber security. The payloads are data packages with event frames, it can combine one or more levels of data acquisition (Table I).

Depending on the asset importance and the desired acquisition level, the gateway must be able to execute high-level data processing, over-the-air firmware updates and data operation to arrange and compact the data into adequate payloads.

For Greenfield plants, the data acquisition is performed using the latest technologies, which can be integrated and tested at manufacturing stages. In general, these new equipment show a superior level of connectivity.

For Brownfield assets, it is more complex; in some cases, dedicated data acquisition system for generators can be used apart from the operational sensors. In both cases, advanced monitoring devices for electric machines can be partial discharge, vibration acquisition system, digital fault recorder (high frequency acquisition), rotor flux sensors, rotor ground detection system, shaft voltage/current and winding vibration measurement. In Fig.2, those elements are presented at main asset block, shown as Dedicated Data Acquisition System. Note that each specific measurement requires a dedicated acquisition hardware and specific data analysis.

d. Cloud Infrastructure & Cloud Computing

In the past, the industrial and non-industrial IIoT applications were constrained by limitations of: edge-to-cloud communication, cloud infrastructure and cyber security (by electronics technology and cost too). In the past decade, those aspects got tremendous improvements that became these applications feasible and cost accessible. The cloud infrastructure services comprise of a full stack solution, which combine back-end, front-end, cloud computing resources for data manipulation, analytics, data storage and other features.

The cloud computing is performed using several techniques; the container approach is gaining popularity; it fractionates the data processing and analytics into micro services. After developing a robust data analysis process, to product Data-Driven insights, these algorithms are organized into a pipeline architecture. Those pipelines, or workflows, are fitted into containers to run at edge and/or cloud level, allowing the scalability with high value.

The cloud receives the raw and/or pre-processed data (payload) from the gateway from one or multiple assets. The advanced analysis is performed at cloud (or edge) using high level computing and algorithms. This approach leverages the Data-Driven services, bringing to the user valuable insights from an asset or a fleet.

e. Data Cleaning, Preparation & Feature Engineering

Before any analysis, the data cleaning and preparation must be performed. Fig. 4 suggests a workflow for that.

It is an important and time-consuming task, especially for large data sets. Activities related to this process consist of filling or removing missing and inconsistent data, statistical checking as distribution and outliers, data frame merging from different sources, timestamping adjustment, per unitization, identification of asset status, feature engineering, scaling/standardizing techniques and, depending on the forward analysis, the date time resampling. After establishing this process, the operational code can be fitted into a pipeline/container.

The filling technique of missing data must be selected carefully, which can use interpolation, the mean of last n samples or other approaches. It depends on the acquisition level, on the missing period, data nature, among other factors. In some cases, the missing periods must be removed from the data frame to avoid parsing errors. In any case, the missing data is always a data science concern.

In general, the scaling methods, important for models, are sensitive to outliers, inconsistent and missing data, due to that, the data cleaning must be performed previously. Feature engineering uses the domain knowledge and data science skills to create virtual data from original real data. The real and virtual data sets are used as algorithm's inputs, for model(s) train, test, evaluation, deployment, and production. A good feature engineering surely leverages the model(s) outcomes.

Fig. 4 – Suggested workflow to data cleaning and preparation

f. Data Analysis Process and Value Creation

The process of extracting value from data is challenging, very iterative, and depends directly on the interface between the domain knowledge team and the data science team. This process has sequential steps that can vary depends on the team's organizations and the problem-solving approach.

The Fig. 5 shows a suggested workflow approach to create such value via IIoT Solutions, which have basically three levels of deliverable, first is the asset descriptive reports/analysis, second the diagnostic and prescriptive analysis and finally the predictive analysis. Those analysis creates the Data-Informed and Data-Driven insights.

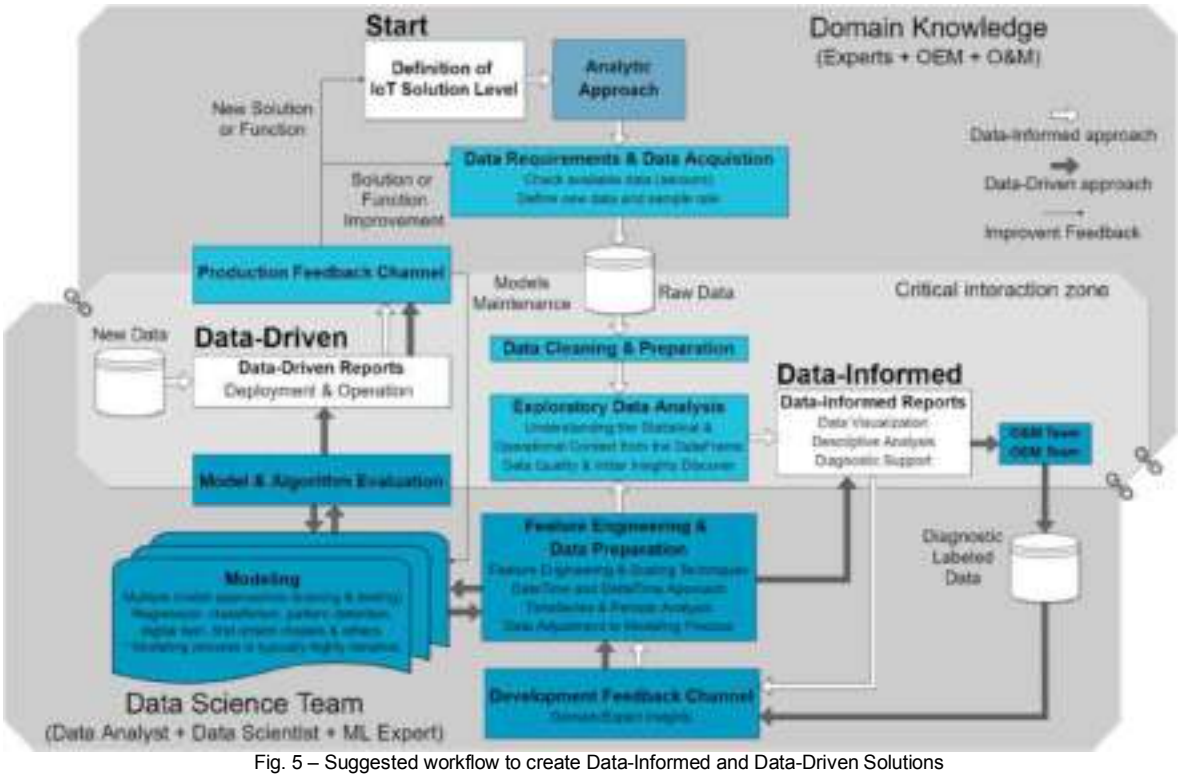

Fig. 5 – Suggested workflow to create Data-Informed and Data-Driven Solutions

The proposed workflow is based on CRISP-DM methodology (Cross Industry Standard Process for Data Mining), presented by [15] and [16], which indicates a well-defined flow to organize the data and the algorithm creation. The interpretation of this workflow starts at above white block, named as "Definition of IoT Level Solution" and goes to the Data-Informed block, via white arrows. The creation of Data-Driven solution is presented by gray arrows, as a sequence and closing the loop with new data.

The descriptive reports are used by OEM and O&M teams for troubleshooting analysis. These reports are created using adequate sample rate and showing the data in such a way that accelerates the root cause analysis process. This event frames data with relevant occurrences are labeled, properly stored, and used also into development feedback channel to create the autonomous diagnostics. This channel is essential to training the machine learning algorithms and improve it over the IIoT Solution lifecycle.

The diagnostic, prescriptive and predictive analysis inside Data-Driven consists of the use of such trained algorithms to identify patterns from new incoming data and to indicate what is normal, abnormal, or similar to previous diagnostic labeled data.

To put it into production, the steps described above must be organized into specific codes and algorithms. After evaluation, testing and deployment, those algorithms are fitted into containers to run at edge or cloud level. During the solution life cycle, the algorithms can receive upgrading from production feedback channel, resulting three possible actions: new solution/function, existing solution/function improvement or model maintenance.

Creating such algorithms and enriching them with experience and expertise is a remarkable task. It must be faced as a journey, with sequential milestones.

g. Analytic Approach Importance

Some aspects of analytic approach that orientates the value creation are: focus on data quality instead quantity; focus on causality first instead correlation and proper creation of diagnostic labeled data set.

In general, the machine learning process is highly dependent on the data distribution and stationary behavior. To obtain this, the parameters under analysis must be adjusted using scaling techniques. Additionally, the time series data from different devices can introduce unmatched timestamping, it must be also adjusted, to reproduce the asset behavior properly and digitally.

h. Machine Learning and Model Approach

There are three types of machine learning process: supervised, unsupervised and reinforcement. Some references show that those models can be data-based, physical-based or even hybrid; each one has its own pros, cons and specifications. Choosing a model is not trivial and requires machine learning background. For robust solutions, multiple model approaches are sometimes required, it is called as ensemble models.

Fig. 6 shows a basic workflow to construct machine learning algorithms. The first input is the raw data, it is used by OEM and O&M team to create the diagnostic labeled dataset, which is divided into three distinct datasets, for training, validation and evaluation tasks.

Before an algorithm release, the performance (accuracy) must be properly evaluated. From time to time, the algorithm effectiveness must be re-evaluated too, if needed, the algorithm can be enhanced with retraining, improvement or re-design approach. The feedback channel (black arrow shown in Fig. 5) supports this task.

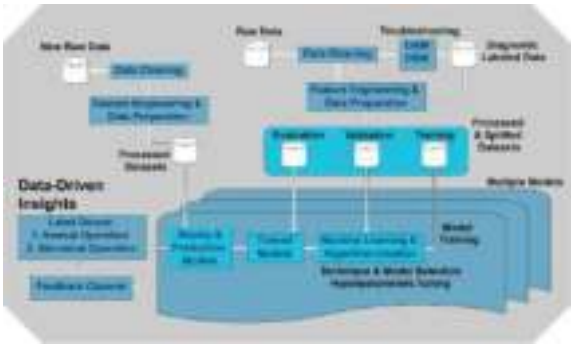

Fig. 6 – Suggested workflow to construct machine learning model

From a basic perspective, the learning process is the model's hyperparameters tuning (diagonal arrows in Fig.7 from [9]), which "learns" the relationship between the input and output data (as presented in Fig. 8 from [10]).

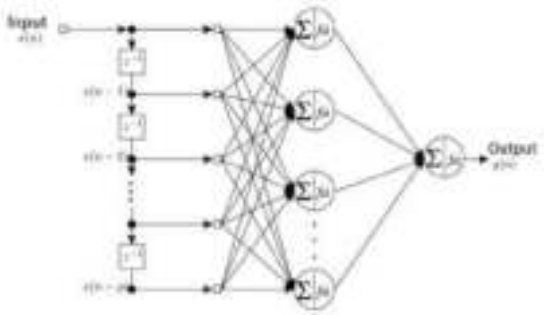

Fig. 7 – Example of machine learning model, a recurrent neural network TLFN focused

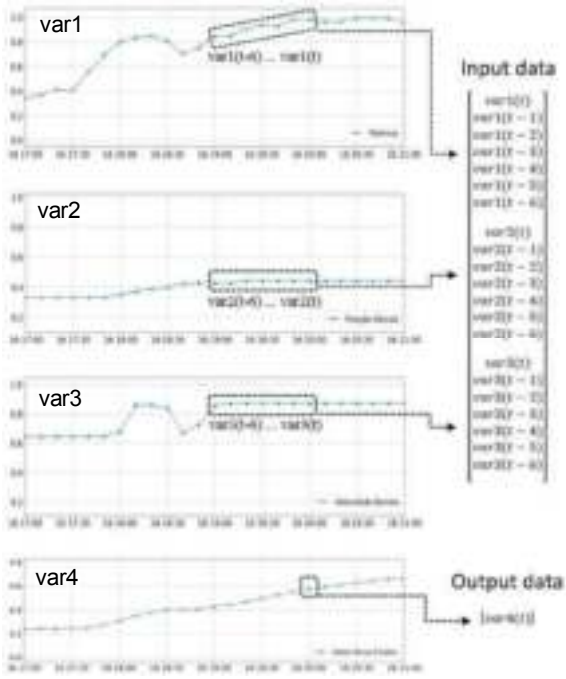

Fig. 8 – Model's input and output vector from 1-hour multivariate time series data (4 hours plot)

Get a tuned model with adequate performance is challenging and represents a high value inside an IIoT Solution. There are some ways to evaluate the model outcomes, however it is not the subject of this paper.

A permanent concern during an algorithm creation are the overfitting, underfitting, variance and bias. It must be considered in such a way to get the algorithms able to identify the patterns properly, over an asset or a fleet. In some cases, each asset has its own data preparation and model training requirements.

For data science, correlation factors are very important and dominate the machine learning models. From physic perspective, causality is the key factor and dominates the asset behavior. A good data science and IIoT Solution should combine correlation and causality properly. Otherwise, weak models are created.

Table II is created based on the Zhou (et al.) [13] and JI (et al.) [14] studies, which explore the physics-based and data-based models. To leverage the model's outcome, the hybrid approaches can combine the best of both worlds. For example, the physic-based model equations can orientate the creation of input vector for a data-based models, which have the benefits of machine learning training with real data.

Table II – Physics-based and Data-based model comparison

Physics-based model	Data-based model
Behavior explainable by well-known equations.	"Black box", hard to explain due to the learning dynamics.
Asset constructive parameters required.	Ability to abstract the asset constructive parameters.
In general, it needs few operating asset data, compared to data-based model.	In general, it needs a large amount of (structured) data.
Computational power required for model optimization process.	High level of computational power required for model training process.
Domain knowledge required during the model creation.	Domain knowledge required during the model evaluation.
Currently, it´s human dependent and will continue to be.	It is currently quite artisanal, but it can be automated.
Outcome leveraged when combined with data-based approach.	Requires cloud infrastructure.

i. Resources

To create an IIoT Solution, there are many activities at hardware level; however, the major part is in software. The hardware perspective consists of creation and installation of sensors, data acquisitions system, gateways, etc.

The software tasks are varied and require multiple skills as data architecture, back-end, front-end developers, security analyst, data analyst, data scientist, among others.

Fig. 9 shows the main actors required for an IIoT Solution development, some ones are itinerant over applications and others are specific for each solution.

III. EXPLORATORY DATA ANALYSIS

The data used in this paper is based on a real medium size generator, it is anonymized due to obvious reason.

An exploratory data analysis is conducted in order to understand the statistical and operational data context. The period under evaluation is around sixty days, starting at 45th day of the year.

a. Statistical Context Evaluation

At this stage, the data quality investigation is under focus. This evaluation is performed using a statistical approach, observing the distribution, outliers, finding inconsistent data, minimum values, maximum values, mean, median, IQR (Interquartile Range), standard deviation, p-value, Dickey-Fuller test and others hypothesis testing. It helps the data team to understand the data context and supports the data preparation for model usage.

b. Operational Context Evaluation

To analyze and understand the asset operational context, many types of graphic can be used. The time series plot is largely used, presented in Fig. 10. Another type is the scatter plots, with operational data and limits, as presented in Fig. 11. The domain knowledge contribution, combining the data plots, equipment limits (IEC60034-3 standard limit) and rate values, are very useful on this task.

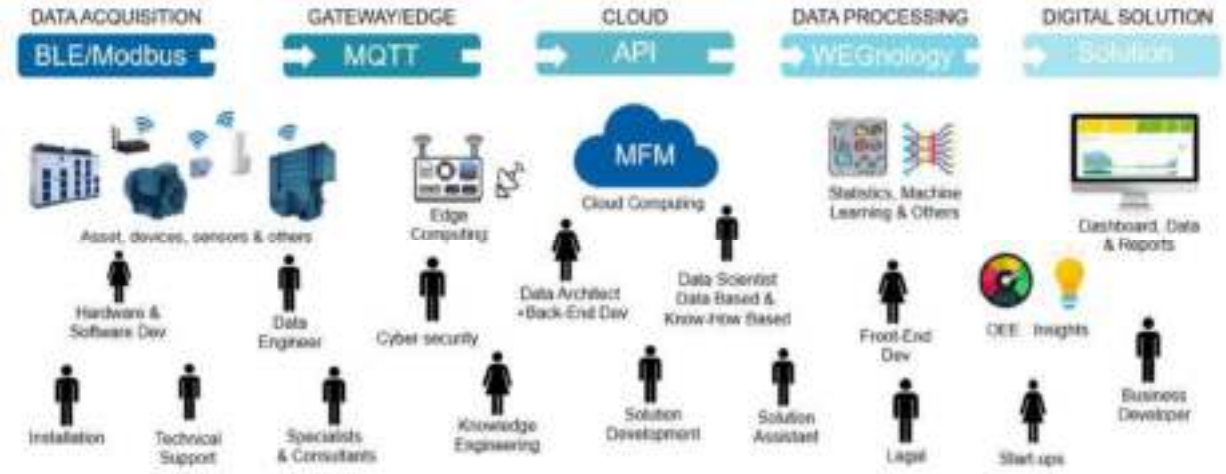

Fig. 9 – Digital solution work frame overview

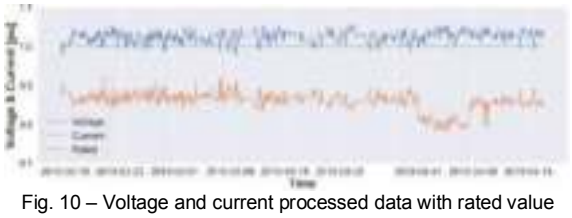

Fig. 10 – Voltage and current processed data with rated value

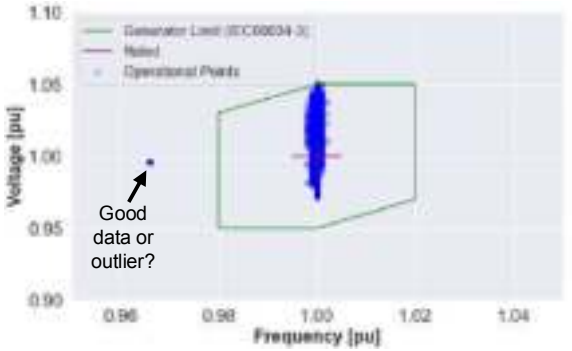

Fig. 11 – Scatter plot for voltage and frequency with IEC limit

The capability curve (Fig. 12) shows the generator operational active and reactive power and the asset limit curve. It is very important to evaluate how the asset is been operated, checking if the asset safe limits were exceeded and near the generator operates near the rated power.

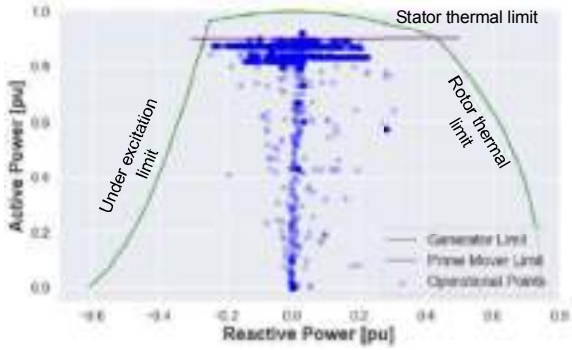

Fig. 12 – Generator capability curve/limits and operational points

Fig. 13 shows the generator hour meter by small ranges of active power with histogram plot. It is useful to see what is the amount of hours by power range demanded by the system. It is also easy to compare the behavior over the fleet units and support the asset health studies due to the operational aging.

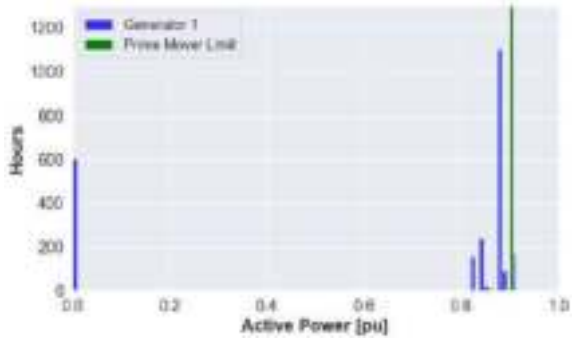

Fig. 13 – Generator hour meter by Active Power (histogram)

Fig. 14 shows the drive-end and the non-drive-end bearing vibration over time. Some correlation analysis was performed, which indicates weak correlation with other operational parameters, as power and bearing temperature. In this case, the vibration values behave near stochastically. Fig. 15 shows the histogram of such vibration values. As noted, the drive-end bearing has the mean value 0,9 mm/s and non-drive-end 1,1 mm/s.

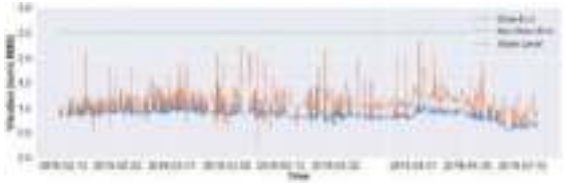

Fig. 14 – Bearing vibration over time

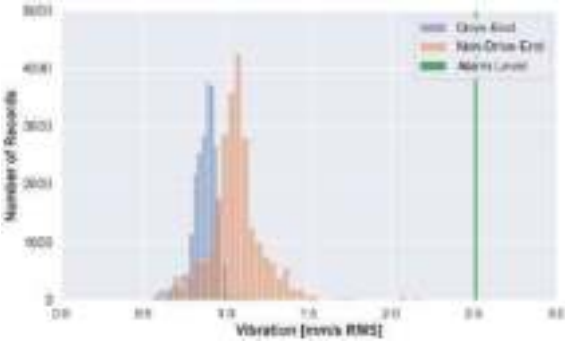

Fig. 15 – Bearing vibration histogram

IV. PATTERN DETECTION

a. Pattern detection with multivariate data

Fig. 16 represents sixty days of generator operation, starting at 45th day of the year, with eight parameters: bearing vibration, stator current/voltage, active power, stator temperature, bearing temperatures and excitation.

The algorithm uses hourly-resampled data. Each boxplot represents one day. This data was cleaned and prepared as presented before.

In this demonstration, the bearing temperature sensor number two has two patterns, it changes at the 59th day. The first part is designated pattern A and the rest is normal operation. The active power shows a stable condition with two distinct levels, it changes from 90% to 83% at the 90th day and returns to 90% at the 99th day. The 83% level is called pattern B and the rest is normal operation. Pattern A is an inconsistency at the temperature sensor number two and the pattern B is a power reduction.

The proposed algorithm detects those two patterns from the normal operational conditions. At first try, the pattern recognition does not work properly, the algorithm output is shown in Fig. 17. It identifies the pattern B, but it was unable to identify the others. Noting that, the scaling method is changed from StandardScaler to MinMaxScaler, then it runs properly, as shown in Fig. 18.

All three patterns are well identified. The output indicates pattern A until hour 336 (59th day), then change to normal operation pattern. The pattern B is observed between 1080 hours (90th day) and 1296 hours (99th day).

The algorithm pointed out some false positives around the points: 380, 600 and 1300 hours.

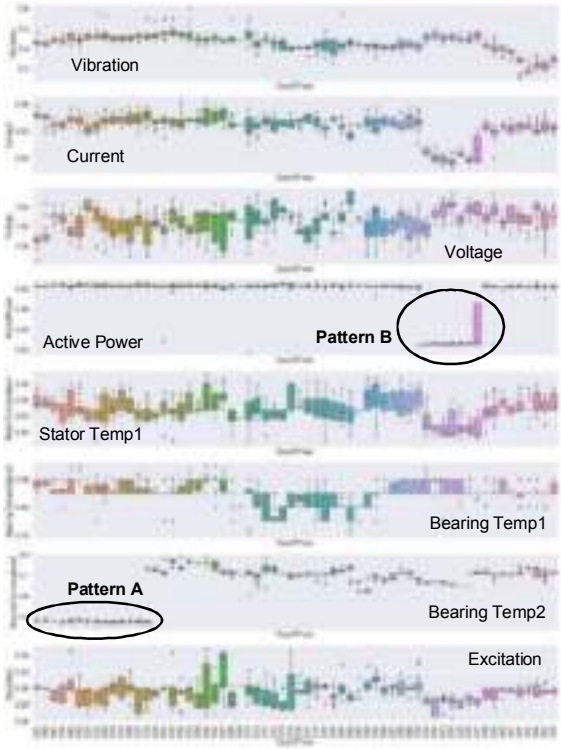

Fig. 16 – Generator operation, daily boxplots & hour resampling

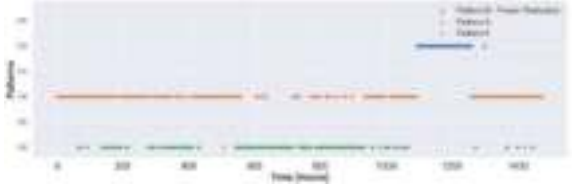

Fig. 17 – Pattern identification results at initial approaches, failed

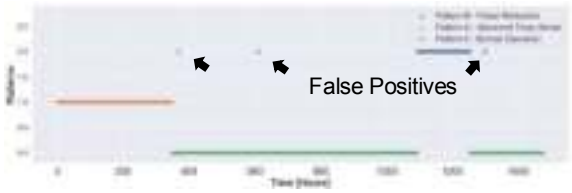

Fig. 18 – Pattern identification results after proper scaling

b. Pattern identification with univariate data

A similar approach is used to identify normal and abnormal condition from a single parameter. Fig. 19 shows a temperature sensor with sample rate of 2 minutes. Fig. 20 shows the daily boxplot temperature with daily resample. Fig. 21 shows the algorithm output with hourly samples; the pattern 1 (blue) represents the abnormal pattern identification.

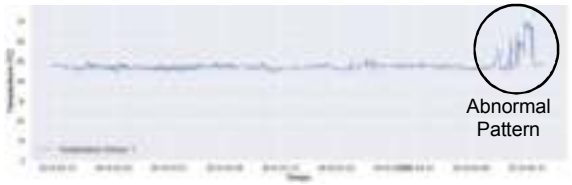

Fig. 19 – Temperature sensor with normal & abnormal operation

Fig. 20 – Temperature sensor, daily boxplots & hour resampling

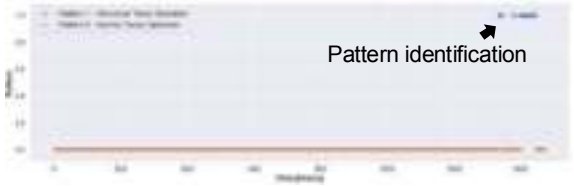

Fig. 21 – Pattern identification results

For univariate time series analysis, the decomposition function can be applied, as shown in Fig. 22. It extracts the trend, the seasonality and the residual component. These constituent parts can be used at featuring engineering stage, which can improve the model results.

In general, the pattern identification of univariate data presents a weak value, because the relevant behavior of the majority of equipment of industry are multivariate. Besides that, the use of traditional threshold alarms from SCADA is a low cost and feasible way to identify the univariate rise or decrease trend, which is well known and used in industry.

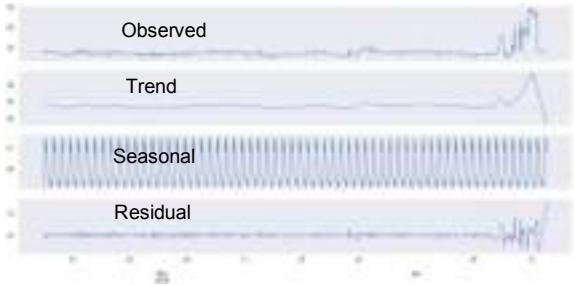

Fig. 22 – Decomposition of temperature sensor

V. DEPLOYMENT & PRODUCTION

a. Deployment & Production

Considering a development context, deployment is putting all the parts together into a final solution and running it at production level. The activities involved at this stage depends on the IIoT platform and related technologies. Using a high-level platform helps with these tasks, simplifying and shortening the deployment process, which can be a time-consuming task.

Deploying an IIoT Solution into production requires a multidisciplinary team. It is highly recommended to start with the Data-Informed level solution, stablishing its operation and get real data. Secondly, initiate the data science approach, creating the big data (structured) and constructing the Data-Driven features.

b. Data-Informed Dashboard

Data-Informed dashboards and reports contain the asset operational history from one or multiple assets, with data visualization, basic statistics, failure numbers, hour meters, relevant events, etc. This information helps the O&M team

to understand the asset's past operation and condition, which supports/orientates the maintenance scheduling.

Additionally, these descriptive reports show the data in such a way that helps the O&M team during the diagnostic and troubleshooting activities.

The final solution might involve multiple perspectives, such as the asset owner, partners, O&M, OEM and others. These perspectives will guide the IIoT Solution creation. In general, the deliverables are dashboards, reports, notifications (messages/e-mail), data exchange (APIs), insights about the normal and abnormal pattern operation, cross analysis about fleet/sites, advanced analysis tools, troubleshooting frameworks and other features.

The next five figures show an example of Data-Informed dashboard of a diesel generator unit, dedicated to O&M team. The application overview is displayed in Fig. 23, with asset location (gps), asset status (test mode, running, etc), speed and output power, general view of sensors at schematic, a histogram and a heat map of active power.

Fig. 24 shows the grid monitor with actual voltage and frequency level, voltage time series plot, Volts/Hertz chart (scatter plot) with regulatory limits and a heat map of voltage level. It helps to verify holistically the voltage and frequency behavior during the last week.

The diesel unit monitoring is shown in Fig. 25, with time series plots of output power, turbo pressure, inlet air and oil temperature, oil and fuel pressure, fuel consumption, block temperature and block vibration. The on-line readings of number of starts, total running hours, battery voltage and other are displayed. A scatter plot with output power and consumption is used to track that behavior. The generator monitoring is shown in Fig. 26, displaying the on-line readings and time series plots of output power, power factor, current, voltage, frequency, temperature and vibration. The generator capability curve with operational values, the Volts/Hertz chart with IEC limits and the unbalanced current monitor are also exhibited.

Fig. 27 shows the event list and alarms.

c. Data-Driven Insights

Data-Driven dashboards and reports go deeper into troubleshooting cases, advanced statistics/analytics, and patterns detection as normal and potential abnormal conditions.

Some Data-Driven insights are created using the OEM and O&M orientation. It generates useful operational condition-based insights for maintenance planning that prevents the unexpected asset downtime. Examples of than can be a pre-alarm indication based on multivariate pattern detection, which is not trivial to detect.

For univariate cases, traditional alarm and shutdown threshold are feasible, which are well known and used in industry for a long time.

Those pattern detection algorithms can operate with different window scan periods. Depending on the parameters and issue nature, it can be minutes, hours, days, weeks and even months. Events that can be tracked using those algorithms are heat exchange thermal condition combined with output power, bearing vibration combined with operational condition and others.

Additionally, other Data-Driven insights can be the maintenance scheduling activities based on hour meter and output power history, evaluation of asset controlling performance, troubleshooting tools, fleet cross analysis, calculations of MTBF (Mean Time Between Failures) and OEE (Overall equipment effectiveness), etc.

Fig. 23 – Data-Informed Dashboard - Part I - Application overview

Fig. 24 – Data-Informed Dashboard - Part II - Grid monitor

Fig. 25 – Data-Informed Dashboard - Part III - Diesel Monitor

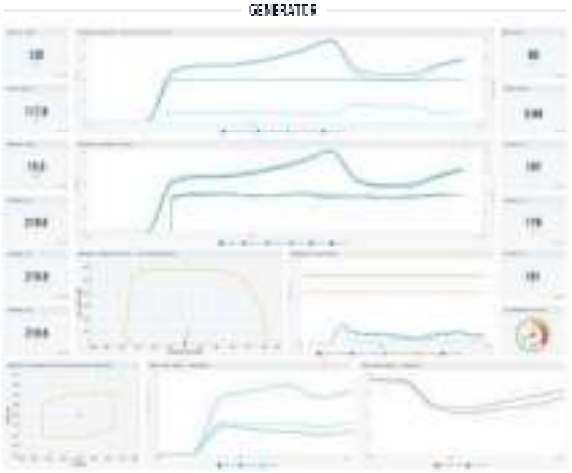

Fig. 26 – Data-Informed Dashboard - Part IV - Generator Monitor

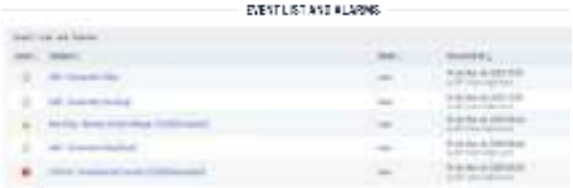

Fig. 27 – Data-Informed Dashboard - Part V - Event List

The below example (Fig. 28) shows an output from a recurrent neural network TLFN focused model (Fig. 7), which estimates the generator temperature considering the cooling parameters data. The input data and output data used in this case are presented in Fig. 8. The green arrow indicates when an abnormal pattern is detected.

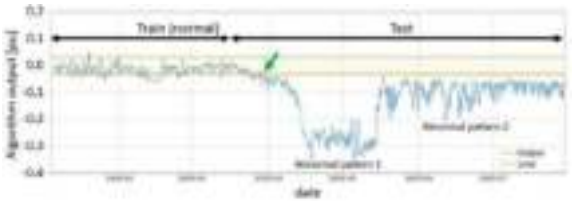

Fig. 28 – TLFN model output, difference of estimated generator temperature based on multivariate parameters input

VI. CONCLUSIONS

The creation and deployment of an IIoT Solution and pattern detection algorithm for multivariate data is an advanced and multidisciplinary task, which generates high value. To overcome it, the use of a robust IIoT Platform and the engagement between the data science and domain knowledge team must be considered as strategic.

The proper data acquisition is decisive. The sensor and gateway must play this role observing the cyber security requirements, with data synchronization, fast data processing and capability to perform over-the-air updates.

New IIoT projects must focus on Data-Informed Solution first and Data-Driven Solution secondly. The proposed workflow helps on create a robust and trustworthy approach to construct such solution, observing the team's interactions.

To leverage the Data-Driven model's outcome, the hybrid approaches can be a good option, which combine the best of both worlds. In this case, the physic-based model equations can orientate the creation of input and output vector for a data-based models, which have the benefits of machine learning training process with real data.

The creation of such technology is a journey. This quick demonstration suggests to starting simple, using a robust IIoT platform, implementing the feedback channel, forming the teams' engagement and seeking for the continuous development practice.

VII. ACKNOWLEDGEMENTS

I would like to thank WEG, UDESC (Santa Catarina State University) and University Center SATC (Charitable Association of the Industry of Santa Catarina).

I also would like to thank my professor Ademir Nied, for his advising during my master´s degree and on this paper, and to my colleagues João Vitor da Silva, Heron Pereira, Alexandre Weihermann, Kelvin C. de Andrade, Carlos Ogawa, Elissa S. de Carvalho, Giovani M. Pradi, Lucas H.S. Tavares, Gregory C. Manchesan and Luiz Felipe Manke, which contributed at solution concept development and/or enrich this paper with review, suggestions and corrections.

VIII. REFERENCES

[1] Rollins, J. B., Foundational Methodology for Data Science, IBM Analytics, White Paper, 2015.
[2] Silipo, R., Zimmer, M. A., Data and Machine Architecture for the Data Science Lab, Brane and Knime, 2015.
[3] IEC Standard 60034-3:2007, Rotating electrical machines - Part 3: Specific requirements for synchronous generators driven by steam turbines or combustion gas turbines.
[4] Blumenthal, R., et al., Secure, Reliable And Efficient Energy Supply In Production Processes Using Cloud-Based Technologies, PCIC Europe EUR19_33, 2019.
[5] Related posts at Quora.com, Towardsdatascience.com, Machinelearningmastery.com and Medium.com.
[6] Grus, J., Data Science from Scratch, O'Reilly, 2016.
[7] Mckinney, W., Python for Data Analysis, O'Reilly, 2018.
[8] Géron, A., Hands-On Machine Learning with Scikit-Learn & TensorFlow, O'Reilly, 2019.
[9] Nied, Ademir. Training about neural recurrent network. Universidade Federal de Minas Gerais, 2007.
[10] Oliveira, Mateus N., Case study on the use of machine learning algorithm to detect operational deviation in electric generation assets and IIOT solutions, Master degree, 2020.
[11] Niehaus, Karl; Hilbert, Marc. Thermal analysis of a wind turbine generator by applying a model on real measurement data. IEEE, 2012.
[12] WELTE, Thomas M. et al., Research project on industry 4.0 and digitalization applied to fault detection and maintenance of hydropower plants, 2018.
[13] ZHOU, Datong, et al., Model comparison of a data-driven and a physical model for simulating hvac systems., 2016.
[14] JI, J, et al., Comparison of a data-driven model and a physical model for flood forecasting, 2012.
[15] CHAPMAN, Pete et al. The crisp-dm user guide. In: 4th CRISP-DM SIG Workshop in Brussels in March, 1999.
[16] WIRTH, Rüdiger; HIPP, Jochen. CRISP-dm: Towards a standard process model for data mining. In: SPRINGER-VERLAG LONDON, UK., 2000.

IX. NOMENCLATURE

IIoT	- Industrial Internet of Things
OEM	- Original Equipment Manufacture;
O&M	- Operation & Maintenance team;
Data frame	- Set of raw or processed data;
Event frame	- Data from specific period;
Payload	- Data frame and event frame;
EDA	- Exploratory data analysis;
Asset parameters	- Asset sensors data or specific data;
RMS	- Root mean square;
Greenfield	- New site or installation;
Brownfield	- Existing site or installation;
Feature engineering	- Creating virtual parameters from asset parameters to fits at machine learning requirements or leverage the results;
Data-Informed Solutions	- Reporting past and basic data visualization, bring initial insights;
Data-Driven Solutions	- Reporting relevant events using advanced analysis and data visualization, bringing relevant insights to owner and O&M team;
Full Stack	- Back-end, front-end, data storage, cloud computing resources, etc;
Pipeline	- Structured data processing;

Domain knowledge	- Application expert, OEM & O&M knowledge on how to construct, operate and troubleshoot the asset;
API	- Application Program Interface;
TLFN	- Time Lagged Feedforward Network
SCADA	- Supervisory Control & Data Acquisition

X. VITA

Mateus Nicoladelli de Oliveira received the B.Sc. degree in electrical engineering from SATC, Criciúma, Brazil, in 2010, the M.Sc. degree in electrical engineering from Santa Catarina State University (UDESC), Joinville, Brazil, in 2020 and pursuing the MBA in Digital Business from USP/Esalq, São Paulo, Brazil. Works at WEG Equipamentos Elétricos since 2010. He has five years global experience with commissioning & start-up of large electric machines, six years with engineering, research and development of medium voltage rotating machinery and related monitoring system. Since end of 2020, Mateus is Digital Business Developer at WEG Digital Solutions department, acting as Product Manager to support and conduct the technical improvement and the commercial expansion of WEG Motion Fleet Management Solution, an industry 4.0 worldwide product for industrial fleet monitoring and asset management.
nicoladelli@weg.net

Ademir Nied received the B.Sc. degree in electrical engineering from the Federal University of Santa Maria, Santa Maria, Brazil, in 1987, the M.Sc. degree in industrial informatics from the Federal Technological University of Parana, Curitiba, Brazil, in 1995 and the Ph.D. degree in electrical engineering from the Federal University of Minas Gerais, Belo Horizonte, Brazil, in 2007. Since 1996, he has been a Professor with the Department of Electrical Engineering, State University of Santa Catarina, Joinville, Brazil. From 2015 to 2016, he was a Visiting Professor with the WEMPEC, University of Wisconsin Madison, Madison, WI, USA. His research interests include electrical machines, control of electrical drives, and renewable energy.
ademir.nied@udesc.br

EXCITATION OF NATURAL FREQUENCY IN LARGE MOTORS BY DOUBLE FREQUENCY TEST

Lucas Selonke Klaas
WEG
Jaraguá do Sul, SC
Brazil
lucask@weg.net

Abstract - The double frequency test is a method widely used due to several factors that make it more attractive compared to other methods of testing electric motors. The advantages of the test method for large motors will be evaluated presenting two cases of resonance.

The first case is an induction motor with a shaft center height of 630 mm, six poles that has arrived for technical assistance for shaft recovery. In the initial condition, the vibration was satisfactory. During the double frequency test the rotor increased vibration over time. Near temperature stabilization, the amplitude reached levels of 10 mm/s r.m.s.

In the second case, an induction motor with a shaft center height of 710 mm, eight poles, the vibration amplitude above 50 mm / s r.m.s was detected in the heat exchanger during the double frequency test.

The positive points reinforce the advantage of the test method and both examples demonstrate the necessary care with excitation of natural frequencies in rotating and static parts of motors. Those cases are related to the acceptance tests at factory.

Index Terms — Natural frequency, double frequency test.

I. INTRODUCTION

There are several tests performed to approve a large electric motor at the manufacturer. Besides the electrical test determined in API 541 [1], one of most significant in terms of importance are the vibration and temperature rise tests. Usually these kinds of tests are witnessed by the customer and are the last to be done before finishing and shipping the motor to the customer.

These tests are critical for checking the electrical and mechanical performance of the motor. In most of time the excitation frequencies of electric motor are the rotational speed, the power supply line frequency and twice power supply line frequency for free run. In cases of tests coupling the motor to a dynamometer, it is great amount of excitation is introduced as misalignment, unbalance of coupling, transmission of vibration through the shaft or through the base. It is important to mention that in most of the times it is necessary to adjust the shaft high of the motor that will be tested in relation to the dynamometer resulting in not ideal setup for vibration testing. Between the motor and the seismic base will have a pedestal lowering the stiffness of the support.

II. TEMPERATURE RISE TEST

The aim of this analysis is the double frequency test but there are many methods to evaluate the temperature rise of induction motors under full load. The most accepted are: Direct Load, Graphic Method, Back-to-Back, Forward Short Circuit, Double Frequency Superposition Method. The notable difference is that Double Frequency is the only test that does not demand mechanical coupling between the laboratory machine and the machine under test. [2]

The double frequency test method feed two different frequencies into the stator terminals of the induction motor under test. For example, the main source is 60 Hz and the auxiliary 50 Hz. The rotor tries to follow this speed variation accelerating and decelerating alternately. This behavior generates losses on the rotor and stator as heat. Despite using two frequency sources, the speed of the machine is very close to the frequency of the main source.

In addition to the rotor heating phenomenon, which is desired for this type of test, there is also the appearance of multiple frequencies of the difference of the power supply line. For example, if the motor is powered with 50 and 60 Hz, the difference is 10 Hz and during the test, multiples of this difference will appear in the spectrum.

III. EXCITATION OF NATURAL FREQUENCY

The natural frequency excitation depends on the application. It can be well seen in the case of musical instruments, or undesirable in the case of electric motors. Concerning the motor only and not the driven load, the natural frequency excitation represents an increase of the amplitude of vibration that may result in the vibration not being within limits during a test performed by the manufacturer.

Following API 541 [1] recommendations, natural frequencies should avoid the excitation frequencies of the electric motor. Therefore, natural frequencies close to 1x and 2x running frequency and 1x and 2x power line frequency are not recommended.

When an electric motor is designed, the natural frequencies of the rotating and static parts are calculated in order to avoid resonances. Then the natural frequencies of the rotor and the structure are analyzed, such as housing, stator, covers, terminal box, heat exchanger.

Taking as example the six-pole motor with the power supply of 60 Hz, the frequencies to be avoided are 20, 40, 60 and 120 Hz. When performing the double frequency test due to the appearance of multiple harmonics, it is necessary to removal natural frequencies from 10, 20, 30 Hz and so on. Considering the 15% of separation margin between the natural and excitation frequency, it results in wide range in which there can be no natural frequencies.

Considering small motors, i.e. with shaft center height

less than 355 mm, this criterion is not difficult to meet. However, when dealing with large motors, as an example, which has a shaft center height of 630 mm, 710 mm and higher, moving natural frequencies, becomes a difficult or almost impossible task.

It is important to keep in mind that even if there are excitation frequencies equal or near natural frequencies, vibration amplitude will only increase if the force can excite the shape mode - an excitation force in the axial direction is unlikely to excite a horizontal or vertical shape mode.

Therefore, during the double frequency test, it is possible to have natural frequencies excited which will result in increased vibration. As a reference for determining if the level of vibration is acceptable and ensuring it does not cause damage to the equipment, it should be recommended operating under the limit of zone C of ISO 20816-1 [3]. The zones are defined as a qualitative assessment of vibration. Normally new machines fall in zone A and vibration levels in zone C are not recommended for long-term continuous operation. Generally, the duration of the double frequency temperature test for large motor is about 04 hours; however, it depends on the motor as it takes into account the cooling system, mechanical and electrical losses.

IV. VIBRATION ANALYSIS

Vibration analysis is an important diagnostic method for understanding the source and for correcting the cause that produces it. The most widely used tool among analyzers is the spectrum FFT. In the presented cases, it were used besides the analysis of the vibration spectrum, bump tests, dynamic rotor calculation and numerical modal analysis.

The above-mentioned motors presented high vibration during the double frequency test. Both were above zone C, requiring intervention to enable the hot test to be performed. A third example represents most of the motors tested by the double frequency method. The amplitude increased during the test but the vibration levels are within limits of zone A of ISO 20816-1 [3]. In this case, there is no need of intervention.

A. Motor, shaft height 630 mm, VI poles, 60 Hz

The motor had the shaft replaced and the rotor rewound. After the recovery process, the motor presented low vibration levels at no load in cold condition. However, during the double frequency test, vibration increased considerably. The amplitude presented at No Load Hot in Table I were immediately after the double frequency test. The corresponding temperatures of stator windings are in Table II.

TABLE I
Vibration readings at different conditions

Measuring Position mm/s r.m.s	Condition		
	No Load Cold	Double Frequency Hot	No Load Hot (after Double Frequency)
DE-H	1.73	8.82	1.41
DE-V	0.76	8.97	1.20
DE-A	0.60	2.69	0.66
NDE-H	1.74	10.8	0.89
NDE-V	0.54	9.92	1.06
NDE-A	0.17	4.58	0.51

TABLE II
Absolute temperature of stator windings

Stator Temperature (°C)	Condition		
	No Load Cold	Double Frequency Hot	No Load Hot (after Double Frequency)
	43.6	102.2	98.02

Figure 1, 2 and 3 present the spectrum FFT for the Drive End Horizontal direction in different conditions. The horizontal axis is in Hertz. The red arrows represent the multiple harmonics of rotational speed. Comparing the vibration between cold and hot conditions at no load, there was a slight reduction of 1x amplitude. The other harmonics did not change significantly.

Along the double frequency test, the motor present high increase of 1x vibration, appearance of 10 and 28 Hz. The rotor dynamic analysis indicates natural frequency at 28.4 Hz. The corresponding mode shape of the rotor is presented at Figure 4.

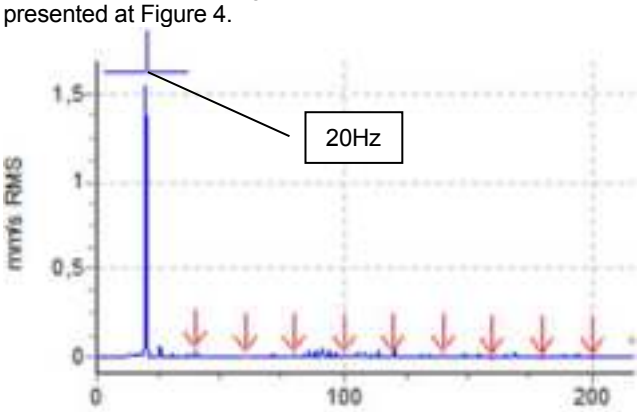

Fig. 1 Cold condition – drive end bearing, horizontal direction.

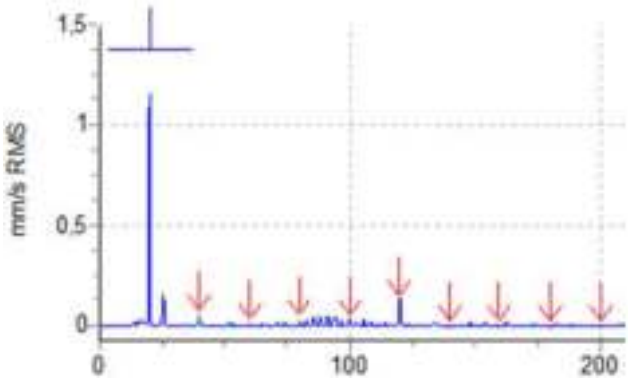

Fig. 2 Hot condition – drive end bearing, horizontal direction.

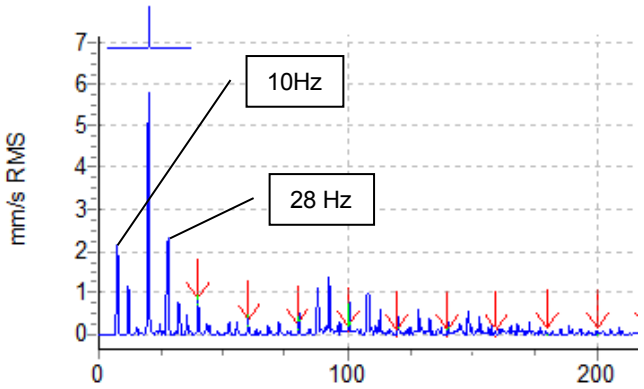

Fig. 3 During double frequency increase 1x amplitude. Appearance of 10 Hz and of 28 Hz.

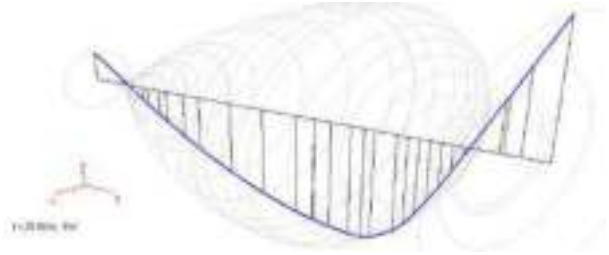

Fig. 4 Mode shape of rotor.

Two actions were taken in order to attenuate the vibration amplitude. In the first action was performed the balance of the rotor at a third plane in the middle point between bearings as indicated by red dot in the Figure 5.

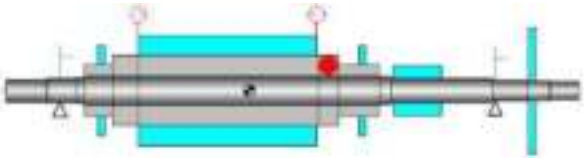

Fig. 5 Representation of rotor.

In the second action was performed the heating test by applying the back-to-back method as shown at Figure 6. This required the manufacturing of coupling between the motors and the existence of another motor with similar power.

Fig. 6 At the left side the motor used for test and at the right side the motor evaluated.

As shown at Figure 6, the left side motor is smaller. This difference of size also reflects reduced power. The drive motor was unable to reach the same temperature as the double frequency test shown in Table IV. The double frequency test was repeated in order to reach a higher temperature.

Comparing the condition double frequency hot on Table I and III is possible to evaluate the influence of the balancing in the third plane of the rotor. The maximum amplitude was reduced from 10.8 to 3.93 mm/s r.m.s. In Table III, comparing cold and hot back-to-back conditions, there is no excitation of natural frequency and low increase in vibration amplitude.

TABLE III
Vibration readings for coupled test

Measuring Position mm/s r.m.s	Condition		
	Back-to-back Cold	Back-to-back Hot	Double Frequency Hot
DE-H	0.48	0.82	3.93
DE-V	0.23	0.22	1.41
DE-A	0.31	0.90	0.73
NDE-H	0.54	1.04	2.59
NDE-V	0.37	0.44	1.36
NDE-A	0.22	0.48	0.89

TABLE IV
Absolute temperature for coupled test

Stator Temperature (°C)	Condition		
	Back-to-back Cold	Back-to-back Hot	Double Frequency Hot
	45.6	87.1	99.8

B. Motor, shaft height 710 mm, VIII poles, 50 Hz

In this case, the detection of the high vibration amplitude cause was easier. The motor analyzed showed high vibration at the heat exchanger in the beginning of the double frequency test. The bump test was performed to verify the natural frequencies of the heat exchanger mounted over the stator frame. The Figure 7 present responses at 19, 25 and 42 Hz for the bump test executed on the heat exchanger. The motor has eight poles and 50 Hz power line frequency. Therefore, the rotational frequency is 12.5 Hz.

In the double frequency test, excitation frequencies appear at 10, 20, 30 and 40 Hz. As the natural frequency at 19 Hz is very close to the excitation in 20Hz, a high vibration amplitude around 50 mm/s r.m.s appeared at 20 Hz.

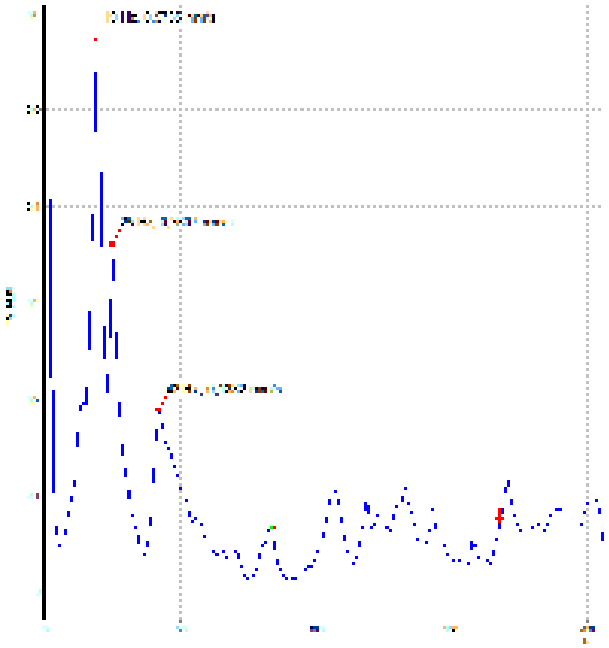

Fig. 7 Bump test at heat exchanger.

Through the numerical modal analysis, it was found the that mode shape at 19 Hz is horizontal with greater amplitude in the upper part of the heat exchanger (Fig. 8).

In order to decrease the vibration amplitude and allow the motor to be tested by the double frequency method, the bolts have been loosened. The change in fixation of the heat exchanger relative to the stator frame was necessary to modify the mode shape and the natural frequency. In this way, the amplitude of vibration was reduced.

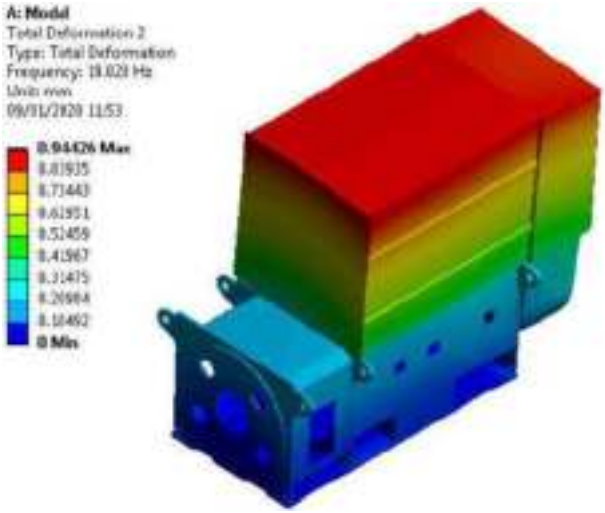

Fig. 8 Mode shape of vibration at 19 Hz.

C. Motor, shaft height 630 mm, IV poles, 50 Hz

There are regular cases are in which the motor is double frequency tested and has a slight increase in vibration. There is no natural frequency excitation.

The following spectrum is of new motor with shaft center height of 630 mm, four poles. The vibration readings are much lower than the limit of IEC 60034-14 [4] at cold and hot condition. During the double frequency, although the amplitude increased around six times, the motor still presented low vibration levels according the Table V.

TABLE V
Vibration readings at different conditions

Measuring Position mm/s r.m.s	Condition		
	No Load Cold	Double Frequency Hot	No Load Hot
DE-H	0.33	2.00	0.39
DE-V	0.23	1.26	0.22
DE-A	0.29	0.55	0.41
NDE-H	0.31	2.09	0.39
NDE-V	0.24	0.29	0.24
NDE-A	0.22	0.49	0.30

Table VI presents the temperature of the stator according the vibration readings.

TABLE VI
Absolute temperature of stator windings

Stator Temperature (°C)	Condition		
	No Load Cold	Double Frequency Hot	No Load Hot
	41.5	133.0	130.0

According to Table V, the amplitude is stable between cold and hot condition with no load. The spectrum of Figures 9 and 10 shows the influence of the double frequency test. There is an increase of amplitude on the rotational frequency, 25 Hz. The major influence of the double frequency test is represented by the harmonic of 10 Hz.

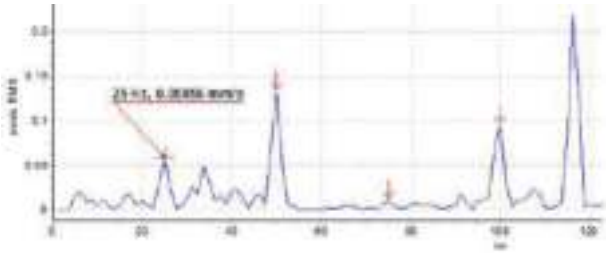

Fig. 9 Hot condition – drive end bearing, horizontal direction.

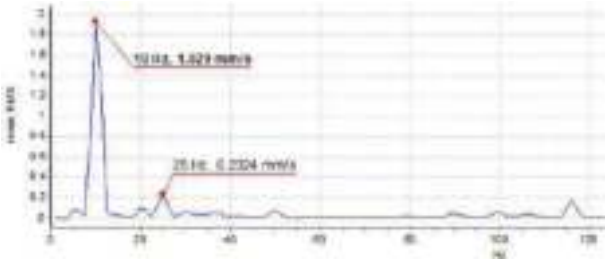

Fig. 10 Along double frequency test – drive end bearing, horizontal direction.

V. CONCLUSIONS

The double frequency test is widely employed mainly due to being able to avoid having to use a coupling and a driving motor with similar characteristics. It is economically impractical for electric motor manufacturers to have a large variety of motors dedicated for back-to-back tests, mainly due to a great combination of characteristics as power, voltage, shaft center height and polarity.

However, attention is required during the test to avoid natural frequency excitation and excessive amplitude. Therefore, vibration measurement during a double frequency test is recommended to ensure that the limits of ISO 20816-1 [3], zone C are not exceeded during the test.

VI. REFERENCES

[1] API 541, fifth edition. Form-wound Squirrel Cage Induction Motors – 375 kW (500 Horsepower) and Larger.

[2] C. Glauco, R. Fredemar, W Stephen. “Comparative analyses of standards temperature rise test methods for induction machines”, PCIC Europe Conference Record”, 2009.

[3] ISO 20816-1, first edition. Mechanical vibration – Measurement and evaluation of machine vibration - Part 1: General guidelines.

[4] IEC 60034-14, fourth edition. Rotating electrical machines – Part 14: Mechanical vibration of certain machines with shaft heights 56 mm and higher – Measurement, evaluation and limits of vibration severity.

VII. VITA

Lucas Selonke Klaas received his B.S. and M.S. degree in mechanical engineering and science and engineering of materials from the State University of Santa Catarina, Brazil, in 2007 and 2013 respectively. Currently is study doctoral in electrical engineering. His research interest is bearingless motor. He is design engineer and vibration specialist of WEG Energy since 2008.

MIN. TERMINAL VOLTAGE ON RUNNING SYNCHRONOUS MOTORS DURING LARGE MOTORS STARTING

Paper No. PCIC Europe 22_36

Ali Alameer
Saudi Aramco,
Dhahran, Saudi Arabia
ali.alameer.1@aramco.com

Rami Dabbousi
Saudi Aramco,
Dhahran, Saudi Arabia
rami.dabbousi@aramco.com

Hussain Al-Marzoug
Saudi Aramco,
Dhahran, Saudi Arabia
hussain.marzoug@aramco.com

Zeyad T. Balkhyour
Saudi Aramco,
Dhahran, Saudi Arabia
zeyad.balkhyour@aramco.com

Abstract - This paper presents the influence of power system voltage drop caused by starting large motors on the performance of Direct Online (DOL) running three-phase brushless synchronous motors that are connected on the same bus. The principal contribution of this paper is to propose a method to calculate tolerable terminal voltage on the synchronous motors, both salient-pole, and cylindrical rotor designs, under the condition of large motors starting. This paper suggests that the motor pull-out torque at rated voltage and frequency is the main criteria to be used for calculating tolerable voltage drop that will secure the motor from the out-of-step conditions. Based on that, the paper proposes minimum terminal voltage for synchronous motors that are calculated using International Standards pull-out torque values. A dynamic simulation, utilizing power system software, for the performance of running Medium Voltage brushless synchronous motor under large motor starting, endorsed the calculated minimum voltage values.

Index Terms — synchronous motor, power distribution system, terminal voltage, starting large motors, direct online.

NOMENCLATURE

V	Motor rated terminal voltage (pu).
E	Rotor rated back e.m.f (pu).
T_{CR}	Cylindrical design pull-out torque (pu)
T_{SP}	Salient-pole design pull-out torque (pu)
X_d	d-axis machine's reactance (pu)
X_q	q-axis machine's reactance (pu).
δ	Power angle (rad)

I. INTRODUCTION

Industrial power distribution system (PDS) quality is crucial for achieving reliable continuous operation for a facility. This is usually attained through designing a power system with high conservative requirements. One of the challenging requirements that have to be carefully evaluated during the system design phase is the voltage drop on running motors during the startup of large motors connected on the same switchgear bus or in a nearby location in the power system that might be affected. Therefore, the voltage drop on a running motor terminal, under the condition of a large motor starting connected on the same bus, is crucial to be understood carefully.

The voltage drop will impact synchronous motors' torque, and in extreme dips, the motor will have considerable speed and power angle oscillation, and therefore loss of sync condition may occur. On the other hand, if the requirement for voltage drop on running motors is exaggerated, it will be highly challenging to design the power system and could lead to an overdesigned system with considerably higher costs. From experience in the industry, it is a common practice to limit the voltage drop on running motors to around 85 to 80% of the motor nominal voltage.

In IEEE Std 399 [1], a fundamental procedure for calculating the minimum terminal voltage of three-phase induction motors during the start-up of an adjacent motor is discussed. Although calculating this voltage for cylindrical rotor synchronous motors (CRSM) is as trivial as for induction motors, the mathematical approach for calculating this value for salient-pole synchronous motors (SPSM), where the rotor saliency is considered in the torque equation, is quite complicated. The motivation of this paper is to present a detailed technical approach on how to specify that minimum tolerable terminal voltage, for both CRSM and SPSM, to enhance the cost and the quality of the PDS design when considering the voltage drop during motor starting as a design criterion.

A technical background about voltage-torque relationships for synchronous motors will be discussed in II. In III, formulae for calculating the minimum tolerable terminal voltage of synchronous motors during adjacent large motor starting are established. After that, in IV, a dynamic simulation, utilizing power system software, for the performance of running Medium Voltage synchronous motor under large induction motor starting will be deliberated to endorse the calculated minimum voltage drop values; and demonstrate the minimal impact these motors could have in case of maintaining their terminal voltage at that minimum calculated value.

II. SYNCHRONOUS MOTORS VOLTAGE TORQUE RELATIONSHIP

Voltage drop on a running synchronous motor terminal, under the condition of large direct online motor starting connected on the same bus, is crucial to be understood carefully. The voltage drop will impact the motor torque, and in extreme dips, the motor will have considerable deceleration and therefore stall conditions may occur.

Synchronous motors torque at synchronism, the steady-state running condition, depends on the terminal voltage, but it also depends on the rotor back e.m.f (excitation) as well as a sinusoidal component, which is the motor power angle. Consequently, during a tolerable voltage drop, the power angle, and hence the speed, will momentarily oscillate until it finally stabilizes again at the synchronous speed. If the voltage drop is severe, the speed oscillation will continue until it completely collapses and consequently,

the motor will have a loss of sync condition (as it will be shown in a power system simulation later in this paper).

For synchronous motors, pull-out torque is the main criteria to calculate minimum voltage drop at its terminals. The pull-out torque is defined in NEMA MG-1 [2] as the maximum sustained torque which the motor will develop at synchronous speed with rated voltage applied at rated frequency and with normal excitation. The feature of sustaining synchronous speed at the pull-out torque is of high importance which makes it vastly advantageous in terms of considering it as the criteria of minimum tolerable terminal voltage for brushless synchronous motors, both SPSM and CRSM. The developed torque at synchronism of a synchronous motor depends on its rotor design, either SPSM or CRSM [3]. SPSM design has the advantage of developing two torque components, which are the synchronous and the reluctance torques. However, a CRSM only develops a synchronous torque component. It is vital to evaluate the pull-out torque under steady-state operation to understand how it varies with respect to excitation and terminal voltage, and consequently develop minimum terminal voltage requirements during adjacent motor starting.

A. Pull-Out Torque at Steady State

1) Cylindrical rotor synchronous motors (CRSM)

A cylindrical rotor design develops only one torque component, which is the synchronous torque, given by equation (1) per unit [3]:

$$T_s = V\frac{E}{X_d}sin(\delta) \tag{1}$$

where:

T_s synchronous torque;

The maximum (pull-out) torque occurs at δ = 90º independently of the machine design, where it is the maximum value of the synchronous torque. Thus, the per unit pull-out torque of a CRSM is given as:

$$T_{CR} = \frac{VE}{X_d} \tag{2}$$

It can be seen that the pull-out torque depends on the d-axis reactance, terminal voltage, and rotor back e.m.f. Unlike induction motors, it is proportional “linearly” with the motor terminal voltage.

2) Salient-pole synchronous motor (SPSM)

Salient-pole design motors develop an additional component to the synchronous component developed by the CRSM, which is the reluctance torque, given in per unit by (3) [3]:

$$T_{rel} = V^2\frac{1}{2}\left(\frac{1}{X_q}-\frac{1}{X_d}\right)sin(2\delta) \tag{3}$$

where:

T_{rel} reluctance torque;

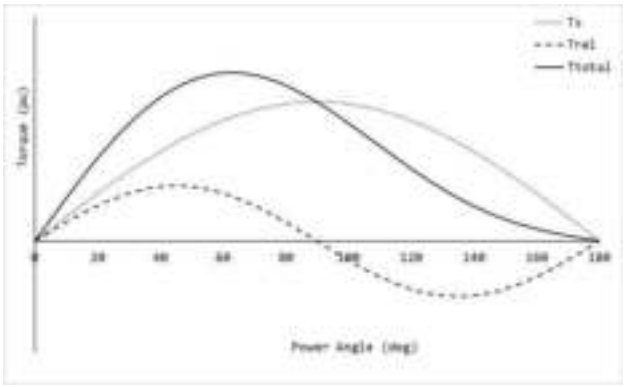

Fig.1 SPSM Torque-Power angle curve

The motor total developed torque is the sum of both components, reluctance and synchronous, and given as in (4):

$$T_{total} = T_s + T_{rel} \tag{4}$$

Explicitly:

$$T_{total} = V\frac{E}{X_d}sin(\delta) + V^2\frac{1}{2}\left(\frac{1}{X_q}-\frac{1}{X_d}\right)sin(2\delta) \tag{5}$$

A typical salient-pole design torque Vs power angle plot is illustrated in Fig.1. It can be seen that the SPSM has two torque components, one of them is linearly proportional with the terminal voltage (synchronous component), and the other has square relation with the voltage (reluctance component). Consequently, the pull-out torque will occur at a power angle δ < 90º.

For calculating the pull-out torque, first, (5) should be differentiated concerning the power angle as follows:

$$\frac{dT_{total}(\delta)}{d\delta} = V\frac{E}{X_d}cos(\delta) + V^2\left(\frac{1}{X_q}-\frac{1}{X_d}\right)cos(2\delta) \tag{6}$$

$$\frac{dT_{total}(\delta)}{d\delta} = \alpha\, cos(\delta) + \beta\, cos(2\delta) \tag{7}$$

where:

α $V\frac{E}{X_d}$;

β $V^2\left(\frac{1}{X_q}-\frac{1}{X_d}\right)$.

The non-linear equation (7) then has to be solved to find the power angle for which the torque is at maximum:

$$\frac{dT_{total}(\delta)}{d\delta} = \alpha\, cos(\delta) + \beta\, cos(2\delta) = 0 \tag{8}$$

Equation (8) appears to have a maximum of two real solutions in the range of $0 \le \delta \le \pi$, which are given as:

$$\delta_{max1} = \pi - cos^{-1}\left[\frac{\alpha - \sqrt{\alpha^2 + 8\beta^2}}{4\beta}\right]$$

$$\delta_{max2} = \pi + cos^{-1}\left[\frac{\alpha - \sqrt{\alpha^2 + 8\beta^2}}{4\beta}\right]$$

(9)

Since the motor case is being evaluated rather than the generator case, only the solutions occurring in the range $0 \leq \delta \leq \pi$ shall be considered. Thus, δ_{max2} can be discarded. This power angle should then be substituted in (5) above to find the pull-out torque of a SPSM:

$$T_{SP} = \alpha\, sin(\delta_{max1}) + \frac{\beta}{2} sin(2\delta_{max1})$$

(10)

B. Pull-Out Torque during Adjacent Motor Starting

Direct online motor starting requires high reactive power and consequently is associated with extensive high inrush current. This high current causes a considerable voltage drop in the network depending on the started motor design, available short circuit from the source, and system component impedances. The impact of motor starting on running brushless synchronous motors is therefore of a high concern during the design of a power system. As it was shown previously, the running motor torque will reduce with the voltage drop on its terminals. Therefore, to secure minimum disturbance in the speed and power angle to achieve successful reacceleration after adjacent motor starting is concluded, the voltage drop must be limited to a value that will secure the pull-out torque to be at least at 1.0 pu of the motor rated torque.

III. Minimum Synchronous Motor Terminal Voltage

The pull-out torque equation (2) for CRSM and (10) for SPSM above is the basic equation to find formulae for calculating minimum voltage on the motor terminals.

A. Cylindrical Rotor Synchronous Motor

From (2), a formula for calculating the minimum voltage at CRSM terminals can be found by simply employing the criteria of achieving at least 1 pu as a pull-out torque during the starting of a large motor:

$$1 = \frac{V_{CR-min} E}{X_d}$$

(11)

Rearranging for $V_{CR\text{-}min}$:

$$V_{CR-min} = \frac{X_d}{E}$$

(12)

That is also:

$$V_{CR-min} = \frac{1}{T_{CR,n}}$$

(13)

Where $V_{CR\text{-}min}$ is the minimum tolerable terminal voltage and $T_{CR,n}$ is the rated pull-out torque, respectively for a CRSM.

Since $V_{CR\text{-}min}$ for round rotor design can be found using only the rated pull-out torque value in (13), it makes it easier to identify $V_{CR\text{-}min}$ during the Power Distribution System (PDS) design phase by only using NEMA MG-1 [2] and IEC 60034 [4] pull-out torque standard values. This is unlike the case of salient-pole design where parameters related to the machine's design are required to calculate $V_{CR\text{-}min}$ as it will be shown later. Tolerable terminal voltages of CRSM using NEMA MG-1 [2] and IEC 60034 [4] pull-out torque standard values is shown in Table I.

Table I
Minimum CRSM tolerable terminal voltage using NEMA/IEC pull-out torque

International Standards	Power Factor	Min. Pull-Out Torque in pu	$V_{CR\text{-}min}$ in pu
API 546 [5]/ NEMA MG-1 [2]	1.00	1.50	0.67
	0.80	1.75	0.57
IEC 60034 [4]	All	1.35	0.75

B. Salient-Pole Synchronous Motor

For a SPSM (unlike the CRSM), the minimum terminal voltage on a Salient-pole machine cannot be directly related to the pull-out torque due to the nonlinear relationship as shown in (10). The pull-out torque of SPSM described in (10) can be explicitly written as:

$$T_{SP} = V\frac{E}{X_d} sin(\delta_{max1}) + V^2 \frac{1}{2}\left(\frac{1}{X_q} - \frac{1}{X_d}\right) sin(2\delta_{max1})$$

(14)

For the minimum terminal voltage, T_{SP} is substituted with 1 pu and (14) becomes:

$$1 = V_{SP-min}\frac{E}{X_d} sin(\delta_{max1}) + V_{SP-min}^2 \frac{1}{2}\left(\frac{1}{X_q} - \frac{1}{X_d}\right) sin(2\delta_{max1})$$

(15)

Rearranging for $V_{SP\text{-}min}$:

$$V_{SP-min} = \frac{X_d}{E\, sin(\delta_{max1})}\left[1 - \frac{V_{SP-min}^2}{2}\left(\frac{1}{X_q} - \frac{1}{X_d}\right) sin(2\delta_{max1})\right]$$

(16)

Equation (16) is non-linear, and conveniently it can be solved iteratively since all parameters, other than $V_{SP\text{-}min}$, are constants. Equation (16) clearly shows the fact that $V_{SP\text{-}min}$ for salient-pole is higher than that of round rotor design, considering both designs have same E and X_d. This can be observed through comparing (13) with (16), assuming that usually $X_q \approx X_d$ and $sin(\delta_{max1}) < 1$ in (16).

IV. Power System Software Simulation

A power system software simulation for running salient-pole synchronous motor performance using transient stability analysis was conducted in order to verify the proposed calculation method. Note that transient study was used instead of dynamic motor starting since the software neglects the excitation parameter and considers the machine as induction in dynamic motor starting studies.

A. System Model

The simple power network model associated with the simulated motors are displayed in Fig.2. The simulated motor model data are illustrated in Table II. The simulated motor (Syn1) will be examined during the start-up of the large induction motor (Mtr1). For conservative simulation, the exciter model was chosen as "Fixed" type in order to neglect the excitation response for supporting the bus voltage during the startup of the induction motor (Mtr1). For the simulated motor Syn1, with its data shown in Table II, the minimum tolerable terminal voltage given in equation (16) is found at 0.73 pu, which was calculated as follows.

The rated *E* of the motor was found to be 1.46 pu using (17) [6]:

$$E = V\cos\delta + X_d I_a \sin(\theta + \delta) \quad (17)$$

Where I_a is the rated current, θ is the power factor angle and δ is the power angle at rated power that is found to be 0.509 rad (29.16º) using (18) [6]:

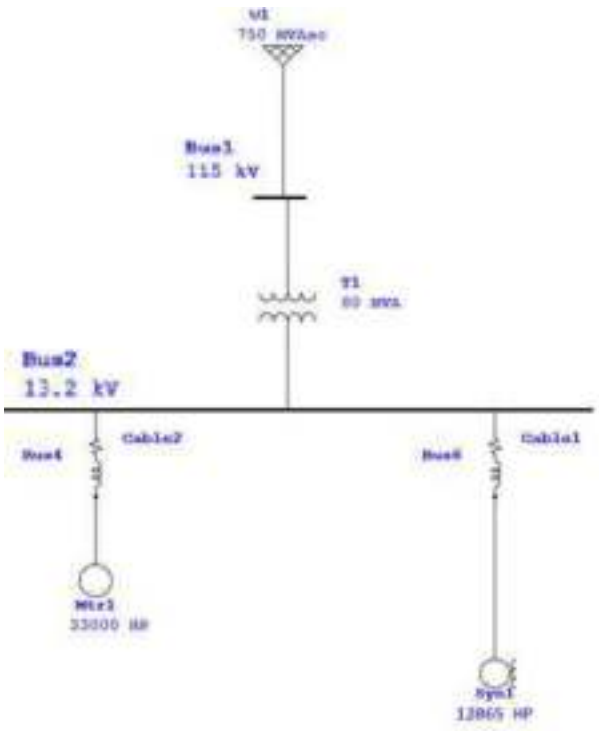

Fig.2 SPSM system simulation: power network model

Table II
Simulated running SPSM (Syn1) model data

Parameter	Value
Rated Voltage	13.2 kV (1.0 pu)
Rated Current	403 A (1.0 pu)
Power Factor	1.00
Rated Power	9 MW (0.98 pu)
Speed (f/# of poles)	1,800 RPM (1.0 pu)
X_d	1.204 pu
X_q	0.558 pu
Excitation	"Fixed Type"

Table III
SPSM ETAP simulation events

Time	Event
0 sec	Syn1 is running at full load and rated speed
1 sec	Mtr1 started
15 sec	End of simulation

$$\delta = tan^{-1}\left(\frac{X_q I_a cos\theta}{V + X_d I_a sin\theta}\right) \quad (18)$$

These will result in a δ_{max1}, calculated as in (9), to be 1.10 rad (63º), with a resultant pull-out torque using (10) of 1.50 pu. Consequently, the iteratively calculated $V_{min\text{-}SP}$ in (16) is 0.73 pu.

The general simulated events are shown in Table III. Two scenarios were examined as follows:

1. Selecting a Utility short circuit ratio that will achieve a voltage drop on the motor bus during the start-up of the motor Mtr1 slightly above the calculated voltage (0.73 pu).

2. Selecting a Utility short circuit ratio that will achieve a voltage drop on the motor bus during the start-up of the motor Mtr1 slightly below the calculated voltage (0.73 pu).

B. Simulation Results

The speed of Syn1 with its terminal voltage for Scenario (1) are plotted in Fig.3 and Fig.4 respectively. On the other hand, the speed and voltage for Scenario (2) are illustrated in Fig.5 and Fig.6 respectively.

C. Results Analysis

In Scenario (1) and at the 1st second in the plots, where the large motor Mtr1 was started, the speed (Fig.3) has a minor swinging from 1,770 to almost 1,825 RPM. Moreover, the speed oscillation was damped successfully and reached a stable condition at 1,800 RPM although that the start-up of the large motor was not successful, and the voltage drop was at around 73% (Fig.4) for extended period of time. On the other hand, for Scenario (2), it can be observed that at the startup of Mtr1, the voltage on Syn1 terminal was at around 72% (Fig.6), which caused the speed of the motor (Fig.5) to collapse after almost two seconds only. Therefore, from the simulated two scenarios above, it can be concluded that the calculated $V_{SP\text{-}min}$ value is confirmed to achieve successful stability and the motor would not experience loss of sync condition even in worst case scenario of unsuccessful start-up for the large motor (Mtr1).

V. Conclusion

The voltage-torque relationship for three-phase brushless synchronous motors was discussed in detail in this article and it was shown clearly that the torque is sensitive with respect to the motor terminal voltage. It was also shown that the motor pull-out torque is only affected by the terminal voltage in adjacent motor starting conditions. A technical base line for calculating the minimum tolerable terminal voltage on three-phase brushless synchronus

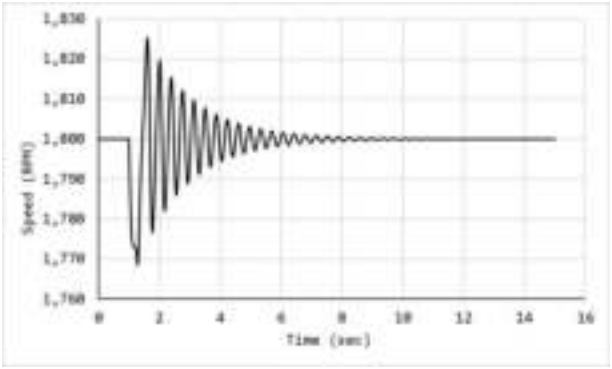

Fig.3 SPSM simulation results: Scenario (1) speed

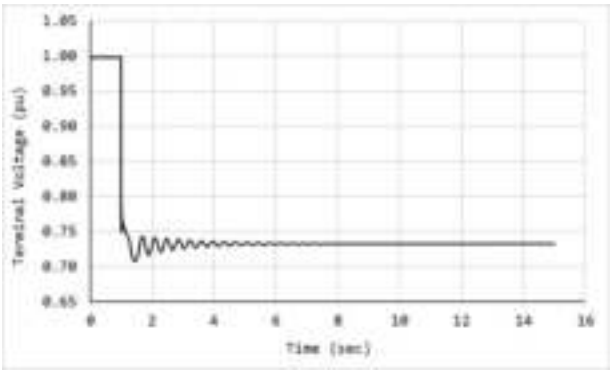

Fig.4 SPSM simulation results: Scenario (1) terminal volt.

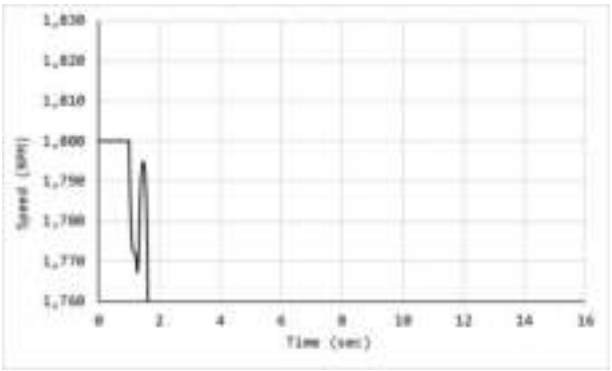

Fig.5 SPSM simulation results: Scenario (2) speed

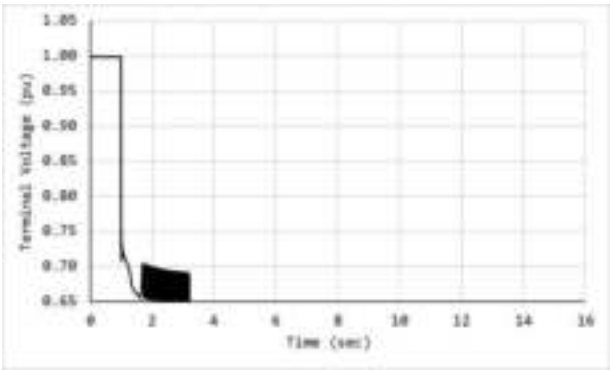

Fig.6 SPSM simulation results: Scenario (2) terminal volt.

motors, both salient-pole and cylindrical rotor designs, was discussed and proven, by simulation results, to be useful for the design of PDS when considering voltage drop associated with large motor starting as a design criterion. As a future work, it is highly recommended to validate the theoretical calculations and the simulation results presented here with a practical experiment. Afterwards, results may be shared with the standards committee of API [5] and IEC [4] for consideration.

VI. References

[1] IEEE Std. 399-1997", IEEE Recommended Practice for Industrial and Commercial Power Systems Analysis, 1997.
[2] NEMA MG 1-2016", Motors & Generators, 2016.
[3] J. F. Gieras, Electrical Machines: Fundamentals of Electromechanical Energy Conversion,. Boca Raton, US: CRC Press, 2017, pp. 293-358.
[4] IEC-60034-1-2017", Rotating electrical machines – Part 1: Rating and performance, 2017.
[5] API Std 546, Brushless Synchronous Machines—500 kVA and Larger, 2008 3rd Edition.
[6] H. Saadat, Power System Analysis, 2nd ed, New York, US: The McGraw-Hill Companies, 1999, pp. 468.

VII. VITA

Ali A. Al-Ameer (M' 19) received his BEng degree in Electrical & Electronics Engineering from The University of Leeds, United Kingdom in 2015. Ali joined Saudi Aramco in 2015; he worked for Safaniya Onshore Plants Operation Department as Motors Engineer. Then, in 2018 he transferred to the engineering head office, Consulting Services Department. Ali has a deep interest in electric machines and control systems.

Rami M. O. Dabbousi obtained his BScEE from King Fahd University of Petroleum and Mineral, Saudi Arabia, in 1996 and his MSc from Texas A&M University in 2002. He has been working with Saudi Aramco since 1996 with the Consulting Services Department, in Dhahran, and worked in different organizations within the company; including Refining, Maintenance, and Projects, as well as an intern assignment with ABB Machines in Sweden. He is an IEEE Senior Member, active in the IEEE local section, and has authored several IEEE papers.

Hussain J. Al-Marzoug (M' 18) received his BEng degree in Electrical Engineering in 2003 and Master of Engineering in Construction and Engineering Management in 2009 from King Fahad University of Petroleum & Minerals, Saudi Arabia. Hussain received Master of Electrical Engineering in Power System form Texas A&M, College Station, Texas, USA. Hussain has16 years of diversified experience in Oil & Gas and Petrochemical in design, construction, operation and maintenance. Hussain has a deep interest in Power System Analysis, Protection and Automation.

Zeyad T. Balkhyour received his B.S degree in Electrical Engineering from University of Missouri – Columbia, USA in 2010 and MS degree from University of Colorado – Denver, USA in 2016. Zeyad has been working with Saudi Aramco – Consulting Services Department since 2010, and has a deep interest in the field of Electrical Motors.

TABLE OF CONTENTS

PCIC Europe

ISBN: 978-3-9524799-7-1

Organization

Justin Mason, Trydanol Energy Solutions

Paul Donnellan, Shell

Diedrich Thaden, Wintershall

Chris Thomason

Luigi Bellofatto, IMESA Spa